Metabolomics: A Promising Tool to Improve the Understanding of the Developmental Origins of Obesity and Metabolic Disease.

by

Jennifer L. LaBarre

A dissertation submitted in partial fulfillment
of the requirements for the degree of
Doctor of Philosophy
(Nutritional Sciences)
in The University of Michigan
2020

Doctoral Committee:

Professor Charles F. Burant, Chair
Assistant Professor Katherine W. Bauer
Professor Dana C. Dolinoy
Professor Karen E. Peterson
Professor Peter X.K. Song

Jennifer L. LaBarre

jenlab@umich.edu

ORCID ID: 0000-0003-3100-1770

©Jennifer L. LaBarre 2020

DEDICATION

The contents of this doctoral dissertation titled “Metabolomics: A Promising Tool to Improve the Understanding of the Developmental Origins of Obesity and Metabolic Disease” are dedicated to each pediatric patient I see in my practice as a Registered Dietitian. My patients provide the inspiration to create innovative solutions to address the complex pathophysiology of obesity and type 2 diabetes.

ACKNOWLEDGMENTS

My heart is full of gratitude as I conclude my doctoral degree at the University of Michigan. First and foremost, I would like to thank my adviser and mentor, Dr. Chuck Burant, who has an unmatched, contagious zeal for research. I approached Chuck at the beginning of my time at Michigan, expressing interest in the field of metabolomics. Chuck has gone above and beyond in creating research opportunities and collaborations that match my goals and passions. I am most grateful for his support. I am impressed by Chuck's ability to balance a strong research portfolio with time in the clinic as an endocrinologist; as I desire to pursue a career as a clinical dietitian and researcher. I will cherish every Saturday morning meeting, with fresh donuts, during my time at Michigan.

My dissertation committee is composed of truly exceptional scientists, with a broad range of expertise, strengthening my dissertation. I am so grateful for their shared knowledge and countless hours devoted to my development. Dr. Karen Peterson was the first professor at Michigan in which I expressed my research interests. Her understanding of growth and development is unmatched, providing input and guidance on the implications of puberty on the metabolome. I am grateful for the contributions from Dr. Dana Dolinoy; a leading researcher in the field of epigenetics and environmental exposures. Dana always impresses me with her crisp and confident composure as a researcher and her incredible advocacy for the training of young scientists. I am thankful for the contributions from Dr. Kate Bauer as an epidemiologist who classifies the social and behavioral determinants of obesity. She challenges me to reflect on the

public health implications of my deeply molecular, metabolomics dissertation. Lastly, I have valued collaborating with Dr. Peter Song; an innovative biostatistician who has profoundly contributed to each chapter in this dissertation. He helped create strong statistical pipelines for working with metabolomics data.

Each committee member played a vital role in my training. Their diverse expertise strengthened me as a scientist; training me to think as a molecular biologist, a statistician, and an epidemiologist. This aspect of my PhD training is truly unique to the School of Public Health within the University of Michigan. Thank you to each of my committee members for your time and talents, as well as many laughs along the way.

I am grateful for the collaborations with the Michigan Mother Infant Pairs (MMIP) cohort research team, led by Dr. Vasantha Padmanabhan. Clinical data for the mother-infant dyads was retrieved by Dr. Muraly Puttabyatappa. I am especially thankful for the efforts of Dr. Jackie Goodrich and Carly McCabe, as they provided guidance and training for analyzing EPIC bead array DNA methylation data.

I have enjoyed the opportunity to collaborate with countless researchers within the Early Life Exposures in Mexico to ENvironmental Toxicants project. Dr. Wei Perng provided guidance on analyzing metabolomics data. I'm grateful for the countless hours of collaboration with Dr. Peter Song's biostatistics doctoral students, Dr. Lu Tang, Dr. Ling Zhou, and Wei Hao. I am thankful for the coordinators of the ELEMENT project, Laura Arboleda and Robin Lee, and the field work team in Mexico.

I have loved being a member of the Burant lab, managed by Mary Treutelaar, kept afloat by Dr. Heidi IglayReger, and supported by eager graduate students with a passion for metabolism. It has

been a joy to journey on this doctoral degree with Jim Casey, a fellow nutritional sciences PhD student. I'm grateful for the staff at the Michigan Regional Comprehensive Metabolomics Resource Core for my metabolomics training, including Dr. Maureen Kachman and Dr. Alla Karnovsky. Lastly, I want to thank my funding sources as I was supported by a training grant from Dr. Burant, the Michigan Nutrition and Obesity Center (P30 DK089503), and the Michigan Regional Comprehensive Metabolomics Resource Core (R24 DK097153).

I am especially thankful for the passionate University of Michigan nutritional science colleagues and friends that I met along the way, in particular Rachel Caty and Claire Roess for being a source of inspiration in helping my find my niche in the field. I am grateful for my conversations with Dr. Sue Cole, providing a voice of reason during each step of my degree.

My journey would not have been possible without the love and support from my parents, John and Lynn LaBarre, my brother and his wife, John and Jana LaBarre, and my best friends, Alex Meijer and Claire Ouimet.

TABLE OF CONTENTS

DEDICATION ii
ACKNOWLEDGMENTS iii
LIST OF TABLES viii
LIST OF FIGURES x
LIST OF ABBREVIATIONS xiii
ABSTRACT xv
CHAPTER 1
Introduction 1
Obesity and Type 2 Diabetes: A Growing Public Health Challenge. 1
The Developmental Origins of Obesity and Metabolic Disease. 4
A Systems Biology Approach Utilizing Metabolomics Techniques 7
Using the Metabolome to Classify the Intrauterine Environment 12
Intrauterine Influences on the Epigenome 13
Mitochondrial Dysfunction in the Pathogenesis of Obesity and Metabolic Disease 16
Metabolite Biomarkers of Obesity and Insulin Resistance 18
Specific Aims and Hypotheses 21
References 25
CHAPTER 2
Maternal Lipid Levels across Pregnancy Impact the Umbilical Cord Blood Lipidome and Infant Birth Weight 36
Abstract 36
Introduction 37
Subjects and Methods 39
Results 42
Discussion 48
Conclusion 53
References 96

CHAPTER 3
Lipidome across Pregnancy Influences the Establishment of Umbilical Cord Blood Leukocyte Genome-Wide DNA Methylation. 101
Abstract 101
Introduction 101
Subjects and Methods 104
Results 108
Discussion 111
Conclusion 115
References 134
CHAPTER 4
Evidence for Intrinsic Mitochondrial Nutrient Utilization Underlying the Association between Metabolite Levels and Insulin Resistance in Adolescents. 139
Abstract 139
Introduction 140
Subjects and Methods 142
Results 147
Discussion 154
Conclusion 158
References 198
CHAPTER 5
Conclusion 203
Significance of Research Findings 203
Study Strengths and Limitations 208
Future Studies and Applications 211
Public Health Relevance 217
References 223

LIST OF TABLES

Table 2.1	Lipid species class, abbreviation, and number of lipids annotated from lipidomics analysis.	56
Table S2.1	Lipid group classifications.	57
Table 2.2	Characteristics of the MMIP participants, stratified by sex (n=106).	60
Table S2.2	Comparison of M1-M3 lipid raw peak intensities.	63
Table S2.3	Comparison of M3-CB lipid raw peak intensities.	74
Table 3.1	Characteristics of the MMIP participants (n=100)	118
Table 3.2	Number of significant differentially methylated CpG probes in umbilical cord blood leukocytes associated with maternal lipid groups.	119
Table 3.3	Classification of significant differentially methylated CpG probes in umbilical cord blood leukocytes associated with maternal lipid groups.	121
Table 3.4	Classification of differentially methylated regions in umbilical cord blood leukocytes associated with maternal lipid groups.	123
Table S3.1	Enriched gene ontologies (GO) from differentially methylated probes associated with M3 LysoPC-sat.	126
Table S3.2	Enriched KEGG pathways from differentially methylated probes associated with M3 LysoPC-sat.	131
Table 4.1	Characteristics of the ELEMENT participants, stratified by sex (n=206).	161
Table S4.1	Association between annotated metabolites and BMIz (n=206).	165
Table S4.2	Association between annotated metabolites and BMIz in boys (n=98).	168

Table S4.3	Association between annotated metabolites and BMIz in girls (n=108).	171
Table S4.4	Association between annotated metabolites and HOMA-CP (n=206).	178
Table S4.5	Association between annotated metabolites and HOMA-CP in boys (n=98).	180
Table S4.6	Association between annotated metabolites and HOMA-CP in girls (n=108).	182
Table S4.7	Linear relationship between energy adjusted macronutrient intake with BMIz and HOMA-CP.	185
Table S4.8	Classification of clusters.	188
Table S4.9	Path analysis demonstrating the relationship between macronutrient intake with BMIz through metabolome clusters, adjusting for age, sex and puberty onset.	191
Table S4.10	Path analysis demonstrating the relationship between macronutrient intake with HOMA-CP through metabolome clusters, adjusting for age, sex and puberty onset.	194
Table S4.11	Differences in IGF-1 levels between pubteral and pre-pubertal children.	197
Table 5.1	Effect of weight loss on clinical measures.	220

LIST OF FIGURES

Figure 1.1	Study Objective.	23
Figure 1.2	Study Cohort.	24
Figure 2.1	Timeline of clinical study visits.	55
Figure S2.1	Relationship between maternal baseline BMI, gestational weight gain, and Fenton BW percentile.	61
Figure 2.2	Dynamic changes in maternal and cord blood plasma lipidome during pregnancy.	62
Figure 2.3	Pearson correlation of maternal first trimester plasma lipidome.	84
Figure 2.4	Pearson correlation of maternal delivery plasma lipidome.	85
Figure 2.5	Pearson correlation of cord blood lipidome**.**	86
Figure 2.6	Correlation between lipid groups differs between maternal and cord blood samples.	87
Figure S2.2	Associations between maternal and cord blood lipid groups with maternal BMI at baseline.	88
Figure S2.3	Associations between maternal and cord blood lipid groups with maternal gestational weight gain.	89
Figure 2.7	Distinct maternal and cord blood lipid groups are related to birth weight.	90
Figure 2.8	Association between triglycerides and birth weight in male and female infants.	91
Figure 2.9	Maternal lipids correlate with cord blood lysophospholipids.	92

Figure 2.10	Maternal lipids correlate with cord blood polyunsaturated triglycerides.	94
Figure 3.1	Maternal term saturated lysophospholipids are associated with differential DNA methylation in promoter regions of infant leukocyte genes.	124
Figure S3.1	Maternal term saturated lysophospholipid levels are associated with differential DNA methylation within the CpG Island of *DBI*.	125
Figure 3.2	Top 10 significantly enriched gene ontologies and biological pathways associated with M3 LysoPC-sat.	133
Figure S4.1	Relationship between insulin and C-peptide at baseline.	160
Figure S4.2	Clinical phenotypes and metabolic biomarkers exhibit strong correlations, sex-stratified.	163
Figure S4.3	Association of metabolite features with BMIz, within the entire cohort and sex-stratified.	164
Figure 4.1	Association of diglycerides and amino acids with BMIz exhibits sex differences.	174
Figure S4.4	Fatty acids and diglycerides stratified by sex and obese (BMIz ≥2) vs. normal weight (-2≤BMIz<1).	175
Figure 4.2	Relationship between fatty acid chain length and number of double bonds with BMIz, sex-stratified.	176
Figure S4.5	Association of metabolite features with HOMA-CP, within the entire cohort and sex-stratified.	177
Figure 4.3	Insulin resistance is inversely associated with short- and medium-chain acylcarnitine metabolites.	184
Figure 4.4	Structure of path analysis.	186
Figure 4.5	Clustering of annotated metabolites.	187
Figure 5.1	Proposed influence of the maternal and cord blood lipidome on birth weight.	218
Figure 5.2	Proposed differences in mitochondrial oxidation in an insulin resistance and insulin sensitive cell.	219
Figure 5.3	Effect of weight loss on the plasma lipidome.	221

Figure 5.4 Relationship between the Institute of Medicine gestational weight gain recommendations, pre-pregnancy BMI category, and Fenton BW percentile. 222

LIST OF ABBREVIATIONS

AA	arachidonic acid
AC	acylcarnitine
BCAA	branched chain amino acid
BMIz	BMI z-score
BP	biological processes
BW	birth weight
CB	cord blood
CC	cellular components
CE	cholesterol ester
Cer	ceramide
CI	confidence interval
DBP	diastolic blood pressure
DG	diglyceride
DHA	docosahexaenoic acid
DiC	dicarboxylic group
DMR	differentially methylated region
DOHaD	Developmental Origins of Health and Disease
EFA	essential fatty acid
ELEMENT	Early Life Exposure in Mexico to ENvironmental Toxicants
FA	fatty acid
FAO	fatty acid oxidation
FC	fold change
FDR	false discovery rate
FFA	free fatty acid
FFM	fat free mass
FFQ	food frequency questionnaire
GO	gene ontology
GWG	gestational weight gain
HDL	high density lipoprotein
HOMA-CP	homeostatic model assessment of insulin resistance using C-peptide
HOMA-IR	homeostatic model assessment of insulin resistance
IGF-1	insulin-like growth factor 1
IOM	Institute of Medicine
IR	insulin resistance
KEGG	Kyoto Encyclopedia of Genes and Genomes
LC	long-chain
LDL	low density lipoprotein

LysoPC	lysophosphatidylcholine
LysoPE	lysophosphatidylethanolamine
LysoPL	lysophospholipid
M1	maternal first trimester
M3	maternal delivery
MC	medium-chain
MF	molecular function
MFSD2a	major facilitator superfamily domain-containing protein 2
MG	monoglyceride
MMIP	Michigan Mother-Infant Pairs
MS	mass spectrometry
mTOR	mammalian target of rapamycin
MUAFA	mid-upper arm fat area
MUAMA	mid-upper arm muscle area
MUFA	monounsaturated fatty acid
PA	phosphatidic acid
PC	phosphatidylcholine
PE	phosphatidylethanolamine
PG	phosphatidylglycerol
PI	phosphatidylinositol
PL	phospholipid
PL-PC	plasmenyl-phosphatidylcholine
PL-PE	plasmenyl-phosphatidylethanolamine
PS	phosphatidylserine
PUFA	polyunsaturated fatty acid
REE	resting energy expenditure
SBP	systolic blood pressure
SFA	saturated fatty acid
SM	sphingomyelin
SP	suprailiac skinfold
SS	subscapular skinfold
T2D	type 2 diabetes
TG	triglyceride
TR	triceps skinfold
TR+SS	total subcutaneous adiposity
SS/TR	central subcutaneous adiposity
VLDL	very low density lipoprotein
WC	waist circumference
WHtR	waist to height ratio
WL	weight loss

ABSTRACT

The prevalence of obesity and type 2 diabetes continues to rise in the pediatric and adult population. This increase in metabolic disease may be partially due to programming during sensitive periods of development. Metabolomics is a powerful tool to identify molecular biomarkers and mechanistic insights into adverse health outcomes. This dissertation describes the use of metabolomic profiling to define the metabolic environment in two human cohorts, during gestation and the pubertal transition, and relate them mechanistically to growth and metabolism outcomes.

Lipidomic profiles performed on first trimester maternal plasma (M1), delivery maternal plasma (M3), and infant umbilical cord plasma (CB) in 106 mother-infant dyads showed selective transport of long-chain polyunsaturated fatty acids (PUFA) as well as lysophosphatidylcholine (LysoPC) and lysophosphatidylethanolamine (LysoPE) into CB. Using linear models, CB LysoPC and LysoPE groups were positively associated with birth weight, a commonly assessed indicator of gestational implications on fetal growth. M1 PUFA containing triglycerides and phospholipids appear to modulate the levels of the CB lysophospholipids related to BW. Furthermore, epigenome-wide DNA methylation was measured in CB leukocytes to determine how the maternal lipidome across gestation may influence fetal programming. M3 saturated LysoPCs and LysoPEs were associated with differential methylation in CpG islands within genes pertaining to cell proliferation and growth. These results highlight the influence of the maternal lipidome on the infant epigenome.

A growing body of evidence suggests a relationship between the metabolome and metabolic health in adults, however, less is known in children and adolescents in the pubertal transition, who have changing hormonal patterns and accumulation of muscle and fat tissue. Using untargeted metabolomics, metabolites associated with BMI z-score include positive associations with diglycerides among girls and positive associations with branched chain and aromatic amino acids in boys. In contrast to that found in adults, medium-chain acylcarnitines were inversely associated with insulin resistance (IR), suggesting less imbalance in the delivery and oxidation of substrates in adolescents, perhaps due to the increased substrate utilization to fuel tissue and linear growth. Path analysis identified metabolites that underlie the relationship between energy-adjusted macronutrient intake with IR. Carbohydrate intake is positively associated with IR through decreases in intermediates of β-oxidation, while fat intake is positively associated with IR through increases in extra-mitochondrial fatty acid metabolism, the latter identified by accumulation of dicarboxylic fatty acids. Thus, biomarkers of IR and mitochondrial oxidative capacity may depend on the relative nutrient mix and an individual's intrinsic mitochondrial metabolism.

These studies demonstrate the ability to generate inferential hypotheses about metabolism by acquiring high dimensional metabolomics data. The suggested modulation of uptake of lysophospholipids into the developing fetus, potentially influencing birth weight, by PUFAs exposure in the first trimester could be tested in larger cohorts or experimentally by timed PUFA intake. Longitudinal follow-up is needed to identify if fetal programming, via the establishment of DNA methylation patterns at birth, influences risk of adult metabolic disease. During adolescence, our findings confirm and extend associations between the metabolome with obesity and IR, emphasizing sex-specific differences due to variations in muscle and fat tissue

accumulation in puberty. These results suggest that adolescents prone to IR have an increase in selection of carbohydrates for fuel, exacerbated by elevated habitual carbohydrate consumption. Using controlled feeding studies, intrinsic differences in mitochondrial metabolism and the consequence of habitual macronutrient intake on IR could be directly tested.

CHAPTER 1

Introduction

Obesity and Type 2 Diabetes: A Growing Public Health Challenge.

One of the top public health crises our world currently is challenged by is the increase in the prevalence of obesity. Between 1980 and 2014, the worldwide prevalence of obesity has more than doubled (1). In the United States, 39.8% of adults have obesity and 18.5% of children and adolescents aged 2-19 years have obesity (2). The high prevalence of obesity is increasing in both developed and developing nations (3). Higher levels of obesity are found in people with lower socioeconomic status, less education, and within Hispanic and non-Hispanic black (4).

Obesity is defined by excessive growth of adipose tissue depots, typically due to an imbalance between energy intake and the energetic needs of an individual. The obesity pandemic is related to increased intake of calorically dense foods, in particular highly processed foods, paired with increases in sedentary activity (5). Through the incorporation of genome-wide analyses, common genetic variants of obesity risk have been identified (6). Depending on the population studied, the genetic influence of obesity varies from 40-70% (7,8). Common genes associated with obesity have previously been reviewed highlighting 190 known associated loci, accounting for <10% of obesity risk (6). Therefore, genetics alone cannot explain the rise in obesity prevalence and it is clear that the interaction between environmental factors and genetic variants influences the risk of disease.

In parallel to the obesity pandemic, the global prevalence of type 2 diabetes (T2D) has rapidly increased over the past four decades (9). In a study including 180 countries, the global prevalence of T2D in people ages 20-79 years was 8.8% in 2015 (10). The burden of diabetes influences low-income and middle-income countries more than high-income countries with the highest T2D trends in Polynesia and Micronesia followed by Melanesia, the Middle East, and northern Africa (9). Epidemiologic studies link T2D with obesity, including the Nurses' Health Study (11), suggesting that T2D risk increases with higher BMI. Studies highlight the importance of fat distribution in the development to T2D. Visceral adiposity, rather than subcutaneous adiposity, contributes to T2D, potentially due to lipid accumulation around key internal organs including the liver (12). The increased ability to store excess lipids in subcutaneous adipose tissue is hypothesized to be protective from developing T2D (13).

T2D development is associated with a fall in the production of the hormone insulin. Insulin is an anabolic hormone produced by β-cells of the pancreas in the fed state to maintain blood glucose homeostasis. Insulin binds to insulin receptors on the cell surface, inducing autophosphorylation of the insulin receptors and stimulating a signaling cascade to maintain glucose homeostasis (14). The regulatory effect of the insulin transduction pathway differs by cell type – stimulating uptake of glucose in myocytes and adipocytes, inhibiting glucose release in hepatocytes, promoting lipid synthesis and storage in hepatocytes and adipocytes, and stimulating protein synthesis and inhibiting protein degradation in myocytes (14).

The origins of T2D begin as tissues become resistant, or non-responsive, to insulin signaling. To compensate, pancreatic β-cells increase the production of insulin to lower blood glucose levels. Overtime, the resistance to insulin action paired with an intrinsic susceptibility to dysfunction and death of β-cells to produce leads to inadequate insulin secretion for the prevailing insulin

sensitivity (15). Indeed, genes attributing to the development of type 2 diabetes seem to be primarily associated with β-cell development, signaling, and failure to compensate for increased demands (16). Without the production of insulin, blood glucose homeostasis is not maintained. Elevations in the blood glucose level is paired with increases in free fatty acids (FFA), triglycerides (TG), and LDL-cholesterol (LDL-C) (17). The gold standard for measuring insulin resistance is a hyperinsulinemic-euglycemic clamp (18), however, estimates can be obtained through the homeostatic model assessment of insulin resistance (HOMA-IR) or through a frequently sampled intravenous glucose tolerance test (FSIVGTT). Systemic changes in glucose homeostasis are a result of impaired insulin action on multiple metabolically active organs, including skeletal muscle, the liver, and adipose tissue. Although the complete mechanisms in the pathogenesis of T2D are not yet fully understood, researchers are beginning to describe how tissues become insulin resistant, highlighting the connection between obesity and T2D (19).

This dissertation describes the use of metabolomic profiling to define the metabolic environment in two human cohorts, during gestation and the pubertal transition, and relate them mechanistically to growth and metabolism outcomes, potentially highlight risk of developing metabolic diseases (**Figure 1.1**). To address this objective, we incorporated untargeted metabolomics and lipidomics techniques to two human cohorts; the Michigan Mother-Infant Pairs (MMIP) cohort and the Early Life Exposure in Mexico to ENvironmental Toxicants (ELEMENT) cohort (**Figure 1.2**). During gestation, the maternal lipidome was related to the infant birth weight and the umbilical CB lipidome to determine how nutrient exposure influences fetal growth. Additionally, we assessed the influence of the maternal lipidome on establishing infant umbilical CB leukocyte DNA methylation patterns, providing insight on fetal programming via epigenetic mechanisms. Lastly, during adolescence, we determined how the

metabolome is associated with insulin resistance, which may be exacerbated by habitual dietary intake. The remainder of this chapter will focus the developmental origins of susceptibility to type 2 diabetes on the application of metabolomics to probe the potential biology underlying risk for insulin resistance and diabetes.

The Developmental Origins of Obesity and Metabolic Disease.

Both external and internal exposures may influence the trajectory of development and alter disease risk in adult life. The Developmental Origins of Health and Disease (DOHaD) field describes how insults during the gestational and postnatal periods can permanently program an individual altering their risk of human disease during adulthood (20). David Barker and his colleagues were the original pioneers of the DOHaD approach which originated from their epidemiological studies of infant and adult mortality published in *The Lancet* (21–23). These findings generated the Fetal Origins Hypothesis, which proposes that the gestational period has a significant impact on an individual's health and wellbeing in adulthood. Barker demonstrated that the fetus is not immune to harmful exposures and events that happen during gestation can impact future health in adulthood.

The DOHaD approach acknowledges that an organism will adapt to best fit its external environment to increase chance of survival. Developmental plasticity describes the ability of a given genotype to produce differing phenotypes in response to environmental cues (24). Plasticity can be evolutionary advantageous as environmental cues can influence structural changes to enhance the survival of the organism within the extant environment. Sensitive periods of development denote times when environmental insults have a larger effect than the same exposure during other periods. Examples of sensitive periods include in utero, newborn, infancy, and puberty. Infant birth weight (BW) is the most common health outcome studied to determine

if the maternal intrauterine environment influences the development of the fetus. Both low and high BW have been associated with increased T2D rates, proposing a U-shaped curve with higher T2D rates in both tails of the distributions (25,26).

Maternal nutrient availability and offspring health outcomes

The origins of the DOHaD field began in the 1900s, as scientists were collecting experimental evidence that manipulating pregnant animals can alter the phenotype of the offspring (27). Famines during World War II provided rare experiments to observe how conditions during gestational development influenced offspring (28). The strongest evidence of the influence of exposures during gestation occurred in Rotterdam and The Hague, two cities in the western Netherlands that experienced a well-documented famine after a railway strike during World War II. From November 1944 through February 1945, the German occupants limited rations to 400-800 calories/day for all people, including pregnant women. After the complete restriction, the Netherlands returned back to their complete diet relatively quickly. The Dutch Hunger Winter created a controlled human cohort of intrauterine deprivation and long-term health implications (29). This study and others (30,31) have revealed implications of exposure timing, as some pregnant women were exposed to the famine in early gestation, while others exposed in late gestation. Nutrient restriction in utero during the first trimester was associated with elevated rates of obesity, altered lipid profiles, and cardiovascular disease (32). Exposure to famine in the third trimester was associated with lower birth weight and lower rates of adult obesity (32) as well as decreased glucose tolerance (33). Additionally, prenatal famine exposure in the first trimester was associated to differentially methylated DNA regions related to genes involved in growth and metabolism (34), suggesting the influence of famine of the epigenome. Epidemiologic studies have identified outcomes from other cohorts of individuals exposed to famine across the entire

gestational period demonstrating increased risk of adult T2D and hyperglycemia (35) and hypertension (36). Stemming from results of famine studies, dietary manipulation studies during pregnancy have demonstrated changes in the risk of adult metabolic disease among offspring (37). These studies have demonstrated the nutrient factors, including energy intake, fatty acids (37,38), protein (39,40), micronutrients (41), and vitamins, including folic acid (42), have profound influence on fetal programming, varying by timing of exposure.

Maternal phenotypes and offspring metabolic health

Studies have demonstrated that maternal phenotypes influence the offspring development. There is an increase in pregnant women that are overweight or obese, which influences both maternal and infant health. Maternal obesity during pregnancy is associated with an increased risk of gestational diabetes mellitus (GDM) and elevated infant fat mass and birth weight at delivery as well as an increase in adult risk of obesity and insulin resistance (43). During pregnancy, both excessive and inadequate maternal gestational weight gain influence maternal and infant outcomes (44). In 2009, the Institute of Medicine (IOM) issued guidelines on gestational weight gain for optimal maternal and infant health based on pre-pregnancy BMI (45). Independent of pre-pregnancy BMI, women who gained more weight than the IOM recommendations had newborns with increased risk of childhood adiposity, hypertension and insulin resistance (46). Additionally, women who gained less weight than the IOM recommendations had newborns with increased risk of hypertension and insulin resistance (46). These results suggest that pre-pregnancy BMI and GWG have distinct pathways influencing offspring's risk of metabolic health.

The Pima Indians from the Gila River Indian Community of Arizona are a population with a high prevalence of diabetes and obesity that have been followed in a longitudinal study since the

1960s (47). Through this group of people, the effect of maternal T2D on offspring health has been assessed. During adolescence, the offspring of diabetic mothers weighed 140% more than their desirable weight, directly relating maternal diabetes to offspring obesity (48). Interestingly, maternal diabetes was predictive of obesity in adolescence, independent of maternal pre-pregnancy BMI and infant birth weight (49). From these studies, the Hyperglycemia and Adverse Pregnancy Outcome (HAPO) study began; a renowned study assessing the influence of mild maternal glycemia with adverse pregnancy outcomes (50). The HAPO study demonstrated that maternal hyperglycemia, even at levels below the GDM diagnosis threshold, were associated with large-for-gestational-age offspring (51). Exposure to elevated glucose levels in utero is associated with childhood adiposity, independent of maternal BMI (52). At childhood, offspring exposed to untreated GDM during pregnancy are more insulin resistance with limited β-cell compensation (53).

A Systems Biology Approach Utilizing Metabolomics Techniques

As analytical techniques and computational methods are advancing, there is an opportunity to classify the complexity of a biological system at the molecular, cellular, and organismal level. The field of systems biology is a collaboration between chemist, biologists, mathematicians, physicists, and engineers incorporating multiple omics approaches (e.g. genomics, epigenomics, transcriptomics, proteomics, and metabolomics) (54). Applying these omics techniques creates a holistic approach in the study of a biological system. As omics technologies are becoming more accessible, the incorporation of multi-omics techniques in a research design presents computational challenges and difficulties in interpretations of the findings. Despite these complexities, systems biology approaches are being applied to understand the development and progression of disease states.

Metabolomics is the analysis of the chemical reactions within cells, tissues, or biological systems. Metabolites are small molecular weight compounds (<1,500 Da) that are both intermediates and products of metabolism. Each metabolite plays a critical role in keeping cells healthy and functioning properly, including providing substrates for energy production, participating in cell signaling, and regulating enzymes through inhibiting or stimulating their activity. The metabolome varies between individuals due to age (55) and dietary intake (56), as well as biological differences in individual phenotypes based on genetics, epigenetics, and the external environmental. Analytical chemistry instrumentation is used for metabolomics assays. A common platform couples a separation method, such as gas chromatography, liquid chromatography, or capillary electrophoresis, with mass spectrometry (MS) to ionize and detect the compounds within the sample. Another method called nuclear magnetic resonance (NMR) spectroscopy can detect metabolites through the application of magnetic fields to measure the re-emitted electromagnetic radiation from nuclei with the sample. Targeted metabolomics approaches use standards to quantitatively measure specific groups of metabolites of interest, generally favored for hypothesis-driven approaches. Untargeted metabolomics detects all low molecular weight compounds in a biological sample, known as the metabolome, generally favored for hypothesis-generating approaches. Challenges in untargeted metabolomics include the large number of unannotated "features" that may be redundant or a fragmentation of the ionization techniques.

Classifying the metabolome of different cell-types and tissue-types is important to understand localized influences of a disease-state (57). However, many biological samples require invasive procedures to obtain, such as biopsies. Blood is a commonly used biological fluid for metabolomics analyses, as it requires minimally invasive procedures and has the potential to

reflect the complex interplay of many tissues within the human body. There is a desire to classify differential metabolites in a disease state in blood, potentially identifying biomarkers to assess in other populations. Plasma is the liquid in which blood cells are suspended and is obtained when anti-coagulants are introduced. If anti-coagulants are not introduced, the blood is allowed to clot and the supernatant fluid is called the serum. Slight differences have been observed between the serum and plasma metabolome (58), however similar biological and clinical associations have been seen.

The metabolome is the complete set of small-molecular weight compounds in a sample, composed of amino acids, organic acids, nucleic acids, fatty acids, sugars, amines, vitamins, co-factors, and exogenous chemicals, such as drugs or food additives. Multiple databases are available for compound identification and classification of metabolites including the Human Metabolome Database (HMDB) (59), KEGG (60), Lipid Maps (61), and Metlin (62). Each metabolite contributes to the human body in different ways. Nucleic acids and amino acids are the building blocks for DNA, RNA, and proteins. Carbohydrates are a major source of energy during the fed state and can be stored in tissues, primarily liver and muscle as glycogen. Lipids are the most structurally diverse and abundant metabolites in human plasma (63). The main groups of lipids are fatty acyls, glycerolipids, phospholipids, sphingolipids, and sterol lipids (61). Each lipid group will be discussed below.

Fatty acyls are the fundamental category of lipids, including fatty acids, eicosanoids, fatty alcohols, and esters. The basic structure of a fatty acid is a hydrocarbon chain with a terminal carboxyl group, varying in chain length and the number of double bonds. The terminal carboxyl group can be substituted for an alcohol group, forming a fatty alcohol. The structure of fatty

acids determines their biological functions, including energy storage, signal-transduction, and lipid synthesis.

The highest proportion of total lipids in the plasma is within the glycerolipids class, which is comprised of monoglycerides, diglycerides, and triglycerides. Glycerolipids are composed of a glycerol backbone with one, two, or three fatty acyl groups. These lipids are transported through the body via lipoproteins to be distributed to tissues. In adipose tissue, glycerolipids are the main energy storage. Plasma glycerolipid levels change based on the fasted or fed state (63). Elevated triglycerides can results from an unhealthy diet, pregnancy, weight gain, genetics, and the use of some medications (64). Hypertriglyceridemia is a common risk factor for cardiovascular disease (64).

Phospholipids are the main component of cell membranes, containing a glycerol backbone with two fatty acyl tails attached with ester linkages to the sn-1 and sn-2 carbons and a polar molecule attached to the sn-3 carbon. Typically, a polyunsaturated fatty acid tail is attached to the sn-2 position. The human body has a wide variety of phospholipids differing by organelle and cell type (65). This diversity suggests specificity in phospholipid's involvement in many physiological processes; although it is uncertain how cell-specific phospholipid composition is established and maintained. Phospholipids can be converted to each other rapidly, suggesting the high correlation between many types of phospholipids. The simplest phospholipid is phosphatidic acid, with a phosphate group attached to the sn-3 carbon. Phosphatidic acid is a precursor for other lipid synthesis and is rapidly converted to diglyceride molecules for cell signaling (65). Phosphatidylcholine is the most abundant phospholipid in the cell, comprising 40-50% of total phospholipids within all organelles (65), and contains a choline head-group. Phosphatidylethanolamine N-methyltransferase (PEMT) converts a phosphatidylethanolamine

lipid to a phosphatidylcholine via the addition of three methyl groups. Phosphatidylethanolamine is enriched in the inner membrane of the mitochondria, comprising 35-40% of total phospholipids (65). Additional polar head groups attaching to the phosphate group on the sn-3 carbon include glycerol (phosphatidylglycerol), inositol (phosphatidylinositol), and serine (phosphatidylserine) among other combinations.

The fatty acyl group on the sn-1 carbon of a phospholipid can be altered. The hydrolysis of the fatty acyl group on the sn-1 carbon forms a lysophospholipid, a lipid class important for cell signaling. Plasmalogens contain a fatty alcohol radical and a cis double bond at the sn-1 carbon. Plasmalogens are named by the polar head-group in the sn-3 position making the most abundant plasmenyl-phosphatidylcholine and plasmenyl-phosphatidylethanolamine (66). Because polyunsaturated fatty acids are typically attached to the sn-2 carbon, plasmalogens are considered reservoirs of polyunsaturated fatty acids in membranes (67).

Sphingolipids contain a polar head group, known as an amino alcohol called a sphingosine, and two nonpolar tails. Variations in the r-group attached to the oxygen on the sphingosine determine its class. A sphingolipid with a hydrogen R-group is called a ceramide, which can participate in a variety of cell signaling. A sphingolipid with a phosphocholine R-group is called a sphingomyelin, which is found in cell membranes in the myelin sheath at high abundance.

Sterols contain one hydroxyl group on a 4-ring structure. The most abundant sterol in human plasma is cholesterol, existing in both free and fatty acyl-esterified forms. Sterols are precursors to vitamin and steroid hormone synthesis and are components of the cell membrane.

Using the Metabolome to Classify the Intrauterine Environment

The maternal metabolome has been used to obtain an objective measurement of the metabolic environment in which the developing fetus is exposed. Changes in the maternal metabolome across gestation occur to support the developing needs to the fetus (68), suggesting the importance of analyzing multiple measures of the metabolome across gestation. The application of metabolomics to developmental studies can identify changes in maternal nutrient availability across pregnancy (69,70) while identifying how maternal characteristics, such as pre-pregnancy BMI (71–73), hyperglycemia (74,75), and other lifestyle/clinical factors (76), influence nutrient availability and alter fetal growth, typically measured by birth weight. Using a targeted metabolomics approach, our research group previously reported an increase in plasma long-chain fatty acids and corresponding long-chain acylcarnitines in maternal plasma from first trimester to term, supporting rapid fetal growth (77). The metabolome of the maternal plasma across gestation can be paired with the metabolome of infant umbilical cord blood. Maternal metabolite levels, placental transfer, and interaction with other metabolites, such as inhibition by competition or metabolite-induced changes in placental transport activity, can all affect the relative levels of the umbilical cord blood metabolome.

Metabolomics analyses have been applied to identify trimester-specific maternal metabolites associated with infant birth weight and adiposity (71,72,74,78,79), accounting for maternal characteristics such as pre-pregnancy BMI (72). The metabolome from cord blood has been correlated with BW finding positive associations with branched chain amino acids (80), AC (81,82), and phosphatidylcholines (PC) (82,83) along with inverse associations with TGs (81). Other studies have found that cord blood lysophosphatidylcholine (LysoPC) metabolites with

varying chain length and saturation are positively associated with newborn BW (83–85), as well as with weight at 6 months of age (83).

Intrauterine Influences on the Epigenome

There is growing evidence that epigenetic mechanisms are an important contributor to developmental programming (86). Epigenetics is defined as mitotically heritable changes in gene expression that occur without altering the DNA sequence. Two epigenetic modifications include DNA methylation and alterations to chromatin folding via histone modifications. DNA methylation is the most extensively studied epigenetic modification. Methyl-groups are covalently attached to the 5' carbon of a cytosine, commonly preceding a guanine, generating a 5-methylcytosine. Across most tissues, 70% of CpG sites are methylated (87). Regions in the genome with high CpG site frequency are called CpG islands, which are often located at the 5' promotor of genes. In general, transcriptionally active genes have unmethylated CpG islands upstream of the promoter. Another way that genes are regulated is through altering chromatin structure, the complex of DNA and its histone protein. Histone proteins can be modified through methylation, phosphorylation, acetylation, and ubiquitination; impacting gene expression through either promoting or preventing transcription factor binding. Other epigenetic mechanisms with a potential role in the development of disease include noncoding RNAs (86).

The ability to modify the epigenome through a variety of mechanisms allows for control of gene expression in a cellular and tissue-specific manner. Epigenetic responses fluctuate between different cell-types, allowing for specificity in gene expression dependent upon localization. Modifications can remain present through cell divisions (mitosis) and, although rare, may last for multiple generations (meiosis) (88), highlighting the inter-generational heritability of epigenetic modifications. During mammalian development, genome-wide epigenetic reprogramming erases

epigenetic marks, followed by the establishment of a new set of marks (89). As an individual develops, the epigenome is vulnerable to insults. One particularly vulnerable period is during embryogenesis, where DNA synthesis rates are high and establishing the epigenome is crucial for normal development (90).

During sensitive periods of development, environmental exposures have the capability to influence the epigenome and protect or predispose an organism to disease development. A well-known example of maternal diet influencing epigenetic changes in the offspring is found in the viable yellow *Agouti* (A^{vy}) mouse model (91). The *agouti* gene encodes the agouti-signaling protein, which is responsible for distributing melanin pigment. During development, the *agouti* gene is expressed in the skin modulating hair color. In mice, the wild type *agouti* allele (*A*) produces a brown phenotype. The viable yellow mutation (A^{vy}) expression differs from the wild type because the *agouti* gene is ectopically expressed across all tissues during the lifespan of the mouse, not just during development. The A^{vy} metastable epiallele, an allele in which epigenetic regulation is established during early development and highly maintained throughout mitotic divisions, is formed from an insertion of an intracisternal A-particle (IAP) upstream of the transcription site (92). The methylation of the IAP influences the phenotype of the mouse. When the IAP is unmethylated, there is an increase in transcription of the *agouti* gene, resulting in mice with yellow fur that are obese, hyperinsulinemic, hyperglycemic, and have an increased risk of cancer (92). A fully methylated IAP produces healthy brown mice. The viable yellow *Agouti* (A^{vy}) mouse model has been used across multiple types of studies assessing how nutrition influences the offspring development. Maternal diets supplemented with methyl donors, such a folic acid, increase the methylation of the IAP insert in the *Agouti* (A^{vy}) gene, reducing its expression (91).

Alterations in maternal nutrition during gestation in the form of under- or over-nutrition, protein restriction, alterations in fat type, sugar content, and micronutrients have induced epigenetic changes in the offspring (93,94). Polyunsaturated fatty acids are thought to influence DNA methylation via directly influencing enzymes responsible for methylation and/or contributing to one carbon metabolism via choline from phosphatidylcholine. During pregnancy, clinical trials have supplemented polyunsaturated fatty acids finding conflicting results, potentially due to timing in gestation and cell-type analyzed (95,96). DNA methylation is dependent upon micronutrient intake providing substrates (folate, methionine, choline, and betaine) and co-factors (vitamins B12, B6, and B2) for one carbon metabolism (97). Additionally, maternal hyperglycemia (98) and body composition (99) have been analyzed for associations with infant DNA methylation.

Metabolomics provides an objective and quantifiable measurement of how the maternal environment influences the offspring epigenome. Previous work from our group (77) provided some of the first evidence for a relationship between specific metabolites in the maternal plasma across gestation with DNA methylation in umbilical cord blood leukocytes. The correlations were quantified between a targeted group of metabolites with global methylation (LINE-1) and methylation at candidate loci including *ESR1*, *PPARα*, *IGF2*, and *H19*, which have previously been associated with growth and future cardiovascular disease risk (100–102). The results revealed significant correlations of essential fatty acids, conditionally essential fatty acids, medium-chain acylcarnitines, and long-chain acylcarnitines in maternal first trimester and term blood with DNA methylation in infant cord blood at LINE1, *ESR1*, and *PPARα* (77). A recent study (103) assessed how the maternal lipidome at ~26 weeks gestation influences DNA methylation in umbilical cord blood cells. These results found that maternal phospholipids and

lysophospholipids were associated with methylation, suggesting the importance of that lipids fraction in establishing methylation patterns.

Mitochondrial Dysfunction in the Pathogenesis of Obesity and Metabolic Disease

Mitochondrial dysfunction has been identified as a key component in the pathogenesis of T2D as connections between the mitochondria and insulin resistance were first identified over 40 years ago (104). The mitochondria is the site for β-oxidation; the main pathway of fatty acid oxidation (105). This organelle produces the majority of a cell's ATP through the oxidation of glucose, amino acids, and fatty acids and oxidative phosphorylation in the electron transport chain within the mitochondrial matrix. As insulin is the predominant hormone involved in fuel metabolism, altered mitochondrial function has been discussed as the cause, the consequence, and a non-related correlation with insulin resistance (106–108).

To begin to understand the role of mitochondria in insulin resistance, it is necessary to consider how the mitochondria responds to different energy substrates. Humans possess the capability to oxidize carbohydrates and fat for energy production. Oxidation of each fuel does not occur in isolation, but rather, occurs simultaneously. There is a reciprocal relationship between the utilization of carbohydrates and fat (109). The steady-state of this relationship is dictated by (1) the fasted or fed state, (2) being at rest or during exercise, and (3) the availability of substrates. Being able to shift between oxidizing carbohydrates and fat is evolutionary advantageous for humans, allowing for the metabolic response to fluctuations in energy supply and demand.

The reciprocal relationship between carbohydrate and fat oxidation was established by Randle et al. in the 1960s (110). It was observed that in skeletal muscle, there is competition between selecting carbohydrates or fat for energy production in the fasted and fed states, dependent upon the presence of free fatty acids (110). These experiments found that elevated plasma free fatty

acids increased fatty acid oxidation and decreased glucose oxidation (110). During a fast, skeletal muscle in lean individuals relies mainly on lipid metabolism, as originally observed by Andres et al. (111). Later experiments identified that elevated fatty acid oxidation increased the production of acetyl-CoA, citrate, and glucose-6-phosphate, which reduced glucose oxidation via the inhibition of pyruvate dehydrogenase, phosphofructokinase, and hexokinase (112). In contrary, in the fed state when glucose availability increases, fatty acid oxidation is suppressed via the inhibition of carnitine palmitoyltransferase 1 (CPT1) by malonyl-CoA (113). The elegant transition between fatty acid and carbohydrate oxidation in the fasted and fed state is controlled by a variety of endocrine and metabolic signals (114).

In the fed state, metabolic adaptations must occur to respond to fluctuations in the supply of carbohydrates and fat to produce energy. An organism's ability to select fuel for energy production depending on environmental demand is defined as metabolic flexibility, coined by Kelley et al. in 1999 (115). Metabolic flexibility is related to the metabolic health of an organism. For instance, Kelley et al. observed differences in adaptations to fuel preference between obese individuals with insulin resistance and lean individuals in both the fasting state and after an insulin infusion (115). At rest during fasting, Kelley et al. found that obese individuals with insulin resistance have a lesser reliance on fatty acid oxidation than lean individuals. Upon insulin infusion, obese individuals with insulin resistance were not able to reduce fatty acid oxidation and did not increase glucose oxidation in comparison to lean individuals. Kelley classified obese individuals with insulin resistance as having a state of metabolic inflexibility (112).

In insulin resistance, skeletal muscle has an increase in fatty acid uptake (116) paired with a decreased mitochondrial oxidative capacity, measured by enzymatic activity (107,117,118) and

rates of fatty acid oxidation (119,120). In adults, these alterations leads to lipotoxicity and incomplete fatty acid oxidation with increases in acylcarnitine intermediates (121) and incompletely oxidized fatty acids (122,123). Levels of intramyocellular lipids are positively associated with worsening insulin resistance, independent of obesity (124) and observed in muscles of multiple fiber types (125). Incompletely oxidized fatty acids are partitioned towards the synthesis of other metabolites that have been linked to insulin signaling such as diacylglycerols, triglycerides, and ceramides (126). These lipids may impair insulin signaling through other mechanisms including activation of the diacylglycerol-protein kinase C pathway (126). Overall, the obese and insulin resistant state is marked by alterations in fuel selection, metabolic flexibility, and oxidative capacity.

Metabolite Biomarkers of Obesity and Insulin Resistance

Metabolomics has been used to identify biomarkers of obesity (127) and insulin resistance (128), increasing the understanding of the pathogenesis. Obesity and insulin resistance alter the oxidative capacity and metabolic fate of a subset of essential amino acids (129). Branched chain amino acids (BCAA), leucine, isoleucine, and valine, and their metabolites and carnitines esters are elevated with obesity, insulin resistance, and T2D, first demonstrated 50 years ago (130). Elevated plasma BCAAs are associated with an increased risk for T2D (131,132). Risk of becoming insulin resistant is increased with the presence of genetic polymorphisms near the *PPM2* gene (encoding for branched chain ketoacid dehydrogenase [BCKDH] phosphate), which alters BCAA metabolism (133). Individuals with insulin resistance have decreased BCAA catabolism in hepatocytes and adipocytes, leading to the accumulation of plasma BCAAs and their metabolites (134). Excess BCAAs may contribute to insulin resistance via activation of mTORC1 signaling, though this remains controversial (135). Additional amino acids that are

elevated with obesity and insulin resistance include sulfur-containing methionine and cysteine (136,137) and the aromatic amino acids tyrosine and phenylalanine (130,137).

Metabolomics analyses have revealed significant associations between fatty acid oxidation intermediates, such as acylcarnitines, and insulin resistance. The carnitine shuttle transports fatty acyl-CoAs into the mitochondria via their carnitine ester through carnitine palmitoyltransferase 1 (CPT1), which regulates fatty acid oxidation flux (138). Once inside the inner mitochondrial membrane, carnitine palmitoyltransferase 2 (CPT2) transports the acylcarnitine into the mitochondrial matrix converting it back to free carnitine and the fatty acyl-CoA. In adults with obesity and insulin resistance, there is an imbalance between entry of acyl-CoA into the mitochondria and fatty acid oxidation rates, resulting in elevated acylcarnitines (121) and incompletely oxidized FA (122,123). Skeletal muscle insulin resistance is associated with increased acylcarnitine accumulation in the muscle or circulation (123,139). These results lead to the hypothesis that if fatty acid oxidation rates outpace the TCA cycle, there will be an accumulation of fatty acid oxidation intermediates, which may influence insulin resistance.

Risk of adult obesity and insulin resistance will be classified during adolescence; a period physical transition marked by the onset of puberty. Pediatric studies highlight differences in the fluctuations of the metabolome with obesity and insulin resistance compared to adults. BCAAs and their short-chain acylcarnitine metabolites, propionylcarnitine and butyrylcarnitine, have been consistently increased in obese adolescents (140–142). However, studies are inconsistent regarding the relationship between BCAA and insulin resistance in adolescents with findings reporting positive associations (140–142), inverse associations (143), and sex differences (144–146) which may be due to differences in analytical methodologies as well as the variability in the size and characteristic in study populations. Some metabolomics analyses in youth have also

identified divergent associations of metabolite levels and metabolic phenotypes compared to those observed in adults. In contrast to adults, free fatty acids were not associated with BMI or insulin resistance at 15 years of age (147,148). Additionally, lower levels of fatty acid oxidation intermediates, such as dicarboxylic fatty acids (141) and medium chain acylcarnitines (143), were reported in children with T2D and obesity. These results suggest less imbalance in the delivery and oxidation of substrates in these individuals, perhaps due to the increased substrate utilization to fuel tissue and linear growth in the pubertal period. Sex differences may be explained by changes in muscle and fat mass accompanied by puberty.

Specific Aims and Hypotheses

The Developmental Origins of Health and Disease hypothesis suggests that exposures during sensitive periods of development have the potential to cause permanent changes in metabolic pathways increasing the risk of obesity and insulin resistance (149). **The aim of this dissertation was to classify the metabolic environment using metabolomics during sensitive periods of early development to identify alterations in the risk of developing obesity, insulin resistance, and metabolic diseases.** Our goal was to define the potential metabolite mediators that are associated with alterations in metabolism arising during fetal development that persist into adolescence. To achieve this goal, we determined the metabolome's relationship to the development and metabolic state of infants and adolescents through the following Specific Aims:

SPECIFIC AIM 1: Determine the dynamic changes in the maternal lipidome during pregnancy and identify maternal nutrient exposures that are critical for the modulation of birthweight and the umbilical cord blood lipidome using the Michigan Mother-Infant Pairs cohort. To determine the timing and effect of maternal nutrients on offspring development, untargeted lipidomics profiling of mother-infant dyads was performed in plasma samples collected from maternal first trimester (M1) and delivery (M3) and infant umbilical cord blood plasma (CB). Fluctuations in the metabolome across pregnancy were identified, inferring the role of placenta transport proteins. We classified maternal and CB lipids associated with maternal characteristics and infant birth weight, considering sex differences. We identified maternal lipids that may modulate the CB lipidome that is related to birth weight.

SPECIFIC AIM 2: Investigate how the maternal lipidome relates to infant DNA methylation patterns to understand how nutrient exposures influence epigenetic programming. DNA methylation in CB leukocytes was assessed using the Infinium

MethylationEPIC (EPIC) bead array. Using empirical Bayes modeling, we analyzed how the maternal lipidome (M1 and M3) influences infant DNA methylation, highlighting differential methylation in genes associated with lipid metabolism and adiposity.

SPECIFIC AIM 3: Expand on the relationship between the metabolome with obesity and insulin resistance during the pubertal period, defining sex-specific alterations using the Early Life Exposure in Mexico to ENvironmental Toxicants cohort. To assess the metabolite alterations that are related to metabolic health, untargeted metabolomics profiling of adolescents was performed using serum samples. Using linear models, the relationship between the metabolome with obesity and insulin resistance was quantified, assessing sex-specific alterations given differences in pubertal hormones and the accumulation of muscle and fat tissue. We determined if recalled dietary intake could provide additional information on the underlying difference in metabolism that leads to insulin resistance.

After the completion of these studies, we have developed an initial model for how intrauterine exposure can lead to altered metabolism in later life. Confirmation that specific metabolite patterns are associated with postnatal risk for metabolic disease, we may have the opportunity to modify intrauterine nutrient exposure through diet to modulate the long-term risks of the offspring

Figure 1.1. Study Objective. Classification of the metabolic environment during sensitive periods of development to identify alterations in the risk of developing obesity, type 2 diabetes, and metabolic diseases.

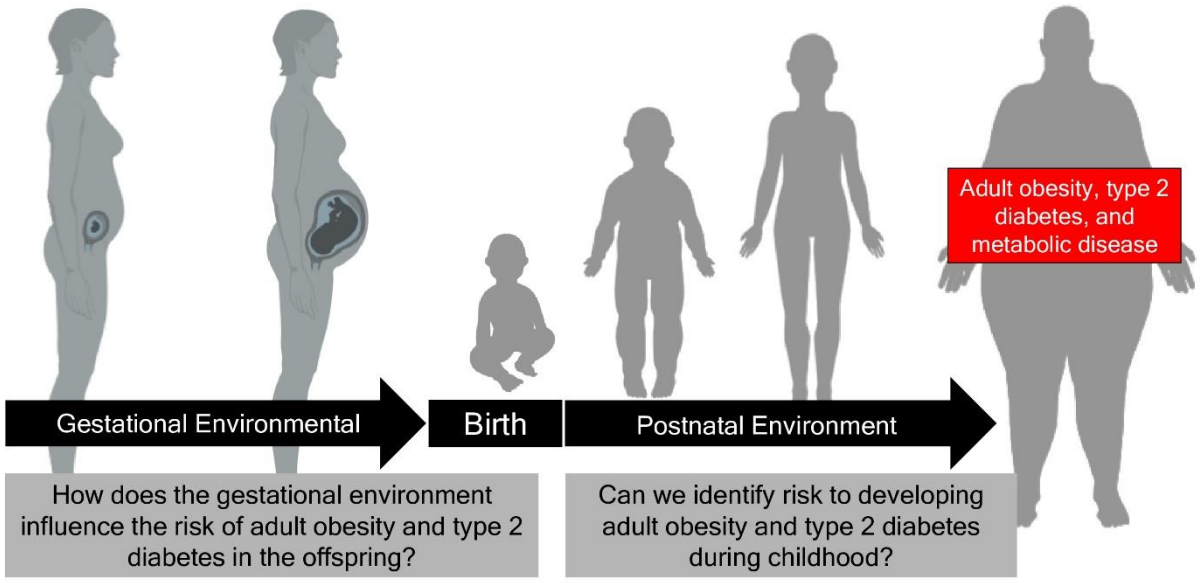

Figure 1.2. Study cohort. To classify the metabolic environment during development, we will incorporate untargeted metabolomics and lipidomics techniques to two human cohorts; the Michigan Mother-Infant Pairs (MMIP) cohort and the Early Life Exposure in Mexico to ENvironmental Toxicants (ELEMENT) cohort. The novelty of this dissertation is the incorporation of multiple metabolome measurements with the epigenome to gain a broader understanding of a biological system.

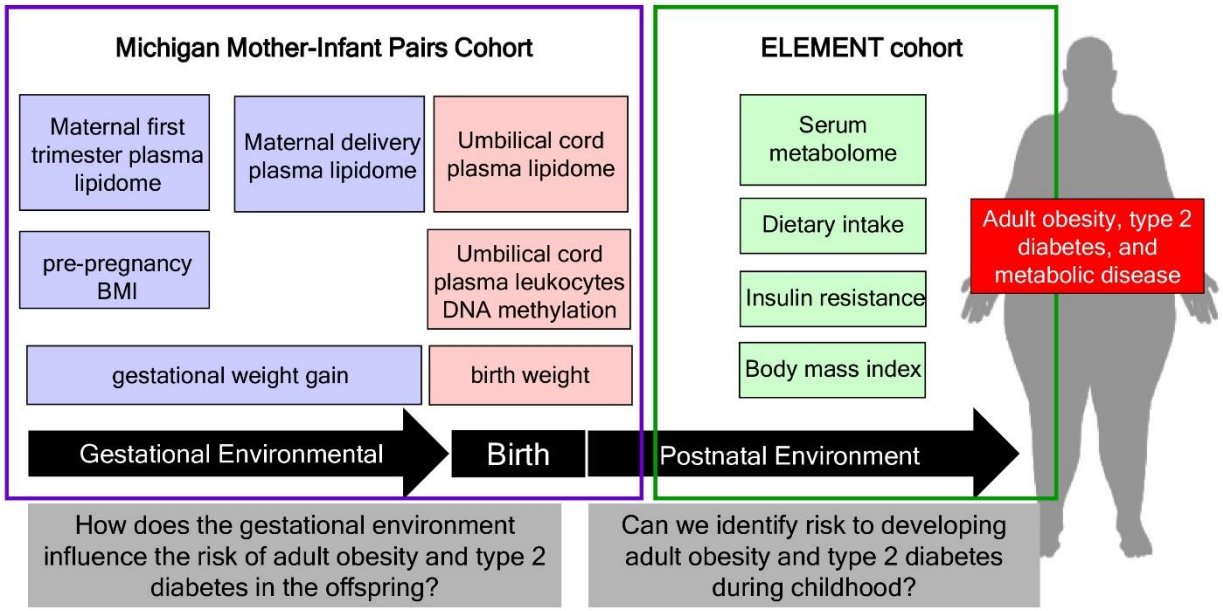

References

1. World Health Organization. Obesity and Overweight 2018. 2018;
2. NCHS, National Health and Nutrition Examination Survey, 2015–2016.
3. Ng M, Fleming T, Robinson M, Thomson B, Graetz N, Margono C, Mullany EC, Biryukov S, Abbafati C, Abera SF, et al. Global, regional, and national prevalence of overweight and obesity in children and adults during 1980-2013: A systematic analysis for the Global Burden of Disease Study 2013. Lancet. 2014;384:766–81.
4. Wang Y, Beydoun MA. The Obesity Epidemic in the United States—Gender, Age, Socioeconomic, Racial/Ethnic, and Geographic Characteristics: A Systematic Review and Meta-Regression Analysis. Epidemiol Rev. 2007;29:6–28.
5. Mcallister EJ, Dhurandhar N V, Keith SW, Aronne LJ, Barger J, Baskin M, Benca RM, Biggio J, Boggiano MM, Eisenmann JC, et al. Ten putative contributors to the obesity epidemic. Crit Rev Food Sci Nutr. 2009;49:868–913.
6. Andersen MK, Sandholt CH. Recent Progress in the Understanding of Obesity: Contributions of Genome-Wide Association Studies. Curr Obes Rep. 2015;4:401–10.
7. Stunkard AJ, Harris JR, Pedersen NL, McClearn GE. The body-mass index of twins who have been reared apart. N Engl J Med. 1990;322:1483–7.
8. Maes HHM, Neale MC, Eaves LJ. Genetic and Environmental Factors in Relative Body Weight and Human Adiposity. Behav Genet. 1997;27:325–51.
9. Collaboration NRF. Worldwide trends in diabetes since 1980: a pooled analysis of 751 population-based studies with 4.4 million participants. Lancet. NCD Risk Factor Collaboration. Open Access article distributed under the terms of CC BY; 2016;387:1513–30.
10. Bommer C, Sagalova V, Heesemann E, Manne-goehler J, Atun R, Barnighausen T, Davies J, Vollmer S. Global Economic Burden of Diabetes in Adults: Projections From 2015 to 2030. Diabetes Care. 2018;41:963–70.
11. Colditz GA, Willett WC, Rotnitzky A, Manson JE. Weight gain as a risk factor for clinical diabetes mellitus in women. Ann Intern Med. 1995;122:481–6.
12. Hardy OT, Czech MP, Corvera S. What causes the insulin resistance underlying obesity? Curr Opin Endocrinol Diabetes Obes. 2012;19:81–7.
13. Vasan SK, Osmond C, Canoy D, Christodoulides C, Neville MJ, Gravio C Di, Fall C, Karpe F. Comparison of regional fat measurements by dual-energy X-ray absorptiometry and conventional anthropometry and their association with markers of diabetes and cardiovascular disease risk. Int J Obes. Nature Publishing Group; 2018;42:850–7.
14. Meyts P. The Insulin Receptor and Its Signal Transduction Network. Feingold K, Anawalt B, Boyce A, editors. Endotext; 2016.
15. Defronzo RA. Banting Lecture. From the triumvirate to the ominous octet: a new

paradigm for the treatment of type 2 diabetes mellitus. Diabetes. 2009;58:773–95.

16. Lawlor N, Stitzel ML. (Epi)genomic heterogeneity of pancreatic islet function and failure in type 2 diabetes. Mol Metab [Internet]. Elsevier GmbH; 2019;27:S15–24. Available from: https://doi.org/10.1016/j.molmet.2019.06.002

17. Reaven GM. Banting Lecture 1988 Role of Insulin Resistance in Human. Diabetes. 1988;37:1595–607.

18. Ralph A, Tobin JD. Glucose clamp technique: a method for quantifying insulin secretion and resistance. Am J Physiol. 2019;237:E214-23.

19. Petersen MC, Shulman GI. Mechanisms of Insulin Action and Insulin Resistance. Physiol Rev. 2018;98:2133–223.

20. Barker DJP. The origins of the developmental origins theory. J Intern Med. 2007;261:412–7.

21. Barker DJP, Osmond C. Infant mortality, childhood nutrition, and ischaemic heart disease in England and Wales. Lancet. 1986;1:1077–87.

22. Barker DJP, Winter PD, Osmond C, Margetts B, Simmonds SJ. Weight in infancy and death from ischaemic heart disease. Lancet. 1989;2:577–80.

23. Barker DJP, Gluckman PD, Godfrey KM, Harding J, Owens J, Robinson J. Fetal nutrition and cardiovascular disease in adult life. Lancet. 1993;341:938–41.

24. Bateson P, Barker D, Clutton-brock T, Deb D, D'Udine BD, Foley RA, Gluckman P, Godfrey K, Kirkwood T, Lahr M, et al. Developmental plasticity and human health. Nature. 2004;430:419–21.

25. Pettitt DJ, Jovanovic L. Birth weight as a predictor of type 2 diabetes mellitus: the U-shaped curve. Curr Diab Rep. 2001;1:78–81.

26. Barker DJP, Eriksson JG, Forsén T, Osmond C. Fetal origins of adult disease: Strength of effects and biological basis. Int J Epidemiol. 2002;31:1235–9.

27. Walton A, Hammond J. The maternal effects on growth and conformation in Shire horse-Shetland pony crosses. Proc R Soc B Biol Sci. 1938;125:311–35.

28. Dohad D, Past C, Gluckman PD, Buklijas T, Hanson MA. The Epigenome and Developmental Origins of Health and Disease. 2016. 1–15 p.

29. Schulz LC. The Dutch Hunger Winter and the developmental origins of health and disease. Proc Natl Acad Sci U S A. 2010;107:16757–8.

30. Lumey LH, Stein AD, Susser E. Prenatal Famine and Adult Health. Annu Rev Public Heal. 2011;32:211–20.

31. Sun C, Burgner DP, Ponsonby A-L, Saffery R, Huang R-C, Vuillermin PJ, Cheung M, Craig JM. Effects of early-life environment and epigenetics on cardiovascular disease risk in children: highlighting the role of twin studies. Pediatr Res. 2013;73:523–30.

32. Susser M, Stein Z. Timing in Prenatal Nutrition: A Reprise of the Dutch Famine Study.

Nutr Rev. 1994;52:84–94.

33. Ravelli ACJ, Meulen JHP Van Der, Michels RPJ, Osmond C, Barker DJP, Hales CN, Bleker OP. Glucose tolerance in adults after prenatal exposure to famine. Lancet. 1998;351:173–7.

34. Tobi EW, Goeman JJ, Monajemi R, Gu H, Putter H, Zhang Y, Slieker RC, Stok AP, Thijssen PE, Müller F, et al. DNA methylation signatures link prenatal famine exposure to growth and metabolism. Nat Commun. 2014;5.

35. Wang J, Li Y, Han X, Liu B, Hu H, Wang F, Li X, Yang K, Yuan J, Yao P, et al. Exposure to the Chinese Famine in Childhood Increases Type 2 Diabetes Risk in Adults. J Nutr. 2016;146:2289–95.

36. Huang C, Li Z, Wang M, Martorell R. Early life exposure to the 1959-1961 Chinese famine has long-term health consequences. J Nutr. 2010;140:1874–8.

37. Kereliuk SM, Brawerman GM, Dolinsky VW. Maternal Macronutrient Consumption and the Developmental Origins of Metabolic Disease in the Offspring. Int J Mol Sci. 2017;18:1–27.

38. Mennitti L V., Oliveira JL, Morais CA, Estadella D, Oyama LM, Oller do Nascimento CM, Pisani LP. Type of fatty acids in maternal diets during pregnancy and/or lactation and metabolic consequences of the offspring. J Nutr Biochem [Internet]. Elsevier Inc.; 2015;26:99–111. Available from: http://dx.doi.org/10.1016/j.jnutbio.2014.10.001

39. de Brito Alves J, de Oliveira J, Ferreira D, Barros M, Noqueira V, Alves D, Vidal H, Leandro C, Laqranha C, Pirola L, et al. Maternal protein restriction induced-hypertension is associated to oxidative disruption at transcriptional and functional levels in the medulla oblongata. Clin Exp Pharmacol Physiol. 2016;43:1177–84.

40. Chen J, Martin-gronert MS, Tarry-adkins J, Ozanne SE. Maternal Protein Restriction Affects Postnatal Growth and the Expression of Key Proteins Involved in Lifespan Regulation in Mice. PLoS One. 2009;4:1–7.

41. Haider B, Bhutta Z. Multiple-micronutrient supplementation for women during pregnancy. Cochrane Database Syst Rev. 2017;

42. Pannia E, Cho CE, Kubant R, Diana S, Huot PSP, Anderson GH. Role of maternal vitamins in programming health and chronic disease. Nutr Rev. 2016;74:166–80.

43. Nicholas LM, Morrison JL, Rattanatray L, Zhang S, Ozanne SE, Mcmillen IC. The early origins of obesity and insulin resistance: timing, programming and mechanisms. Int J Obes [Internet]. Nature Publishing Group; 2016;40:229–38. Available from: http://dx.doi.org/10.1038/ijo.2015.178

44. Group LP-MO and COS. Association of Gestational Weight Gain With Adverse Maternal and Infant Outcomes. JAMA. 2019;321:1702–15.

45. Rasmussen KM, Yaktine AL, Guidelines PW, Board N. Weight Gain During Pregnancy: Reexamining the Guidelines [Internet]. 2009. Available from: http://www.nap.edu/catalog/12584

46. Tam CHT, Ma RCW, Yuen LY, Ozaki R, Li AM, Hou Y, Chan MHM, Ho CS, Yang X, Chan JCN, et al. The impact of maternal gestational weight gain on cardiometabolic risk factors in children. Diabetologia. Diabetologia; 2018;61:2539–48.

47. Bennett P, Rushforth N, Miller M, LeCompte P. Epidemiologic studies of diabetes in the Pima Indians. Recent Prog Horm Res. 1976;32:333–76.

48. Pettitt DJ, Baird H, Aleck K, Bennett PH, Knowler WC. Excessive obesity in offspring of Pima Indian women with diabetes during pregnancy. N Engl J Med. 1983;308:242–5.

49. Pettitt DJ, Knowler WC, Bennett PH, Aleck KA, Baird HR. Obesity in offspring of diabetic Pima Indian women despite normal birth weight. Diabete Care. 1987;10:76–80.

50. Group HSCR. The Hyperglycemia and Adverse Pregnancy Outcome (HAPO) Study. Int J Gynaecol Obstet. 2002;78:69–77.

51. The HAPO Study Cooperative Research Group. Hyperglycemia and adverse pregnancy outcomes. N Engl J Med. 2008;358:1991–2002.

52. HAPO Follow-up Study Coorperative Research Group. Maternal glucose levels during pregnancy and childhood adiposity in the Hyperglycemia and Adverse Pregnancy Outcome Follow-up Study. Diabetologia. 2019;62:598–610.

53. Lowe WL, Scholtens DM, Kuang A, Linder B, Lawrence JM, Lebenthal Y, Mccance D, Hamilton J, Nodzenski M, Talbot O, et al. Hyperglycemia and Adverse Pregnancy Outcome Follow-up Study (HAPO FUS): Maternal Gestational Diabetes Mellitus and Childhood Glucose Metabolism. Diabetes Care. 2019;42:372–80.

54. Pinu FR, Beale DJ, Paten AM, Kouremenos K, Swarup S, Schirra HJ, Wishart D. Systems biology and multi-omics integration: Viewpoints from the metabolomics research community. Metabolites. 2019;9:1–31.

55. Chaleckis R, Murakami I, Takada J, Kondoh H, Yanagida M. Individual variability in human blood metabolites identifies age-related differences. Proc Natl Acad Sci U S A. 2016;113:4252–9.

56. Brennan L, Hu FB. Metabolomics Based Dietary Biomarkers in Nutritional Epidemiology- Current Status and Future Opportunities. Mol Nutr Food Res [Internet]. 2018;1701064. Available from: http://doi.wiley.com/10.1002/mnfr.201701064

57. Heinemann M, Zenobi R. Single cell metabolomics. Curr Opin Biotechnol. Elsevier Ltd; 2011;22:26–31.

58. Yu Z, Kastenmüller G, He Y, Belcredi P, Möller G, Prehn C, Mendes J, Wahl S, Roemisch-Margl W, Ceglarek U, et al. Differences between human plasma and serum metabolite profiles. PLoS One. 2011;6:1–6.

59. Wishart DS, Feunang YD, Marcu A, Guo AC, Liang K, Vázquez-Fresno R, Sajed T, Johnson D, Li C, Karu N, et al. HMDB 4.0: The human metabolome database for 2018. Nucleic Acids Res. 2018;46:D608–17.

60. Kanehisa M, Sato Y, Kawashima M, Furumichi M, Tanabe M. KEGG as a reference

resource for gene and protein annotation. Nucleic Acids Res. 2016;44:457–62.

61. Fahy E, Sud M, Cotter D, Subramaniam S. LIPID MAPS online tools for lipid research. Nucleic Acids Res. 2007;35:606–12.

62. Guijas C, Montenegro-Burke JR, Domingo-Almenara X, Palermo A, Warth B, Hermann G, Koellensperger G, Huan T, Uritboonthai W, Aisporna AE, et al. METLIN: A Technology Platform for Identifying Knowns and Unknowns. Anal Chem. 2018;90:3156–64.

63. Quehenberger O, Dennis EA. The human plasma lipidome. N Engl J Med. 2011;365:1812–23.

64. Reiner Ž. Hypertriglyceridaemia and risk of coronary artery disease. Nat Publ Gr. Nature Publishing Group; 2017;14:401–11.

65. Vance JE. Phospholipid Synthesis and Transport in Mammalian Cells. Traffic. 2015;16:1–18.

66. Nagan N, Zoeller RA. Plasmalogens: Biosynthesis and functions. Prog Lipid Res. 2001;40:199–229.

67. Sugiura K, Soga WN, Nitta H, Waku K. Occurrence of Alkyl Ether Phospholipids in Rabbit Platelets: Compositions and Fatty Chain Profiles. J Biochem. 1983;94:1719–22.

68. Lindsay KL, Hellmuth C, Uhl O, Buss C, Wadhwa PD, Koletzko B, Entringer S. Longitudinal metabolomic profiling of amino acids and lipids across healthy pregnancy. PLoS One. 2015;10:e0145794.

69. Pinto J, Barros S, Rosa M, Domingues M, Goodfellow BJ, Galhano E, Pita C, Ceu Almeida M do, Carreira IM, Gil AM. Following Healthy Pregnancy by NMR Metabolomics of Plasma and Correlation to Urine. J Proteome Res. 2015;14:1263–74.

70. Luan H, Meng N, Liu P, Feng Q, Lin S, Fu J, Davidson R, Chen X, Rao W, Chen F, et al. Pregnancy-Induced Metabolic Phenotype Variations in Maternal Plasma. J Proteome Res. 2014;13:1527–36.

71. Hellmuth C, Lindsay KL, Uhl O, Buss C, Wadhwa PD, Koletzko B, Entringer S. Association of maternal pre-pregnancy BMI with metabolomic profile across gestation. Int J Obes. Nature Publishing Group; 2017;41:159–69.

72. Sandler V, Reisetter AC, Bain JR, Muehlbauer MJ, Nodzenski M, Stevens RD, Ilkayeva O, Lowe LP, Metzger BE, Newgard CB, et al. Associations of maternal BMI and insulin resistance with the maternal metabolome and newborn outcomes. Diabetologia. Diabetologia; 2016;60:518–30.

73. Desert R, Canlet C, Costet N, Cordier S, Bonvallot N. Impact of maternal obesity on the metabolic profiles of pregnant women and their offspring at birth. Metabolomics. Springer US; 2015;11:1896–907.

74. Scholtens DM, Bain JR, Reisetter AC, Muehlbauer MJ, Nodzenski M, Stevens RD, Ilkayeva O, Lowe LP, Metzger BE, Newgard CB, et al. Metabolic networks and

metabolites underlie associations between maternal glucose during pregnancy and newborn size at birth. Diabetes. 2016;65:2039–50.

75. Scholtens DM, Muehlbauer MJ, Daya NR, Stevens RD, Dyer AR, Lowe LP. Metabolomics reveals broad-scale metabolic perturbations in hyperglycemic mothers during pregnancy. Diabetes Care [Internet]. 2014;37. Available from: https://doi.org/10.2337/dc13-0989

76. Maitre L, Villanueva CM, Lewis MR, Ibarluzea J, Santa-Marina L, Vrijheid M, Sunyer J, Coen M, Toledano MB. Maternal urinary metabolic signatures of fetal growth and associated clinical and environmental factors in the INMA study. BMC Med. BMC Medicine; 2016;14:1–12.

77. Marchlewicz EH, Dolinoy DC, Tang L, Milewski S, Jones TR, Goodrich JM, Soni T, Domino SE, Song PXK, Burant CF, et al. Lipid metabolism is associated with developmental epigenetic programming. Sci Rep. Nature Publishing Group; 2016;6:1–13.

78. Hellmuth C, Lindsay KL, Uhl O, Buss C, Wadhwa PD, Koletzko B, Entringer S. Maternal Metabolomic Profile and Fetal Programming of Offspring Adiposity: Identification of Potentially Protective Lipid Metabolites. Mol Nutr Food Res. 2019;63:e1700889.

79. Scholtens DM, Muehlbauer MJ, Daya NR, Stevens RD, Dyer AR, Lowe LP, Metzger BE, Newgard CB, Bain JR, Lowe WL. Metabolomics reveals broad-scale metabolic perturbations in hyperglycemic mothers during pregnancy. Diabetes Care. 2013;37:158–66.

80. Perng W, Rifas-Shiman SL, McCulloch S, Chatzi L, Mantzoros C, Hivert MF, Oken E. Associations of cord blood metabolites with perinatal characteristics, newborn anthropometry, and cord blood hormones in project viva. Metabolism. Elsevier Inc.; 2017;76:11–22.

81. Lowe WL, Bain JR, Nodzenski M, Reisetter AC, Muehlbauer MJ, Stevens RD, Ilkayeva OR, Lowe LP, Metzger BE, Newgard CB, et al. Maternal BMI and glycemia impact the fetal metabolome. Diabetes Care. 2017;40:902–10.

82. Robinson O, Keski-Rahkonen P, Chatzi L, Kogevinas M, Nawrot T, Pizzi C, Plusquin M, Richiardi L, Robinot N, Sunyer J, et al. Cord Blood Metabolic Signatures of Birth Weight: A Population-Based Study. J Proteome Res. 2018;17:1235–47.

83. Patel N, Hellmuth C, Uhl O, Godfrey K, Briley A, Welsh P, Pasupathy D, Seed P, Koletzko B, Poston L, et al. Cord Metabolic Profiles In Obese Pregnant Women; Insights Into Offspring Growth And Body Composition. J Clin Endocrinol Metab. 2017;103:346–55.

84. Hellmuth C, Uhl O, Standl M, Demmelmair H, Heinrich J, Koletzko B, Thiering E. Cord Blood Metabolome Is Highly Associated with Birth Weight, but Less Predictive for Later Weight Development. Eur J Obes. 2017;10:85–100.

85. Lu Y-P, Reichetzeder C, Prehn C, Yin L-H, Yun C, Zeng S, Chu C, Adamski J, Hocher B. Cord Blood Lysophosphatidylcholine 16:1 is Positively Associated with Birth Weight. Cell Physiol Biochem. 2018;45:614–24.

86. Gluckman P, Hanson M, Cooper C, Thornburg KL. Effect of In Utero and Early-Life Conditions on Adult Health and Disease. N Engl J Med. 2008;359:61–73.

87. Gu J, Stevens M, Xing X, Li D, Zhang B, Payton JE, Oltz EM, Jarvis JN, Jiang K, Cicero T, et al. Mapping of Variable DNA Methylation Across Multiple Cell Types Defines a Dynamic Regulatory Landscape of the Human Genome. G3. 2016;6:973–86.

88. Jirtle RL, Skinner MK. Environmental epigenomics and disease susceptibility. Nat Rev Genet. 2007;8:253–62.

89. Morgan H, Santos F, Green K, Dean W, Reik W. Epigenetic reprogramming in mammals. Hum Mol Genet. 2005;14:R47-58.

90. Dolinoy DC, Das R, Weidman JR, Jirtle RL. Metastable epialleles, imprinting, and the fetal origins of adult diseases. Pediatr Res. 2007;61:30R-37R.

91. Dolinoy DC. The agouti mouse model: an epigenetic biosensor for nutritional and environmental alterations on the fetal epigenome. Nutr Rev. 2008;66:S7-11.

92. Bernal AJ, Jirtle RL. Epigenomic Disruption: The Effects of Early Developmental Exposures. Birth Defects Res Part A Clin Mol Teratol. 2010;88:938–44.

93. Jimenez-Chillaron J, Diaz R, Martinez D, Pentinat T, Ramon-Krauel M, Ribo S, Plosch T. The role of nutrition on epigenetic modifications and their implications on health. Biochimie. 2012;94:2242–63.

94. James P, Sajjadi S, Tomar AS, Saffari A, Fall CHD, Prentice AM, Shrestha S, Issarapu P, Yadav DK, Kaur L, et al. Candidate genes linking maternal nutrient exposure to offspring health via DNA methylation: a review of existing evidence in humans with specific focus on one-carbon metabolism. Int J Epidemiol. 2018;47:1910–37.

95. Amarasekera M, Noakes P, Strickland D, Saffery R, Martino DJ, Prescott SL. Epigenome-wide analysis of neonatal CD4(+) T-cell DNA methylation sites potentially affected by maternal fish oil supplementation. Epigenetics. 2014;9:1570–6.

96. Dijk SJ Van, Zhou J, Peters TJ, Buckley M, Sutcliffe B, Oytam Y, Gibson RA, Mcphee A, Yelland LN, Makrides M, et al. Effect of prenatal DHA supplementation on the infant epigenome: results from a randomized controlled trial. Clin Epigenetics. Clinical Epigenetics; 2016;8:1–13.

97. Anderson OS, Sant KE, Dolinoy DC. Nutrition and epigenetics: An interplay of dietary methyl donors, one-carbon metabolism and DNA methylation. J Nutr Biochem [Internet]. Elsevier Inc.; 2012;23:853–9. Available from: http://dx.doi.org/10.1016/j.jnutbio.2012.03.003

98. Hajj N El, Schneider E, Lehnen H, Haaf T. Epigenetics and life-long consequences of an adverse nutritional and diabetic intrauterine environment. Reproduction. 2014;148:R111–20.

99. Sharp GC, Lawlor DA, Richmond RC, Fraser A, Simpkin A, Suderman M, Shihab HA, Lyttleton O, McArdle W, Ring SM, et al. Maternal pre-pregnancy BMI and gestational weight gain, offspring DNA methylation and later offspring adiposity: Findings from the

Avon Longitudinal Study of Parents and Children. Int J Epidemiol. 2015;44:1288–304.

100. Haggarty P, Hoad G, Horgan GW, Campbell DM. DNA Methyltransferase Candidate Polymorphisms, Imprinting Methylation, and Birth Outcome. PLoS One. 2013;8:1–8.

101. Tabano S, Colapietro P, Cetin I, Grati FR, Zanutto S, Mandò C, Antonazzo P, Pileri P, Rossella F, Larizza L, et al. Epigenetic modulation of the IGF2/H19 imprinted domain in human embryonic and extra-embryonic compartments and its possible role in fetal growth restriction. Epigenetics. 2010;5:313–24.

102. Sébert SP, Lecannu G, Kozlowski F, Siliart B, Bard JM, Krempf M, Champ MM-J. Childhood obesity and insulin resistance in a Yucatan mini-piglet model: putative roles of IGF-1 and muscle PPARs in adipose tissue activity and development. Int J Obes. 2005;29:324–33.

103. Tindula G, Lee D, Huen K, Bradman A, Eskenazi B, Holland N. Pregnancy lipidomic profiles and DNA methylation in newborns from the CHAMACOS cohort. Environ Epigenetics. 2019;5:1–11.

104. Yamada T, Ida T, Yamaoka Y, Ozawa K, Takasan H, Honjo I. Two distinct patterns of glucose intolerance in icteric rats and rabbits. Relationship to impaired liver mitochondria function. Transl Res. 1975;86:38–45.

105. Kunau W, Dommes V, Schulz H. Beta-oxidation of fatty acids in mitochondria, peroxisomes, and bacteria: a century of continued progress. Prog Lipid Res. 1995;34:267–342.

106. Boushel R, Gnaiger E, Schjerling P, Skovbro M, Kraunsoe R, Dela F. Patients with type 2 diabetes have normal mitochondrial function in skeletal muscle. Diabetologia. 2007;50:790–6.

107. Kelley DE, He J, Menshikova E V, Ritov VB. Dysfunction of Mitochondria in Human Skeletal Muscle in Type 2 Diabetes. 2002;51.

108. Petersen KF, Dufour S, Befroy D, Garcia R, Shulman GI. Impaired Mitochondrial Activity in the Insulin-Resistant Offspring of Patients with Type 2 Diabetes. N Engl J Med. 2004;350:664–71.

109. Spriet LL. New Insights into the Interaction of Carbohydrate and Fat Metabolism During Exercise. Sport Med. 2014;44:S87-96.

110. Randle PJ, Garland PB, Hales CN, Newsholme EA. the Glucose Fatty-Acid Cycle Its Role in Insulin Sensitivity and the Metabolic Disturbances of Diabetes Mellitus. Lancet. 1963;281:785–9.

111. Andres R, Cader G, Zierler KL, Andres R, Cader G, Zierler KL. The quantitatively minor role of carbohydrate in oxidative metabolism by skeletal muscle in intact man in the basal state; measurements of oxygen and glucose uptake and carbon dioxide and lactate production in the forearm. J Clin Invest. 1956;35:671–82.

112. Kelley DE, Mandarin LJ, Mandarino LJ. Fuel selection in human skeletal muscle in insulin resistance: a reexamination. Diabetes [Internet]. 2000;49:677–83. Available from:

10905472

113. Winder WW, Arogyasami J, Elayan M, Cartmill D. Time course of exercise-induced decline in malonyl-CoA in different muscle types. Am J Physiol. 1990;259:E266-71.

114. Smith RL, Soeters MR, Wust RC, Houtkooper RH. Metabolic Flexibility as an Adaptation to Energy Resources and Requirements in Health and Disease. Endocr Rev. 2018;39:489–517.

115. Kelley DE, Goodpaster B, Wing RR, Simoneau J. Skeletal muscle fatty acid metabolism in association with insulin resistance, obesity, and weight loss. Am J Clin Nutr. 1999;277:E1130-41.

116. Bonen A, Parolin ML, Steinberg GR, Calles-escandon J, Tandon N, Glatz J, Luiken J, Heigenhauser G, Dyck DJ. Triacylglycerol accumulation in human obesity and type 2 diabetes is associated with increased rates of skeletal muscle fatty acid transport and increased sarcolemmal FAT/CD36. FASEB J. 2004;18:1144–66.

117. Simoneau J-A, Kelley DE. Altered glycolytic and oxidative capacities of skeletal muscle contribute to insulin resistance in NIDDM. J Appl Physiol. 1997;83:166–71.

118. He J, Watkins S, Kelley DE. Skeletal Muscle Lipid Content and Oxidative Enzyme Activity in Relation to Muscle Fiber Type in Type 2 Diabetes and Obesity. Diabetes. 2001;50:817–23.

119. Simoneau J-A, Veerkamp JH, Turcotte LP, Kelley DE. Markers of capacity to utilize fatty acids in human skeletal muscle: relation to insulin resistance and obesity and effects of weight loss. FASEB J. 1999;13:2051–60.

120. Lowell BB, Shulman GI. Mitochondrial Dysfunction and Type 2 Diabetes. Science (80-). 2005;307:384–7.

121. Ribel-madsen A, Ribel-madsen R, Brøns C, Newgard CB, Vaag AA, Hellgren LI. Plasma acylcarnitine profiling indicates increased fatty acid oxidation relative to tricarboxylic acid cycle capacity in young , healthy low birth weight men. Physiol Rep. 2016;4:e12977.

122. Mihalik SJ, Goodpaster BH, Kelley DE, Chace DH, Vockley J, Toledo FGS, DeLany JP. Increased Levels of Plasma Acylcarnitines in Obesity and Type 2 Diabetes and Identification of a Marker of Glucolipotoxicity. Obesity. 2010;18:1695–700.

123. Koves TR, Ussher JR, Noland RC, Slentz D, Mosedale M, Ilkayeva O, Bain J, Stevens R, Dyck JRB, Newgard CB, et al. Mitochondrial Overload and Incomplete Fatty Acid Oxidation Contribute to Skeletal Muscle Insulin Resistance. Cell Metab. 2008;7:45–56.

124. Jacob S, Machann J, Rett K, Brechtel K, Volk A, Renn W, Maerker E, Matthaei S, Schick F, Claussen C, et al. Association of Increased Intramyocellular Lipid Content With Insulin Resistance in Lean Nondiabetic Offspring of Type 2 Diabetic Subjects. Diabetes. 1999;48:1113–9.

125. Malenfant P, Joanisse D, Theriault R, Goodpaster B, Kelley D, Simoneau J-A. Fat content in individual muscle fibers of lean and obese subjects. Int J Obes. 2001;25:1316–21.

126. Morino K, Petersen KF, Shulman GI. Molecular mechanisms of insulin resistance in humans and their potential links with mitochondrial dysfunction. Diabetes. 2006;55:S9–15.

127. Rangel-Huerta O-D, Pastor-Villaescusa B, Gil A. Are we close to defining a metabolomic signature of human obesity? A systematic review of metabolomics studies. Metabolomics. Springer US; 2019;15:1–31.

128. Pallares-méndez R, Aguilar-salinas CA, Cruz-bautista I, Bosque-plata L del. Metabolomics in diabetes, a review. Ann Med. 2016;48:89–102.

129. Adams SH. Emerging Perspectives on Essential Amino Acid Metabolism in Obesity and the insulin resistant state. Adv Nutr. 2011;2:445–56.

130. Felig P, Marliss E, Cahill GF. Plasma Amino Acid Levels and Insulin Secretion in Obesity. N Engl J Med. 1969;281:811–6.

131. Liu J, Semiz S, Lee SJ Van Der, Spek A Van Der, Verhoeven A, van Klinken JB, Sijbrands E, Harms A, Hankemeier T, van Dijk K, et al. Metabolomics based markers predict type 2 diabetes in a 14-year follow-up study. Metabolomics. Springer US; 2017;13:1–11.

132. Wang TJ, Larson MG, Vasan RS, Cheng S, Rhee EP, Mccabe E, Lewis GD, Fox CS, Jacques PF, Fernandez C, et al. Metabolite profiles and the risk of developing diabetes. Nat Med. 2011;17:448–54.

133. Lotta LA, Scott RA, Sharp SJ, Burgess S, Luan J, Tillin T, Schmidt AF, Imamura F, Stewart ID, Perry RB, et al. Genetic Predisposition to an Impaired Metabolism of the Branched-Chain Amino Acids and Risk of Type 2 Diabetes: A Mendelian Randomisation Analysis. PLoS. 2016;13:1–22.

134. Newgard CB. Interplay between lipids and branched-chain amino acids in development of insulin resistance. Cell Metab [Internet]. Elsevier Inc.; 2012;15:606–14. Available from: http://dx.doi.org/10.1016/j.cmet.2012.01.024

135. Lynch CJ, Adams SH. Branched-chain amino acids in metabolic signalling and insulin resistance. Nat Rev Endocrinol. Nature Publishing Group; 2014;10:723–36.

136. Huffman K, Shah S, Stevens R, Bain J, Muehlbauer M, Slentz C, Tanner C, Kuchibhatla M, Houmard J, Newgard CB, et al. Relationships between circulating metabolic intermediates and insulin action in overweight to obese, inactive men and women. Diabetes Care. 2009;32:1678–83.

137. Tai ES, Tan MLS, Stevens RD, Low YL, Muehlbauer MJ, Goh DLM, Ilkayeva OR, Wenner BR, Bain JR, Lee JJM, et al. Insulin resistance is associated with a metabolic profile of altered protein metabolism in Chinese and Asian-Indian men. Diabetologia [Internet]. 2010;53:757–67. Available from: http://link.springer.com/10.1007/s00125-009-1637-8

138. Schooneman MG, Vaz FM, Houten SM, Soeters MR. Acylcarnitines: Reflecting or Inflicting Insulin Resistance? Perspect Diabetes. 2013;62:1–8.

139. Adams SH, Hoppel CL, Lok KH, Zhao L, Wong SW, Minkler PE, Hwang DH, Newman JW, Garvey WT. Plasma acylcarnitine profiles suggest incomplete long-chain fatty acid beta-oxidation and altered tricarboxylic acid cycle activity in type 2 diabetic African-American women. J Nutr. 2009;139:1073–81.

140. Perng W, Gillman MW, Fleisch AF, Michalek RD, Watkins SM, Isganaitis E, Patti M-E, Oken E. Metabolomic profiles and childhood obesity. Obesity. 2014;22:2570–8.

141. Butte NF, Liu Y, Zakeri IF, Mohney RP, Metha N, Voruganti VS, Goring H, Cole SA, Comuzzie AG. Global metabolomic profiling targeting childhood obesity in the hispanic Population. Am J Clin Nutr. 2015;102:256–67.

142. Mccormack SE, Shaham O, Mccarthy MA, Deik AA, Wang TJ, Gerszten RE, Clish CB, Mootha VK, Grinspoon SK, Fleischman A. Circulating branched-chain amino acid concentrations are associated with obesity and future insulin resistance in children and adolescents. Pediatr Obes. 2013;8:52–61.

143. Mihalik SJ, Michaliszyn SF, De Las Heras J, Bacha F, Lee S, Chace DH, De Jesus VR, Vockley J, Arslanian SA. Metabolomic Profiling of Fatty Acid and Amino Acid Metabolism in Youth With Obesity and Type 2 Diabetes. Diabetes Care. 2012;35:605–11.

144. Mastrangelo A, Martos-Moreno G, García A, Barrios V, Rupérez FJ, Chowen JA, Barbas C, Argente J. Insulin resistance in prepubertal obese children correlates with sex-dependent early onset metabolomic alterations. Int J Obes. 2016;40:1494–502.

145. Newbern D, Gumus Balikcioglu P, Balikcioglu M, Bain J, Muehlbauer M, Stevens R, Ilkayeva O, Dolinsky D, Armstrong S, Irizarry K, et al. Sex Differences in Biomarkers Associated With Insulin Resistance in Obese Adolescents: Metabolomic Profiling and Principal Components Analysis. J Clin Endocrinol Metab. 2014;99:4730–9.

146. Perng W, Tang L, Song PXK, Tellez-rojo MM, Cantoral A, Peterson KE. Metabolomic profiles and development of metabolic risk during the pubertal transition: a prospective study in the ELEMENT Project. Pediatr Res. 2019;85:262–8.

147. Jensen MD, Haymond MW, Rizza RA, Cryer PE, Miles JM. Influence of body fat distribution on free fatty acid metabolism in obesity. J Clin Invest. 1989;83:1168–73.

148. Frohnert BI, Jacobs DR, Steinberger J, Moran A, Steffen LM, Sinaiko AR. Relation between serum free fatty acids and adiposity, insulin resistance, and cardiovascular risk factors from adolescence to adulthood. Diabetes. 2013;62:3163–9.

149. Reinehr T. Type 2 diabetes mellitus in children and adolescents. World J Diabetes. 2013;4:270–81.

CHAPTER 2

Maternal Lipid Levels across Pregnancy Impact the Umbilical Cord Blood Lipidome and Infant Birth Weight

Abstract

Major alterations in metabolism occur during pregnancy enabling the mother to provide adequate nutrients to support infant development, affecting birth weight (BW) and potentially long-term risk of obesity and cardiometabolic disease. We classified dynamic changes in the maternal lipidome during pregnancy and identified lipids associated with Fenton BW z-score and the umbilical cord blood (CB) lipidome. Lipidomics was performed on first trimester maternal plasma (M1), delivery maternal plasma (M3), and CB plasma in 106 mother-infant dyads. Shifts in the maternal and CB lipidome were consistent with the selective transport of long-chain polyunsaturated fatty acids (PUFA) as well as lysophosphatidylcholine (LysoPC) and lysophosphatidylethanolamine (LysoPE) species into CB. Partial correlation networks demonstrated fluctuations in correlations between lipid groups at M1, M3, and CB, signifying differences in lipid metabolism. Using linear models, LysoPC and LysoPE groups in CB were positively associated with BW. M1 PUFA containing triglycerides (TG) and phospholipids were correlated with CB LysoPC and LysoPE species and total CB polyunsaturated TGs. These results indicate that early gestational maternal lipid levels influence the CB lipidome and its relationship with BW, suggesting an opportunity to modulate maternal diet and improve long-term offspring cardiometabolic health.

Introduction

The Developmental Origins of Health and Disease (DOHaD) theory describes how insults during early life can permanently program the fetus/offspring, altering their risk of adult chronic disease (1). To adapt to the intrauterine environment (i.e. maternal nutrient supply), structural changes and functional modifications occur in fetal organs and tissues to ensure survival of the newborn, indicative of their developmental plasticity (2). Barker and Osmond developed this hypothesis in response to observations from the Dutch Famine birth cohort, a well-documented famine in the Netherlands during World War II. Within this cohort, nutrient restriction in utero in the first trimester was associated with increased risk of obesity, dyslipidemia and cardiovascular disease, while restriction in the third trimester was associated with decreased risk of metabolic disease independent of birth weight (BW) (3), affirming existence of distinct susceptibility windows for producing differing outcomes. Infant BW is the most common health outcome studied to determine if the maternal intrauterine environment influences the development of the fetus. Both low and high BW have been associated with an increased risk of obesity and cardiometabolic diseases, including type 2 diabetes (T2D) (4, 5).

In recent years, profiling of small molecular weight compounds in a biological sample by metabolomics has been used to obtain an objective measurement of the metabolic environment in which the developing fetus is exposed. Metabolite levels are influenced by dietary intake (6) and can both reflect and influence changes in metabolism (7). The application of metabolomics to developmental studies can identify changes in maternal nutrient availability across pregnancy (8–11). Using a targeted metabolomics approach, we previously reported an increase in plasma long-chain fatty acids and corresponding long-chain acylcarnitines (AC) in maternal plasma from first trimester to term (10). These results reflect the increase in lipolysis during late-

gestation to fuel rapid fetal growth. Using a larger cohort and a comprehensive lipidomics platform, we aim to expand our previous findings and detail changes in phospholipids, ceramides (Cer), cholesteryl esters (CE), and triglycerides (TG) during pregnancy.

Metabolomics analyses have been applied to identify trimester-specific maternal metabolites associated with infant BW and adiposity (12–16), accounting for maternal characteristics such as pre-pregnancy BMI (13). Maternal metabolite levels, placental transfer, and interaction with other metabolites, such as inhibition by competition or metabolite-induced changes in placental transport activity, can all affect the relative levels of the umbilical cord blood (CB) metabolome. The CB metabolome is influenced by maternal characteristics such as pre-pregnancy BMI (17, 18).

The metabolome from CB has been correlated with BW finding positive associations with branched chain amino acids (19), AC (18, 20), and phosphatidylcholines (PC) (20, 21) along with inverse associations with TGs (18). Other studies have found that CB lysophosphatidylcholine (LysoPC) metabolites with varying chain length and saturation are positively associated with newborn BW (21–23), as well as with weight at 6 months of age (21). However, what remains unclear is how the maternal lipidome influences that establishment of CB lipids related to BW. In this study we profiled 573 lipid species in 106 mother-infant dyads from maternal first trimester (M1) and delivery blood (M3) as well as umbilical CB. We confirm the strong association of CB lysophospholipids (LysoPL) and BW. In addition, we find that maternal first trimester and delivery plasma lipid profiles seem to influence the levels of CB LysoPLs. Some of these effects appear to have sex-specific influences in the developing fetus (24). The results of this study indicate that starting in early gestation, the maternal metabolite

environment may have an important effect on offspring weight and potentially, long-term cardiometabolic risk, consistent with developmental origins of health and disease (1).

Subjects and Methods

Study Population. The subjects used in this study are part of the Michigan Maternal Infant Pair (MMIP) birth cohort study (2010-present). Briefly, pregnant women were recruited at their first prenatal appointment between 8 and 14 weeks of gestation. Eligibility criteria for MMIP were: age between 18 and 42 years old, had a spontaneously conceived singleton pregnancy, and intended to deliver at the University of Michigan Hospital. A subset of MMIP participants from among these were chosen for lipidomics measures. Criteria for inclusion for the current study include the mother-infant pairs having complete demographic, survey and health information at their initial study visit and availability of all biospecimen at all-time points from mother and child. Study procedures were approved by the UM Medical School Institutional Review Board, and all participants provided written informed consent.

During the initial study visit at 8-14 week of pregnancy, participants provided a blood sample (**M1**) and anthropometry information (weight and height) to calculate an estimated baseline BMI. Information obtained at delivery include maternal weight for calculating gestational weight gain (GWG) from the initial visit. Maternal venous blood samples (**M3**) and cord blood (**CB**) samples via venipuncture from the umbilical cord were collected. Physician measured anthropometry was adjusted for gestation age and infant sex using Fenton growth curves for BW (25) and growth curves developed by the Canadian Institute of Health Research for head circumference (26). All 106 mother-infant pairs met additional inclusion criteria for this study including infant BW greater than 2500 grams, maternal BMI > 18.5, full term, and no pregnancy complications (i.e. gestational diabetes mellitus). Study design represented in **Figure 2.1.**

Lipidomics sample preparation. Metabolomics analysis were conducted by the Michigan Regional Comprehensive Metabolomics Resource Core. Maternal plasma (M1 and M3) samples were stored at -80°C prior to analysis. Lipids were extracted using a modified Bligh-Dyer Method (27). At room temperature, the extraction used water/methanol/dichloromethane (2:2:2, v/v/v) after spiking internal standards. The organic layer was collected, dried under nitrogen, and resuspended in 100µL of Buffer B (10:90 acetonitrile/isopropyl alcohol) with 10mM Na4OAc. Lipid extracts were analyzed using a lipid chromatography tandem mass spectrometry platform (28)

Shotgun lipidomics analysis. Lipid extracts were injected into a 1.8 µm particle 50 x 2.1 mm internal diameter Waters Acquity HSS T3 column (Waters, Milford, MA) and heated to 55°C. For chromatography, a linear gradient using solvents was created over the 20 minute total run time. Solvent A contained acetonitrile/water (40:60, v/v) with 10mM ammonium acetate. Solvent B contained acetonitrile/water/isopropanol (10:5:85, v/v/v) with 10 mM ammonium acetate. For the first ten minutes, a 60% Solvent A and 40% Solvent B was used. For the next seven minutes, the gradient increased in a linear fashion to 100% Solvent B. For the final three minutes, the gradient switched back to 60% Solvent B and 40% Solvent A. The flow rate used for these experiments was 0.4 mL/min and the injection volume was 5µL. The column was equilibrated for three minutes before the next injection and run at a flow rate of 0.400uL/min for a total run time of 20 min. Samples were ionized in positive and negative ionization model using a Triple TOF 5600 (AB Sciex, Concord Canada). Pooled human plasma samples and pooled experimental samples were randomized and ran for quality control (29).

From detected features, lipids were classified using LIPIDBLAST (30), a computer generated tandem mass spectral library containing 119,200 compounds from 26 lipid classes. Raw feature

data files with mass and retention time were searched against LIPIDBLAST using Multiquant 1.1.0.26 (ABsciex, Concord, Canada) (31). Lipid compounds were excluded with (1) a relative standard deviation greater than 40% in the pooled samples and/or (2) less than 70% presence in the samples. Missing data were imputed using the K-nearest neighbor method. After processing, 573 lipids from multiple lipid classes were identified (**Table 2.1**). All lipids will be mentioned with the nomenclature as X:Y, where X is the length of the carbon chain and Y, the number of double bonds.

Statistics. Prior to the main analysis, we examined differences in maternal and newborn characteristics stratified by sex of the newborn. Pearson chi-square tests were used to identify sex-differences in categorical variables. Paired t-tests were used to identify sex-differences in continuous variables.

To observe changes in the lipid profile across pregnancy, raw peak intensities of each lipid were standardized (mean=0, standard deviation=1) across M1, M3, and CB. Paired t-tests were used to identify differences in raw peak intensities of individual lipids between M1-M3, to represent change in maternal metabolome during pregnancy, and M3-CB, to represent transfer of lipids through the placenta. We calculated FC for M1-M3 (log2[M3/M1]) and for M3-CB (log2[CB/M3]) to quantify change between time points (α=0.05/573). Using Pearson's correlations, the correlations between individual lipids within time points was measured.

Due to biological constraints on metabolism, many metabolites are highly correlated. In response, we created lipid groups separating individual lipids by class and number of double bonds, yielding 41 groups (**Table S2.1**). To create lipid group scores, unsupervised Principal Component Analysis was run retaining the first principal component, accounting for the largest portion of variance using PROC FACTOR in SAS. Within the principal component, each lipid

receives a factor loading, which is the correlation coefficient between the lipid and the component. Score were created by (1) multiplying the lipid factor loading by the lipid standardized peak intensity and (2) adding together these values for all lipids within a lipid group, using PROC SCORE in SAS. Mother-infant dyads received lipid group scores for M1, M3, and CB, separately. Using Debiased Sparse Partial Correlations, the correlations between lipid groups within time points was measured. As this is an exploratory analysis, we present correlations that have an adjusted p-value<0.2.

Linear regression was used to classify the relationship between maternal baseline BMI and GWG with M1, M3, and CB lipid groups, adjusting for sex, parity, maternal age, and gestational age (unadjusted p-value<0.05). Linear regression was used to identify M1, M3, and CB lipid groups associated with Fenton BW z-score, adjusting for sex, parity, maternal age, gestational age, maternal baseline BMI, and GWG (unadjusted p-value<0.05). Sex-stratified models were run. Furthermore, linear models were used to explore sex differences between individual CB triglycerides (mean 0, standard deviation 1) and Fenton BW z-score, stratified by infant sex and adjusted for parity, maternal age, gestational age, maternal baseline BMI, and GWG (unadjusted p-value<0.05). Non-parametric regression curves were plotted to classify how the relationship between TGs and BW is related to the number of double bonds in TGs. CB lipid groups associated with BW were correlated with M1 and M3 individual lipids and lipid groups to determine if maternal lipids modulate the levels with CB, using Pearson Correlations (p<0.05).

Unless otherwise state, all statistical analyses were performed using SAS 9.4 (Cary, North Carolina). Figures were created using GraphPad Prism version 7.4 (La Jolla, California).

Results

Subject Demographics

Women were recruited during the first trimester and followed through delivery (**Figure 2.1**). Average maternal age at their first trimester visit was 32.1 ± 3.6 years and the majority of women had a lean baseline BMI (62%) (**Table 2.2**). On average, women gained 13.2±5.2 kg between the baseline visit and term and 72% of infants were born vaginally. Offspring analysis was stratified by males (n=51) and females (n=55). We observed no significant difference in Fenton BW percentile between males and females.

Maternal BMI was inversely associated with gestational weight gain (GWG) ($r2 = 0.18$, $p<0.001$), indicating that leaner women gained more weight during pregnancy (**Figure S2.1a**). In contrast, maternal BMI was positively associated with Fenton BW percentile ($r2=0.06$, $p=0.014$) (**Figure S2.1b**); and while not significant, maternal GWG trended towards a positive association with Fenton BW percentile ($r2=0.03$, $p=0.070$) (**Figure S2.1c**).

Fluctuations in the Lipidome between M1, M3, and CB

We next examined the changes in the plasma lipidome across pregnancy (M1 to M3) and between maternal delivery plasma and cord blood (M3 to CB), the latter as a potential surrogate for placental transfer and fetal exposure. **Figure 2.2a** displays a Heatmap of lipids organized by class with individual lipid peak intensities normalized across M1, M3, and CB. **Figures 2.2b** and **Table S2.2** show fold changes (FC) of lipids from M1 to M3. **Figure 2.2c** and **Table S2.3** shows FC of lipids between M3 and CB. Most classes of lipids increased in levels from M1 to M3, consistent with previous observations of generalized increase in lipoproteins and associated lipids with advancing pregnancy (8,32). A subset of lipid species was reduced in M3 compared to M1 including polyunsaturated CEs and a variety of LysoPC and LysoPE species. Most of the polyunsaturated fatty acid (PUFA) containing lipids that were lower in M3 were significantly increased in CB plasma (**Figure 2.2a, 2.2c**). In addition, several lipid species that are statistically

unchanged from M1 to M3 were higher in CB compared to M3, including SM and TG enriched in PUFAs. These results are consistent with the known specific transfer of PUFAs across the placenta to the fetus (33), perhaps mediated by LysoPLs (see below) (34).

Pearson Correlations of Individual Lipids within Each Time-Point

Networks were generated for individual lipids at M1 (**Figure 2.3**), M3 (**Figure 2.4**), and CB (**Figure 2.5**) using Pearson's correlations. In maternal plasma, clusters of lipid classes were observed between (1) TGs, DGs, PCs, and PEs; (2) Cers and SMs; (3) PL-PC and PL-PE; and (4) LysoPCs and LysoPEs. FFA and AC tended to cluster by themselves, independent of the other lipid networks. Interestingly, in CB plasma, individual lipids all clustered together

Partial Correlation Network of Lipid Groups within Each Time-Point

Given the specific patterns within lipid classes containing PUFAs, lipid clusters were created by grouping lipids based on a priori knowledge of lipid class and the number of double bonds in each lipid species, resulting in 41 groups at each time point (**Table S2.1**). Using a Debiased Sparse Partial Correlation algorithm (35), we estimated partial correlation networks for lipid groups within M1, M3, and CB, using an adjusted p-value less than 0.2 (**Figure 2.6**). At each time point, the majority of correlations were positive, signifying the connectivity of lipids across classes. In particular, multiple positive correlations were observed between (1) TGs, DGs, and phospholipids; (2) Cers and SMs; (3) PL-PC and PL-PE; and (4) LysoPCs and LysoPEs. Most positive correlations occurred between lipid groups containing lipids with similar number of double bonds. CEs are correlated with a variety of lipid classes including LysoPCs, phospholipids, DGs, SMs, and TGs; potentially suggesting their interaction with a variety of lipid metabolic pathways. Noteworthy, in M1, M3, and CB, CE-poly is inversely associated with

DG-mono and, excluding M1, with TG-mono. Both M3 and CB have more significant correlations than M1 (**Figure 2.6**), potentially due to the increase in maternal lipolysis and delivery fatty acids to the fetal circulation during late gestation, resulting in proportional distribution to different lipids species.

Relationship between Maternal Characteristics with the Maternal and Cord Blood Lipidome

The next objective was to assess the relationship between maternal characteristics, baseline BMI and GWG, and the lipidome at M1, M3, and CB. At each time point, multiple lipid classes were associated with BMI and GWG, adjusting for sex, maternal age, parity, and gestational age. Maternal BMI was inversely associated with PCs and PEs and was positively associated with SM-mono and SM-poly at both M1 and M3 (**Figure S2.2**). In CB, saturated PGs and SM-poly are positively associated with maternal BMI, while CE displayed inverse correlations. Associations of GWG with lipid groups were largely in the opposite direction, due to the inverse correlation between BMI and GWG (**Figure S2.1a**). GWG was positively associated with LysoPC and LysoPE clusters at both M1 and M3, independent of the number of double bonds in the fatty acid tails (**Figure S2.3**). GWG was inversely associated with SM-mono and SM-poly at both M1 and M3. Few associations between GWG and CB lipids groups were observed.

Relationship between Maternal and Cord Blood Lipidome and Birth Weight

As infant BW is associated with obesity and future cardiometabolic risk (4,5), we sought to identify maternal and CB lipid groups associated with Fenton BW z-score using linear regression, adjusting for sex, maternal age, parity, gestational age, GWG, and BMI (**Figure 2.7**). Sex stratified models determined if sex influences the relationship between the lipidome and BW.

In the combined model, the early gestation lipidome (M1) was not associated with infant BW in the combined model, however, M1 lipid groups were associated with BW in males in the sex-stratified models (**Figure 2.7A**) displaying positive associations with saturated free fatty acids (FFA) and negative associations with CER-mono, CER-poly, PC-mono, SM-sat, and SM-mono. Within M3, significant positive correlations were observed between BW and DG-sat, LysoPE-sat, PL-PC-sat, SM-mono, SM-poly, and TG-sat (**Figure 2.7B**). The direction of these associations was consistent within males and females, however in the sex-stratified models, the relationship reached significance in females, but not in males.

Within the CB, all LysoPC and LysoPE lipids groups are positively associated with BW, independent of the number of double bonds and was consistent in both male and female infants (**Figure 2.7C**). Additionally, CB DG-poly and TG-poly are inversely associated with BW, driven by female infants, and CE-poly is inversely associated with BW, driven by male infants. In response to the unique relationship between CB TG-poly and BW, sex-stratified regression models determined the relationship between individual CB TGs (97 triglycerides) and Fenton BW z-score, adjusting for maternal age, parity, gestational age, GWG, and BMI. **Figure 2.8** represents the beta coefficients from the sex-stratified models, plotted by the number of double bonds in the TGs. Observing non-linear trends, we used non-parametric regression to fit polynomial lines to each curve, emphasizing the evident sex differences in the relationship between polyunsaturated TGs and BW, again driven by females.

Influence of Maternal Lipidome on Cord Blood Lysophospholipids

Our results indicated that CB LysoPLs of varying chain length and number of double bonds are elevated in the CB compared to M3 (**Figure 2.2**) and are significantly associated with BW, independent of sex (**Figure 2.7**). To assess if maternal lipids during pregnancy can influence the

level of CB LysoPLs, M1 and M3 lipidome was correlated with individual CB LysoPCs and LysoPEs, as well as the score of LysoPC and LysoPE subgroups (Sat, Mono and Poly) and the score of all LysoPLs (LysoPL-total). **Figure 2.9** displays a Heatmap of lipids from M1 and M3 that are significantly correlated with the CB LysoPL-total group. In M1, 13 lipids positively correlated, and 47 lipids inversely correlated with CB total LysoPL levels. Lipids with a positive correlation include AC 18:0 and LysoPC species (16:0, 17:0, 18:0, 19:0, and 20:0), as well as the saturated LysoPC lipid group. Lipids with an inverse correlation mainly include individual lipids and lipid groups with PUFA containing DG, PC, phosphatidylethanolamine (PE), and TGs, suggesting that early maternal levels of PUFAs within multiple lipid class modulate levels of CB LysoPL-total.

In M3, 34 lipids were positively correlated, and 7 lipids were inversely correlated with CB LysoPL levels. M3 saturated LysoPC and LysoPE lipid groups, as well as individual LysoPL, are positively associated with CB LysoPL-total, proposing that higher M3 levels results in higher CB levels. CER and SM containing saturated and monounsaturated TGs are positively associated with CB LysoPL-total. Interesting, inverse associations were observed between M3 LysoPE 20:3 and 22:5 with CB LysoPL-total, suggesting differences based on the fatty acid tail.

Most correlations between the significant M1 and M3 individual lipids and individual CB LysoPCs and LysoPEs were in the same direction as CB LysoPL-total. Subtle variations in the correlation patterns are observed for LysoPC 18:2, 18:3, 20:5, and 26:4 and LysoPE 18:2, 20:3, 20:4, 22:6, and 24:0, potentially suggesting differences in how the maternal lipidome modulates these CB polyunsaturated LysoPL.

Influence of the Maternal Lipidome on Cord Blood Polyunsaturated Triglycerides

The apparent preferential transfer of lipids containing PUFAs into the CB (**Figure 2.2**) and an inverse association between Fenton BW z-score and CB lipid groups containing PUFAs (**Figure 2.7 and 2.8**) prompted us to determine if maternal lipids might modulate the levels of PUFA in CB. The M1 and M3 lipidome was correlated with CB TGs. **Figure 2.10** displays a Heatmap of lipids from M1 and M3 that are significantly correlated with the CB TG-poly group. A variety of M1 PUFA containing lipids, including PC, PL-PC, DG, and TG, are positively associated with CB TG-poly. In M3, there are positive correlations between PCs and PEs, 75% of these phospholipids contained PUFAs, with CB TG-poly, suggesting the mobilization of PUFAs within PCs and PEs to the placenta for transport. Lastly, M3 monounsaturated and polyunsaturated SM are inversely associated with CB TG-poly, noting that these lipids were found to be positively associated with maternal BMI (**Figure S2.2**) and Fenton BW z-score (**Figure 2.7**).

Discussion

Using a comprehensive lipidomics platform including almost six hundred lipid species, this study objectively classified the maternal metabolic environment during the first trimester and at delivery, as well as the infant lipidome, reflecting infant metabolism. We found dynamic shifts in the maternal lipidome across pregnancy and evidence for selective transfer of lipids containing PUFA from maternal to fetal circulation. We further identified associations between the lipidome and BW, emphasizing the inverse correlations observed with CB DGs and TGs containing PUFAs and positive correlations observed with CB LysoPL. Lastly, we identified maternal lipids that may modulate CB lipid levels influential in growth.

Early in gestation, insulin sensitivity is enhanced to increase maternal energy storage (36). However, as pregnancy advances, maternal insulin resistance increases with elevations in lipid

parameters such as lipoproteins, TGs, and total cholesterol to support the necessary metabolic changes for pregnancy maintenance and fetal growth (8). Of the 573 lipid species analyzed, 35% were significantly increased while only 10% were decreased in M3 compared to M1 (**Figure 2.2b**). Between M1 and M3, we observed higher levels of PC, PE, DG, CER, SM, TG, and FFA, many containing fatty acids with 16-18 carbons. The majority of lipids species reduced in M3 are increased in CB and are enriched in long-chain PUFAs, suggesting specific transfer of these entities across the placenta to the fetus to provide LC-PUFAs to support brain development (37). While several studies have demonstrated the apparent transfer of individual PUFAs into the fetal circulation during the later stages of pregnancy (33,38,39), our study is the first to document the transfer of a wide variety of lipid species containing LC-PUFA including CE, LysoPL, TG, and SM as well as free LC-PUFA.

The transport of PUFA from maternal circulation to the fetus is dependent upon fetal requirements of PUFAs, which increase during late gestation. PUFAs such as arachidonic acid (20:4n-6) (AA) and docosahexaenoic acid (22:6n-3) (DHA) are essential for establishing cell membranes in the brain and retina (40). Within the maternal liver, these fatty acids are derived from the essential fatty acids (EFA) linoleic acid and alpha-linolenic acid via elongation by liver Δ5 and Δ6 desaturases. Fetal supply of very LC-PUFAs is dependent on placental transfer because placenta lacks the enzymes Δ5 and Δ6 desaturases (41) and the fetus only has limited desaturase activity (42).

Correlations between the maternal and CB lipidome can infer the role of transport proteins. Our results suggest that starting early in gestation, M1 PUFA levels within PC, PL-PC, DG, and TG are positively associated with CB TG-poly (**Figure 2.10**). Therefore, maternal PUFA levels early in gestation are crucial to establish infant PUFA levels. Since there is no evidence of direct

placental transport of TG from maternal to fetal circulation (43), these results suggest a diversion of PUFAs from the maternal TG pool with re-esterification in CB TGs. This diversion could occur during hepatic TG elongation and desaturation of EFAs, with increased esterification of PUFA or by TG lipolysis in placenta and selective uptake of PUFA at the maternal-fetal interface (44,45). Maternal fatty acids are transported to the fetus across the placenta via a variety of fatty acid transport proteins as well as passive diffusion (46).

Using ^{13}C-labeled fatty acids administered to women 12-hours prior to scheduled Cesarean delivery, Gil-Sánchez et al. demonstrated that the esterification of fatty acids into different lipid fractions influences placental transfer to the fetus (46). In maternal plasma at the time of delivery, ^{13}C-fatty acid enrichment was detected with the incorporation of saturated fatty acid ^{13}C-palmitate and monounsaturated fatty acid ^{13}C-oleate in TGs while the PUFAs ^{13}C-linoleic and ^{13}C-DHA were found in both TGs and phospholipids (46). Within the placenta, 90% of labeled FA were found in the phospholipid fraction with significant enrichment of ^{13}C-DHA in CB compared to both maternal and placental samples. These results suggest that the incorporation of essential PUFA into maternal phospholipids may be important for placental transfer at the end of gestation. Our results found M3 polyunsaturated FA within PCs and PEs, rather than DGs and TGs, are positively associated with CB TG-poly (**Figure 2.10**), supporting the importance of the phospholipid fraction in the transfer of PUFA late in gestation.

Our results indicated a sexual dimorphic effect of CB DG- and TG-poly with BW, with a larger effect seen in the females (**Figure 2.7** and **2.8**). Previous studies that have looked at the effect of PUFA supplementation during pregnancy on infant BW have yielded mixed results (47), potentially due to differences in gestation length, baseline characteristics of the participants, and source, timing, and dose of n-3 PUFA supplement. PUFAs supplementation has been associated

with longer gestation and an increase in fetal weight, especially in women at risk for intrauterine growth retardation (48). However, O'Tierney-Ginn, et al. (49) found that total CB saturated fatty acids was positively associated with high skinfold thickness at birth (but not birthweight BMI z-score), as well as increased BMI-z trajectory in early infancy, while PUFA levels were inversely correlated with BMI-z trajectory. Hauner, et al. (50) demonstrated that dietary n-3 LC-PUFA supplementation of women had no effect on BW in randomized trial of 208 women but had a larger effect on the gene expression profile in female placentas. Sedlmeier, et al. observed placental gene expression to be more responsive to maternal omega-3 supplementation in females than males (51). The reason for the sexually dimorphic differences is not yet clear.

We observed a positive association between CB LysoPE and LysoPCs and Fenton BW z-score (**Figure 2.7**), independent of the chain length and the number of double bonds. This confirms findings from other studies that CB LysoPCs with varying chain length and saturation are positively associated with newborn BW (21–23), as well as with weight at age 6 months (21). The associations between LysoPL and BW were not as apparent in M1 and M3, with an exception being M3 LysoPE-sat are positively associated with BW (**Figure 2.7**). Additionally, we found that maternal GWG is positively associated with M1 and M3 LysoPC and LysoPE lipid groups of varying number of double bonds, suggesting an influence of maternal characteristics during pregnancy on LysoPL (**Figure S2.3**).

Recently, the Major Facilitator Super Family Domain Containing 2a (MFSD2a) protein has been proposed as a NA+-dependent LysoPL transporter in the brain (52) and placenta (53). This transporter provides a mechanism for the active transport of LysoPL from maternal plasma, consistent with our study findings that (1) LysoPC and LysoPE are depleted in maternal plasma

and elevated in CB (**Figure 2.2**) and (2) M1 and M3 LysoPLs, mainly containing saturated FA, are positively correlated with total CB LysoPL levels (**Figure 2.9**).

Since the sn-2 position of phospholipids tend to be occupied by PUFAs (54), it has been hypothesized that specific placental endothelial lipases cleave sn-1 fatty acids, allowing transport of the PUFA-containing LysoPL to the fetal circulation, perhaps enhancing delivery to the developing fetal brain (34,55). An intriguing possibility suggested by our data is that there is an interaction between PUFA during development and later transfer of LysoPL to the fetus. We see a significant inverse association of PUFA-containing lipids M1 and LysoPC levels in the CB of infants and conversely, a positive association of M1 (and M3) lipids enriched in saturated fatty acids (**Figure 2.9**). This might imply early programming of LysoPL transport capacity. Control of MFSD2a expression in placenta has not been established, but is potentially regulated by diet. In mice, cortical and subcortical brain MFSD2a levels increased in rodents fed a high fat diet, with PUFA-containing diets having a greater effect at lower concentrations than a lard-containing diet (56). Additionally, MFSD2a expression in placenta is positively correlated with CB DHA levels (53), supporting its role in PUFA transport and implying it responds to the levels of DHA.

Of interest, polyunsaturated SM are decreased between M3 and CB (**Figure 2.2**), suggesting that maternal late gestation SM may be (1) directly transferred to the fetus to provide PUFAs or (2) converted into LysoPL, the preferential transfer method of PUFAs. Multiple significant correlations were observed between M3 SM and the CB lipidome. CB polyunsaturated TGs are inversely correlated with M3 SM-mono and SM-poly individual lipids and lipid groups (**Figure 2.10**), suggesting that elevated late gestation polyunsaturated SM may result in lower levels of polyunsaturated containing TG in the CB. Supporting these results, we found that M3 SM-mono

and M3 SM-poly are positively associated with maternal baseline BMI (**Figure S2.3**) and positively associated with newborn BW (**Figure 2.7**). These results suggest that inability to convert SM to transfer the monounsaturated and polyunsaturated fatty acids across the placenta results in less favorable fetal development, potentially linked to maternal BMI. Lastly, M3 saturated and monounsaturated SM were positively associated with CB LysoPL-total levels. These results highlight the importance of the SM lipid fraction during gestation, which potentially is related to the pathogenesis of obesity, T2D, and various metabolic diseases (57).

Conclusion

The finding that the lipids that show the greatest differences between maternal and fetal circulation at term are also associated with BW is a novel finding in these studies and suggests a complex interaction between PUFA intake, incorporation into specific lipid subtypes and transport to the developing fetus. Future longitudinal studies with a larger sample size are desired to assess if changing the maternal metabolic environment to a more favorable lipidome will improve infant outcomes. Collection of maternal dietary intake can help elucidate the relationship between nutrient intake and blood concentrations of very long-chain FA, as the metabolome doesn't solely represent dietary intake, but rather a combination of genetics, diet, and phenotypes. Maternal blood collection at delivery may not be representative of the metabolic states during the third trimester due to the stress of parturition, although we observed no differences in lipidome components based on route of delivery. Collecting multiple blood samples throughout pregnancy will help to further classify lipidome changes throughout pregnancy. Collection of placenta samples and quantifying gene expression of key transport proteins (i.e. MFSD2a) would provide details on preferential transfer of lipid species.

Authorship

Jennifer L. LaBarre, Muraly Puttabyatappa, Peter X.K. Song, Jaclyn M. Goodrich, Ling Zhou, Thekkelnaycke M. Rajendiran, Tanu Soni, Steven E. Domino, Marjorie C. Treadwell, Dana C. Dolinoy, Vasantha Padmanabhan, and Charles F. Burant

Acknowledgements

We would like to acknowledge Samantha Milewski and Steven Rogers for help with recruitment, processing of samples, and retrieval of clinical data.

Funding Support

University of Michigan NIEHS/EPA Children's Environmental Health and Disease Prevention Center P01 ES022844/RD 83543601 (VP, DCD, PS, JG), NIH Children's Health Exposure Analysis Resource (CHEAR), 1U2C ES026553 (DD, JG, CFB), Michigan Lifestage Environmental Exposures and Disease (M-LEEaD) NIEHS Core Center P30 ES017885 (VP, DCD, JG, PS, CFB), NIH/NIEHS UG3 OD023285 (VP, DCD), Molecular Phenotyping Core, Michigan Nutrition and Obesity Center P30 DK089503 (CFB, DCD) and Michigan Regional Metabolomics Resource Core R24 DK097153 (CFB), Ruth L. Kirschstein Institutional Training Grant from the NIEHS T32 ES007062 (MP) and The A. Alfred Taubman Research Institute (CFB).

Study Approval

The MMIP study was approved by the University of Michigan Institutional Review Board (HUM00017941). Written informed consent was received from all participants and all plasma samples and metadata were deidentified prior to analysis.

Figure 2.1. Timeline of clinical study visits.

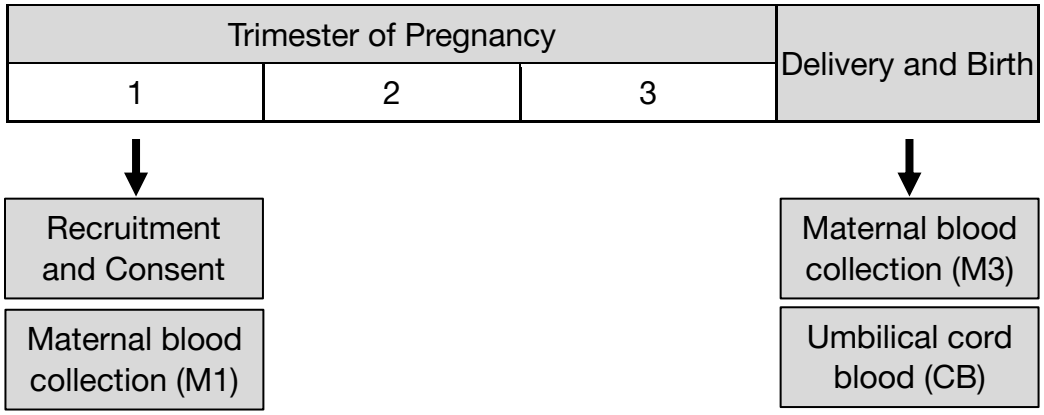

Lipidomics was conducted on maternal first trimester (M1), term (M3) and cord blood (CB) plasma (n=106). Maternal and infant phenotypes were collected throughout the study.

Table 2.1. Lipid species class, abbreviation, and number of lipids annotated from lipidomics analysis.

Lipid Class	Abbreviation	Number
acylcarnitine	AC	6
ceramide	CER	51
cholesteryl ester	CE	13
diacylglycerol	DG	30
free fatty acid	FFA	16
glucosylceramidase	GlcCer	9
lysophosphatidylcholine	LysoPC	29
lysophosphatidylethanolamine	LysoPE	9
phosphatidic acid	PA	4
phosphatidylcholine	PC	96
phosphatidylethanolamine	PE	44
plasmenyl-phosphatidylcholine	PL-PC	54
plasmenyl-phosphatidylethanolamine	PL-PE	36
phosphatidylglycerol	PG	8
phosphatidylinositol	PI	12
phosphatidylserine	PS	2
sphingomyelin	SM	65
triacylglycerol	TG	97

Table S2.1. Lipid group classifications. Lipidomics dataset was collapsed into groups of lipids based on the lipid class and the number of double bonds within the fatty acid tails. A list of the individual lipids within each group are reported.

Lipid Group	Lipid Species
AC	Acylcarnitine 16:0, Acylcarnitine 18:0, Acylcarnitine 24:0, Acylcarnitine 26:0, Acylcarnitine 18:1, Acylcarnitine 18:2
CE	16:0 CE, 18:0 CE, 16:1 CE, 17:1 CE, 18:1 CE
CE-poly	18:2 CE, 18:3 CE, 20:3 CE, 20:4 CE, 22:4 CE, 20:5 CE, 22:5 CE, 22:6 CE
CER-sat	Cer[NDS] 34:0, Cer[NDS] 36:0, Cer[NDS] 38:0, Cer[NDS] 40:0, Cer[NDS] 41:0, Cer[NDS] 42:0, Cer[EODS] 53:0, Cer[NP] 34:0, Cer[NP] 40:0, Cer[NP] 42:0,
CER-mono	Cer[NS] 32:1, Cer[NS] 33:1, Cer[NS] 34:1, Cer[NS] 35:1, Cer[NS] 36:1, Cer[NS] 37:1, Cer[NS] 38:1, Cer[NS] 39:1, Cer[NS] 40:1, Cer[NS] 41:1, Cer[NS] 42:1, Cer[NS] 43:1, Cer[NS] 44:1, Cer[AS] 41:1, Cer[EODS] 49:1, Cer[NP] 42:1
CER-poly	Cer[NS] 34:2, Cer[NS] 36:2, Cer[NS] 38:2, Cer[NS] 39:2, Cer[NS] 40:2, Cer[NS] 41:2, Cer[NS] 42:2, Cer[NS] 43:2, Cer[AS] 42:2, Cer[EODS] 57:2, Cer[NS] 41:3, Cer[NS] 42:3, Cer[NS] 43:3, Cer[NS] 33:4, Cer[NS] 37:4
DG-sat	DG 30:0, DG 31:0, DG 32:0, DG 33:0, DG 34:0, DG 36:0, DG 38:0, DG 30:1, DG 32:1, DG 33:1, DG 35:1, DG 36:1, DG 38:1
DG-mono	DG 32:2, DG 34:2, DG 35:2, DG 36:2, DG 38:2, DG 34:3, DG 35:3, DG 36:3, DG 38:3
DG-poly	DG 36:4, DG 38:4, DG 36:5, DG 38:5, DG 38:6, DG 38:7, DG 40:7, DG 40:8
FFA-sat	FFA18:0, FFA16:0, FFA20:0, FFA22:0, FFA24:0
FFA-mono	FFA18:1, FFA20:1, FFA22:1, FFA24:1
FFA-poly	FFA18:2, FFA20:2, FFA22:2, FFA24:2, FFA22:3, FFA24:3, FFA20:4
GlcCer	GlcCer[NS] 32:1, GlcCer[NS] 34:1, GlcCer[NS] 38:1, GlcCer[NS] 40:1, GlcCer[NS] 41:1, GlcCer[NS] 42:1, GlcCer[NS] 43:1, GlcCer[NS] 41:2, GlcCer[NS] 42:2
LysoPC-sat	LysoPC 14:0, LysoPC 15:0, LysoPC 16:0, LysoPC 17:0, LysoPC 18:0, LysoPC 19:0, LysoPC 20:0, LysoPC 22:0, LysoPC 24:0, LysoPC 26:0
LysoPC-mono	LysoPC 16:1, LysoPC 17:1, LysoPC 18:1, LysoPC 19:1, LysoPC 20:1, LysoPC 24:1, LysoPC 26:1
LysoPC-poly	LysoPC 18:2, LysoPC 20:2, LysoPC 26:2, LysoPC 18:3, LysoPC 20:3, LysoPC 20:4, LysoPC 22:4, LysoPC 24:4, LysoPC 26:4, LysoPC 20:5, LysoPC 22:5, LysoPC 22:6
LysoPE-sat	LysoPE 16:0, LysoPE 18:0, LysoPE 24:0
LysoPE-poly	LysoPE 18:2, LysoPE 20:3, LysoPE 20:4, LysoPE 22:5, LysoPE 22:6
PC-sat	PC 22:0, PC 23:0, PC 24:0, PC 26:0, PC 28:0, PC 29:0, PC 30:0, PC 31:0, PC 32:0, PC 33:0, PC 34:0, PC 36:0, PC 40:0, PC 25:1, PC 26:1, PC 28:1, PC 30:1, PC 31:1, PC 32:1, PC 33:1, PC 34:1, PC 35:1, PC 36:1, PC 37:1, PC 38:1, PC 40:1, PC 42:1
PC-mono	PC 30:2, PC 31:2, PC 32:2, PC 33:2, PC 34:2, PC 35:2, PC 36:2, PC 37:2, PC 38:2, PC 40:2, PC 42:2, PC 44:2, PC 30:3, PC 32:3, PC 33:3, PC 34:3, PC 35:3, PC 36:3, PC 37:3, PC 38:3, PC 39:3, PC 40:3, PC 42:3, PC 44:3
PC-poly	PC 40:10, PC 42:10, PC 42:11, PC 32:4, PC 34:4, PC 35:4, PC 36:4, PC 37:4, PC 38:4, PC 39:4, PC 40:4, PC 42:4, PC 44:4, PC 46:4, PC 34:5, PC 35:5, PC 36:5, PC 37:5, PC 38:5, PC 39:5, PC 40:5, PC 41:5, PC 42:5, PC 44:5, PC 46:5, PC 35:6, PC 36:6, PC

	37:6, PC 38:6, PC 39:6, PC 40:6, PC 41:6, PC 42:6, PC 44:6, PC 35:7, PC 36:7, PC 37:7, PC 38:7, PC 39:7, PC 40:7, PC 42:7, PC 40:8, PC 42:8, PC 40:9, PC 42:9
PE-sat	PE 30:0, PE 32:0, PE 33:0, PE 34:0, PE 35:0, PE 36:0, PE 32:1, PE 33:1, PE 34:1, PE 35:1, PE 36:1, PE 38:1
PE-mono	PE 32:2, PE 33:2, PE 34:2, PE 35:2, PE 36:2, PE 37:2, PE 38:2, PE 40:2, PE 34:3, PE 35:3, PE 36:3, PE 37:3, PE 38:3
PE-poly	PE 42:10, PE 34:4, PE 35:4, PE 36:4, PE 37:4, PE 38:4, PE 40:4, PE 36:5, PE 37:5, PE 38:5, PE 40:5, PE 36:6, PE 37:6, PE 38:6, PE 39:6, PE 40:6, PE 38:7, PE 40:7, PE 40:8
PG-sat	PG 32:0, PG 33:0, PG 34:0, PG 36:0, PG 32:1, PG 34:1
PG-mono	PG 34:2, PG 36:2
PI-sat	PI 34:1, PI 36:1
PI-mono	PI 34:2, PI 36:2, PI 36:3, PI 38:3
PI-poly	PI 36:4, PI 38:4, PI 38:5, PI 40:5, PI 38:6, PI 40:6
PLPC-sat	PL-PC 24:0, PL-PC 26:0, PL-PC 30:0, PL-PC 32:0, PL-PC 34:0, PL-PC 35:0, PL-PC 36:0, PL-PC 40:0, PL-PC 42:0, PL-PC 32:1, PL-PC 34:1, PL-PC 35:1, PL-PC 36:1, PL-PC 37:1, PL-PC 40:1, PL-PC 42:1, PL-PC 44:1
PLPC-mono	PL-PC 34:2, PL-PC 35:2, PL-PC 36:2, PL-PC 37:2, PL-PC 40:2, PL-PC 42:2, PL-PC 44:2, PL-PC 34:3, PL-PC 35:3, PL-PC 36:3, PL-PC 37:3, PL-PC 38:3, PL-PC 40:3, PL-PC 42:3, PL-PC 43:3, PL-PC 44:3
PLPC-poly	PL-PC 34:4, PL-PC 36:4, PL-PC 37:4, PL-PC 38:4, PL-PC 40:4, PL-PC 41:4, PL-PC 42:4, PL-PC 43:4, PL-PC 44:4, PL-PC 46:4, PL-PC 36:5, PL-PC 38:5, PL-PC 39:5, PL-PC 40:5, PL-PC 42:5, PL-PC 44:5, PL-PC 36:6, PL-PC 37:6, PL-PC 38:6, PL-PC 40:6, PL-PC 44:6
PLPE-sat	PL-PE 32:0, PL-PE 32:1, PL-PE 34:1, PL-PE 35:1, PL-PE 36:1, PL-PE 38:1, PL-PE 40:1
PLPE-mono	PL-PE 32:2, PL-PE 34:2, PL-PE 35:2, PL-PE 36:2, PL-PE 37:2, PL-PE 38:2, PL-PE 40:2, PL-PE 34:3, PL-PE 36:3, PL-PE 38:3, PL-PE 40:3
PLPE-poly	PL-PE 34:4, PL-PE 35:4, PL-PE 36:4, PL-PE 37:4, PL-PE 38:4, PL-PE 39:4, PL-PE 40:4, PL-PE 42:4, PL-PE 36:5, PL-PE 37:5, PL-PE 38:5, PL-PE 40:5, PL-PE 36:6, PL-PE 37:6, PL-PE 38:6, PL-PE 39:6, PL-PE 40:6, PL-PE 42:6
SM-sat	SM 30:0, SM 32:0, SM 33:0, SM 34:0, SM 36:0, SM 38:0, SM 40:0, SM 41:0, SM 29:1, SM 30:1, SM 31:1, SM 32:1, SM 33:1, SM 34:1, SM 35:1, SM 36:1, SM 37:1, SM 38:1, SM 39:1, SM 40:1, SM 41:1, SM 42:1, SM 43:1, SM 44:1
SM-mono	SM 30:2, SM 32:2, SM 33:2, SM 34:2, SM 35:2, SM 36:2, SM 37:2, SM 38:2, SM 39:2, SM 40:2, SM 41:2, SM 42:2, SM 43:2, SM 44:2, SM 34:3, SM 36:3, SM 38:3, SM 39:3, SM 40:3, SM 41:3, SM 42:3, SM 43:3, SM 44:3
SM-poly	SM 36:4, SM 38:4, SM 40:4, SM 42:4, SM 43:4, SM 44:4, SM 45:4, SM 38:5, SM 40:5, SM 42:5, SM 44:5, SM 47:5, SM 35:6, SM 42:6, SM 44:6, SM 42:7, SM 43:7, SM 44:7
TG-sat	TG 36:0, TG 38:0, TG 39:0, TG 40:0, TG 41:0, TG 42:0, TG 43:0, TG 44:0, TG 45:0, TG 46:0, TG 47:0, TG 48:0, TG 49:0, TG 50:0, TG 51:0, TG 52:0, TG 53:0, TG 54:0, TG 56:0, TG 40:1, TG 42:1, TG 44:1, TG 45:1, TG 46:1, TG 47:1, TG 48:1, TG 49:1, TG 50:1, TG 51:1, TG 52:1, TG 53:1, TG 54:1, TG 55:1, TG 56:1, TG 58:1, TG 62:1, TG 42:2, TG 44:2, TG 46:2, TG 47:2, TG 48:2, TG 49:2, TG 50:2, TG 51:2, TG 52:2, TG 53:2, TG 54:2, TG 55:2, TG 56:2, TG 58:2

TG-mono	TG 42:3, TG 46:3, TG 47:3, TG 48:3, TG 49:3, TG 50:3, TG 51:3, TG 52:3, TG 53:3, TG 54:3, TG 55:3, TG 56:3, TG 58:3, TG 48:4, TG 50:4, TG 51:4, TG 52:4, TG 53:4, TG 54:4, TG 56:4, TG 58:4, TG 50:5, TG 51:5, TG 52:5, TG 53:5, TG 54:5, TG 56:5, TG 58:5
TG-poly	TG 50:6, TG 52:6, TG 54:6, TG 56:6, TG 58:6, TG 54:7, TG 56:7, TG 58:7, TG 54:8, TG 56:8, TG 58:8, TG 56:9, TG 58:9, TG 56:10, TG 58:10, TG 60:10, TG 58:11, TG 60:11, TG 60:12, TG 62:12, TG 62:14

Table 2.2. Characteristics of the MMIP participants, stratified by sex (n=106).

Categorical Variables	All n (%)	Males n (%)	Females n (%)	p-value[A]
Parity				
0	33 (31%)	16 (31%)	17 (31%)	0.988
1	45 (42%)	21 (41%)	24 (44%)	
2	21 (20%)	11 (22%)	10 (18%)	
≥3	7 (7%)	3 (6%)	4 (7%)	
Baseline BMI (kg/m²)				
18.5-24.9	64 (62%)	30 (61%)	34 (63%)	0.5037
25.0-29.9	18 (17%)	11 (22%)	7 (13%)	
30.0-34.9	12 (12%)	4 (8%)	8 (15%)	
≥ 35.0	9 (9%)	4 (8%)	5 (9%)	
Delivery Mode				
Vaginal	76 (72%)	35 (69%)	41 (75%)	0.4992
Caesarean Section	30 (28%)	16 (31%)	14 (25%)	
Continuous Variables	All mean±SD (n)	Males mean±SD (n)	Females mean±SD (n)	p-value[B]
Maternal Baseline Characteristics				
Age (years)	32.1±3.6	32.4±4.1	31.7±3.2	0.3233
Weight (kg)	71.1±17.6	69.4±13.9	72.6±20.4	0.3465
Height (cm)	165±7 (103)	165±6 (49)	165±7 (54)	0.8589
BMI (kg/m²)	25.8±6.0 (103)	25.4±5.3 (49)	26.2±6.6 (54)	0.5238
Maternal and Newborn Delivery Characteristics				
Gestation age (days)	278±7	278±8	278±6	0.9812
GWG (kg)	13.2±5.2	13.9±4.5	12.6±5.8	0.2058
Birth weight (g)	3510±436 (105)	3638±467	3390±370 (54)	0.0032
Fenton BW z-score	0.09±0.87 (105)	0.20±0.95	-0.01±0.78 (54)	0.2055
Fenton BW percentile	53.1±26.1 (105)	56.0±28.2	50.4±23.8 (54)	0.2701
Head Circumference (cm)	35±1 (101)	35.2±1.2 (48)	34.7±1.3 (53)	0.049
Fenton HC z-score	0.10±0.86 (101)	0.16±0.72 (48)	0.04±0.96 (53)	0.4847
Fenton HC percentile	52.5±25.5 (101)	54.9±22.9 (48)	50.4±27.6 (53)	0.3749

Values are n(%) or mean±SD. Stratified by males (n=51) and females (n=55). [A]Represents Pearson's chi-square test for categorical variables. [B]Represents paired t-test for continuous variables. If sample size differs, mean±SD (n).

Figure S2.1. Relationship between maternal baseline BMI, gestational weight gain, and Fenton BW percentile.

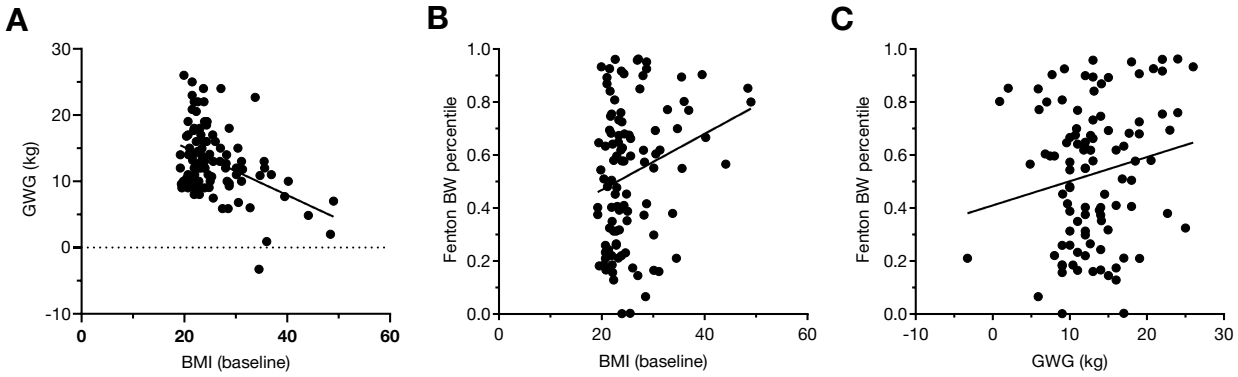

(A) Maternal baseline BMI is inversely associated with gestational weight gain (r^2 0.18, P<0.001). **(B)** Maternal baseline BMI is positively associated with Fenton BW percentile (r^2 0.06, p=0.0014). **(C)** Maternal gestational weight gain is trending towards a positive association with Fenton BW percentile (r^2 0.03, p=0.070).

Figure 2.2. Dynamic changes in maternal and cord blood plasma lipidome during pregnancy.

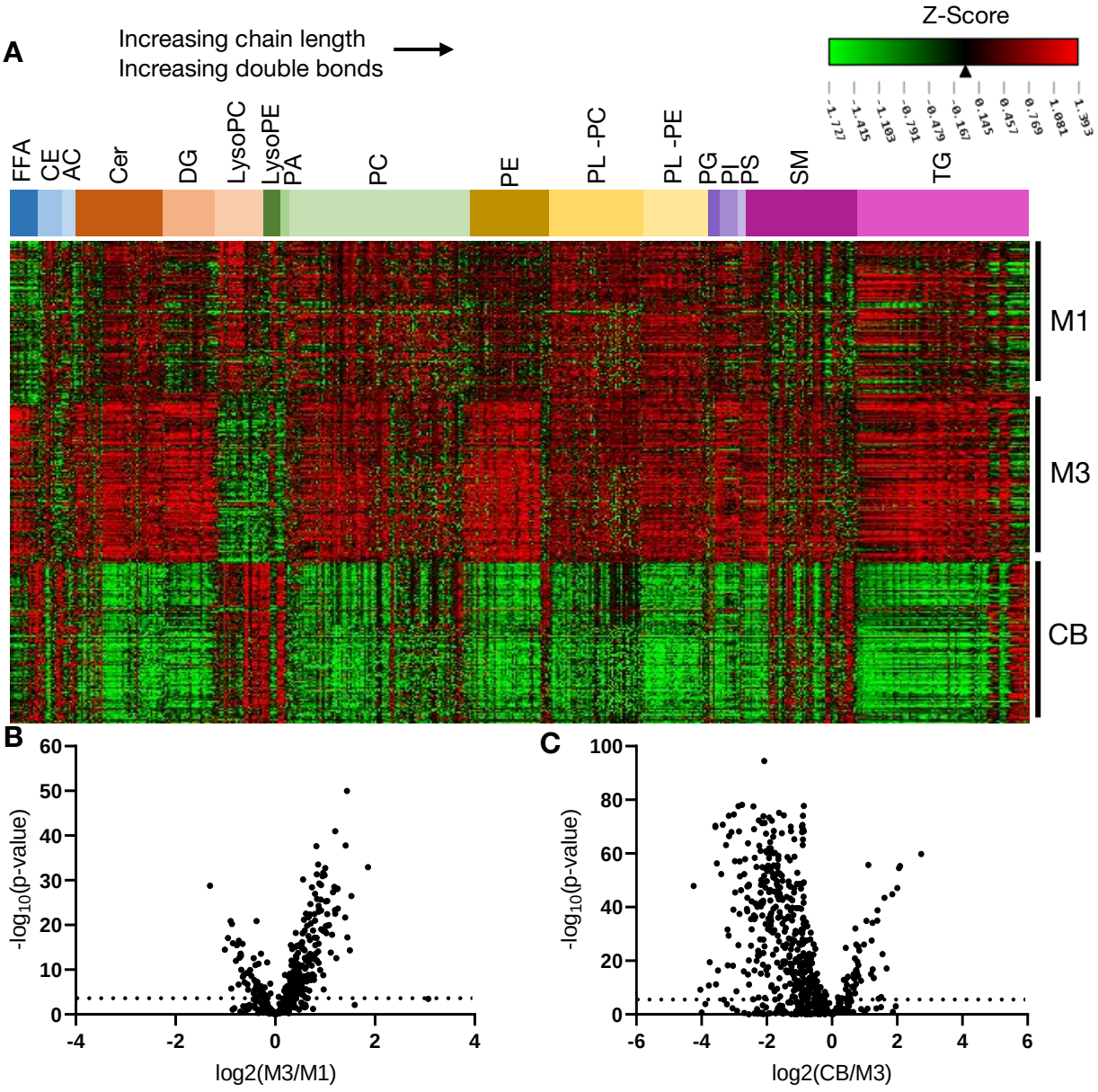

(A) Heat Map of standardized peak intensity for individual lipids (mean 0, standard deviation 1). Lipids are grouped by lipid class with increasing total chain length and double bond from left to right in each lipid class. **(B)** Differences between M1 and M3 lipidome using log2FC. Lipids that are greater in M1 than M3 have a positive log2FC. Of the 573 lipid species analyzed, 35% were significantly increased and 10% were decreased (Bonferroni adjusted, α=0.05/573). **(C)** Differences between M3 and CB lipidome using log2FC. Of the 573 lipid species analyzed, 10% were significantly increased and 61% were decreased (Bonferroni adjusted, α=0.05/573). Lipids that are greater in M3 than CB have a positive log2FC.

Table S2.2. Comparison of M1-M3 lipid raw peak intensities. Paired t-tests identified differences in raw peak intensities of individual plasma lipids between M1 to M3. The fold change between lipids in M1 and M3 was calculated by $\log_2$(M3/M1), where a positive FC indicates increases in that lipid between M1 and M3 and a negative FC indicates decreases in that lipid between M1 and M3. Significance highlighted in red (Bonferroni adjusted, α=0.05/573).

Metabolite	M1		M3		M1 M3 t-test		
	Mean	Std dev	Mean	Std dev	$\log_2$(M3/M1)	p-value	-log10(p-value)
FFA(16:0)	5.68E+07	8.07E+06	7.06E+07	1.39E+07	0.314	3.46E-16	15.461
FFA(18:0)	6.89E+07	5.46E+06	7.23E+07	7.23E+06	0.071	1.13E-04	3.948
FFA(18:1)	2.37E+07	1.42E+07	5.46E+07	2.45E+07	1.203	3.16E-23	22.501
FFA(18:2)	1.62E+07	8.75E+06	3.37E+07	1.50E+07	1.055	1.29E-20	19.889
FFA(20:0)	1.99E+06	2.46E+05	2.10E+06	3.40E+05	0.083	4.17E-03	2.380
FFA(20:1)	4.66E+05	2.38E+05	1.34E+06	6.81E+05	1.526	3.46E-27	26.461
FFA(20:2)	4.17E+05	2.33E+05	9.58E+05	4.24E+05	1.199	4.63E-24	23.335
FFA(20:4) Arachidonic acid	1.45E+06	6.69E+05	1.73E+06	6.73E+05	0.260	2.22E-03	2.653
FFA(22:0)	5.59E+05	1.43E+05	6.46E+05	2.71E+05	0.208	3.99E-03	2.399
FFA(22:1)	1.41E+05	4.34E+04	2.58E+05	1.57E+05	0.871	3.09E-12	11.510
FFA(22:2)	3.64E+04	1.30E+04	8.29E+04	3.39E+04	1.186	3.01E-29	28.521
FFA(22:3)	4.85E+04	1.69E+04	8.90E+04	3.17E+04	0.877	2.20E-24	23.657
FFA(24:0)	3.76E+05	1.53E+05	3.86E+05	1.73E+05	0.039	6.47E-01	0.189
FFA(24:1)	2.62E+05	6.80E+04	3.83E+05	1.08E+05	0.548	7.64E-19	18.117
FFA(24:2)	7.47E+04	2.29E+04	1.21E+05	3.54E+04	0.690	4.02E-23	22.396
FFA(24:3)	1.23E+04	4.71E+03	1.72E+04	6.76E+03	0.487	3.69E-09	8.433
16:0 Cholesteryl ester	4.57E+04	1.20E+04	4.72E+04	1.76E+04	0.046	4.75E-01	0.324
16:1 Cholesteryl ester	2.22E+04	1.04E+04	3.32E+04	1.51E+04	0.582	2.96E-09	8.528
17:1 Cholesteryl ester	6.55E+03	2.87E+03	7.14E+03	2.74E+03	0.123	1.32E-01	0.881
18:0 Cholesteryl ester	1.89E+04	8.57E+03	1.78E+04	7.35E+03	-0.083	3.38E-01	0.471
18:1 Cholesteryl ester	5.79E+05	1.19E+05	6.98E+05	1.59E+05	0.269	3.76E-09	8.424
18:2 Cholesteryl ester	3.30E+06	5.46E+05	3.19E+06	6.38E+05	-0.048	1.91E-01	0.720
18:3 Cholesteryl ester	1.15E+04	2.65E+04	9.06E+03	2.09E+04	-0.339	4.65E-01	0.333
20:3 Cholesteryl ester	3.50E+05	8.97E+04	3.10E+05	8.99E+04	-0.175	1.37E-03	2.863
20:4 Cholesteryl ester	1.48E+04	9.05E+03	1.67E+04	1.00E+04	0.175	1.47E-01	0.832
20:5 Cholesteryl ester	9.86E+04	7.82E+04	5.35E+04	5.23E+04	-0.883	1.63E-06	5.789
22:4 Cholesteryl ester	1.52E+04	5.45E+03	1.17E+04	4.62E+03	-0.384	6.65E-07	6.177
22:5 Cholesteryl ester	4.07E+04	1.25E+04	3.39E+04	1.24E+04	-0.263	1.03E-04	3.985
22:6 Cholesteryl ester	2.33E+05	8.96E+04	1.77E+05	8.09E+04	-0.398	3.11E-06	5.507
Acylcarnitine 16:0	6.54E+04	2.02E+04	6.95E+04	2.48E+04	0.089	1.81E-01	0.741
Acylcarnitine 18:0	3.10E+04	1.05E+04	2.88E+04	1.39E+04	-0.108	1.89E-01	0.723
Acylcarnitine 18:1	1.22E+05	5.05E+04	1.32E+05	5.46E+04	0.111	1.79E-01	0.747
Acylcarnitine 18:2	7.63E+04	3.84E+04	7.12E+04	3.93E+04	-0.100	3.40E-01	0.469
Acylcarnitine 24:0	1.82E+03	1.08E+03	1.86E+03	9.37E+02	0.031	7.77E-01	0.109
Acylcarnitine 26:0	2.69E+03	1.69E+03	2.53E+03	1.42E+03	-0.090	4.47E-01	0.350
Cer[NDS] 34:0	1.07E+05	2.19E+04	1.20E+05	2.95E+04	0.168	2.68E-04	3.572
Cer[NDS] 36:0	3.58E+04	1.20E+04	7.37E+04	2.97E+04	1.042	4.28E-26	25.369
Cer[NDS] 38:0	3.60E+03	1.19E+03	5.22E+03	1.99E+03	0.536	1.19E-11	10.924
Cer[NDS] 40:0	3.17E+05	1.07E+05	5.04E+05	1.39E+05	0.667	1.86E-22	21.731
Cer[NDS] 41:0	2.10E+04	6.63E+03	3.03E+04	8.43E+03	0.532	1.61E-16	15.792
Cer[NDS] 42:0	5.53E+04	1.80E+04	8.59E+04	2.46E+04	0.637	1.55E-20	19.809
Cer[NDS] 42:1	3.19E+05	8.69E+04	4.38E+05	1.19E+05	0.454	1.85E-14	13.732
Cer[NS] 32:1	3.63E+04	1.06E+04	3.90E+04	1.14E+04	0.102	7.91E-02	1.102
Cer[NS] 33:1	2.97E+04	6.80E+03	2.79E+04	8.19E+03	-0.095	6.88E-02	1.163

Cer[NS] 33:4	3.42E+03	2.51E+03	3.45E+03	2.51E+03	0.011	9.38E-01	0.028
Cer[NS] 34:1	1.59E+04	3.85E+03	2.09E+04	5.73E+03	0.398	1.56E-12	11.806
Cer[NS] 34:2	2.34E+04	6.03E+03	2.49E+04	7.48E+03	0.088	1.18E-01	0.928
Cer[NS] 35:1	1.53E+07	1.62E+06	1.37E+07	1.52E+06	-0.161	2.35E-12	11.630
Cer[NS] 36:1	1.34E+05	3.17E+04	2.18E+05	6.55E+04	0.705	2.21E-25	24.655
Cer[NS] 36:2	2.02E+04	5.61E+03	2.62E+04	9.87E+03	0.375	1.45E-07	6.839
Cer[NS] 37:1	6.74E+04	1.52E+04	8.99E+04	3.30E+04	0.416	1.11E-09	8.956
Cer[NS] 37:4	1.80E+04	8.47E+03	1.51E+04	6.43E+03	-0.258	4.64E-03	2.334
Cer[NS] 38:1	2.14E+05	5.79E+04	3.19E+05	8.17E+04	0.576	6.52E-22	21.186
Cer[NS] 38:2	2.88E+04	7.67E+03	4.12E+04	1.20E+04	0.514	1.77E-16	15.751
Cer[NS] 39:1	2.70E+05	7.50E+04	3.53E+05	9.12E+04	0.386	8.94E-12	11.049
Cer[NS] 39:2	3.59E+04	1.12E+04	4.50E+04	1.32E+04	0.326	1.88E-07	6.727
Cer[NS] 40:1	1.24E+06	3.51E+05	1.76E+06	4.98E+05	0.508	4.65E-16	15.333
Cer[NS] 40:2	2.29E+05	6.42E+04	2.95E+05	7.92E+04	0.365	2.34E-10	9.630
Cer[NS] 41:1	8.06E+04	2.31E+04	1.06E+05	2.94E+04	0.401	1.66E-11	10.779
Cer[NS] 41:2	4.06E+05	1.04E+05	4.99E+05	1.31E+05	0.298	3.08E-08	7.512
Cer[NS] 41:3	5.03E+04	1.54E+04	6.46E+04	2.18E+04	0.362	9.47E-08	7.024
Cer[NS] 42:1	3.19E+05	8.69E+04	4.38E+05	1.19E+05	0.454	1.85E-14	13.732
Cer[NS] 42:2	1.43E+06	3.51E+05	1.95E+06	4.83E+05	0.441	4.24E-16	15.373
Cer[NS] 42:3	8.38E+03	2.99E+03	1.10E+04	4.27E+03	0.389	6.82E-07	6.166
Cer[NS] 43:1	6.74E+05	2.14E+05	6.77E+05	2.27E+05	0.006	9.28E-01	0.032
Cer[NS] 43:2	1.56E+04	5.20E+03	1.63E+04	5.83E+03	0.065	3.48E-01	0.458
Cer[NS] 43:3	7.39E+03	2.98E+03	1.02E+04	3.55E+03	0.459	3.96E-09	8.402
Cer[NS] 44:1	2.63E+04	5.83E+03	2.62E+04	7.21E+03	-0.009	8.51E-01	0.070
Cer[AS] 41:1	2.26E+04	9.70E+03	3.75E+04	1.71E+04	0.726	3.98E-13	12.401
Cer[AS] 42:2	8.56E+04	2.81E+04	9.28E+04	3.52E+04	0.116	1.02E-01	0.990
Cer[EODS] 49:1	4.93E+03	2.44E+03	8.42E+03	3.86E+03	0.772	1.87E-13	12.727
Cer[EODS] 53:0	1.03E+04	3.45E+03	7.86E+03	2.90E+03	-0.386	1.06E-07	6.976
Cer[EODS] 57:2	9.93E+03	3.94E+03	9.66E+03	4.45E+03	-0.040	6.41E-01	0.193
Cer[NP] 34:0	5.17E+03	2.63E+03	4.12E+03	1.99E+03	-0.328	1.18E-03	2.930
Cer[NP] 40:0	6.95E+04	2.58E+04	7.25E+04	2.53E+04	0.061	3.94E-01	0.404
Cer[NP] 42:0	1.12E+05	3.24E+04	1.07E+05	3.07E+04	-0.062	2.78E-01	0.557
Cer[NP] 42:1	6.83E+04	2.58E+04	6.41E+04	2.34E+04	-0.092	2.14E-01	0.670
GlcCer[NS] 32:1	3.15E+03	1.60E+03	3.77E+03	1.69E+03	0.256	7.17E-03	2.145
GlcCer[NS] 34:1	1.43E+05	3.15E+04	1.92E+05	5.62E+04	0.426	2.00E-13	12.699
GlcCer[NS] 38:1	8.90E+03	4.03E+03	1.19E+04	3.71E+03	0.418	5.68E-08	7.245
GlcCer[NS] 40:1	1.90E+05	5.23E+04	2.47E+05	7.97E+04	0.380	3.48E-09	8.459
GlcCer[NS] 41:1	1.56E+04	4.32E+03	1.84E+04	5.62E+03	0.237	7.59E-05	4.120
GlcCer[NS] 41:2	8.91E+03	4.44E+03	1.15E+04	5.62E+03	0.368	2.55E-04	3.593
GlcCer[NS] 42:1	5.01E+04	1.29E+04	6.22E+04	1.56E+04	0.310	4.44E-09	8.352
GlcCer[NS] 42:2	3.98E+04	8.63E+03	4.67E+04	1.24E+04	0.231	4.40E-06	5.357
GlcCer[NS] 43:1	6.97E+03	4.72E+03	7.32E+03	3.69E+03	0.071	5.46E-01	0.263
MG 26:4	2.53E+04	7.84E+03	2.82E+04	9.60E+03	0.157	1.63E-02	1.786
DG 30:0	9.81E+03	1.07E+04	1.92E+04	1.69E+04	0.969	2.57E-06	5.591
DG 30:1	5.04E+03	4.75E+03	7.92E+03	6.32E+03	0.651	2.36E-04	3.628
DG 31:0	2.56E+03	2.31E+03	4.10E+03	2.47E+03	0.680	4.77E-06	5.321
DG 32:0	2.57E+04	2.42E+04	7.25E+04	5.16E+04	1.496	4.77E-15	14.321
DG 32:1	3.57E+04	2.92E+04	8.35E+04	5.58E+04	1.225	2.70E-13	12.569
DG 32:2	1.56E+04	1.04E+04	2.62E+04	1.35E+04	0.746	1.10E-09	8.959
DG 33:0	3.24E+03	2.15E+03	5.29E+03	2.92E+03	0.709	2.10E-08	7.677
DG 33:1	6.15E+03	4.88E+03	1.15E+04	6.45E+03	0.901	1.13E-10	9.946
DG 34:0	2.57E+04	1.47E+04	4.58E+04	2.29E+04	0.835	8.80E-13	12.056
DG 34:2	1.39E+05	7.30E+04	3.33E+05	1.56E+05	1.257	2.19E-24	23.660
DG 34:3	3.50E+04	1.82E+04	6.81E+04	2.90E+04	0.961	2.10E-19	18.678
DG 35:1	6.72E+03	3.75E+03	1.18E+04	5.17E+03	0.812	2.52E-14	13.599

DG 35:2	7.43E+03	3.41E+03	1.36E+04	6.14E+03	0.869	1.45E-16	15.840
DG 35:3	4.03E+03	2.12E+03	6.92E+03	3.10E+03	0.780	1.28E-13	12.894
DG 36:0	1.17E+04	3.30E+03	1.31E+04	3.47E+03	0.167	2.38E-03	2.623
DG 36:1	4.31E+04	2.17E+04	8.75E+04	4.14E+04	1.023	6.93E-19	18.159
DG 36:2	2.14E+05	8.10E+04	4.33E+05	2.02E+05	1.015	1.61E-20	19.792
DG 36:3	2.49E+05	9.74E+04	4.97E+05	2.38E+05	0.996	2.80E-19	18.553
DG 36:4	1.65E+05	7.44E+04	2.68E+05	1.15E+05	0.704	2.90E-13	12.538
DG 36:5	1.99E+04	1.04E+04	2.72E+04	1.26E+04	0.447	8.37E-06	5.077
DG 38:0	1.91E+03	1.05E+03	2.18E+03	1.29E+03	0.192	9.33E-02	1.030
DG 38:1	8.37E+03	4.37E+03	1.00E+04	5.02E+03	0.257	1.24E-02	1.907
DG 38:2	9.77E+03	3.62E+03	2.18E+04	8.99E+03	1.158	4.64E-28	27.334
DG 38:3	1.33E+04	4.85E+03	2.52E+04	9.48E+03	0.918	6.15E-24	23.211
DG 38:4	2.09E+04	7.51E+03	3.53E+04	1.28E+04	0.756	1.68E-19	18.775
DG 38:5	3.91E+04	2.01E+04	6.20E+04	2.42E+04	0.664	1.96E-12	11.708
DG 38:6	3.47E+04	1.92E+04	5.16E+04	2.16E+04	0.572	7.70E-09	8.114
DG 38:7	4.72E+03	3.52E+03	5.74E+03	4.20E+03	0.282	5.64E-02	1.249
DG 40:7	1.39E+04	8.78E+03	2.38E+04	1.38E+04	0.775	2.41E-09	8.619
DG 40:8	6.18E+03	4.52E+03	9.19E+03	6.13E+03	0.572	6.62E-05	4.179
LysoPC 14:0	3.99E+04	1.99E+04	2.54E+04	1.39E+04	-0.652	3.78E-09	8.423
LysoPC 15:0	5.10E+04	1.94E+04	2.80E+04	1.18E+04	-0.868	6.30E-21	20.201
LysoPC 16:0	5.11E+06	1.26E+06	3.79E+06	1.21E+06	-0.433	2.58E-13	12.589
LysoPC 16:1	9.38E+04	4.87E+04	6.13E+04	3.52E+04	-0.615	7.06E-08	7.151
LysoPC 17:0	1.71E+06	1.72E+05	1.59E+06	1.36E+05	-0.102	1.38E-07	6.861
LysoPC 17:1	2.28E+04	7.89E+03	1.45E+04	5.35E+03	-0.654	1.62E-16	15.790
LysoPC 18:0	3.87E+06	1.24E+06	2.50E+06	1.85E+06	-0.628	1.43E-09	8.844
LysoPC 18:1	1.81E+06	5.76E+05	1.09E+06	5.57E+05	-0.730	3.46E-17	16.461
LysoPC 18:2	2.12E+06	9.32E+05	8.57E+05	3.15E+05	-1.309	1.62E-29	28.791
LysoPC 18:3	2.71E+04	1.22E+04	1.50E+04	6.29E+03	-0.851	1.14E-16	15.943
LysoPC 19:0	3.41E+04	8.11E+03	2.59E+04	8.42E+03	-0.397	9.64E-12	11.016
LysoPC 19:1	1.08E+04	3.58E+03	7.28E+03	4.33E+03	-0.573	5.56E-10	9.255
LysoPC 20:0	2.18E+04	7.88E+03	1.35E+04	6.94E+03	-0.696	2.77E-14	13.558
LysoPC 20:1	3.83E+04	1.54E+04	2.61E+04	1.76E+04	-0.556	1.86E-07	6.730
LysoPC 20:2	2.99E+04	1.01E+04	1.85E+04	1.04E+04	-0.692	5.50E-14	13.260
LysoPC 20:3	2.20E+05	8.09E+04	1.29E+05	6.79E+04	-0.771	3.46E-16	15.461
LysoPC 20:4	5.37E+05	2.00E+05	2.78E+05	1.99E+05	-0.947	8.73E-18	17.059
LysoPC 20:5	1.28E+05	7.98E+04	7.71E+04	5.79E+04	-0.736	2.23E-07	6.652
LysoPC 22:0	9.32E+03	4.06E+03	6.36E+03	3.83E+03	-0.552	1.28E-07	6.894
LysoPC 22:4	1.93E+04	8.41E+03	1.33E+04	9.91E+03	-0.544	2.89E-06	5.539
LysoPC 22:5	3.69E+04	1.45E+04	2.24E+04	1.22E+04	-0.718	2.18E-13	12.662
LysoPC 22:6	1.06E+05	4.29E+04	6.59E+04	2.97E+04	-0.691	9.88E-14	13.005
LysoPC 24:0	1.60E+04	5.61E+03	1.13E+04	4.50E+03	-0.504	1.21E-10	9.916
LysoPC 24:1	5.54E+03	2.03E+03	3.98E+03	1.61E+03	-0.477	2.75E-09	8.561
LysoPC 24:4	1.71E+03	1.13E+03	1.66E+03	1.05E+03	-0.038	7.65E-01	0.116
LysoPC 26:0	4.15E+03	1.86E+03	2.58E+03	1.46E+03	-0.682	1.08E-10	9.968
LysoPC 26:1	3.10E+03	1.43E+03	2.29E+03	1.25E+03	-0.435	1.91E-05	4.718
LysoPC 26:2	1.97E+03	1.02E+03	1.50E+03	9.88E+02	-0.391	8.22E-04	3.085
LysoPC 26:4	3.24E+03	1.33E+03	3.44E+03	1.53E+03	0.087	3.10E-01	0.508
LysoPE 16:0	1.55E+05	6.14E+04	1.55E+05	6.77E+04	-0.004	9.63E-01	0.016
LysoPE 18:0	8.39E+04	2.66E+04	8.77E+04	4.12E+04	0.064	4.27E-01	0.369
LysoPE 18:1	1.95E+05	8.73E+04	1.46E+05	6.46E+04	-0.424	4.32E-06	5.364
LysoPE 18:2	2.06E+05	1.18E+05	1.02E+05	4.49E+04	-1.011	3.51E-15	14.454
LysoPE 20:3	3.49E+04	1.69E+04	2.02E+04	1.07E+04	-0.790	1.06E-12	11.974
LysoPE 20:4	1.67E+05	6.62E+04	8.94E+04	3.36E+04	-0.897	1.35E-21	20.870
LysoPE 22:5	4.24E+04	1.93E+04	3.50E+04	1.80E+04	-0.279	3.97E-03	2.401
LysoPE 22:6	6.29E+04	2.52E+04	5.04E+04	1.80E+04	-0.320	4.62E-05	4.335

LysoPE 24:0	9.07E+03	3.88E+03	7.91E+03	4.07E+03	-0.198	3.39E-02	1.469
PA 34:1	9.75E+03	7.24E+03	9.89E+03	6.66E+03	0.020	8.89E-01	0.051
PA 34:2	1.64E+04	5.27E+03	1.35E+04	4.59E+03	-0.281	2.84E-05	4.546
PA 36:4	9.95E+03	3.41E+03	9.76E+03	4.57E+03	-0.028	7.30E-01	0.137
PA 38:6	7.13E+03	4.15E+03	7.91E+03	3.48E+03	0.150	1.40E-01	0.854
PC 22:0	1.59E+03	1.41E+03	1.35E+03	1.31E+03	-0.237	1.99E-01	0.701
PC 23:0	1.85E+03	1.21E+03	2.02E+03	1.22E+03	0.126	3.13E-01	0.505
PC 24:0	4.10E+03	4.20E+03	2.87E+03	2.12E+03	-0.516	7.52E-03	2.124
PC 25:1	2.28E+03	3.17E+03	1.50E+03	1.35E+03	-0.600	2.16E-02	1.666
PC 26:0	1.28E+04	1.35E+04	9.75E+03	7.57E+03	-0.395	4.20E-02	1.377
PC 26:1	1.73E+03	1.39E+03	1.29E+03	1.05E+03	-0.422	1.04E-02	1.984
PC 28:0	8.03E+04	7.80E+04	9.11E+04	6.28E+04	0.182	2.69E-01	0.570
PC 28:1	8.05E+03	6.91E+03	7.82E+03	5.30E+03	-0.043	7.79E-01	0.109
PC 29:0	2.40E+04	1.60E+04	2.65E+04	1.47E+04	0.139	2.49E-01	0.604
PC 30:0	1.64E+05	7.27E+04	1.90E+05	7.95E+04	0.208	1.56E-02	1.806
PC 30:1	1.25E+05	7.92E+04	1.83E+05	1.18E+05	0.547	4.07E-05	4.390
PC 30:2	1.72E+04	1.46E+04	1.77E+04	1.04E+04	0.040	7.81E-01	0.107
PC 30:3	1.29E+04	9.52E+03	1.32E+04	6.80E+03	0.040	7.52E-01	0.124
PC 31:0	8.26E+04	3.49E+04	7.40E+04	2.69E+04	-0.160	4.37E-02	1.360
PC 31:1	4.51E+04	2.32E+04	6.01E+04	2.94E+04	0.412	5.75E-05	4.241
PC 31:2	2.26E+05	8.75E+04	6.02E+05	2.24E+05	1.411	1.60E-38	37.796
PC 32:0	1.68E+06	2.75E+05	1.92E+06	2.82E+05	0.195	1.45E-09	8.837
PC 32:1	1.61E+06	6.87E+05	2.54E+06	9.93E+05	0.662	9.78E-14	13.010
PC 32:2	1.36E+06	5.07E+05	1.90E+06	6.89E+05	0.481	6.26E-10	9.203
PC 32:3	4.11E+04	2.06E+04	5.38E+04	2.72E+04	0.388	1.71E-04	3.766
PC 32:4	1.80E+04	9.48E+03	2.19E+04	1.06E+04	0.279	5.62E-03	2.250
PC 33:0	1.12E+05	3.65E+04	1.13E+05	3.21E+04	0.010	8.73E-01	0.059
PC 33:1	8.58E+04	4.12E+04	1.01E+05	3.96E+04	0.237	6.33E-03	2.198
PC 33:2	5.05E+05	1.75E+05	1.01E+06	3.15E+05	1.004	1.96E-33	32.708
PC 33:3	3.83E+04	1.32E+04	4.32E+04	1.43E+04	0.174	1.00E-02	1.999
PC 34:0	4.29E+05	1.14E+05	5.48E+05	2.09E+05	0.356	5.40E-07	6.267
PC 34:1	1.99E+06	1.21E+06	3.89E+06	2.85E+06	0.964	1.64E-09	8.784
PC 34:2	1.05E+07	1.92E+07	8.78E+07	2.18E+08	3.068	3.38E-04	3.471
PC 34:3	3.37E+06	8.83E+05	4.51E+06	1.16E+06	0.417	8.90E-14	13.051
PC 34:4	4.91E+05	2.05E+05	5.28E+05	2.02E+05	0.104	1.91E-01	0.720
PC 34:5	1.11E+04	8.95E+03	9.07E+03	7.99E+03	-0.287	8.74E-02	1.058
PC 35:1	3.78E+04	2.42E+04	3.47E+04	1.01E+04	-0.121	2.34E-01	0.631
PC 35:2	1.06E+05	5.47E+04	1.14E+05	5.57E+04	0.099	3.20E-01	0.495
PC 35:3	2.56E+05	5.62E+04	2.22E+05	4.20E+04	-0.209	9.09E-07	6.041
PC 35:4	3.41E+05	1.00E+05	2.94E+05	8.74E+04	-0.212	3.82E-04	3.418
PC 35:5	2.97E+04	1.89E+04	2.69E+04	1.67E+04	-0.143	2.53E-01	0.596
PC 35:6	3.24E+05	1.32E+05	6.11E+05	1.79E+05	0.916	1.15E-29	28.938
PC 35:7	1.28E+04	6.29E+03	2.64E+04	1.07E+04	1.042	3.56E-23	22.449
PC 36:0	1.38E+05	3.98E+04	1.48E+05	4.18E+04	0.101	7.41E-02	1.130
PC 36:1	3.31E+06	9.70E+05	4.02E+06	1.07E+06	0.280	9.13E-07	6.040
PC 36:2	4.42E+05	7.54E+05	7.46E+05	1.48E+06	0.756	6.00E-02	1.222
PC 36:3	2.90E+06	5.33E+05	3.29E+06	6.56E+05	0.179	5.40E-06	5.268
PC 36:4	3.39E+06	8.01E+05	3.52E+06	7.26E+05	0.051	2.43E-01	0.615
PC 36:5	2.18E+04	6.35E+04	1.34E+04	3.57E+04	-0.700	2.38E-01	0.623
PC 36:6	2.56E+05	1.13E+05	2.71E+05	1.26E+05	0.083	3.61E-01	0.443
PC 36:7	5.00E+04	1.61E+04	4.55E+04	1.24E+04	-0.135	2.51E-02	1.600
PC 37:1	3.78E+04	1.43E+04	3.79E+04	1.22E+04	0.003	9.63E-01	0.016
PC 37:2	5.18E+04	3.34E+04	5.13E+04	3.66E+04	-0.013	9.21E-01	0.036
PC 37:3	7.08E+04	3.42E+04	6.88E+04	3.05E+04	-0.042	6.49E-01	0.188
PC 37:4	6.32E+05	2.21E+05	4.73E+05	1.74E+05	-0.419	2.11E-08	7.676

PC 37:5	9.04E+04	3.49E+04	1.79E+05	5.53E+04	0.987	7.36E-32	31.133
PC 37:6	1.70E+05	6.28E+04	1.49E+05	5.64E+04	-0.195	9.11E-03	2.040
PC 37:7	5.07E+04	2.20E+04	8.81E+04	2.84E+04	0.798	1.04E-21	20.981
PC 38:1	5.42E+04	1.49E+04	5.84E+04	1.49E+04	0.107	4.19E-02	1.378
PC 38:2	1.48E+05	3.85E+04	1.51E+05	4.51E+04	0.036	5.19E-01	0.285
PC 38:3	1.18E+06	3.13E+05	1.10E+06	2.54E+05	-0.100	4.49E-02	1.348
PC 38:4	1.21E+07	2.62E+06	9.57E+06	2.38E+06	-0.337	4.83E-12	11.316
PC 38:5	8.91E+05	2.14E+05	8.46E+05	2.05E+05	-0.075	1.20E-01	0.922
PC 38:6	1.18E+07	3.38E+06	1.20E+07	3.04E+06	0.023	6.70E-01	0.174
PC 38:7	1.41E+05	5.15E+04	1.65E+05	5.24E+04	0.227	8.81E-04	3.055
PC 39:3	3.37E+04	1.17E+04	3.03E+04	1.10E+04	-0.154	2.90E-02	1.538
PC 39:4	9.13E+04	2.26E+04	7.48E+04	2.36E+04	-0.288	4.64E-07	6.334
PC 39:5	3.76E+03	4.20E+03	3.90E+03	5.10E+03	0.054	8.22E-01	0.085
PC 39:6	2.06E+05	7.64E+04	1.49E+05	5.71E+04	-0.469	3.25E-09	8.488
PC 39:7	2.12E+04	8.48E+03	1.81E+04	6.38E+03	-0.228	2.93E-03	2.534
PC 40:0	3.98E+03	2.10E+03	4.83E+03	3.48E+03	0.281	3.15E-02	1.502
PC 40:1	1.20E+04	6.27E+03	1.32E+04	6.40E+03	0.139	1.67E-01	0.777
PC 40:2	3.82E+04	2.49E+04	4.37E+04	2.78E+04	0.193	1.32E-01	0.878
PC 40:3	6.18E+04	2.86E+04	6.68E+04	2.66E+04	0.112	1.89E-01	0.724
PC 40:4	1.49E+05	5.06E+04	1.46E+05	3.56E+04	-0.032	5.90E-01	0.229
PC 40:5	2.61E+05	7.93E+04	2.57E+05	6.99E+04	-0.023	6.88E-01	0.163
PC 40:6	2.67E+06	7.44E+05	2.39E+06	6.05E+05	-0.160	3.02E-03	2.520
PC 40:7	9.51E+04	2.64E+04	8.81E+04	2.03E+04	-0.112	2.98E-02	1.526
PC 40:8	2.32E+05	5.99E+04	2.05E+05	4.74E+04	-0.179	3.22E-04	3.492
PC 40:9	1.44E+04	6.30E+03	1.38E+04	6.02E+03	-0.067	4.39E-01	0.358
PC 40:10	3.06E+04	8.89E+03	2.50E+04	7.74E+03	-0.291	1.97E-06	5.705
PC 41:5	1.19E+04	9.14E+03	1.15E+04	1.03E+04	-0.038	8.19E-01	0.087
PC 41:6	1.87E+04	8.05E+03	1.55E+04	7.24E+03	-0.266	3.08E-03	2.512
PC 42:1	1.29E+04	1.03E+04	1.51E+04	2.06E+04	0.225	3.30E-01	0.481
PC 42:2	1.81E+04	1.02E+04	1.71E+04	1.05E+04	-0.078	5.02E-01	0.299
PC 42:3	1.85E+04	1.19E+04	1.93E+04	1.32E+04	0.059	6.52E-01	0.186
PC 42:4	1.47E+04	7.62E+03	1.73E+04	1.09E+04	0.241	4.11E-02	1.386
PC 42:5	4.65E+04	1.41E+04	6.18E+04	1.93E+04	0.409	3.65E-10	9.438
PC 42:6	5.08E+04	1.73E+04	5.40E+04	1.62E+04	0.088	1.66E-01	0.780
PC 42:7	4.94E+04	1.86E+04	4.44E+04	1.79E+04	-0.154	4.78E-02	1.320
PC 42:8	2.81E+04	9.27E+03	2.19E+04	6.56E+03	-0.360	5.62E-08	7.250
PC 42:9	2.99E+04	1.03E+04	3.26E+04	1.01E+04	0.122	6.10E-02	1.215
PC 42:10	5.13E+04	1.99E+04	7.00E+04	2.78E+04	0.448	5.59E-08	7.253
PC 42:11	1.11E+04	3.96E+03	8.85E+03	3.94E+03	-0.320	7.05E-05	4.152
PC 44:2	3.07E+03	1.69E+03	3.58E+03	2.78E+03	0.222	1.07E-01	0.971
PC 44:3	1.62E+03	9.88E+02	1.69E+03	8.60E+02	0.057	6.10E-01	0.215
PC 44:4	1.50E+04	1.01E+04	1.44E+04	9.18E+03	-0.062	6.34E-01	0.198
PC 44:5	9.51E+03	7.25E+03	8.86E+03	5.99E+03	-0.103	4.73E-01	0.325
PC 44:6	4.52E+03	2.51E+03	4.30E+03	2.24E+03	-0.071	5.07E-01	0.295
PC 46:4	1.87E+03	1.66E+03	1.65E+03	9.69E+02	-0.179	2.44E-01	0.613
PC 46:5	1.16E+03	6.62E+02	1.22E+03	9.34E+02	0.071	5.97E-01	0.224
PE 30:0	1.03E+04	7.85E+03	1.53E+04	9.99E+03	0.571	7.44E-05	4.128
PE 32:0	2.08E+04	1.03E+04	2.95E+04	1.04E+04	0.502	5.00E-09	8.301
PE 32:1	6.62E+04	3.84E+04	1.81E+05	1.18E+05	1.446	5.98E-18	17.223
PE 32:2	1.14E+04	6.31E+03	3.00E+04	1.63E+04	1.401	2.23E-22	21.651
PE 33:0	9.31E+03	3.80E+03	8.46E+03	3.93E+03	-0.137	1.13E-01	0.946
PE 33:1	1.50E+04	6.70E+03	2.67E+04	1.08E+04	0.830	7.37E-18	17.132
PE 33:2	1.47E+04	7.15E+03	3.50E+04	1.43E+04	1.253	7.23E-29	28.141
PE 34:0	3.63E+06	3.90E+05	3.39E+06	3.90E+05	-0.096	2.07E-05	4.683
PE 34:1	9.46E+04	3.91E+04	2.56E+05	7.33E+04	1.439	1.07E-50	49.971

PE 34:2	1.26E+06	4.28E+05	2.91E+06	8.93E+05	1.203	1.10E-41	40.957
PE 34:3	2.94E+05	1.67E+05	1.07E+06	5.21E+05	1.858	1.25E-33	32.904
PE 34:4	1.00E+04	5.61E+03	1.82E+04	8.32E+03	0.859	8.46E-15	14.072
PE 35:0	1.46E+04	8.57E+03	1.66E+04	1.05E+04	0.186	1.30E-01	0.885
PE 35:1	2.49E+04	1.33E+04	3.93E+04	1.94E+04	0.660	1.55E-09	8.809
PE 35:2	8.06E+04	3.14E+04	1.52E+05	5.08E+04	0.912	2.23E-26	25.651
PE 35:3	1.66E+04	7.70E+03	2.70E+04	1.05E+04	0.698	2.91E-14	13.536
PE 35:4	2.79E+04	1.28E+04	5.29E+04	2.21E+04	0.921	9.99E-20	19.000
PE 36:0	6.36E+04	1.58E+04	5.99E+04	1.77E+04	-0.086	1.10E-01	0.960
PE 36:1	4.51E+05	1.76E+05	8.77E+05	2.56E+05	0.960	2.13E-32	31.672
PE 36:2	5.05E+05	1.75E+05	1.01E+06	3.15E+05	1.004	1.96E-33	32.708
PE 36:3	1.35E+06	4.76E+05	2.35E+06	6.55E+05	0.798	1.05E-27	26.980
PE 36:4	1.65E+06	5.88E+05	2.99E+06	7.34E+05	0.862	3.04E-34	33.517
PE 36:5	3.39E+05	2.16E+05	7.35E+05	4.43E+05	1.114	1.57E-14	13.804
PE 36:6	1.06E+04	5.98E+03	2.35E+04	1.23E+04	1.142	1.50E-18	17.824
PE 37:2	2.31E+04	9.38E+03	3.48E+04	1.22E+04	0.592	2.32E-13	12.634
PE 37:3	3.04E+04	1.19E+04	4.11E+04	1.44E+04	0.435	1.42E-08	7.848
PE 37:4	1.01E+05	3.20E+04	1.51E+05	4.12E+04	0.587	1.87E-19	18.728
PE 37:5	6.38E+04	1.96E+04	6.41E+04	2.08E+04	0.007	9.13E-01	0.039
PE 37:6	7.32E+04	4.42E+04	1.54E+05	6.70E+04	1.076	1.10E-20	19.960
PE 38:1	3.46E+04	1.67E+04	4.47E+04	1.78E+04	0.370	2.92E-05	4.534
PE 38:2	8.85E+04	2.55E+04	1.20E+05	3.73E+04	0.439	1.17E-11	10.932
PE 38:3	4.86E+05	1.87E+05	7.88E+05	2.79E+05	0.697	2.39E-17	16.621
PE 38:4	5.19E+05	1.36E+05	9.21E+05	2.19E+05	0.826	2.37E-38	37.626
PE 38:5	2.48E+05	7.58E+04	4.42E+05	1.20E+05	0.834	4.69E-32	31.328
PE 38:6	3.24E+05	1.32E+05	6.11E+05	1.79E+05	0.916	1.15E-29	28.938
PE 38:7	6.38E+04	3.21E+04	1.50E+05	6.01E+04	1.232	9.52E-29	28.021
PE 39:6	7.47E+04	3.27E+04	1.02E+05	3.48E+04	0.444	2.48E-08	7.606
PE 40:2	6.70E+03	3.90E+03	6.84E+03	4.46E+03	0.029	8.12E-01	0.091
PE 40:4	1.05E+05	5.53E+04	1.61E+05	7.98E+04	0.611	1.60E-08	7.795
PE 40:5	3.99E+05	1.42E+05	7.35E+05	2.15E+05	0.881	5.03E-30	29.299
PE 40:6	1.31E+06	5.44E+05	2.26E+06	6.80E+05	0.785	3.64E-23	22.438
PE 40:7	3.89E+05	1.78E+05	7.11E+05	2.29E+05	0.868	1.08E-23	22.966
PE 40:8	8.89E+04	3.10E+04	1.41E+05	4.64E+04	0.663	3.02E-18	17.520
PE 42:10	5.86E+03	3.39E+03	7.82E+03	4.25E+03	0.418	2.52E-04	3.599
PL-PC 24:0	4.61E+03	1.96E+03	3.41E+03	2.83E+03	-0.435	4.08E-04	3.389
PL-PC 26:0	2.59E+03	1.69E+03	2.19E+03	1.64E+03	-0.241	8.25E-02	1.083
PL-PC 30:0	1.29E+04	5.65E+03	1.09E+04	5.67E+03	-0.240	1.18E-02	1.930
PL-PC 32:0	9.44E+04	2.66E+04	1.03E+05	4.53E+04	0.127	9.04E-02	1.044
PL-PC 32:1	3.85E+04	2.76E+04	4.20E+04	2.76E+04	0.124	3.63E-01	0.440
PL-PC 34:0	5.59E+05	1.65E+05	6.26E+05	1.25E+05	0.163	9.99E-04	3.001
PL-PC 34:1	4.77E+05	1.39E+05	4.77E+05	1.65E+05	0.000	9.96E-01	0.002
PL-PC 34:2	1.00E+06	2.84E+05	8.45E+05	2.27E+05	-0.247	1.33E-05	4.875
PL-PC 34:3	2.81E+04	1.03E+04	2.75E+04	9.83E+03	-0.034	6.40E-01	0.194
PL-PC 34:4	3.13E+03	1.72E+03	3.67E+03	2.31E+03	0.228	5.72E-02	1.243
PL-PC 35:0	1.86E+04	4.99E+03	1.99E+04	5.59E+03	0.101	6.67E-02	1.176
PL-PC 35:1	1.06E+04	4.37E+03	1.32E+04	6.17E+03	0.324	3.55E-04	3.450
PL-PC 35:2	5.83E+04	2.22E+04	5.12E+04	1.99E+04	-0.186	1.60E-02	1.796
PL-PC 35:3	1.65E+04	8.36E+03	1.26E+04	5.50E+03	-0.395	6.39E-05	4.194
PL-PC 36:0	7.42E+04	2.12E+04	8.51E+04	2.25E+04	0.196	3.92E-04	3.406
PL-PC 36:1	3.02E+05	8.09E+04	3.14E+05	7.47E+04	0.060	2.36E-01	0.628
PL-PC 36:2	3.17E+05	1.07E+05	2.87E+05	1.01E+05	-0.143	3.74E-02	1.427
PL-PC 36:3	1.68E+06	3.67E+05	1.45E+06	2.81E+05	-0.211	7.83E-07	6.106
PL-PC 36:4	1.14E+06	3.13E+05	9.89E+05	2.07E+05	-0.207	4.04E-05	4.394
PL-PC 36:5	6.84E+04	3.31E+04	6.57E+04	2.99E+04	-0.058	5.36E-01	0.271

PL-PC 36:6	2.18E+04	7.49E+03	2.35E+04	6.92E+03	0.105	9.63E-02	1.016
PL-PC 37:1	1.36E+04	4.48E+03	1.53E+04	4.88E+03	0.164	1.13E-02	1.948
PL-PC 37:2	1.06E+04	4.08E+03	1.12E+04	4.32E+03	0.079	3.04E-01	0.517
PL-PC 37:3	1.35E+04	5.41E+03	1.46E+04	4.60E+03	0.106	1.37E-01	0.864
PL-PC 37:4	8.98E+04	3.32E+04	7.11E+04	2.17E+04	-0.337	2.30E-06	5.638
PL-PC 37:6	1.66E+05	6.23E+04	2.05E+05	6.36E+04	0.305	1.07E-05	4.972
PL-PC 38:3	9.36E+05	2.01E+05	8.78E+05	2.49E+05	-0.091	6.66E-02	1.177
PL-PC 38:4	9.85E+05	2.66E+05	8.94E+05	2.78E+05	-0.141	1.50E-02	1.824
PL-PC 38:5	9.67E+04	2.50E+04	9.21E+04	2.31E+04	-0.069	1.74E-01	0.760
PL-PC 38:6	1.66E+05	6.20E+04	1.57E+05	5.12E+04	-0.078	2.67E-01	0.574
PL-PC 39:5	3.04E+04	1.28E+04	2.78E+04	1.32E+04	-0.128	1.50E-01	0.823
PL-PC 40:0	5.27E+04	3.08E+04	6.05E+04	3.15E+04	0.199	6.93E-02	1.159
PL-PC 40:1	8.58E+03	4.71E+03	9.10E+03	3.82E+03	0.085	3.78E-01	0.422
PL-PC 40:2	1.99E+04	5.70E+03	2.16E+04	5.70E+03	0.117	3.20E-02	1.494
PL-PC 40:3	5.85E+04	2.34E+04	6.17E+04	2.61E+04	0.077	3.49E-01	0.458
PL-PC 40:4	3.11E+05	1.09E+05	3.39E+05	9.67E+04	0.124	5.05E-02	1.297
PL-PC 40:5	2.35E+05	6.80E+04	2.72E+05	8.40E+04	0.214	4.45E-04	3.351
PL-PC 40:6	1.98E+05	6.30E+04	2.00E+05	6.24E+04	0.011	8.66E-01	0.062
PL-PC 41:4	2.70E+04	1.99E+04	3.89E+04	2.04E+04	0.528	2.53E-05	4.597
PL-PC 42:0	2.55E+04	1.55E+04	2.69E+04	2.25E+04	0.081	5.79E-01	0.237
PL-PC 42:1	2.67E+04	1.36E+04	2.45E+04	1.55E+04	-0.122	2.80E-01	0.553
PL-PC 42:2	1.52E+05	1.07E+05	1.67E+05	1.15E+05	0.138	3.16E-01	0.500
PL-PC 42:3	6.60E+04	2.58E+04	6.71E+04	2.47E+04	0.023	7.61E-01	0.119
PL-PC 42:4	2.80E+05	1.74E+05	3.47E+05	1.96E+05	0.311	8.83E-03	2.054
PL-PC 42:5	1.40E+05	5.04E+04	1.30E+05	4.43E+04	-0.113	1.06E-01	0.974
PL-PC 43:3	1.08E+04	6.39E+03	1.11E+04	5.70E+03	0.043	6.94E-01	0.159
PL-PC 43:4	1.10E+04	4.90E+03	1.01E+04	5.17E+03	-0.116	2.22E-01	0.654
PL-PC 44:1	9.38E+03	8.70E+03	8.72E+03	1.05E+04	-0.105	6.19E-01	0.209
PL-PC 44:2	4.36E+04	2.28E+04	4.52E+04	2.66E+04	0.053	6.35E-01	0.197
PL-PC 44:3	9.00E+04	4.30E+04	8.82E+04	5.36E+04	-0.029	7.92E-01	0.101
PL-PC 44:4	3.09E+05	1.53E+05	3.20E+05	1.40E+05	0.053	5.65E-01	0.248
PL-PC 44:5	2.73E+05	8.85E+04	2.54E+05	8.36E+04	-0.104	1.11E-01	0.956
PL-PC 44:6	1.04E+05	4.49E+04	1.06E+05	3.74E+04	0.022	7.76E-01	0.110
PL-PC 46:4	5.62E+04	3.48E+04	5.81E+04	3.52E+04	0.049	6.88E-01	0.162
PL-PE 32:0	2.47E+04	7.51E+03	2.91E+04	9.89E+03	0.238	3.15E-04	3.502
PL-PE 32:1	1.57E+04	5.19E+03	1.66E+04	5.13E+03	0.081	2.00E-01	0.700
PL-PE 32:2	9.58E+03	4.46E+03	1.23E+04	8.09E+03	0.357	3.07E-03	2.513
PL-PE 34:1	2.73E+05	7.03E+04	3.02E+05	7.28E+04	0.142	4.37E-03	2.360
PL-PE 34:2	5.78E+05	1.58E+05	6.67E+05	2.08E+05	0.207	5.42E-04	3.266
PL-PE 34:3	2.41E+04	9.61E+03	2.57E+04	1.18E+04	0.095	2.67E-01	0.573
PL-PE 34:4	2.44E+04	1.08E+04	3.69E+04	5.66E+04	0.595	2.67E-02	1.573
PL-PE 35:1	2.18E+04	9.03E+03	2.56E+04	8.77E+03	0.229	2.45E-03	2.611
PL-PE 35:2	4.89E+04	1.83E+04	4.58E+04	1.76E+04	-0.095	2.10E-01	0.679
PL-PE 35:4	2.20E+04	1.11E+04	2.16E+04	2.90E+04	-0.025	9.00E-01	0.046
PL-PE 36:1	2.26E+05	8.75E+04	2.59E+05	7.82E+04	0.196	4.32E-03	2.365
PL-PE 36:2	7.21E+05	1.98E+05	8.49E+05	2.54E+05	0.234	6.75E-05	4.171
PL-PE 36:3	8.63E+05	2.06E+05	8.46E+05	1.97E+05	-0.030	5.28E-01	0.277
PL-PE 36:4	2.11E+06	6.14E+05	1.94E+06	4.68E+05	-0.118	2.84E-02	1.546
PL-PE 36:5	1.46E+05	1.17E+05	1.21E+05	1.15E+05	-0.274	1.14E-01	0.944
PL-PE 36:6	2.54E+04	1.35E+04	3.67E+04	1.73E+04	0.532	2.66E-07	6.576
PL-PE 37:2	1.57E+04	6.27E+03	1.87E+04	6.50E+03	0.250	8.51E-04	3.070
PL-PE 37:4	1.99E+05	8.29E+04	1.38E+05	4.80E+04	-0.528	4.53E-10	9.344
PL-PE 37:5	4.19E+04	2.41E+04	3.82E+04	2.28E+04	-0.133	2.53E-01	0.596
PL-PE 37:6	2.38E+04	1.08E+04	2.97E+04	1.90E+04	0.321	5.77E-03	2.239
PL-PE 38:1	4.17E+04	3.79E+04	5.05E+04	3.98E+04	0.275	1.03E-01	0.988

PL-PE 38:2	1.15E+05	3.74E+04	1.39E+05	4.80E+04	0.275	6.35E-05	4.197
PL-PE 38:3	5.14E+05	1.60E+05	5.33E+05	1.52E+05	0.050	3.96E-01	0.402
PL-PE 38:4	4.85E+05	1.83E+05	4.49E+05	1.39E+05	-0.112	1.07E-01	0.969
PL-PE 38:5	2.66E+06	6.87E+05	2.34E+06	5.17E+05	-0.187	1.50E-04	3.825
PL-PE 38:6	1.65E+06	4.85E+05	1.87E+06	4.78E+05	0.178	1.24E-03	2.906
PL-PE 39:4	5.15E+04	1.92E+04	4.49E+04	1.50E+04	-0.196	6.16E-03	2.211
PL-PE 39:6	1.09E+05	3.72E+04	1.14E+05	3.42E+04	0.070	2.73E-01	0.564
PL-PE 40:1	1.61E+04	7.83E+03	1.85E+04	8.95E+03	0.202	3.73E-02	1.429
PL-PE 40:2	3.82E+04	1.35E+04	4.55E+04	1.67E+04	0.251	5.88E-04	3.230
PL-PE 40:3	1.26E+05	4.37E+04	1.25E+05	3.12E+04	-0.010	8.67E-01	0.062
PL-PE 40:4	3.87E+05	1.12E+05	3.88E+05	1.02E+05	0.000	9.94E-01	0.003
PL-PE 40:5	5.01E+05	1.45E+05	5.50E+05	1.26E+05	0.132	1.03E-02	1.986
PL-PE 40:6	1.66E+05	6.23E+04	2.05E+05	6.36E+04	0.305	1.07E-05	4.972
PL-PE 42:4	7.49E+04	3.02E+04	7.04E+04	2.35E+04	-0.090	2.22E-01	0.654
PL-PE 42:6	1.05E+05	4.11E+04	1.36E+05	4.77E+04	0.372	1.03E-06	5.988
PG 32:0	8.05E+03	4.14E+03	9.91E+03	6.93E+03	0.300	1.84E-02	1.736
PG 32:1	3.55E+03	1.85E+03	4.70E+03	2.51E+03	0.402	2.17E-04	3.664
PG 33:0	3.48E+04	1.21E+04	3.05E+04	1.13E+04	-0.193	7.30E-03	2.136
PG 34:0	4.72E+06	7.29E+05	3.87E+06	7.75E+05	-0.285	2.70E-14	13.568
PG 34:1	4.93E+04	1.49E+04	8.81E+04	2.89E+04	0.839	1.50E-26	25.823
PG 34:2	1.56E+04	5.81E+03	2.08E+04	7.34E+03	0.410	5.18E-08	7.286
PG 36:0	7.34E+04	2.86E+04	5.97E+04	1.23E+04	-0.298	9.76E-06	5.011
PG 36:2	9.73E+04	3.14E+04	1.46E+05	5.07E+04	0.588	4.57E-15	14.340
PI 34:1	7.04E+04	3.45E+04	1.23E+05	4.98E+04	0.800	3.41E-16	15.467
PI 34:2	7.86E+04	4.24E+04	1.19E+05	4.30E+04	0.599	5.95E-11	10.226
PI 36:1	7.01E+04	3.39E+04	9.89E+04	4.84E+04	0.497	1.07E-06	5.970
PI 36:2	3.69E+05	1.85E+05	5.12E+05	1.70E+05	0.475	1.46E-08	7.836
PI 36:3	8.82E+04	5.07E+04	1.05E+05	3.70E+04	0.247	7.37E-03	2.132
PI 36:4	8.89E+04	4.16E+04	1.00E+05	3.94E+04	0.170	4.76E-02	1.322
PI 38:3	7.72E+05	4.67E+05	8.35E+05	3.38E+05	0.114	2.58E-01	0.588
PI 38:4	1.10E+06	4.29E+05	1.06E+06	3.54E+05	-0.050	4.87E-01	0.312
PI 38:5	8.44E+04	3.71E+04	8.16E+04	2.97E+04	-0.048	5.49E-01	0.260
PI 38:6	2.00E+04	1.08E+04	2.27E+04	1.14E+04	0.182	7.72E-02	1.112
PI 40:5	9.35E+04	3.82E+04	1.07E+05	3.85E+04	0.192	1.24E-02	1.907
PI 40:6	7.18E+04	3.38E+04	9.38E+04	3.76E+04	0.386	1.18E-05	4.929
PS 36:1	8.23E+04	3.73E+04	1.66E+05	6.08E+04	1.015	5.50E-26	25.260
PS 38:4	1.35E+04	1.94E+04	1.60E+04	9.77E+03	0.249	2.30E-01	0.638
SM 29:1	2.44E+03	1.13E+03	2.18E+03	8.45E+02	-0.160	6.38E-02	1.196
SM 30:0	6.26E+03	3.19E+03	7.00E+03	3.28E+03	0.161	9.71E-02	1.013
SM 30:1	6.19E+04	2.08E+04	6.85E+04	2.25E+04	0.145	2.87E-02	1.542
SM 30:2	7.68E+03	3.47E+03	7.05E+03	2.52E+03	-0.125	1.28E-01	0.892
SM 31:1	3.97E+04	1.42E+04	4.17E+04	1.49E+04	0.070	3.21E-01	0.494
SM 32:0	7.04E+04	2.50E+04	9.13E+04	3.70E+04	0.375	2.77E-06	5.558
SM 32:1	1.35E+06	3.67E+05	1.73E+06	4.72E+05	0.354	6.63E-10	9.179
SM 32:2	1.62E+05	4.44E+04	1.78E+05	4.71E+04	0.135	1.23E-02	1.909
SM 33:0	6.21E+04	1.79E+04	7.74E+04	2.32E+04	0.318	1.90E-07	6.721
SM 33:1	4.68E+05	1.39E+05	5.44E+05	1.84E+05	0.218	8.01E-04	3.096
SM 33:2	2.74E+04	8.41E+03	3.18E+04	1.01E+04	0.212	8.14E-04	3.089
SM 34:0	2.63E+05	8.26E+04	3.45E+05	1.04E+05	0.393	1.26E-09	8.898
SM 34:1	2.70E+06	4.07E+05	3.41E+06	7.58E+05	0.339	2.38E-15	14.624
SM 34:2	2.01E+06	4.27E+05	2.67E+06	5.44E+05	0.409	6.06E-19	18.217
SM 34:3	1.41E+04	5.00E+03	1.77E+04	5.72E+03	0.323	2.96E-06	5.529
SM 35:1	1.39E+06	2.22E+05	1.07E+06	2.12E+05	-0.376	1.28E-21	20.894
SM 35:2	3.30E+04	1.23E+04	3.56E+04	1.56E+04	0.109	1.82E-01	0.741
SM 35:6	4.31E+03	2.74E+03	5.58E+03	3.29E+03	0.372	2.59E-03	2.586

SM 36:0	5.74E+04	1.85E+04	8.36E+04	2.30E+04	0.542	6.36E-17	16.196
SM 36:1	2.20E+06	4.68E+05	2.75E+06	5.96E+05	0.327	9.74E-13	12.011
SM 36:2	1.20E+06	3.09E+05	1.48E+06	4.16E+05	0.303	7.36E-08	7.133
SM 36:3	1.58E+05	4.76E+04	2.01E+05	6.01E+04	0.342	4.33E-08	7.364
SM 36:4	3.16E+04	7.64E+03	3.48E+04	8.72E+03	0.138	5.25E-03	2.280
SM 37:1	1.65E+05	7.19E+04	1.84E+05	8.26E+04	0.158	7.36E-02	1.133
SM 37:2	5.11E+04	1.56E+04	4.73E+04	1.49E+04	-0.110	7.51E-02	1.124
SM 38:0	1.63E+05	3.76E+04	2.16E+05	4.94E+04	0.403	8.36E-16	15.078
SM 38:1	2.46E+05	1.09E+05	3.24E+05	1.48E+05	0.401	1.67E-05	4.778
SM 38:2	5.86E+05	1.22E+05	5.99E+05	1.54E+05	0.030	5.25E-01	0.280
SM 38:3	5.11E+04	1.90E+04	5.13E+04	1.73E+04	0.005	9.42E-01	0.026
SM 38:4	2.02E+04	8.26E+03	2.53E+04	8.87E+03	0.326	2.19E-05	4.659
SM 38:5	1.56E+04	6.44E+03	1.63E+04	7.30E+03	0.068	4.29E-01	0.368
SM 39:1	2.20E+05	6.58E+04	2.53E+05	7.11E+04	0.200	6.08E-04	3.216
SM 39:2	1.34E+05	3.08E+04	1.40E+05	3.29E+04	0.068	1.44E-01	0.842
SM 39:3	5.32E+04	1.30E+04	4.76E+04	1.35E+04	-0.160	2.48E-03	2.605
SM 40:0	2.53E+05	6.68E+04	3.10E+05	6.20E+04	0.293	8.29E-10	9.081
SM 40:1	1.91E+06	3.93E+05	2.92E+06	4.31E+06	0.612	1.71E-02	1.767
SM 40:2	1.91E+06	1.03E+06	2.06E+06	1.02E+06	0.115	2.63E-01	0.581
SM 40:3	2.43E+05	8.05E+04	2.64E+05	7.22E+04	0.117	5.26E-02	1.279
SM 40:4	3.69E+04	1.02E+04	3.90E+04	1.21E+04	0.079	1.81E-01	0.743
SM 40:5	2.17E+04	8.37E+03	3.23E+04	9.63E+03	0.573	2.76E-15	14.559
SM 41:0	1.74E+05	4.30E+04	2.18E+05	4.67E+04	0.328	1.08E-11	10.968
SM 41:1	1.28E+06	2.58E+05	1.45E+06	2.61E+05	0.176	5.57E-06	5.254
SM 41:2	7.52E+05	1.19E+05	7.43E+05	1.34E+05	-0.017	6.10E-01	0.215
SM 41:3	1.76E+05	4.03E+04	1.86E+05	4.44E+04	0.079	9.13E-02	1.040
SM 42:1	1.91E+06	4.22E+05	2.26E+06	5.43E+05	0.240	4.95E-07	6.305
SM 42:2	3.79E+06	6.13E+05	1.14E+07	2.91E+07	1.593	7.37E-03	2.133
SM 42:3	2.42E+06	4.58E+05	2.80E+06	6.13E+05	0.207	1.07E-06	5.970
SM 42:4	3.40E+05	8.52E+04	3.68E+05	1.10E+05	0.116	3.66E-02	1.436
SM 42:5	8.54E+04	3.69E+04	1.50E+05	7.90E+04	0.815	6.95E-13	12.158
SM 42:6	4.89E+04	2.10E+04	7.78E+04	3.32E+04	0.668	1.34E-12	11.874
SM 42:7	2.13E+04	9.33E+03	3.02E+04	1.42E+04	0.506	1.66E-07	6.779
SM 43:1	4.34E+04	1.48E+04	4.80E+04	1.69E+04	0.145	3.79E-02	1.422
SM 43:2	1.82E+05	5.42E+04	1.69E+05	5.61E+04	-0.105	9.43E-02	1.026
SM 43:3	6.38E+04	1.73E+04	5.97E+04	2.13E+04	-0.095	1.29E-01	0.888
SM 43:4	1.42E+04	9.96E+03	1.40E+04	1.05E+04	-0.024	8.67E-01	0.062
SM 43:7	1.04E+04	4.09E+03	1.18E+04	5.21E+03	0.174	3.83E-02	1.417
SM 44:1	1.36E+04	6.16E+03	1.32E+04	4.71E+03	-0.034	6.78E-01	0.169
SM 44:2	9.18E+03	4.58E+03	9.90E+03	5.42E+03	0.110	2.95E-01	0.531
SM 44:3	4.04E+04	1.98E+04	3.73E+04	2.23E+04	-0.116	2.80E-01	0.553
SM 44:4	1.96E+04	9.00E+03	1.85E+04	9.77E+03	-0.082	4.03E-01	0.394
SM 44:5	1.97E+04	7.85E+03	2.90E+04	1.83E+04	0.558	2.86E-06	5.544
SM 44:6	1.23E+04	6.37E+03	2.10E+04	1.40E+04	0.775	1.79E-08	7.748
SM 44:7	6.45E+03	4.04E+03	7.69E+03	4.55E+03	0.254	3.69E-02	1.432
SM 45:4	1.35E+04	7.58E+03	1.38E+04	8.08E+03	0.031	7.86E-01	0.105
SM 47:5	1.15E+04	7.91E+03	1.38E+04	2.00E+04	0.260	2.78E-01	0.556
TG 36:0	7.49E+04	2.07E+05	4.95E+04	9.20E+04	-0.598	2.48E-01	0.605
TG 38:0	1.43E+05	3.36E+05	7.93E+04	1.68E+05	-0.854	8.06E-02	1.094
TG 39:0	2.15E+04	2.68E+04	1.44E+04	1.26E+04	-0.575	1.49E-02	1.827
TG 40:0	2.49E+05	4.71E+05	1.41E+05	2.69E+05	-0.822	4.13E-02	1.384
TG 40:1	1.11E+05	1.69E+05	1.02E+05	1.29E+05	-0.123	6.62E-01	0.179
TG 41:0	3.41E+04	4.68E+04	2.18E+04	2.02E+04	-0.641	1.45E-02	1.840
TG 42:0	3.59E+05	5.33E+05	2.47E+05	3.28E+05	-0.542	6.59E-02	1.181
TG 42:1	3.00E+05	4.12E+05	2.55E+05	3.66E+05	-0.237	3.98E-01	0.401

TG 42:2	1.60E+05	1.94E+05	1.63E+05	2.08E+05	0.027	9.15E-01	0.039
TG 42:3	2.93E+04	2.83E+04	3.90E+04	3.61E+04	0.412	3.09E-02	1.510
TG 43:0	4.56E+04	5.92E+04	3.19E+04	2.48E+04	-0.515	2.94E-02	1.531
TG 44:0	3.53E+05	4.08E+05	3.22E+05	2.88E+05	-0.133	5.23E-01	0.282
TG 44:1	6.00E+05	6.84E+05	5.99E+05	6.06E+05	-0.002	9.92E-01	0.003
TG 44:2	3.44E+05	3.53E+05	3.41E+05	3.15E+05	-0.012	9.49E-01	0.023
TG 45:0	4.99E+04	5.88E+04	3.98E+04	2.60E+04	-0.326	1.08E-01	0.967
TG 45:1	7.03E+04	7.58E+04	7.05E+04	5.02E+04	0.006	9.75E-01	0.011
TG 46:0	4.04E+05	3.57E+05	5.16E+05	3.05E+05	0.354	1.48E-02	1.829
TG 46:1	1.00E+06	9.21E+05	1.30E+06	1.05E+06	0.382	2.59E-02	1.586
TG 46:2	8.30E+05	6.66E+05	1.01E+06	6.95E+05	0.283	5.58E-02	1.254
TG 46:3	3.00E+05	2.28E+05	3.35E+05	2.10E+05	0.158	2.50E-01	0.602
TG 47:0	5.08E+04	5.17E+04	5.17E+04	2.89E+04	0.026	8.71E-01	0.060
TG 47:1	1.15E+05	1.12E+05	1.29E+05	7.43E+04	0.160	3.01E-01	0.521
TG 47:2	1.01E+05	7.45E+04	1.17E+05	5.76E+04	0.214	7.81E-02	1.107
TG 47:3	4.43E+04	2.62E+04	6.13E+04	2.50E+04	0.471	2.37E-06	5.625
TG 48:0	5.08E+05	3.37E+05	8.43E+05	3.43E+05	0.731	1.26E-11	10.901
TG 48:1	2.06E+06	1.33E+06	3.28E+06	1.67E+06	0.674	1.30E-08	7.887
TG 48:2	2.06E+06	1.10E+06	3.05E+06	1.42E+06	0.571	3.70E-08	7.432
TG 48:3	1.18E+06	6.35E+05	1.47E+06	6.83E+05	0.309	2.02E-03	2.694
TG 48:4	4.53E+05	2.90E+05	4.81E+05	2.48E+05	0.085	4.60E-01	0.337
TG 49:0	6.36E+04	4.66E+04	7.75E+04	3.19E+04	0.287	1.17E-02	1.933
TG 49:1	2.49E+05	1.65E+05	3.34E+05	1.34E+05	0.426	5.14E-05	4.289
TG 49:2	2.62E+05	1.32E+05	3.44E+05	1.21E+05	0.394	3.97E-06	5.401
TG 49:3	1.30E+05	5.20E+04	1.71E+05	5.47E+04	0.394	7.34E-08	7.134
TG 50:0	6.10E+05	3.42E+05	1.05E+06	3.43E+05	0.789	6.85E-18	17.165
TG 50:1	3.48E+06	1.57E+06	6.72E+06	1.81E+06	0.949	1.17E-31	30.933
TG 50:2	4.83E+06	1.60E+06	8.03E+06	1.93E+06	0.734	3.61E-29	28.443
TG 50:3	3.52E+06	1.05E+06	5.39E+06	1.36E+06	0.616	3.15E-23	22.502
TG 50:4	1.65E+06	5.48E+05	2.20E+06	6.47E+05	0.411	2.95E-10	9.530
TG 50:5	3.86E+05	1.68E+05	4.72E+05	1.74E+05	0.290	3.25E-04	3.488
TG 50:6	8.33E+04	4.92E+04	9.27E+04	3.78E+04	0.154	1.22E-01	0.913
TG 51:1	2.33E+05	1.29E+05	3.57E+05	1.27E+05	0.615	2.53E-11	10.597
TG 51:2	5.30E+05	1.70E+05	7.12E+05	1.99E+05	0.427	1.23E-11	10.909
TG 51:3	1.31E+04	9.40E+03	1.61E+04	1.12E+04	0.301	3.41E-02	1.467
TG 51:4	2.34E+05	5.56E+04	2.72E+05	6.88E+04	0.215	1.94E-05	4.712
TG 51:5	9.15E+04	3.74E+04	9.64E+04	3.45E+04	0.076	3.18E-01	0.497
TG 52:0	3.18E+05	1.62E+05	4.87E+05	1.62E+05	0.616	9.11E-13	12.040
TG 52:1	2.43E+06	9.93E+05	3.98E+06	1.15E+06	0.712	4.49E-21	20.348
TG 52:2	8.74E+06	1.87E+06	1.29E+07	2.47E+06	0.556	6.75E-31	30.171
TG 52:4	7.73E+06	2.17E+06	1.07E+07	2.66E+06	0.465	4.18E-16	15.379
TG 52:5	2.36E+06	7.60E+05	3.13E+06	9.51E+05	0.404	7.17E-10	9.145
TG 52:6	5.15E+05	2.00E+05	6.16E+05	2.15E+05	0.258	5.14E-04	3.289
TG 53:0	5.42E+04	2.24E+04	5.09E+04	1.68E+04	-0.091	2.22E-01	0.654
TG 53:1	1.00E+05	5.09E+04	1.39E+05	5.36E+04	0.470	1.95E-07	6.709
TG 53:2	3.12E+05	8.98E+04	4.53E+05	1.42E+05	0.536	1.73E-15	14.762
TG 53:3	3.86E+05	8.44E+04	4.32E+05	1.15E+05	0.164	9.49E-04	3.023
TG 53:4	1.78E+04	1.25E+04	2.19E+04	1.27E+04	0.304	1.72E-02	1.764
TG 53:5	1.15E+05	3.08E+04	1.17E+05	2.69E+04	0.025	6.12E-01	0.213
TG 54:0	8.28E+04	4.96E+04	1.07E+05	4.94E+04	0.367	5.26E-04	3.279
TG 54:1	5.81E+05	3.50E+05	8.30E+05	3.51E+05	0.513	5.57E-07	6.254
TG 54:2	1.92E+06	7.31E+05	2.67E+06	8.45E+05	0.481	3.88E-11	10.411
TG 54:3	2.90E+06	9.43E+05	3.16E+06	8.10E+05	0.127	2.83E-02	1.548
TG 54:4	3.76E+06	1.22E+06	3.85E+06	9.54E+05	0.035	5.39E-01	0.268
TG 54:5	3.40E+06	1.21E+06	3.54E+06	1.02E+06	0.061	3.39E-01	0.470

TG 54:6	2.17E+06	9.75E+05	2.37E+06	8.75E+05	0.129	1.12E-01	0.951
TG 54:7	7.75E+05	4.09E+05	8.54E+05	4.07E+05	0.140	1.59E-01	0.798
TG 54:8	1.69E+05	9.03E+04	1.75E+05	9.19E+04	0.045	6.69E-01	0.174
TG 55:1	2.04E+04	1.28E+04	3.17E+04	1.57E+04	0.631	4.07E-08	7.391
TG 55:2	3.92E+04	1.65E+04	5.49E+04	1.89E+04	0.486	7.84E-10	9.106
TG 55:3	5.28E+04	1.53E+04	7.08E+04	2.33E+04	0.423	2.53E-10	9.597
TG 56:0	1.14E+04	1.04E+04	1.73E+04	1.23E+04	0.606	1.85E-04	3.733
TG 56:1	8.09E+04	8.13E+04	1.16E+05	8.56E+04	0.524	2.24E-03	2.649
TG 56:2	1.69E+05	1.32E+05	2.58E+05	1.36E+05	0.614	2.32E-06	5.635
TG 56:3	2.32E+05	1.27E+05	3.33E+05	1.29E+05	0.520	3.57E-08	7.448
TG 56:4	2.62E+05	7.50E+04	3.12E+05	8.00E+04	0.249	6.20E-06	5.208
TG 56:5	5.58E+05	1.38E+05	5.65E+05	1.26E+05	0.016	7.32E-01	0.136
TG 56:6	7.94E+05	2.13E+05	7.81E+05	1.81E+05	-0.024	6.32E-01	0.199
TG 56:7	9.08E+05	3.17E+05	1.03E+06	3.58E+05	0.175	1.23E-02	1.911
TG 56:8	5.90E+05	2.59E+05	6.79E+05	2.85E+05	0.202	1.86E-02	1.731
TG 56:9	1.70E+05	8.65E+04	1.73E+05	8.41E+04	0.024	8.07E-01	0.093
TG 56:10	2.83E+04	2.02E+04	2.65E+04	2.02E+04	-0.098	5.03E-01	0.298
TG 58:1	2.38E+04	3.33E+04	3.49E+04	3.38E+04	0.551	1.70E-02	1.770
TG 58:2	6.69E+04	1.21E+05	9.33E+04	9.77E+04	0.479	8.20E-02	1.086
TG 58:3	5.57E+04	7.91E+04	8.44E+04	7.43E+04	0.600	6.96E-03	2.157
TG 58:4	3.76E+04	2.38E+04	5.88E+04	2.57E+04	0.646	2.29E-09	8.639
TG 58:5	6.87E+04	2.43E+04	1.25E+05	4.30E+04	0.868	5.19E-25	24.285
TG 58:6	1.14E+05	3.56E+04	1.55E+05	4.67E+04	0.451	5.62E-12	11.250
TG 58:7	1.80E+05	6.57E+04	2.08E+05	7.25E+04	0.202	4.79E-03	2.319
TG 58:8	2.34E+05	9.61E+04	2.47E+05	1.03E+05	0.074	3.67E-01	0.435
TG 58:9	2.12E+05	1.03E+05	2.08E+05	9.06E+04	-0.021	8.15E-01	0.089
TG 58:10	1.37E+05	7.90E+04	1.33E+05	6.60E+04	-0.049	6.47E-01	0.189
TG 58:11	3.89E+04	2.98E+04	3.72E+04	3.01E+04	-0.067	6.68E-01	0.175
TG 60:10	4.46E+04	2.39E+04	4.14E+04	2.12E+04	-0.108	3.02E-01	0.519
TG 60:11	4.57E+04	3.07E+04	4.57E+04	2.99E+04	0.000	9.98E-01	0.001
TG 60:12	3.50E+04	3.21E+04	3.67E+04	3.47E+04	0.072	6.97E-01	0.156
TG 62:1	1.93E+03	4.73E+03	2.33E+03	4.20E+03	0.274	5.12E-01	0.291
TG 62:12	1.03E+04	8.51E+03	1.08E+04	8.37E+03	0.075	6.35E-01	0.197
TG 62:14	6.71E+03	7.30E+03	6.43E+03	7.09E+03	-0.061	7.78E-01	0.109

Table S2.3. Comparison of M3-CB lipid raw peak intensities. Paired t-tests identified differences in raw peak intensities of individual plasma lipids between M3 to CB. The fold change between lipids in M3 and CB was calculated by log2(CB/M3), where a positive FC indicates increases in that lipid between M3 and CB and a negative FC indicates decreases in that lipid between M3 and CB. Significance highlighted in red (Bonferroni adjusted, α=0.05/573).

Metabolite	M3		CB		M3 CB t-test		
	Mean	Std dev	Mean	Std dev	log2(CB/M3)	p-value	-log10(p-value)
FFA(16:0)	7.06E+07	1.39E+07	6.08E+07	1.22E+07	-0.217	3.89E-09	8.410
FFA(18:0)	7.23E+07	7.23E+06	6.83E+07	1.13E+07	-0.083	6.06E-05	4.218
FFA(18:1)	5.46E+07	2.45E+07	2.18E+07	9.47E+06	-1.324	5.17E-29	28.287
FFA(18:2)	3.37E+07	1.50E+07	1.43E+07	6.64E+06	-1.232	7.54E-27	26.123
FFA(20:0)	2.10E+06	3.40E+05	1.86E+06	3.80E+05	-0.178	6.75E-08	7.171
FFA(20:1)	1.34E+06	6.81E+05	3.65E+05	1.28E+05	-1.880	6.52E-34	33.185
FFA(20:2)	9.58E+05	4.24E+05	4.79E+05	1.87E+05	-1.001	3.69E-22	21.433
FFA(20:4) Arachidonic acid	1.73E+06	6.73E+05	2.61E+06	1.77E+06	0.590	1.24E-05	4.908
FFA(22:0)	6.46E+05	2.71E+05	4.64E+05	1.45E+05	-0.477	1.82E-09	8.741
FFA(22:1)	2.58E+05	1.57E+05	1.19E+05	4.13E+04	-1.118	1.61E-16	15.792
FFA(22:2)	8.29E+04	3.39E+04	5.86E+04	2.78E+04	-0.499	8.39E-07	6.076
FFA(22:3)	8.90E+04	3.17E+04	1.56E+05	6.06E+04	0.810	4.24E-19	18.372
FFA(24:0)	3.86E+05	1.73E+05	3.73E+05	1.09E+05	-0.049	3.45E-01	0.462
FFA(24:1)	3.83E+05	1.08E+05	3.24E+05	9.86E+04	-0.243	1.16E-05	4.937
FFA(24:2)	1.21E+05	3.54E+04	1.62E+05	5.02E+04	0.425	4.50E-10	9.347
FFA(24:3)	1.72E+04	6.76E+03	4.08E+04	1.46E+04	1.245	7.19E-35	34.144
16:0 Cholesteryl ester	4.72E+04	1.76E+04	4.50E+04	2.03E+04	-0.068	8.88E-01	0.052
16:1 Cholesteryl ester	3.32E+04	1.51E+04	6.15E+04	4.11E+04	0.887	2.88E-13	12.540
17:1 Cholesteryl ester	7.14E+03	2.74E+03	7.54E+03	3.13E+03	0.079	3.77E-01	0.424
18:0 Cholesteryl ester	1.78E+04	7.35E+03	2.84E+04	1.42E+04	0.670	1.49E-10	9.827
18:1 Cholesteryl ester	6.98E+05	1.59E+05	4.44E+05	1.15E+05	-0.652	3.31E-31	30.480
18:2 Cholesteryl ester	3.19E+06	6.38E+05	1.15E+06	3.77E+05	-1.477	6.08E-75	74.216
18:3 Cholesteryl ester	9.06E+03	2.09E+04	2.87E+03	4.94E+03	-1.658	4.15E-03	2.382
20:3 Cholesteryl ester	3.10E+05	8.99E+04	3.82E+05	9.38E+04	0.300	9.52E-07	6.021
20:4 Cholesteryl ester	1.67E+04	1.00E+04	9.32E+03	8.05E+03	-0.843	2.14E-07	6.670
20:5 Cholesteryl ester	5.35E+04	5.23E+04	4.13E+04	4.71E+04	-0.371	3.27E-01	0.485
22:4 Cholesteryl ester	1.17E+04	4.62E+03	1.95E+04	6.98E+03	0.737	4.07E-17	16.391
22:5 Cholesteryl ester	3.39E+04	1.24E+04	7.05E+04	2.22E+04	1.056	1.38E-35	34.861
22:6 Cholesteryl ester	1.77E+05	8.09E+04	2.87E+05	1.10E+05	0.697	5.82E-14	13.235
Acylcarnitine 16:0	6.95E+04	2.48E+04	1.10E+05	4.37E+04	0.666	1.04E-15	14.985
Acylcarnitine 18:0	2.88E+04	1.39E+04	3.10E+04	1.69E+04	0.107	3.94E-01	0.405
Acylcarnitine 18:1	1.32E+05	5.46E+04	1.04E+05	6.00E+04	-0.345	3.72E-04	3.429
Acylcarnitine 18:2	7.12E+04	3.93E+04	8.88E+04	4.97E+04	0.318	8.42E-03	2.074
Acylcarnitine 24:0	1.86E+03	9.37E+02	1.15E+03	3.77E+05	-0.690	2.28E-01	0.643
Acylcarnitine 26:0	2.53E+03	1.42E+03	1.89E+03	7.42E+03	-0.423	7.19E-01	0.144
Cer[NDS] 34:0	1.20E+05	2.95E+04	1.32E+05	4.24E+04	0.135	4.09E-03	2.389
Cer[NDS] 36:0	7.37E+04	2.97E+04	7.24E+04	1.03E+05	-0.024	2.21E-01	0.655
Cer[NDS] 38:0	5.22E+03	1.99E+03	5.68E+03	3.86E+03	0.123	2.56E-02	1.592
Cer[NDS] 40:0	5.04E+05	1.39E+05	2.94E+05	9.79E+04	-0.774	3.12E-28	27.506
Cer[NDS] 41:0	3.03E+04	8.43E+03	1.26E+04	4.59E+03	-1.271	2.49E-48	47.604
Cer[NDS] 42:0	8.59E+04	2.46E+04	8.64E+04	2.94E+04	0.009	6.42E-01	0.193
Cer[NDS] 42:1	4.38E+05	1.19E+05	1.19E+05	6.62E+04	-1.877	1.23E-62	61.911
Cer[NS] 32:1	3.90E+04	1.14E+04	1.36E+04	6.31E+03	-1.519	1.47E-50	49.833
Cer[NS] 33:1	2.79E+04	8.19E+03	3.21E+04	1.24E+04	0.205	8.26E-03	2.083
Cer[NS] 33:4	3.45E+03	2.51E+03	3.07E+03	1.29E+05	-0.166	1.88E-01	0.726
Cer[NS] 34:1	2.09E+04	5.73E+03	9.68E+03	8.34E+03	-1.112	2.90E-21	20.538
Cer[NS] 34:2	2.49E+04	7.48E+03	1.75E+04	9.27E+03	-0.508	3.82E-10	9.418
Cer[NS] 35:1	1.37E+07	1.52E+06	1.83E+07	3.43E+06	0.425	1.51E-25	24.822
Cer[NS] 36:1	2.18E+05	6.55E+04	9.40E+04	3.96E+04	-1.215	1.64E-40	39.785
Cer[NS] 36:2	2.62E+04	9.87E+03	2.05E+04	8.98E+03	-0.358	1.61E-05	4.793
Cer[NS] 37:1	8.99E+04	3.30E+04	5.31E+04	1.39E+04	-0.759	4.32E-22	21.364
Cer[NS] 37:4	1.51E+04	6.43E+03	6.05E+04	2.32E+04	2.005	7.52E-48	47.124
Cer[NS] 38:1	3.19E+05	8.17E+04	7.21E+04	4.33E+04	-2.146	5.37E-72	71.270

Cer[NS] 38:2	4.12E+04	1.20E+04	1.90E+04	1.04E+04	-1.114	7.88E-32	31.104
Cer[NS] 39:1	3.53E+05	9.12E+04	6.63E+04	3.65E+04	-2.412	2.82E-78	77.550
Cer[NS] 39:2	4.50E+04	1.32E+04	1.40E+04	7.30E+03	-1.684	4.55E-53	52.342
Cer[NS] 40:1	1.76E+06	4.98E+05	3.35E+05	2.32E+05	-2.393	8.99E-70	69.046
Cer[NS] 40:2	2.95E+05	7.92E+04	9.43E+04	3.99E+04	-1.646	7.45E-60	59.128
Cer[NS] 41:1	1.06E+05	2.94E+04	1.46E+04	1.11E+04	-2.869	2.50E-78	77.602
Cer[NS] 41:2	4.99E+05	1.31E+05	1.19E+05	5.51E+04	-2.063	4.53E-72	71.344
Cer[NS] 41:3	6.46E+04	2.18E+04	2.51E+04	1.15E+04	-1.367	7.07E-41	40.151
Cer[NS] 42:1	4.38E+05	1.19E+05	1.19E+05	6.87E+04	-1.877	5.72E-61	60.242
Cer[NS] 42:2	1.95E+06	4.83E+05	5.64E+05	2.43E+05	-1.786	4.30E-69	68.367
Cer[NS] 42:3	1.10E+04	4.27E+03	5.71E+03	6.93E+03	-0.943	5.09E-08	7.293
Cer[NS] 43:1	6.77E+05	2.27E+05	2.13E+05	9.93E+04	-1.664	1.25E-48	47.902
Cer[NS] 43:2	1.63E+04	5.83E+03	5.95E+03	4.37E+03	-1.452	1.39E-31	30.856
Cer[NS] 43:3	1.02E+04	3.55E+03	6.00E+03	2.43E+03	-0.760	5.16E-19	18.287
Cer[NS] 44:1	2.62E+04	7.21E+03	2.15E+04	7.92E+03	-0.285	4.68E-04	3.330
Cer[AS] 41:1	3.75E+04	1.71E+04	8.72E+03	3.36E+05	-2.102	6.87E-01	0.163
Cer[AS] 42:2	9.28E+04	3.52E+04	2.13E+04	1.22E+04	-2.124	6.64E-50	49.178
Cer[EODS] 49:1	8.42E+03	3.86E+03	3.20E+03	1.89E+03	-1.398	8.10E-27	26.091
Cer[EODS] 53:0	7.86E+03	2.90E+03	1.28E+04	3.81E+03	0.706	1.27E-21	20.895
Cer[EODS] 57:2	9.66E+03	4.45E+03	3.63E+03	4.43E+03	-1.413	3.88E-17	16.411
Cer[NP] 34:0	4.12E+03	1.99E+03	2.44E+03	7.06E+03	-0.757	2.38E-01	0.623
Cer[NP] 40:0	7.25E+04	2.53E+04	1.95E+04	1.31E+04	-1.898	4.11E-47	46.386
Cer[NP] 42:0	1.07E+05	3.07E+04	2.96E+04	1.43E+04	-1.856	3.00E-61	60.522
Cer[NP] 42:1	6.41E+04	2.34E+04	2.52E+04	1.06E+04	-1.345	3.29E-37	36.483
GlcCer[NS] 32:1	3.77E+03	1.69E+03	1.39E+03	1.08E+03	-1.441	1.48E-25	24.828
GlcCer[NS] 34:1	1.92E+05	5.62E+04	6.05E+04	2.50E+04	-1.669	2.19E-56	55.660
GlcCer[NS] 38:1	1.19E+04	3.71E+03	5.24E+03	2.23E+03	-1.183	8.76E-38	37.057
GlcCer[NS] 40:1	2.47E+05	7.97E+04	5.42E+04	2.52E+04	-2.188	1.06E-61	60.974
GlcCer[NS] 41:1	1.84E+04	5.62E+03	3.91E+03	2.17E+03	-2.233	1.29E-63	62.889
GlcCer[NS] 41:2	1.15E+04	5.62E+03	4.07E+03	2.70E+03	-1.500	3.08E-26	25.512
GlcCer[NS] 42:1	6.22E+04	1.56E+04	3.38E+04	1.02E+04	-0.878	9.08E-37	36.042
GlcCer[NS] 42:2	4.67E+04	1.24E+04	2.55E+04	8.61E+03	-0.873	1.52E-34	33.819
GlcCer[NS] 43:1	7.32E+03	3.69E+03	3.84E+03	3.30E+03	-0.930	5.93E-10	9.227
MG 26:4	2.82E+04	9.60E+03	1.77E+04	6.37E+03	-0.667	4.52E-17	16.345
DG 30:0	1.92E+04	1.69E+04	3.70E+03	3.23E+03	-2.377	4.07E-17	16.391
DG 30:1	7.92E+03	6.32E+03	1.75E+03	2.67E+03	-2.180	5.67E-16	15.246
DG 31:0	4.10E+03	2.47E+03	1.82E+03	1.18E+03	-1.174	2.52E-15	14.599
DG 32:0	7.25E+04	5.16E+04	1.46E+04	1.99E+04	-2.310	1.06E-20	19.976
DG 32:1	8.35E+04	5.58E+04	1.70E+04	1.68E+05	-2.299	1.13E-02	1.948
DG 32:2	2.62E+04	1.35E+04	5.03E+03	1.01E+05	-2.378	4.26E-01	0.371
DG 33:0	5.29E+03	2.92E+03	2.17E+03	1.11E+03	-1.285	1.01E-19	18.997
DG 33:1	1.15E+04	6.45E+03	2.67E+03	2.37E+03	-2.105	1.44E-28	27.842
DG 34:0	4.58E+04	2.29E+04	1.85E+04	9.80E+03	-1.304	8.87E-23	22.052
DG 34:2	3.33E+05	1.56E+05	6.04E+04	4.52E+04	-2.464	7.13E-43	42.147
DG 34:3	6.81E+04	2.90E+04	1.58E+04	1.03E+04	-2.112	4.55E-43	42.342
DG 35:1	1.18E+04	5.17E+03	2.72E+03	1.59E+03	-2.116	2.66E-42	41.574
DG 35:2	1.36E+04	6.14E+03	2.82E+03	3.33E+05	-2.268	2.85E-01	0.545
DG 35:3	6.92E+03	3.10E+03	1.53E+03	1.15E+03	-2.174	4.91E-41	40.309
DG 36:0	1.31E+04	3.47E+03	1.13E+04	1.60E+04	-0.218	9.04E-01	0.044
DG 36:1	8.75E+04	4.14E+04	1.99E+04	1.55E+04	-2.138	1.38E-37	36.861
DG 36:2	4.33E+05	2.02E+05	7.17E+04	5.57E+04	-2.595	3.29E-44	43.483
DG 36:3	4.97E+05	2.38E+05	6.35E+04	4.86E+04	-2.969	3.37E-46	45.472
DG 36:4	2.68E+05	1.15E+05	4.58E+04	3.29E+04	-2.550	1.13E-48	47.946
DG 36:5	2.72E+04	1.26E+04	7.46E+03	4.70E+03	-1.865	1.45E-35	34.839
DG 38:0	2.18E+03	1.29E+03	1.53E+03	3.20E+03	-0.516	4.90E-01	0.309
DG 38:1	1.00E+04	5.02E+03	2.73E+03	1.70E+03	-1.871	7.37E-32	31.133
DG 38:2	2.18E+04	8.99E+03	3.15E+03	4.41E+03	-2.791	4.74E-47	46.324
DG 38:3	2.52E+04	9.48E+03	8.01E+03	6.31E+03	-1.652	8.82E-37	36.054
DG 38:4	3.53E+04	1.28E+04	2.04E+04	2.13E+04	-0.792	1.32E-09	8.881
DG 38:5	6.20E+04	2.42E+04	2.80E+04	2.04E+05	-1.147	7.22E-01	0.142
DG 38:6	5.16E+04	2.16E+04	2.54E+04	1.89E+04	-1.021	3.41E-16	15.467
DG 38:7	5.74E+03	4.20E+03	3.65E+03	3.45E+03	-0.652	1.46E-03	2.837
DG 40:7	2.38E+04	1.38E+04	1.38E+04	9.38E+03	-0.792	1.88E-08	7.725

DG 40:8	9.19E+03	6.13E+03	5.53E+03	3.62E+03	-0.733	8.60E-07	6.066
LysoPC 14:0	2.54E+04	1.39E+04	4.28E+04	1.52E+04	0.751	3.14E-17	16.503
LysoPC 15:0	2.80E+04	1.18E+04	2.76E+04	1.06E+04	-0.019	7.25E-01	0.140
LysoPC 16:0	3.79E+06	1.21E+06	3.75E+06	1.18E+06	-0.015	5.55E-01	0.255
LysoPC 16:1	6.13E+04	3.52E+04	2.61E+05	8.48E+04	2.091	5.46E-56	55.263
LysoPC 17:0	1.59E+06	1.36E+05	1.63E+06	2.82E+05	0.037	6.88E-01	0.162
LysoPC 17:1	1.45E+04	5.35E+03	2.55E+04	7.75E+03	0.813	5.30E-26	25.276
LysoPC 18:0	2.50E+06	1.85E+06	1.97E+06	7.39E+05	-0.343	4.28E-03	2.369
LysoPC 18:1	1.09E+06	5.57E+05	1.55E+06	4.69E+05	0.506	3.83E-09	8.417
LysoPC 18:2	8.57E+05	3.15E+05	1.47E+06	4.84E+05	0.775	1.92E-20	19.716
LysoPC 18:3	1.50E+04	6.29E+03	2.69E+04	7.91E+03	0.839	1.73E-24	23.763
LysoPC 19:0	2.59E+04	8.42E+03	2.56E+04	8.37E+03	-0.016	5.31E-01	0.275
LysoPC 19:1	7.28E+03	4.33E+03	7.47E+03	3.02E+03	0.037	8.20E-01	0.086
LysoPC 20:0	1.35E+04	6.94E+03	1.15E+04	3.80E+03	-0.222	1.10E-02	1.958
LysoPC 20:1	2.61E+04	1.76E+04	1.88E+04	6.19E+03	-0.474	9.33E-05	4.030
LysoPC 20:2	1.85E+04	1.04E+04	3.23E+04	1.24E+04	0.807	4.84E-15	14.316
LysoPC 20:3	1.29E+05	6.79E+04	5.36E+05	1.75E+05	2.059	2.63E-55	54.580
LysoPC 20:4	2.78E+05	1.99E+05	1.85E+06	6.44E+05	2.734	1.55E-60	59.811
LysoPC 20:5	7.71E+04	5.79E+04	9.50E+04	5.31E+04	0.301	3.93E-02	1.406
LysoPC 22:0	6.36E+03	3.83E+03	5.09E+03	3.04E+03	-0.322	4.39E-02	1.358
LysoPC 22:4	1.33E+04	9.91E+03	3.78E+04	6.30E+04	1.509	3.49E-07	6.457
LysoPC 22:5	2.24E+04	1.22E+04	5.23E+04	1.99E+04	1.219	2.81E-28	27.551
LysoPC 22:6	6.59E+04	2.97E+04	1.73E+05	5.89E+04	1.397	1.68E-39	38.774
LysoPC 24:0	1.13E+04	4.50E+03	1.35E+04	3.71E+03	0.253	1.47E-04	3.833
LysoPC 24:1	3.98E+03	1.61E+03	6.06E+03	2.06E+05	0.605	1.52E-01	0.817
LysoPC 24:4	1.66E+03	1.05E+03	6.45E+03	2.51E+04	1.959	8.66E-04	3.063
LysoPC 26:0	2.58E+03	1.46E+03	8.25E+03	7.06E+03	1.675	7.74E-18	17.111
LysoPC 26:1	2.29E+03	1.25E+03	5.25E+03	3.94E+03	1.195	8.98E-16	15.047
LysoPC 26:2	1.50E+03	9.88E+02	3.95E+03	1.45E+03	1.393	1.02E-35	34.991
LysoPC 26:4	3.44E+03	1.53E+03	6.39E+03	2.56E+04	0.894	1.02E-02	1.991
LysoPE 16:0	1.55E+05	6.77E+04	1.28E+05	4.68E+04	-0.273	3.38E-04	3.472
LysoPE 18:0	8.77E+04	4.12E+04	5.51E+04	1.64E+04	-0.672	2.24E-12	11.650
LysoPE 18:1	1.46E+05	6.46E+04	9.01E+04	3.11E+04	-0.693	2.23E-14	13.652
LysoPE 18:2	1.02E+05	4.49E+04	1.04E+05	4.05E+04	0.017	8.95E-01	0.048
LysoPE 20:3	2.02E+04	1.07E+04	5.71E+04	2.20E+05	1.502	1.98E-03	2.704
LysoPE 20:4	8.94E+04	3.36E+04	3.23E+05	1.23E+05	1.851	1.64E-45	44.785
LysoPE 22:5	3.50E+04	1.80E+04	7.44E+04	2.99E+05	1.090	6.95E-03	2.158
LysoPE 22:6	5.04E+04	1.80E+04	1.53E+05	5.94E+04	1.607	3.66E-44	43.436
LysoPE 24:0	7.91E+03	4.07E+03	8.04E+03	4.32E+03	0.023	4.06E-01	0.392
PA 34:1	9.89E+03	6.66E+03	8.59E+03	4.74E+03	-0.203	2.04E-01	0.690
PA 34:2	1.35E+04	4.59E+03	8.23E+03	3.30E+03	-0.715	1.96E-17	16.708
PA 36:4	9.76E+03	4.57E+03	7.08E+03	5.22E+03	-0.463	1.48E-03	2.829
PA 38:6	7.91E+03	3.48E+03	4.24E+03	2.24E+03	-0.901	1.12E-15	14.949
PC 22:0	1.35E+03	1.31E+03	1.50E+03	9.51E+03	0.161	1.43E-01	0.844
PC 23:0	2.02E+03	1.22E+03	1.68E+03	9.87E+04	-0.268	1.81E-01	0.743
PC 24:0	2.87E+03	2.12E+03	1.76E+03	1.54E+04	-0.705	5.14E-01	0.289
PC 25:1	1.50E+03	1.35E+03	1.67E+03	2.23E+05	0.156	1.55E-01	0.810
PC 26:0	9.75E+03	7.57E+03	2.54E+03	1.94E+05	-1.939	3.97E-01	0.401
PC 26:1	1.29E+03	1.05E+03	7.91E+02	6.12E+03	-0.706	5.80E-01	0.237
PC 28:0	9.11E+04	6.28E+04	1.89E+04	1.29E+04	-2.266	2.04E-24	23.691
PC 28:1	7.82E+03	5.30E+03	2.17E+03	4.91E+03	-1.849	1.39E-11	10.857
PC 29:0	2.65E+04	1.47E+04	7.26E+03	1.99E+04	-1.865	6.52E-11	10.186
PC 30:0	1.90E+05	7.95E+04	1.22E+05	5.60E+04	-0.638	4.11E-12	11.386
PC 30:1	1.83E+05	1.18E+05	5.21E+04	2.97E+04	-1.813	5.52E-23	22.258
PC 30:2	1.77E+04	1.04E+04	3.17E+03	5.27E+03	-2.485	2.18E-26	25.662
PC 30:3	1.32E+04	6.80E+03	4.30E+03	2.48E+03	-1.624	5.97E-28	27.224
PC 31:0	7.40E+04	2.69E+04	7.50E+04	1.95E+05	0.021	1.45E-01	0.840
PC 31:1	6.01E+04	2.94E+04	2.45E+04	3.23E+04	-1.293	3.35E-12	11.475
PC 31:2	6.02E+05	2.24E+05	7.64E+04	9.43E+04	-2.978	7.38E-58	57.132
PC 32:0	1.92E+06	2.82E+05	1.96E+06	5.50E+05	0.033	9.05E-01	0.043
PC 32:1	2.54E+06	9.93E+05	1.98E+06	6.41E+05	-0.361	2.97E-07	6.527
PC 32:2	1.90E+06	6.89E+05	2.00E+05	1.84E+05	-3.249	7.10E-64	63.149
PC 32:3	5.38E+04	2.72E+04	8.91E+03	6.81E+03	-2.594	3.60E-39	38.443

PC 32:4	2.19E+04	1.06E+04	1.11E+04	4.37E+03	-0.976	1.94E-18	17.712
PC 33:0	1.13E+05	3.21E+04	8.48E+04	3.30E+04	-0.412	1.39E-09	8.858
PC 33:1	1.01E+05	3.96E+04	3.06E+04	1.81E+04	-1.726	7.63E-41	40.117
PC 33:2	1.01E+06	3.15E+05	8.49E+04	1.56E+05	-3.575	5.42E-71	70.266
PC 33:3	4.32E+04	1.43E+04	9.80E+03	6.83E+03	-2.139	1.33E-55	54.875
PC 34:0	5.48E+05	2.09E+05	4.21E+05	1.36E+05	-0.382	6.19E-08	7.208
PC 34:1	3.89E+06	2.85E+06	8.24E+05	3.95E+05	-2.239	1.05E-22	21.977
PC 34:2	8.78E+07	2.18E+08	5.95E+06	1.33E+07	-3.883	1.47E-04	3.834
PC 34:3	4.51E+06	1.16E+06	6.66E+05	5.60E+05	-2.759	7.68E-79	78.115
PC 34:4	5.28E+05	2.02E+05	7.45E+04	5.15E+04	-2.827	9.13E-58	57.039
PC 34:5	9.07E+03	7.99E+03	2.09E+03	4.36E+04	-2.114	8.24E-01	0.084
PC 35:1	3.47E+04	1.01E+04	1.50E+04	2.98E+04	-1.208	1.88E-07	6.726
PC 35:2	1.14E+05	5.57E+04	2.91E+04	2.58E+04	-1.965	1.60E-32	31.795
PC 35:3	2.22E+05	4.20E+04	9.25E+04	2.87E+04	-1.260	5.01E-69	68.301
PC 35:4	2.94E+05	8.74E+04	1.18E+05	3.74E+04	-1.314	8.56E-49	48.068
PC 35:5	2.69E+04	1.67E+04	6.42E+03	4.29E+03	-2.067	3.91E-26	25.408
PC 35:6	6.11E+05	1.79E+05	2.33E+05	1.25E+05	-1.389	1.69E-44	43.773
PC 35:7	2.64E+04	1.07E+04	5.45E+03	3.16E+05	-2.274	5.08E-01	0.295
PC 36:0	1.48E+05	4.18E+04	1.08E+05	3.67E+04	-0.456	3.86E-13	12.414
PC 36:1	4.02E+06	1.07E+06	2.18E+06	6.37E+05	-0.884	6.05E-37	36.218
PC 36:2	7.46E+05	1.48E+06	1.72E+05	2.01E+06	-2.115	2.20E-01	0.657
PC 36:3	3.29E+06	6.56E+05	1.47E+06	3.61E+05	-1.159	5.35E-66	65.271
PC 36:4	3.52E+06	7.26E+05	2.38E+06	6.53E+05	-0.561	7.09E-27	26.150
PC 36:5	1.34E+04	3.57E+04	9.62E+03	1.62E+04	-0.478	3.57E-01	0.447
PC 36:6	2.71E+05	1.26E+05	5.30E+04	3.25E+04	-2.353	4.61E-42	41.336
PC 36:7	4.55E+04	1.24E+04	1.22E+04	6.76E+05	-1.901	3.66E-01	0.436
PC 37:1	3.79E+04	1.22E+04	2.21E+04	9.09E+03	-0.779	9.70E-22	21.013
PC 37:2	5.13E+04	3.66E+04	3.33E+04	2.46E+04	-0.626	1.04E-04	3.984
PC 37:3	6.88E+04	3.05E+04	4.35E+04	2.17E+04	-0.663	1.56E-11	10.807
PC 37:4	4.73E+05	1.74E+05	3.55E+05	1.47E+05	-0.412	8.78E-08	7.057
PC 37:5	1.79E+05	5.53E+04	3.94E+04	5.17E+04	-2.188	4.50E-46	45.347
PC 37:6	1.49E+05	5.64E+04	4.81E+04	1.63E+04	-1.630	1.25E-43	42.903
PC 37:7	8.81E+04	2.84E+04	2.73E+04	1.54E+04	-1.690	2.90E-49	48.538
PC 38:1	5.84E+04	1.49E+04	2.87E+04	2.76E+04	-1.024	8.01E-16	15.096
PC 38:2	1.51E+05	4.51E+04	1.28E+05	1.75E+05	-0.241	9.65E-01	0.015
PC 38:3	1.10E+06	2.54E+05	1.27E+06	2.81E+05	0.212	5.09E-05	4.293
PC 38:4	9.57E+06	2.38E+06	1.57E+07	3.50E+06	0.714	9.46E-33	32.024
PC 38:5	8.46E+05	2.05E+05	4.86E+05	1.48E+05	-0.799	4.43E-35	34.354
PC 38:6	1.20E+07	3.04E+06	9.43E+06	2.73E+06	-0.348	7.92E-11	10.101
PC 38:7	1.65E+05	5.24E+04	4.74E+04	2.90E+04	-1.803	7.84E-52	51.106
PC 39:3	3.03E+04	1.10E+04	3.12E+04	1.22E+05	0.041	1.46E-01	0.836
PC 39:4	7.48E+04	2.36E+04	8.30E+04	3.55E+04	0.151	7.37E-02	1.132
PC 39:5	3.90E+03	5.10E+03	2.50E+03	9.98E+03	-0.642	9.05E-01	0.043
PC 39:6	1.49E+05	5.71E+04	1.11E+05	4.10E+04	-0.421	2.41E-07	6.618
PC 39:7	1.81E+04	6.38E+03	1.34E+04	5.88E+04	-0.438	5.89E-01	0.230
PC 40:0	4.83E+03	3.48E+03	2.70E+03	2.29E+06	-0.839	1.62E-01	0.790
PC 40:1	1.32E+04	6.40E+03	7.86E+03	1.02E+04	-0.744	4.42E-04	3.355
PC 40:2	4.37E+04	2.78E+04	2.05E+04	1.56E+04	-1.089	5.89E-12	11.230
PC 40:3	6.68E+04	2.66E+04	4.92E+04	2.40E+05	-0.440	5.11E-01	0.292
PC 40:4	1.46E+05	3.56E+04	1.26E+05	3.94E+04	-0.214	3.15E-05	4.502
PC 40:5	2.57E+05	6.99E+04	2.07E+05	7.56E+04	-0.311	3.17E-07	6.498
PC 40:6	2.39E+06	6.05E+05	2.86E+06	9.08E+05	0.263	4.05E-05	4.392
PC 40:7	8.81E+04	2.03E+04	4.43E+04	1.10E+04	-0.990	2.56E-49	48.592
PC 40:8	2.05E+05	4.74E+04	1.38E+05	3.91E+04	-0.571	5.48E-23	22.261
PC 40:9	1.38E+04	6.02E+03	7.63E+03	4.96E+03	-0.852	1.21E-13	12.917
PC 40:10	2.50E+04	7.74E+03	1.70E+04	1.05E+05	-0.560	5.62E-01	0.250
PC 41:5	1.15E+04	1.03E+04	8.14E+03	5.80E+03	-0.505	6.32E-03	2.200
PC 41:6	1.55E+04	7.24E+03	1.48E+04	1.23E+05	-0.068	1.80E-01	0.744
PC 42:1	1.51E+04	2.06E+04	7.33E+03	6.90E+03	-1.042	8.76E-04	3.058
PC 42:2	1.71E+04	1.05E+04	8.63E+03	6.28E+03	-0.988	2.18E-10	9.661
PC 42:3	1.93E+04	1.32E+04	1.40E+04	1.52E+04	-0.459	6.72E-02	1.173
PC 42:4	1.73E+04	1.09E+04	1.54E+04	2.12E+05	-0.167	1.87E-01	0.727
PC 42:5	6.18E+04	1.93E+04	3.65E+04	1.69E+05	-0.757	8.85E-01	0.053

PC 42:6	5.40E+04	1.62E+04	3.19E+04	5.15E+05	-0.760	3.28E-01	0.484
PC 42:7	4.44E+04	1.79E+04	2.36E+04	8.20E+03	-0.914	2.28E-22	21.642
PC 42:8	2.19E+04	6.56E+03	3.00E+04	9.06E+04	0.456	2.01E-02	1.698
PC 42:9	3.26E+04	1.01E+04	2.55E+04	4.64E+04	-0.355	7.76E-01	0.110
PC 42:10	7.00E+04	2.78E+04	3.24E+04	4.28E+04	-1.114	5.06E-10	9.296
PC 42:11	8.85E+03	3.94E+03	1.02E+04	9.33E+06	0.197	1.58E-01	0.801
PC 44:2	3.58E+03	2.78E+03	1.87E+03	1.84E+04	-0.939	6.58E-01	0.182
PC 44:3	1.69E+03	8.60E+02	1.64E+03	2.44E+05	-0.045	1.58E-01	0.802
PC 44:4	1.44E+04	9.18E+03	1.71E+04	9.27E+03	0.248	3.03E-02	1.519
PC 44:5	8.86E+03	5.99E+03	9.57E+03	1.54E+04	0.112	9.46E-02	1.024
PC 44:6	4.30E+03	2.24E+03	7.34E+03	2.96E+03	0.772	3.77E-16	15.424
PC 46:4	1.65E+03	9.69E+02	2.60E+03	9.09E+04	0.653	1.29E-01	0.890
PC 46:5	1.22E+03	9.34E+02	1.52E+03	9.10E+04	0.321	1.48E-01	0.830
PE 30:0	1.53E+04	9.99E+03	3.56E+03	3.08E+03	-2.101	1.43E-23	22.846
PE 32:0	2.95E+04	1.04E+04	2.20E+04	1.45E+04	-0.424	2.99E-05	4.524
PE 32:1	1.81E+05	1.18E+05	5.31E+04	1.38E+05	-1.766	2.52E-09	8.599
PE 32:2	3.00E+04	1.63E+04	3.98E+03	7.87E+04	-2.911	5.19E-02	1.285
PE 33:0	8.46E+03	3.93E+03	1.06E+04	3.23E+04	0.323	4.21E-02	1.376
PE 33:1	2.67E+04	1.08E+04	7.70E+03	4.61E+03	-1.795	4.26E-40	39.371
PE 33:2	3.50E+04	1.43E+04	3.32E+03	5.70E+03	-3.397	4.97E-53	52.304
PE 34:0	3.39E+06	3.90E+05	3.85E+06	6.61E+05	0.183	4.14E-07	6.382
PE 34:1	2.56E+05	7.33E+04	5.39E+04	3.25E+05	-2.250	5.42E-07	6.266
PE 34:2	2.91E+06	8.93E+05	2.85E+05	4.25E+05	-3.350	2.02E-71	70.695
PE 34:3	1.07E+06	5.21E+05	5.64E+04	1.37E+05	-4.242	1.36E-48	47.867
PE 34:4	1.82E+04	8.32E+03	3.56E+03	4.28E+03	-2.353	4.69E-37	36.329
PE 35:0	1.66E+04	1.05E+04	1.67E+04	2.26E+04	0.010	2.44E-01	0.613
PE 35:1	3.93E+04	1.94E+04	1.59E+04	1.04E+04	-1.303	3.22E-22	21.492
PE 35:2	1.52E+05	5.08E+04	1.70E+04	1.75E+04	-3.156	3.33E-67	66.478
PE 35:3	2.70E+04	1.05E+04	4.62E+03	4.85E+03	-2.547	4.34E-49	48.362
PE 35:4	5.29E+04	2.21E+04	7.40E+03	1.72E+04	-2.837	3.75E-38	37.426
PE 36:0	5.99E+04	1.77E+04	6.19E+04	1.45E+04	0.048	6.36E-01	0.197
PE 36:1	8.77E+05	2.56E+05	1.03E+05	1.57E+05	-3.085	1.09E-68	67.964
PE 36:2	1.01E+06	3.15E+05	8.49E+04	1.58E+05	-3.575	1.27E-70	69.895
PE 36:3	2.35E+06	6.55E+05	2.91E+05	3.35E+05	-3.013	2.94E-75	74.532
PE 36:4	2.99E+06	7.34E+05	8.58E+05	4.50E+05	-1.803	6.13E-67	66.212
PE 36:5	7.35E+05	4.43E+05	7.97E+04	1.78E+05	-3.204	2.53E-32	31.598
PE 36:6	2.35E+04	1.23E+04	2.89E+03	3.32E+03	-3.023	9.82E-40	39.008
PE 37:2	3.48E+04	1.22E+04	8.15E+03	6.56E+03	-2.093	3.70E-50	49.432
PE 37:3	4.11E+04	1.44E+04	1.24E+04	1.24E+05	-1.731	3.25E-01	0.489
PE 37:4	1.51E+05	4.12E+04	4.13E+04	5.76E+04	-1.874	5.48E-35	34.262
PE 37:5	6.41E+04	2.08E+04	4.55E+04	1.19E+05	-0.494	8.40E-01	0.075
PE 37:6	1.54E+05	6.70E+04	1.65E+04	2.65E+05	-3.223	1.67E-04	3.778
PE 38:1	4.47E+04	1.78E+04	1.49E+04	8.31E+03	-1.591	2.85E-37	36.545
PE 38:2	1.20E+05	3.73E+04	3.39E+04	1.95E+04	-1.824	2.26E-53	52.645
PE 38:3	7.88E+05	2.79E+05	2.52E+05	1.30E+05	-1.642	5.51E-45	44.259
PE 38:4	9.21E+05	2.19E+05	2.70E+05	2.64E+05	-1.770	1.56E-46	45.808
PE 38:5	4.42E+05	1.20E+05	1.19E+05	6.05E+04	-1.898	6.56E-65	64.183
PE 38:6	6.11E+05	1.79E+05	2.33E+05	1.24E+05	-1.389	1.44E-44	43.841
PE 38:7	1.50E+05	6.01E+04	2.32E+04	1.83E+04	-2.691	5.34E-53	52.272
PE 39:6	1.02E+05	3.48E+04	2.46E+04	1.17E+04	-2.048	2.72E-55	54.565
PE 40:2	6.84E+03	4.46E+03	5.84E+03	1.09E+04	-0.227	7.75E-01	0.111
PE 40:4	1.61E+05	7.98E+04	7.32E+04	3.95E+04	-1.133	2.94E-20	19.532
PE 40:5	7.35E+05	2.15E+05	1.81E+05	1.09E+05	-2.025	1.77E-61	60.752
PE 40:6	2.26E+06	6.80E+05	5.70E+05	2.89E+05	-1.987	4.89E-61	60.310
PE 40:7	7.11E+05	2.29E+05	1.19E+05	8.74E+04	-2.580	1.54E-64	63.812
PE 40:8	1.41E+05	4.64E+04	5.32E+04	3.51E+05	-1.404	2.31E-01	0.637
PE 42:10	7.82E+03	4.25E+03	1.05E+04	1.62E+04	0.422	7.72E-03	2.112
PL-PC 24:0	3.41E+03	2.83E+03	4.80E+03	5.29E+04	0.493	9.24E-02	1.034
PL-PC 26:0	2.19E+03	1.64E+03	3.58E+03	2.09E+03	0.708	1.31E-08	7.884
PL-PC 30:0	1.09E+04	5.67E+03	1.57E+04	2.15E+04	0.526	7.53E-04	3.123
PL-PC 32:0	1.03E+05	4.53E+04	1.06E+05	3.54E+04	0.043	9.67E-01	0.014
PL-PC 32:1	4.20E+04	2.76E+04	3.45E+04	2.49E+04	-0.284	6.74E-02	1.171
PL-PC 34:0	6.26E+05	1.25E+05	3.24E+05	1.09E+05	-0.949	1.34E-47	46.874

PL-PC 34:1	4.77E+05	1.65E+05	1.45E+05	8.19E+04	-1.714	2.21E-46	45.655
PL-PC 34:2	8.45E+05	2.27E+05	1.79E+05	9.73E+04	-2.241	5.59E-73	72.252
PL-PC 34:3	2.75E+04	9.83E+03	1.42E+04	5.46E+03	-0.954	1.07E-26	25.972
PL-PC 34:4	3.67E+03	2.31E+03	1.27E+03	4.74E+03	-1.525	7.32E-04	3.136
PL-PC 35:0	1.99E+04	5.59E+03	9.32E+03	1.91E+04	-1.095	2.67E-05	4.573
PL-PC 35:1	1.32E+04	6.17E+03	4.90E+03	4.75E+03	-1.433	1.90E-20	19.722
PL-PC 35:2	5.12E+04	1.99E+04	1.13E+04	7.25E+03	-2.176	5.40E-49	48.268
PL-PC 35:3	1.26E+04	5.50E+03	1.08E+04	4.44E+03	-0.224	1.34E-02	1.872
PL-PC 36:0	8.51E+04	2.25E+04	2.64E+04	1.73E+05	-1.686	4.11E-02	1.386
PL-PC 36:1	3.14E+05	7.47E+04	8.28E+04	3.91E+04	-1.925	3.86E-74	73.413
PL-PC 36:2	2.87E+05	1.01E+05	1.57E+05	8.64E+04	-0.866	4.89E-20	19.311
PL-PC 36:3	1.45E+06	2.81E+05	1.26E+06	2.48E+05	-0.206	3.31E-08	7.481
PL-PC 36:4	9.89E+05	2.07E+05	8.88E+05	2.18E+05	-0.155	1.34E-04	3.874
PL-PC 36:5	6.57E+04	2.99E+04	4.48E+04	2.43E+04	-0.551	2.13E-08	7.672
PL-PC 36:6	2.35E+04	6.92E+03	1.25E+04	4.40E+03	-0.911	5.70E-31	30.244
PL-PC 37:1	1.53E+04	4.88E+03	8.32E+03	3.89E+03	-0.877	1.51E-23	22.821
PL-PC 37:2	1.12E+04	4.32E+03	4.75E+03	2.73E+03	-1.232	1.05E-28	27.978
PL-PC 37:3	1.46E+04	4.60E+03	9.86E+03	5.51E+03	-0.564	9.02E-11	10.045
PL-PC 37:4	7.11E+04	2.17E+04	4.50E+04	3.23E+04	-0.660	1.24E-08	7.906
PL-PC 37:6	2.05E+05	6.36E+04	6.56E+04	3.79E+05	-1.641	2.05E-02	1.689
PL-PC 38:3	8.78E+05	2.49E+05	6.88E+05	5.15E+05	-0.352	4.21E-04	3.376
PL-PC 38:4	8.94E+05	2.78E+05	5.73E+05	1.50E+05	-0.642	2.05E-21	20.688
PL-PC 38:5	9.21E+04	2.31E+04	5.46E+04	1.37E+04	-0.755	1.46E-33	32.837
PL-PC 38:6	1.57E+05	5.12E+04	1.60E+05	4.18E+04	0.026	9.39E-01	0.028
PL-PC 39:5	2.78E+04	1.32E+04	2.11E+04	2.99E+05	-0.400	2.35E-01	0.630
PL-PC 40:0	6.05E+04	3.15E+04	2.56E+04	2.02E+04	-1.239	1.35E-18	17.868
PL-PC 40:1	9.10E+03	3.82E+03	4.63E+03	2.74E+03	-0.974	3.81E-19	18.419
PL-PC 40:2	2.16E+04	5.70E+03	9.83E+03	1.83E+04	-1.137	4.56E-07	6.341
PL-PC 40:3	6.17E+04	2.61E+04	2.73E+04	9.53E+03	-1.176	3.37E-28	27.473
PL-PC 40:4	3.39E+05	9.67E+04	1.58E+05	5.37E+04	-1.098	2.58E-40	39.589
PL-PC 40:5	2.72E+05	8.40E+04	1.68E+05	4.55E+04	-0.699	2.32E-23	22.635
PL-PC 40:6	2.00E+05	6.24E+04	1.05E+05	3.20E+04	-0.930	2.05E-32	31.687
PL-PC 41:4	3.89E+04	2.04E+04	2.52E+04	2.70E+05	-0.626	3.77E-01	0.424
PL-PC 42:0	2.69E+04	2.25E+04	1.20E+04	9.58E+03	-1.169	1.29E-09	8.891
PL-PC 42:1	2.45E+04	1.55E+04	1.34E+04	1.40E+04	-0.870	9.37E-07	6.028
PL-PC 42:2	1.67E+05	1.15E+05	7.54E+04	6.54E+04	-1.149	1.19E-11	10.924
PL-PC 42:3	6.71E+04	2.47E+04	3.21E+04	3.59E+04	-1.062	2.30E-12	11.638
PL-PC 42:4	3.47E+05	1.96E+05	1.45E+05	1.01E+05	-1.259	1.51E-17	16.821
PL-PC 42:5	1.30E+05	4.43E+04	5.56E+04	2.46E+04	-1.223	9.34E-36	35.030
PL-PC 43:3	1.11E+04	5.70E+03	5.29E+03	8.46E+06	-1.071	1.61E-01	0.794
PL-PC 43:4	1.01E+04	5.17E+03	7.55E+03	4.04E+03	-0.422	3.40E-04	3.468
PL-PC 44:1	8.72E+03	1.05E+04	2.90E+03	2.72E+03	-1.587	2.14E-07	6.669
PL-PC 44:2	4.52E+04	2.66E+04	1.94E+04	1.49E+04	-1.223	4.10E-16	15.387
PL-PC 44:3	8.82E+04	5.36E+04	4.34E+04	2.76E+04	-1.024	3.79E-13	12.421
PL-PC 44:4	3.20E+05	1.40E+05	1.59E+05	8.36E+04	-1.014	1.15E-20	19.940
PL-PC 44:5	2.54E+05	8.36E+04	1.22E+05	5.60E+04	-1.062	1.79E-31	30.746
PL-PC 44:6	1.06E+05	3.74E+04	6.05E+04	3.39E+05	-0.805	9.82E-01	0.008
PL-PC 46:4	5.81E+04	3.52E+04	3.98E+04	2.09E+04	-0.546	5.54E-06	5.256
PL-PE 32:0	2.91E+04	9.89E+03	1.67E+04	1.42E+04	-0.806	5.81E-10	9.236
PL-PE 32:1	1.66E+04	5.13E+03	1.35E+04	2.51E+05	-0.295	2.02E-01	0.694
PL-PE 32:2	1.23E+04	8.09E+03	2.56E+03	2.88E+03	-2.258	9.24E-24	23.034
PL-PE 34:1	3.02E+05	7.28E+04	2.18E+05	1.00E+05	-0.472	1.50E-11	10.823
PL-PE 34:2	6.67E+05	2.08E+05	9.27E+04	8.18E+04	-2.848	6.30E-69	68.201
PL-PE 34:3	2.57E+04	1.18E+04	5.51E+03	7.54E+04	-2.224	1.81E-01	0.742
PL-PE 34:4	3.69E+04	5.66E+04	4.45E+03	6.44E+04	-3.053	4.84E-03	2.315
PL-PE 35:1	2.56E+04	8.77E+03	9.95E+03	5.57E+03	-1.361	1.07E-36	35.970
PL-PE 35:2	4.58E+04	1.76E+04	6.47E+03	8.04E+03	-2.822	3.51E-52	51.454
PL-PE 35:4	2.16E+04	2.90E+04	4.03E+03	1.58E+04	-2.423	2.55E-06	5.594
PL-PE 36:1	2.59E+05	7.82E+04	8.49E+04	5.88E+04	-1.606	1.72E-45	44.764
PL-PE 36:2	8.49E+05	2.54E+05	9.47E+04	9.25E+04	-3.164	8.32E-75	74.080
PL-PE 36:3	8.46E+05	1.97E+05	2.36E+05	1.10E+05	-1.844	5.96E-73	72.225
PL-PE 36:4	1.94E+06	4.68E+05	9.64E+05	3.96E+05	-1.009	2.31E-40	39.637
PL-PE 36:5	1.21E+05	1.15E+05	2.02E+04	3.00E+04	-2.580	1.23E-15	14.909

PL-PE 36:6	3.67E+04	1.73E+04	1.08E+04	7.27E+03	-1.761	4.43E-32	31.353
PL-PE 37:2	1.87E+04	6.50E+03	3.60E+03	6.90E+03	-2.374	2.83E-36	35.548
PL-PE 37:4	1.38E+05	4.80E+04	6.28E+04	2.74E+04	-1.135	1.18E-30	29.927
PL-PE 37:5	3.82E+04	2.28E+04	1.36E+04	7.89E+03	-1.495	2.15E-20	19.668
PL-PE 37:6	2.97E+04	1.90E+04	9.74E+03	1.34E+04	-1.608	3.75E-14	13.426
PL-PE 38:1	5.05E+04	3.98E+04	1.16E+04	7.03E+03	-2.120	3.07E-19	18.512
PL-PE 38:2	1.39E+05	4.80E+04	2.78E+04	2.18E+04	-2.318	1.03E-55	54.986
PL-PE 38:3	5.33E+05	1.52E+05	1.67E+05	8.21E+04	-1.677	1.47E-55	54.833
PL-PE 38:4	4.49E+05	1.39E+05	1.87E+05	9.04E+04	-1.265	1.92E-39	38.717
PL-PE 38:5	2.34E+06	5.17E+05	8.07E+05	3.15E+05	-1.534	2.65E-68	67.577
PL-PE 38:6	1.87E+06	4.78E+05	8.38E+05	2.98E+05	-1.155	9.01E-48	47.046
PL-PE 39:4	4.49E+04	1.50E+04	2.64E+04	2.98E+04	-0.765	1.10E-05	4.959
PL-PE 39:6	1.14E+05	3.42E+04	4.72E+04	1.86E+04	-1.276	6.74E-44	43.171
PL-PE 40:1	1.85E+04	8.95E+03	5.86E+03	3.99E+03	-1.663	3.87E-30	29.413
PL-PE 40:2	4.55E+04	1.67E+04	1.42E+04	3.75E+04	-1.683	2.72E-10	9.566
PL-PE 40:3	1.25E+05	3.12E+04	8.61E+04	2.64E+05	-0.538	6.99E-01	0.155
PL-PE 40:4	3.88E+05	1.02E+05	2.59E+05	1.42E+05	-0.584	3.07E-13	12.512
PL-PE 40:5	5.50E+05	1.26E+05	1.92E+05	1.95E+05	-1.518	1.28E-34	33.891
PL-PE 40:6	2.05E+05	6.36E+04	6.56E+04	2.55E+04	-1.641	1.40E-53	52.854
PL-PE 42:4	7.04E+04	2.35E+04	5.05E+04	1.32E+05	-0.478	6.89E-01	0.162
PL-PE 42:6	1.36E+05	4.77E+04	4.44E+04	1.87E+04	-1.609	7.41E-46	45.130
PG 32:0	9.91E+03	6.93E+03	6.54E+03	4.48E+03	-0.601	1.89E-04	3.724
PG 32:1	4.70E+03	2.51E+03	2.19E+03	7.65E+03	-1.100	6.01E-02	1.221
PG 33:0	3.05E+04	1.13E+04	3.00E+04	2.30E+05	-0.025	2.48E-01	0.606
PG 34:0	3.87E+06	7.75E+05	4.98E+06	1.08E+06	0.364	1.41E-13	12.852
PG 34:1	8.81E+04	2.89E+04	1.71E+04	1.41E+04	-2.369	4.13E-59	58.384
PG 34:2	2.08E+04	7.34E+03	4.59E+03	5.74E+03	-2.179	1.67E-42	41.778
PG 36:0	5.97E+04	1.23E+04	1.18E+05	4.67E+04	0.982	8.79E-27	26.056
PG 36:2	1.46E+05	5.07E+04	3.45E+04	2.31E+04	-2.083	2.24E-52	51.650
PI 34:1	1.23E+05	4.98E+04	2.20E+04	4.14E+04	-2.481	2.64E-36	35.579
PI 34:2	1.19E+05	4.30E+04	1.88E+04	1.52E+04	-2.665	1.32E-58	57.881
PI 36:1	9.89E+04	4.84E+04	1.62E+04	1.72E+04	-2.610	5.25E-40	39.280
PI 36:2	5.12E+05	1.70E+05	4.43E+04	1.27E+05	-3.531	5.50E-57	56.260
PI 36:3	1.05E+05	3.70E+04	3.51E+04	1.56E+04	-1.578	1.52E-44	43.819
PI 36:4	1.00E+05	3.94E+04	7.91E+04	3.14E+04	-0.339	6.81E-06	5.167
PI 38:3	8.35E+05	3.38E+05	3.76E+05	1.72E+05	-1.153	3.39E-28	27.470
PI 38:4	1.06E+06	3.54E+05	6.19E+05	2.39E+05	-0.780	1.32E-22	21.879
PI 38:5	8.16E+04	2.97E+04	4.61E+04	2.50E+04	-0.823	1.71E-16	15.768
PI 38:6	2.27E+04	1.14E+04	1.33E+04	2.05E+04	-0.772	2.19E-03	2.659
PI 40:5	1.07E+05	3.85E+04	6.11E+04	3.24E+04	-0.807	8.69E-17	16.061
PI 40:6	9.38E+04	3.76E+04	3.45E+04	1.41E+04	-1.443	2.76E-36	35.559
PS 36:1	1.66E+05	6.08E+04	4.04E+04	3.04E+04	-2.042	4.72E-48	47.326
PS 38:4	1.60E+04	9.77E+03	3.21E+04	1.08E+06	1.000	2.15E-01	0.667
SM 29:1	2.18E+03	8.45E+02	9.17E+02	7.86E+03	-1.251	8.11E-01	0.091
SM 30:0	7.00E+03	3.28E+03	4.33E+03	5.53E+03	-0.693	1.75E-03	2.756
SM 30:1	6.85E+04	2.25E+04	1.73E+04	9.99E+03	-1.982	3.35E-54	53.475
SM 30:2	7.05E+03	2.52E+03	3.39E+03	1.80E+03	-1.055	7.05E-25	24.152
SM 31:1	4.17E+04	1.49E+04	1.04E+04	5.88E+03	-1.998	2.48E-50	49.605
SM 32:0	9.13E+04	3.70E+04	5.61E+04	3.94E+04	-0.702	5.43E-09	8.265
SM 32:1	1.73E+06	4.72E+05	4.26E+05	2.09E+05	-2.022	3.89E-68	67.410
SM 32:2	1.78E+05	4.71E+04	7.44E+04	1.94E+05	-1.257	3.32E-05	4.479
SM 33:0	7.74E+04	2.32E+04	2.00E+04	5.03E+04	-1.954	2.60E-18	17.584
SM 33:1	5.44E+05	1.84E+05	1.81E+05	7.03E+04	-1.590	5.46E-48	47.263
SM 33:2	3.18E+04	1.01E+04	9.84E+03	4.65E+03	-1.691	1.80E-50	49.745
SM 34:0	3.45E+05	1.04E+05	2.26E+05	1.02E+05	-0.607	2.20E-15	14.658
SM 34:1	3.41E+06	7.58E+05	1.64E+06	4.62E+05	-1.061	1.74E-53	52.759
SM 34:2	2.67E+06	5.44E+05	1.20E+06	3.82E+05	-1.148	1.60E-59	58.796
SM 34:3	1.77E+04	5.72E+03	6.24E+03	6.23E+04	-1.502	5.53E-01	0.257
SM 35:1	1.07E+06	2.12E+05	2.33E+06	5.32E+05	1.119	2.05E-56	55.689
SM 35:2	3.56E+04	1.56E+04	1.72E+04	3.24E+04	-1.049	2.30E-05	4.639
SM 35:6	5.58E+03	3.29E+03	2.99E+03	2.63E+03	-0.902	6.81E-08	7.167
SM 36:0	8.36E+04	2.30E+04	1.32E+05	5.41E+04	0.665	1.86E-14	13.729
SM 36:1	2.75E+06	5.96E+05	2.37E+06	5.25E+05	-0.220	4.93E-08	7.308

SM 36:2	1.48E+06	4.16E+05	1.70E+06	4.72E+05	0.204	2.42E-03	2.617
SM 36:3	2.01E+05	6.01E+04	5.46E+04	3.37E+04	-1.877	5.15E-55	54.288
SM 36:4	3.48E+04	8.72E+03	1.81E+04	6.04E+03	-0.943	4.16E-40	39.381
SM 37:1	1.84E+05	8.26E+04	1.12E+05	4.65E+04	-0.711	3.10E-13	12.509
SM 37:2	4.73E+04	1.49E+04	4.27E+04	1.33E+04	-0.150	9.15E-03	2.039
SM 38:0	2.16E+05	4.94E+04	2.97E+05	9.73E+04	0.460	8.66E-12	11.063
SM 38:1	3.24E+05	1.48E+05	2.59E+05	1.25E+05	-0.323	7.71E-04	3.113
SM 38:2	5.99E+05	1.54E+05	8.04E+05	1.92E+05	0.425	1.19E-13	12.924
SM 38:3	5.13E+04	1.73E+04	4.78E+04	1.27E+06	-0.102	2.69E-01	0.570
SM 38:4	2.53E+04	8.87E+03	1.54E+04	7.30E+03	-0.712	1.35E-14	13.869
SM 38:5	1.63E+04	7.30E+03	2.72E+04	1.52E+04	0.734	5.47E-12	11.262
SM 39:1	2.53E+05	7.11E+04	1.25E+05	1.48E+05	-1.016	6.84E-12	11.165
SM 39:2	1.40E+05	3.29E+04	6.65E+04	2.16E+04	-1.075	2.53E-49	48.597
SM 39:3	4.76E+04	1.35E+04	4.02E+04	1.15E+04	-0.244	8.24E-06	5.084
SM 40:0	3.10E+05	6.20E+04	3.14E+05	7.62E+04	0.023	9.95E-01	0.002
SM 40:1	2.92E+06	4.31E+06	1.16E+06	4.16E+05	-1.334	3.37E-05	4.472
SM 40:2	2.06E+06	1.02E+06	1.56E+06	1.25E+06	-0.400	1.03E-03	2.989
SM 40:3	2.64E+05	7.22E+04	1.92E+05	5.10E+04	-0.459	5.69E-16	15.245
SM 40:4	3.90E+04	1.21E+04	6.54E+04	1.79E+04	0.746	9.76E-27	26.011
SM 40:5	3.23E+04	9.63E+03	3.34E+04	1.19E+04	0.049	3.17E-01	0.499
SM 41:0	2.18E+05	4.67E+04	8.92E+04	3.68E+04	-1.291	3.52E-58	57.453
SM 41:1	1.45E+06	2.61E+05	3.43E+05	1.58E+05	-2.079	3.66E-95	94.437
SM 41:2	7.43E+05	1.34E+05	3.09E+05	9.86E+04	-1.265	1.15E-70	69.939
SM 41:3	1.86E+05	4.44E+04	1.18E+05	3.37E+04	-0.660	1.00E-28	27.998
SM 42:1	2.26E+06	5.43E+05	1.48E+06	6.11E+05	-0.608	8.14E-20	19.090
SM 42:2	1.14E+07	2.91E+07	2.81E+06	9.60E+05	-2.025	2.38E-03	2.623
SM 42:3	2.80E+06	6.13E+05	1.96E+06	4.20E+05	-0.509	3.54E-25	24.451
SM 42:4	3.68E+05	1.10E+05	5.16E+05	1.32E+05	0.488	1.00E-14	14.000
SM 42:5	1.50E+05	7.90E+04	1.58E+05	4.87E+04	0.074	4.99E-01	0.302
SM 42:6	7.78E+04	3.32E+04	8.62E+04	3.42E+04	0.148	3.51E-02	1.455
SM 42:7	3.02E+04	1.42E+04	2.03E+04	3.80E+05	-0.572	3.56E-01	0.449
SM 43:1	4.80E+04	1.69E+04	2.98E+04	1.04E+04	-0.685	5.69E-18	17.245
SM 43:2	1.69E+05	5.61E+04	1.04E+05	3.28E+04	-0.697	9.56E-21	20.020
SM 43:3	5.97E+04	2.13E+04	5.39E+04	1.65E+04	-0.149	1.73E-02	1.761
SM 43:4	1.40E+04	1.05E+04	1.87E+04	2.20E+04	0.414	5.59E-02	1.252
SM 43:7	1.18E+04	5.21E+03	7.37E+03	4.16E+03	-0.677	2.14E-10	9.669
SM 44:1	1.32E+04	4.71E+03	1.91E+04	3.33E+05	0.530	1.10E-01	0.959
SM 44:2	9.90E+03	5.42E+03	1.20E+04	8.47E+03	0.280	4.68E-03	2.330
SM 44:3	3.73E+04	2.23E+04	5.14E+04	2.55E+04	0.463	4.06E-05	4.391
SM 44:4	1.85E+04	9.77E+03	4.40E+04	3.05E+04	1.253	1.66E-17	16.780
SM 44:5	2.90E+04	1.83E+04	4.46E+04	1.73E+04	0.623	5.32E-11	10.274
SM 44:6	2.10E+04	1.40E+04	2.69E+04	1.18E+05	0.358	6.13E-02	1.213
SM 44:7	7.69E+03	4.55E+03	1.14E+04	5.57E+03	0.566	1.49E-06	5.828
SM 45:4	1.38E+04	8.08E+03	7.03E+03	1.72E+04	-0.976	1.34E-02	1.872
SM 47:5	1.38E+04	2.00E+04	6.52E+03	6.24E+04	-1.076	9.68E-01	0.014
TG 36:0	4.95E+04	9.20E+04	1.63E+04	3.06E+04	-1.601	5.05E-04	3.297
TG 38:0	7.93E+04	1.68E+05	1.82E+04	3.42E+04	-2.124	4.50E-04	3.347
TG 39:0	1.44E+04	1.26E+04	5.23E+03	2.93E+04	-1.465	4.93E-02	1.307
TG 40:0	1.41E+05	2.69E+05	1.41E+04	2.88E+04	-3.320	3.72E-06	5.429
TG 40:1	1.02E+05	1.29E+05	8.62E+03	2.23E+04	-3.558	6.00E-12	11.222
TG 41:0	2.18E+04	2.02E+04	4.83E+03	2.85E+05	-2.177	5.58E-01	0.253
TG 42:0	2.47E+05	3.28E+05	1.80E+04	4.04E+04	-3.775	1.73E-11	10.763
TG 42:1	2.55E+05	3.66E+05	1.55E+04	5.47E+04	-4.035	5.71E-10	9.244
TG 42:2	1.63E+05	2.08E+05	1.02E+04	6.01E+05	-4.000	1.99E-01	0.702
TG 42:3	3.90E+04	3.61E+04	4.25E+03	4.06E+03	-3.199	5.01E-19	18.300
TG 43:0	3.19E+04	2.48E+04	7.89E+03	8.71E+03	-2.016	2.17E-17	16.664
TG 44:0	3.22E+05	2.88E+05	3.91E+04	6.43E+04	-3.039	6.94E-19	18.159
TG 44:1	5.99E+05	6.06E+05	5.30E+04	8.92E+04	-3.498	4.13E-17	16.384
TG 44:2	3.41E+05	3.15E+05	2.53E+04	4.69E+04	-3.752	3.29E-20	19.483
TG 45:0	3.98E+04	2.60E+04	1.24E+04	9.16E+03	-1.682	4.79E-20	19.320
TG 45:1	7.05E+04	5.02E+04	1.46E+04	1.32E+04	-2.273	1.29E-22	21.890
TG 46:0	5.16E+05	3.05E+05	1.12E+05	1.02E+05	-2.203	1.14E-28	27.945
TG 46:1	1.30E+06	1.05E+06	2.23E+05	2.10E+05	-2.550	7.03E-21	20.153

TG 46:2	1.01E+06	6.95E+05	1.38E+05	1.84E+05	-2.868	1.61E-26	25.792
TG 46:3	3.35E+05	2.10E+05	3.72E+04	7.53E+04	-3.172	4.45E-30	29.352
TG 47:0	5.17E+04	2.89E+04	2.00E+04	1.80E+04	-1.372	1.91E-16	15.719
TG 47:1	1.29E+05	7.43E+04	3.93E+04	2.38E+04	-1.713	5.85E-25	24.233
TG 47:2	1.17E+05	5.76E+04	2.82E+04	1.39E+05	-2.058	7.35E-07	6.134
TG 47:3	6.13E+04	2.50E+04	1.01E+04	9.73E+03	-2.596	1.83E-48	47.739
TG 48:0	8.43E+05	3.43E+05	3.15E+05	1.71E+05	-1.419	6.36E-33	32.196
TG 48:1	3.28E+06	1.67E+06	9.31E+05	5.71E+05	-1.817	2.82E-31	30.549
TG 48:2	3.05E+06	1.42E+06	7.91E+05	5.16E+05	-1.950	2.13E-36	35.671
TG 48:3	1.47E+06	6.83E+05	3.01E+05	2.15E+05	-2.287	6.87E-41	40.163
TG 48:4	4.81E+05	2.48E+05	9.12E+04	5.75E+04	-2.399	1.38E-37	36.860
TG 49:0	7.75E+04	3.19E+04	3.51E+04	3.75E+04	-1.143	5.76E-14	13.239
TG 49:1	3.34E+05	1.34E+05	1.01E+05	4.94E+04	-1.721	4.84E-41	40.315
TG 49:2	3.44E+05	1.21E+05	1.07E+05	5.21E+04	-1.683	1.76E-46	45.753
TG 49:3	1.71E+05	5.47E+04	4.42E+04	2.49E+04	-1.954	3.45E-56	55.462
TG 50:0	1.05E+06	3.43E+05	4.20E+05	2.34E+05	-1.327	1.78E-36	35.750
TG 50:1	6.72E+06	1.81E+06	3.12E+06	1.56E+06	-1.537	2.13E-52	51.671
TG 50:2	8.03E+06	1.93E+06	1.73E+06	9.45E+05	-1.363	2.20E-59	58.658
TG 50:3	5.39E+06	1.36E+06	5.91E+05	3.44E+05	-1.644	1.24E-58	57.906
TG 50:4	2.20E+06	6.47E+05	1.30E+05	7.47E+04	-1.896	1.53E-46	45.816
TG 50:5	4.72E+05	1.74E+05	2.51E+04	1.88E+04	-1.863	1.85E-38	37.732
TG 50:6	9.27E+04	3.78E+04	3.46E+05	1.15E+05	-1.883	6.11E-38	37.214
TG 51:1	3.57E+05	1.27E+05	1.18E+05	7.87E+04	-1.605	7.36E-39	38.133
TG 51:2	7.12E+05	1.99E+05	2.12E+05	9.52E+04	-1.747	6.56E-61	60.183
TG 51:3	1.61E+04	1.12E+04	4.07E+03	7.51E+03	-1.985	1.78E-15	14.751
TG 51:4	2.72E+05	6.88E+04	7.14E+04	4.75E+04	-1.927	1.42E-62	61.847
TG 51:5	9.64E+04	3.45E+04	3.03E+04	1.56E+04	-1.669	7.90E-45	44.103
TG 52:0	4.87E+05	1.62E+05	1.70E+05	9.24E+04	-1.515	1.89E-43	42.724
TG 52:1	3.98E+06	1.15E+06	1.32E+06	6.69E+05	-1.591	4.46E-53	52.351
TG 52:2	1.29E+07	2.47E+06	4.17E+06	1.86E+06	-1.623	7.68E-76	75.114
TG 52:4	1.07E+07	2.66E+06	2.49E+06	1.34E+06	-2.102	1.28E-74	73.893
TG 52:5	3.13E+06	9.51E+05	9.07E+05	4.58E+05	-1.786	2.63E-56	55.580
TG 52:6	6.16E+05	2.15E+05	2.58E+05	2.01E+05	-1.257	5.41E-25	24.267
TG 53:0	5.09E+04	1.68E+04	4.92E+04	1.99E+04	-0.050	3.65E-01	0.438
TG 53:1	1.39E+05	5.36E+04	3.65E+04	1.95E+04	-1.928	2.33E-46	45.632
TG 53:2	4.53E+05	1.42E+05	1.19E+05	5.33E+04	-1.932	5.09E-59	58.294
TG 53:3	4.32E+05	1.15E+05	1.23E+05	7.00E+04	-1.813	7.49E-61	60.126
TG 53:4	2.19E+04	1.27E+04	7.36E+03	5.96E+04	-1.574	1.53E-01	0.816
TG 53:5	1.17E+05	2.69E+04	5.23E+04	2.37E+04	-1.164	3.29E-46	45.483
TG 54:0	1.07E+05	4.94E+04	3.87E+04	4.38E+04	-1.463	1.25E-19	18.903
TG 54:1	8.30E+05	3.51E+05	2.26E+05	1.98E+05	-1.875	8.62E-37	36.064
TG 54:2	2.67E+06	8.45E+05	7.82E+05	4.67E+05	-1.774	1.02E-51	50.992
TG 54:3	3.16E+06	8.10E+05	1.26E+06	5.93E+05	-1.331	3.02E-50	49.519
TG 54:4	3.85E+06	9.54E+05	1.42E+06	2.93E+06	-1.439	3.19E-11	10.496
TG 54:5	3.54E+06	1.02E+06	1.53E+06	6.48E+05	-1.216	3.13E-43	42.505
TG 54:6	2.37E+06	8.75E+05	1.17E+06	4.94E+05	-1.012	3.67E-27	26.436
TG 54:7	8.54E+05	4.07E+05	5.22E+05	2.68E+05	-0.711	1.31E-11	10.883
TG 54:8	1.75E+05	9.19E+04	1.20E+05	6.82E+04	-0.539	1.13E-06	5.948
TG 55:1	3.17E+04	1.57E+04	7.70E+03	5.69E+03	-2.039	2.14E-34	33.670
TG 55:2	5.49E+04	1.89E+04	1.22E+04	1.04E+04	-2.170	9.14E-51	50.039
TG 55:3	7.08E+04	2.33E+04	2.12E+04	8.20E+04	-1.740	2.98E-06	5.526
TG 56:0	1.73E+04	1.23E+04	4.02E+03	1.70E+05	-2.110	7.98E-01	0.098
TG 56:1	1.16E+05	8.56E+04	1.81E+04	5.21E+06	-2.688	2.90E-01	0.538
TG 56:2	2.58E+05	1.36E+05	4.67E+04	7.21E+04	-2.465	1.83E-32	31.736
TG 56:3	3.33E+05	1.29E+05	8.99E+04	6.23E+04	-1.887	3.24E-43	42.489
TG 56:4	3.12E+05	8.00E+04	2.15E+05	9.82E+04	-0.535	1.23E-14	13.911
TG 56:5	5.65E+05	1.26E+05	5.46E+05	2.27E+05	-0.048	2.87E-01	0.542
TG 56:6	7.81E+05	1.81E+05	8.57E+05	3.27E+05	0.134	9.21E-02	1.036
TG 56:7	1.03E+06	3.58E+05	1.08E+06	4.65E+05	0.081	4.62E-01	0.335
TG 56:8	6.79E+05	2.85E+05	6.72E+05	3.72E+05	-0.015	7.20E-01	0.143
TG 56:9	1.73E+05	8.41E+04	1.74E+05	1.23E+05	0.009	4.39E-01	0.358
TG 56:10	2.65E+04	2.02E+04	2.52E+04	1.38E+04	-0.070	5.75E-01	0.240
TG 58:1	3.49E+04	3.38E+04	5.99E+03	2.32E+04	-2.541	7.48E-12	11.126

TG 58:2	9.33E+04	9.77E+04	1.22E+04	7.43E+04	-2.929	2.30E-09	8.637
TG 58:3	8.44E+04	7.43E+04	1.30E+04	3.36E+04	-2.700	9.39E-17	16.027
TG 58:4	5.88E+04	2.57E+04	1.98E+04	2.90E+04	-1.572	2.07E-18	17.684
TG 58:5	1.25E+05	4.30E+04	6.68E+04	5.25E+04	-0.909	4.48E-15	14.348
TG 58:6	1.55E+05	4.67E+04	1.31E+05	5.30E+04	-0.245	3.38E-04	3.471
TG 58:7	2.08E+05	7.25E+04	2.35E+05	8.22E+04	0.180	1.75E-02	1.757
TG 58:8	2.47E+05	1.03E+05	3.27E+05	1.22E+05	0.408	1.39E-06	5.858
TG 58:9	2.08E+05	9.06E+04	2.96E+05	1.19E+05	0.508	2.80E-08	7.552
TG 58:10	1.33E+05	6.60E+04	1.98E+05	9.25E+04	0.579	3.65E-08	7.438
TG 58:11	3.72E+04	3.01E+04	4.91E+04	8.27E+04	0.402	1.39E-02	1.858
TG 60:10	4.14E+04	2.12E+04	1.06E+05	4.83E+05	1.361	6.54E-03	2.185
TG 60:11	4.57E+04	2.99E+04	1.23E+05	2.07E+05	1.432	1.41E-06	5.850
TG 60:12	3.67E+04	3.47E+04	8.94E+04	6.04E+04	1.284	2.69E-14	13.570
TG 62:1	2.33E+03	4.20E+03	3.98E+02	1.29E+04	-2.548	8.30E-01	0.081
TG 62:12	1.08E+04	8.37E+03	3.16E+04	1.70E+04	1.548	3.28E-23	22.484
TG 62:14	6.43E+03	7.09E+03	2.35E+04	4.47E+05	1.872	1.15E-01	0.940

Figure 2.3. Pearson correlation of maternal first trimester plasma lipidome.

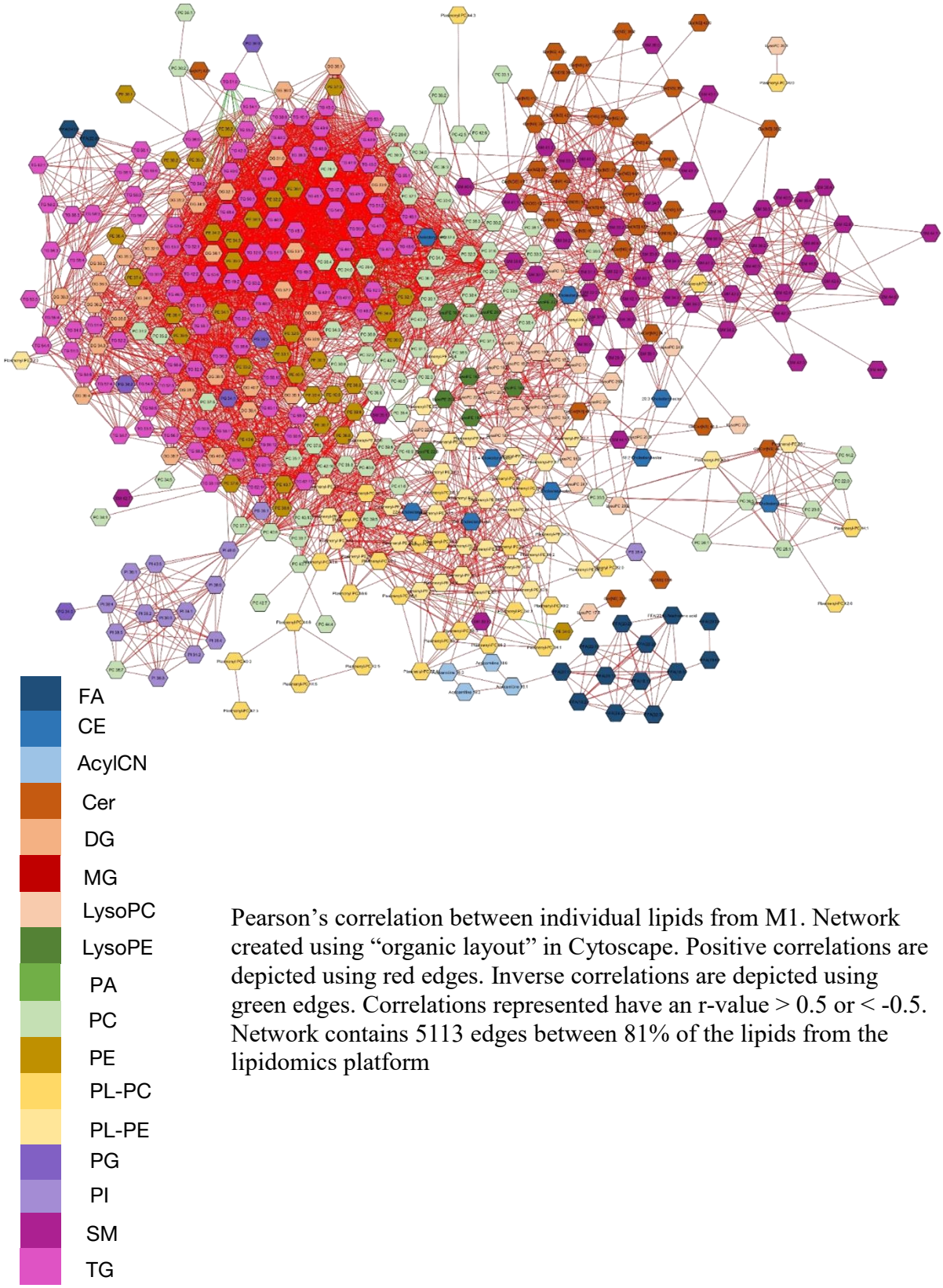

Pearson's correlation between individual lipids from M1. Network created using "organic layout" in Cytoscape. Positive correlations are depicted using red edges. Inverse correlations are depicted using green edges. Correlations represented have an r-value > 0.5 or < -0.5. Network contains 5113 edges between 81% of the lipids from the lipidomics platform

Figure 2.4. Pearson correlation of maternal delivery plasma lipidome.

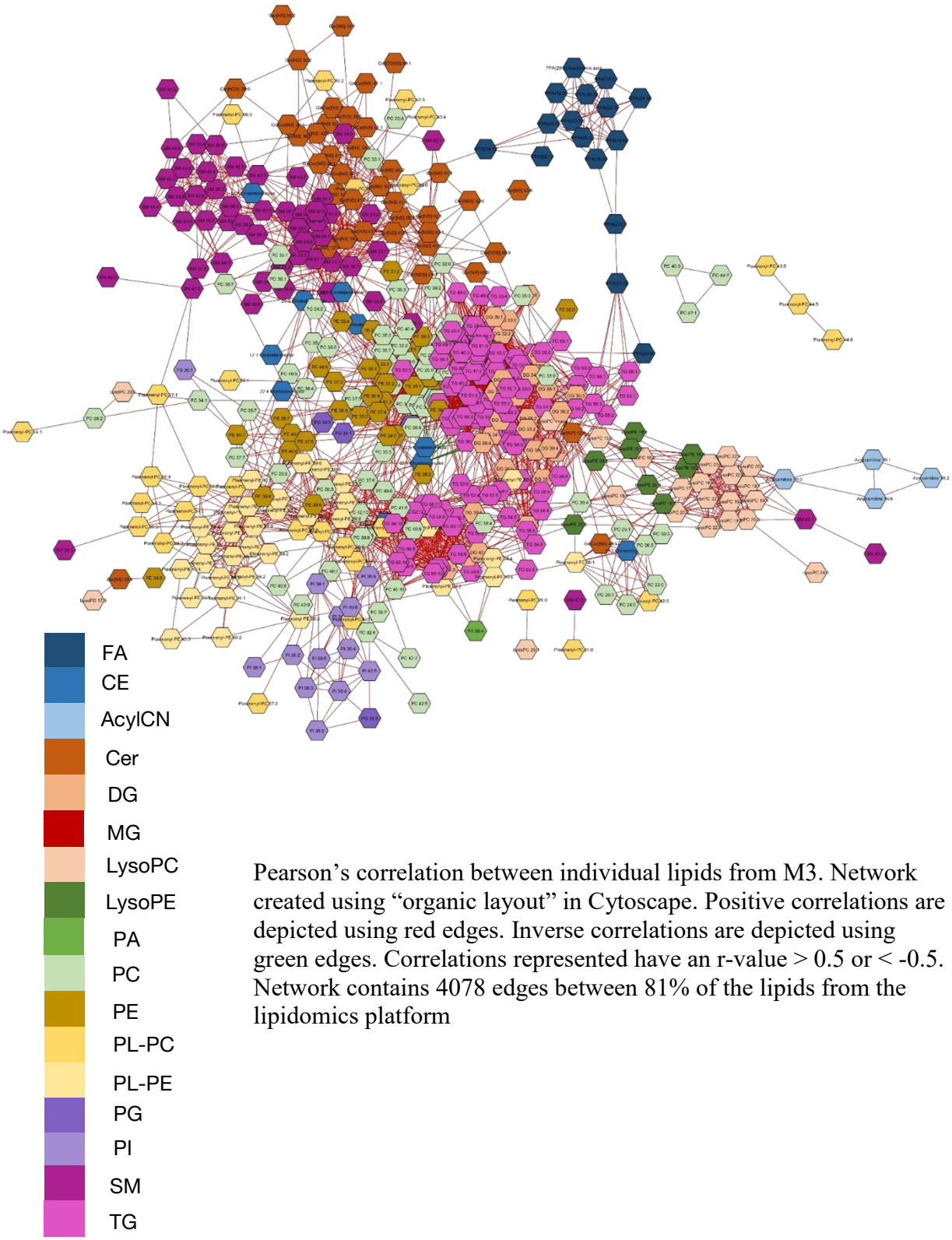

Pearson's correlation between individual lipids from M3. Network created using "organic layout" in Cytoscape. Positive correlations are depicted using red edges. Inverse correlations are depicted using green edges. Correlations represented have an r-value > 0.5 or < -0.5. Network contains 4078 edges between 81% of the lipids from the lipidomics platform

Figure 2.5. Pearson correlation of cord blood lipidome.

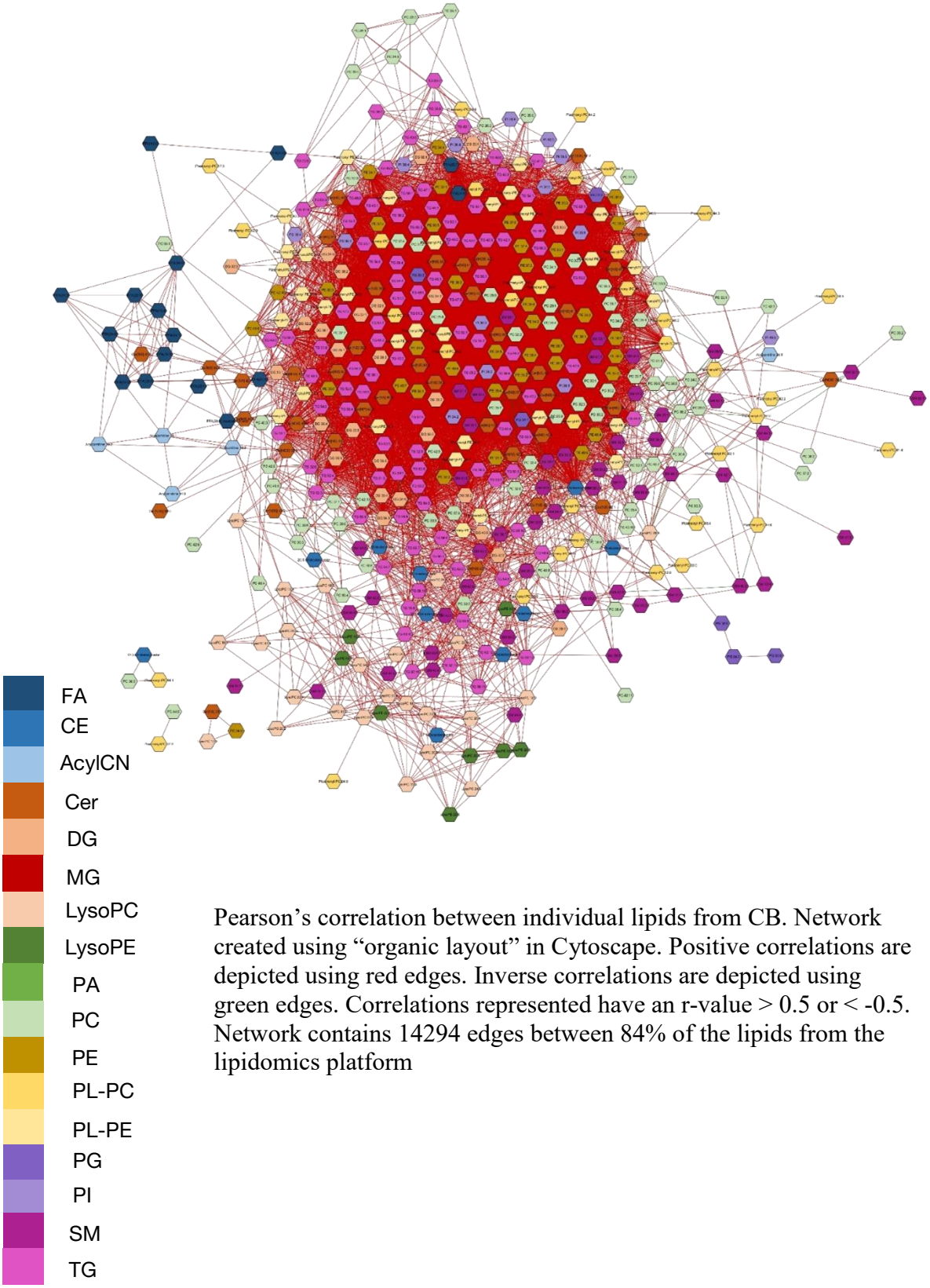

Pearson's correlation between individual lipids from CB. Network created using "organic layout" in Cytoscape. Positive correlations are depicted using red edges. Inverse correlations are depicted using green edges. Correlations represented have an r-value > 0.5 or < -0.5. Network contains 14294 edges between 84% of the lipids from the lipidomics platform

Figure 2.6. Correlation between lipid groups differs between maternal and cord blood samples.

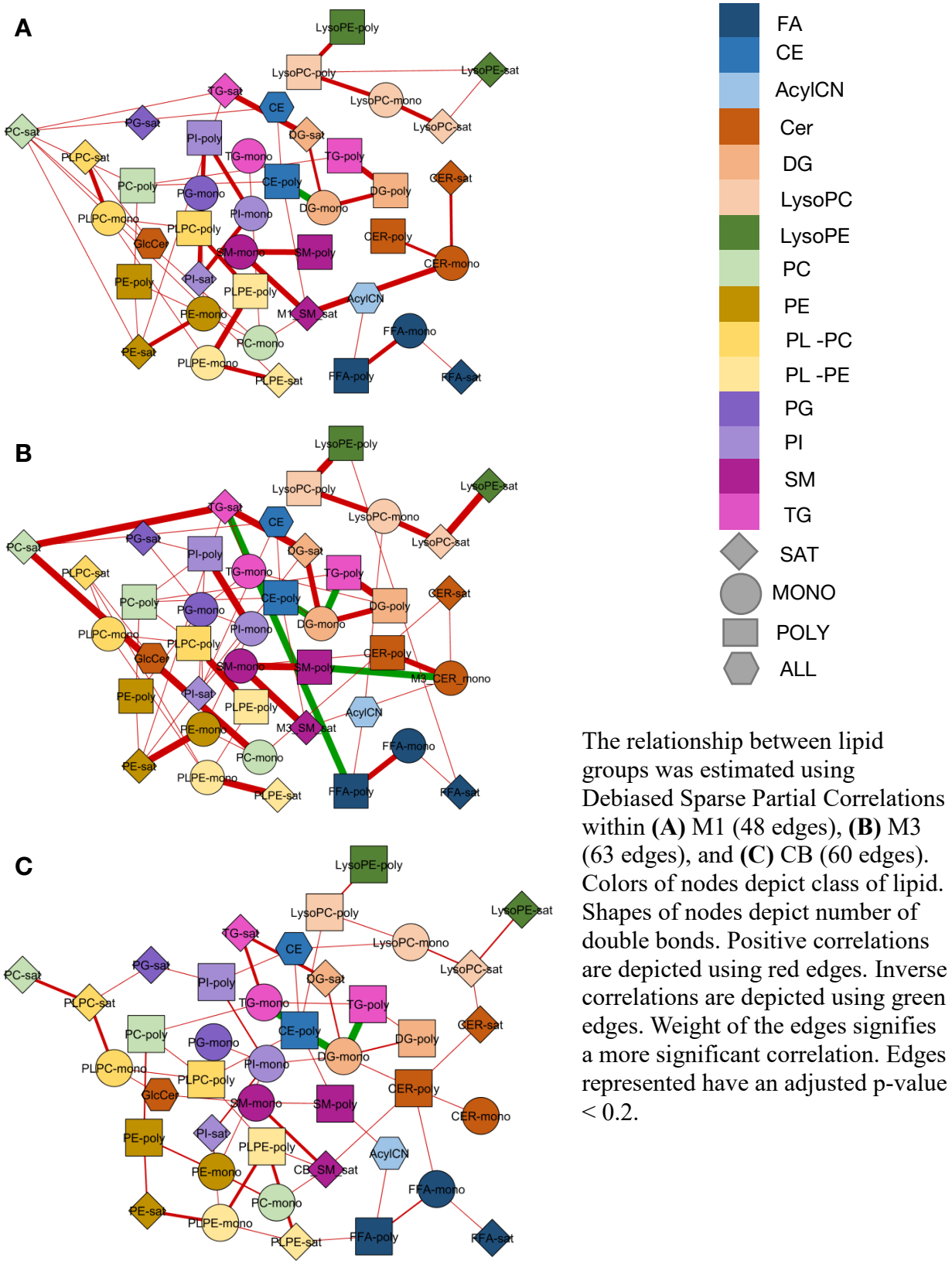

The relationship between lipid groups was estimated using Debiased Sparse Partial Correlations within **(A)** M1 (48 edges), **(B)** M3 (63 edges), and **(C)** CB (60 edges). Colors of nodes depict class of lipid. Shapes of nodes depict number of double bonds. Positive correlations are depicted using red edges. Inverse correlations are depicted using green edges. Weight of the edges signifies a more significant correlation. Edges represented have an adjusted p-value < 0.2.

Figure S2.2. Associations between maternal and cord blood lipid groups with maternal BMI at baseline.

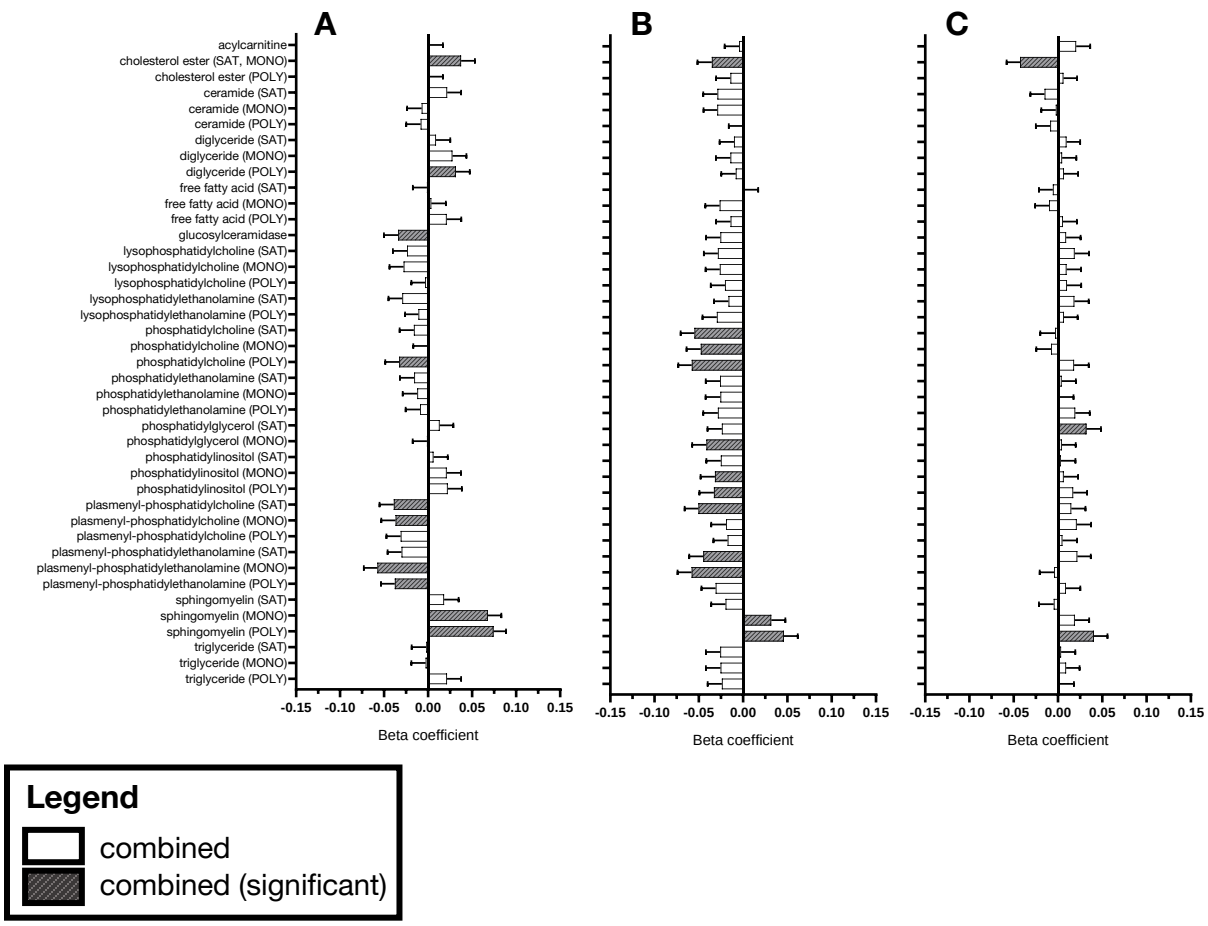

Regression models estimated the linear relationship between maternal BMI at baseline and **(A)** maternal first trimester, **(B)** maternal term, and **(C)** cord blood lipid groups, adjusting for sex, maternal age, parity, and gestational age. Beta coefficients plotted as white bars (β±SE) with significance depicted as gray stripped bars (unadjusted p-value α=0.05).

Figure S2.3. Associations between maternal and cord blood lipid groups with maternal gestational weight gain.

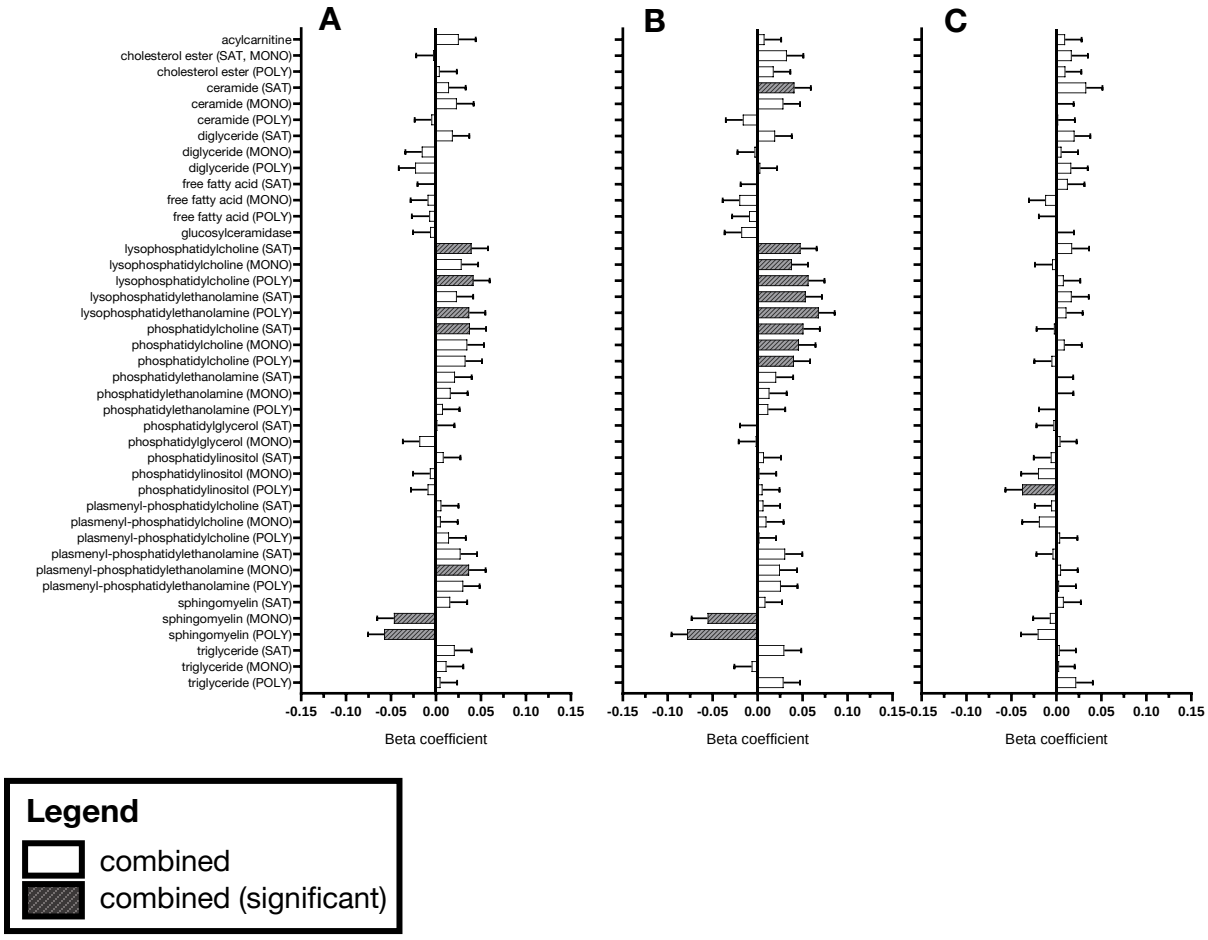

Regression models estimated the linear relationship between maternal GWG (kg) and **(A)** maternal first trimester, **(B)** maternal term, and **(C)** cord blood lipid groups, adjusting for sex, maternal age, parity, and gestational age. Beta coefficients plotted as white bars (β±SE) with significance depicted as gray stripped bars (unadjusted p-value α=0.05).

Figure 2.7. Distinct maternal and cord blood lipid groups are related to birth weight.

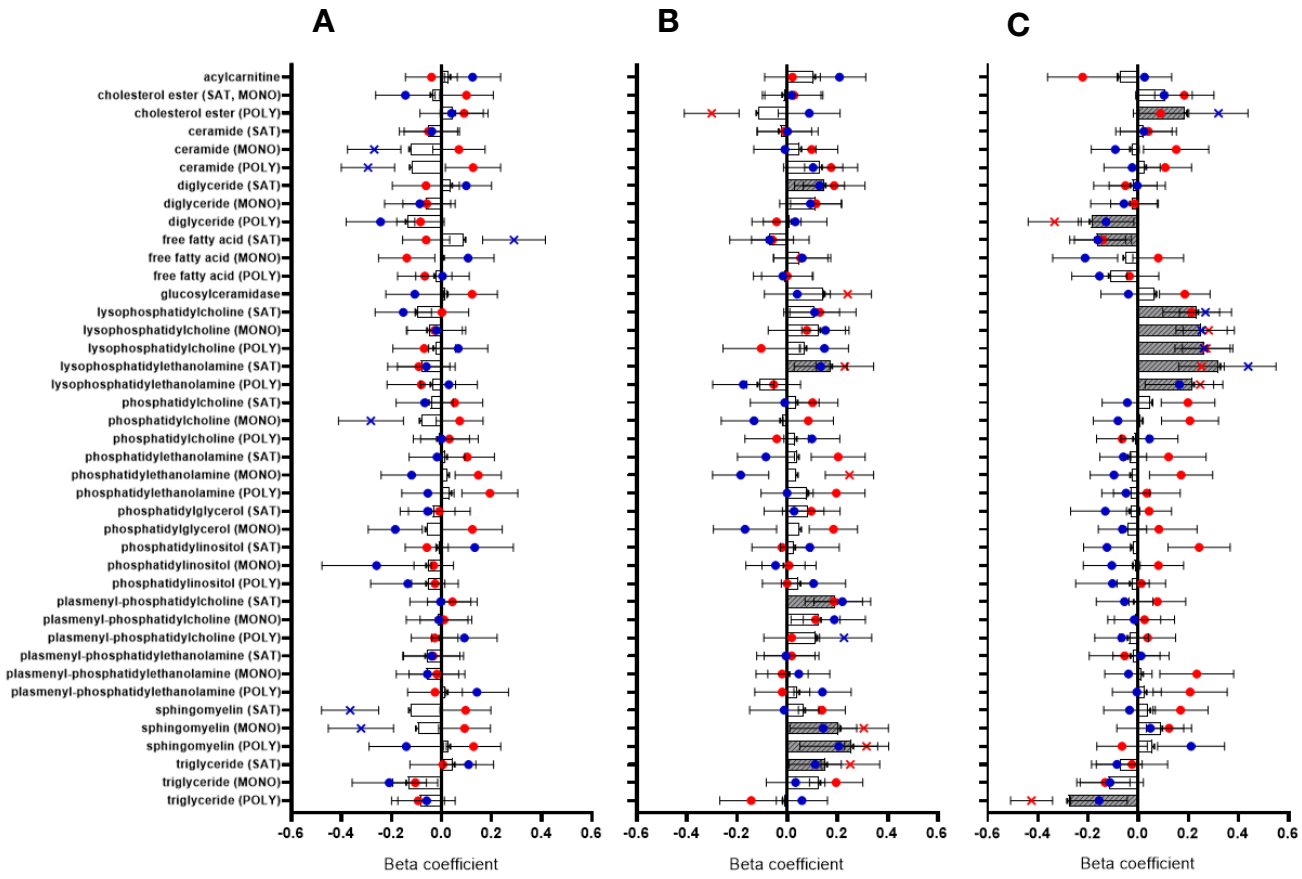

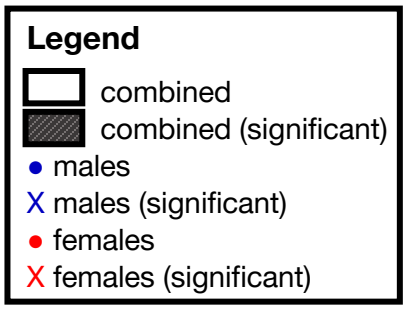

Regression models estimated the linear relationship between lipid groups from **(A)** maternal first trimester, **(B)** maternal term, and **(C)** cord blood and Fenton BW z-score, adjusting for sex, maternal age, parity, gestational age, baseline BMI, and GWG. For the combined model, beta coefficients plotted as gray bars (β±SE) with significance depicted as gray stripped bars (α=0.05). Sex stratified models were run. For males, beta coefficients are plotted as blue dots (β±SE) with significance depicted as blue "X" (α=0.05). For females, beta coefficients are plotted as red dots (β±SE) with significance depicted as red "X" (α=0.05).

Figure 2.8. Association between triglycerides and birth weight in male and female infants.

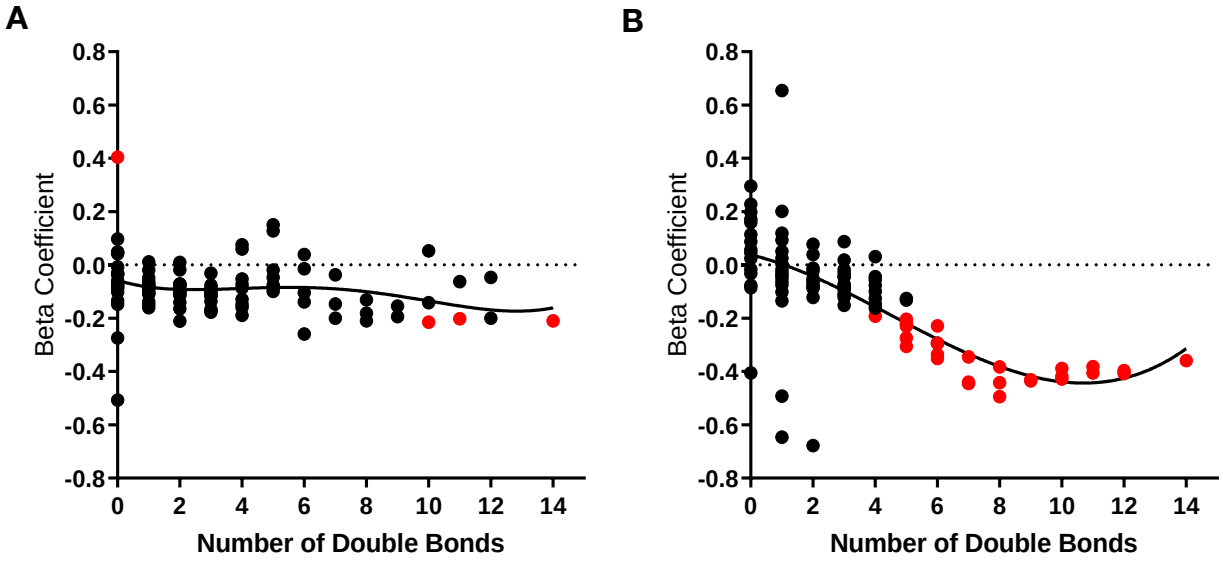

Regression models estimated the linear relationship between cord blood individual triglycerides and Fenton BW z-score in **(A)** males and **(B)** females, adjusting for maternal age, parity, gestational age, baseline BMI, and GWG. Beta coefficients are plotted by the number of double bonds in the fatty acid tails of the TGs. Significant TGs are marked in red (α=0.05). Non-parametric regression fit polynomial lines for each plot.

Figure 2.9. Maternal lipids correlate with cord blood lysophospholipids.

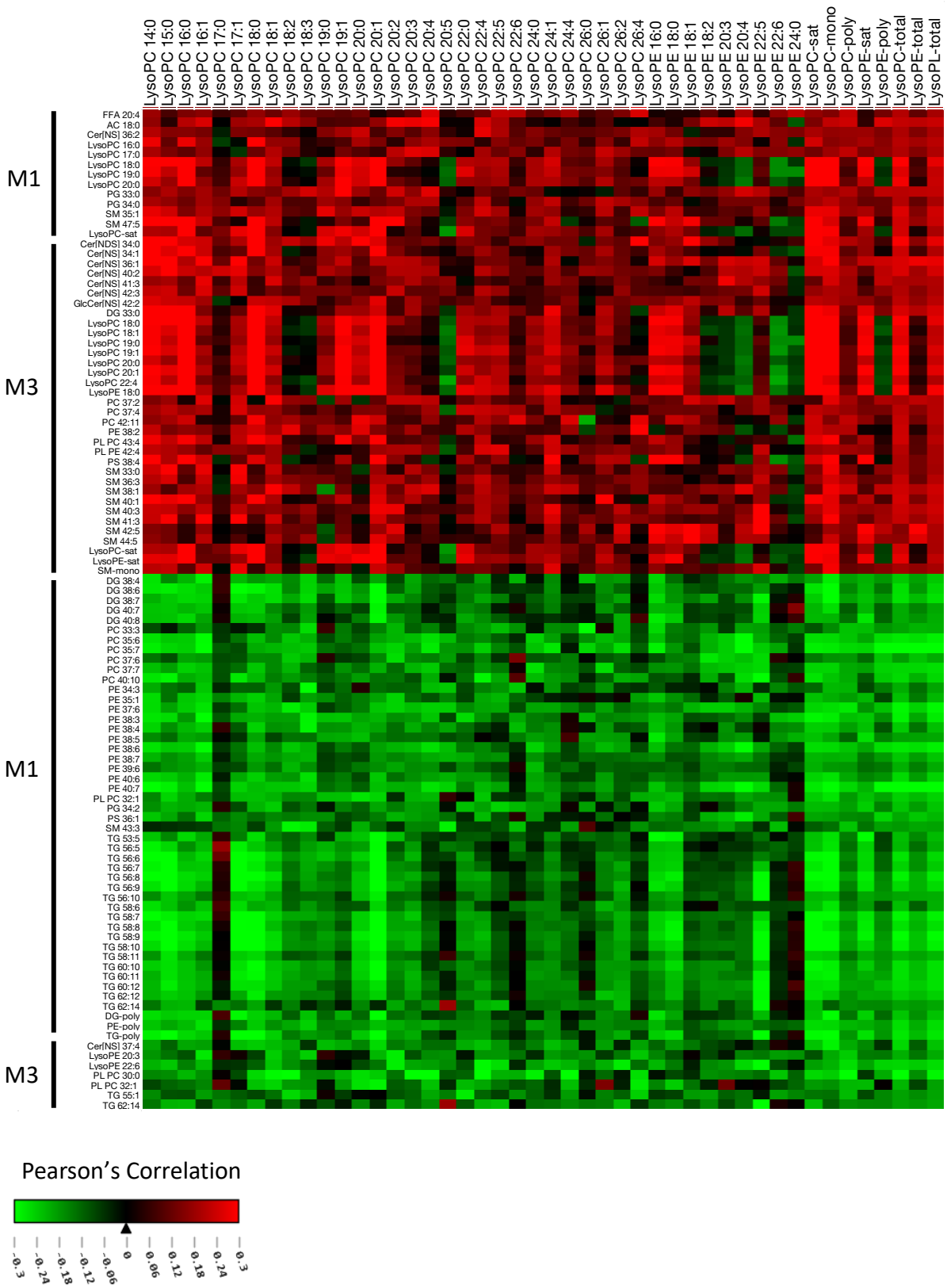

The association between maternal individual lipids and lipid groups with CB LysoPCs, LysoPEs, and total LysoPLs was classified using Pearson's correlations. Maternal lipids listed were significantly correlated with the lipid group CB LysoPL-total (unadjusted p-value α=0.05), suggesting they may modulate CB lysophospholipid levels. Maternal lipids (rows) are broken down by positive and inverse associations. Cord blood lysophospholipids (columns) are ordered by increasing chain length and number of double bonds. CB lipids groups LysoPC-sat, LysoPC-mono, LysoPC-poly, LysoPE-sat, LysoPE-poly, LysoPC-total, LysoPE-total, and LysoPL-total are listed in the last columns.

Figure 2.10. Maternal lipids correlate with cord blood polyunsaturated triglycerides.

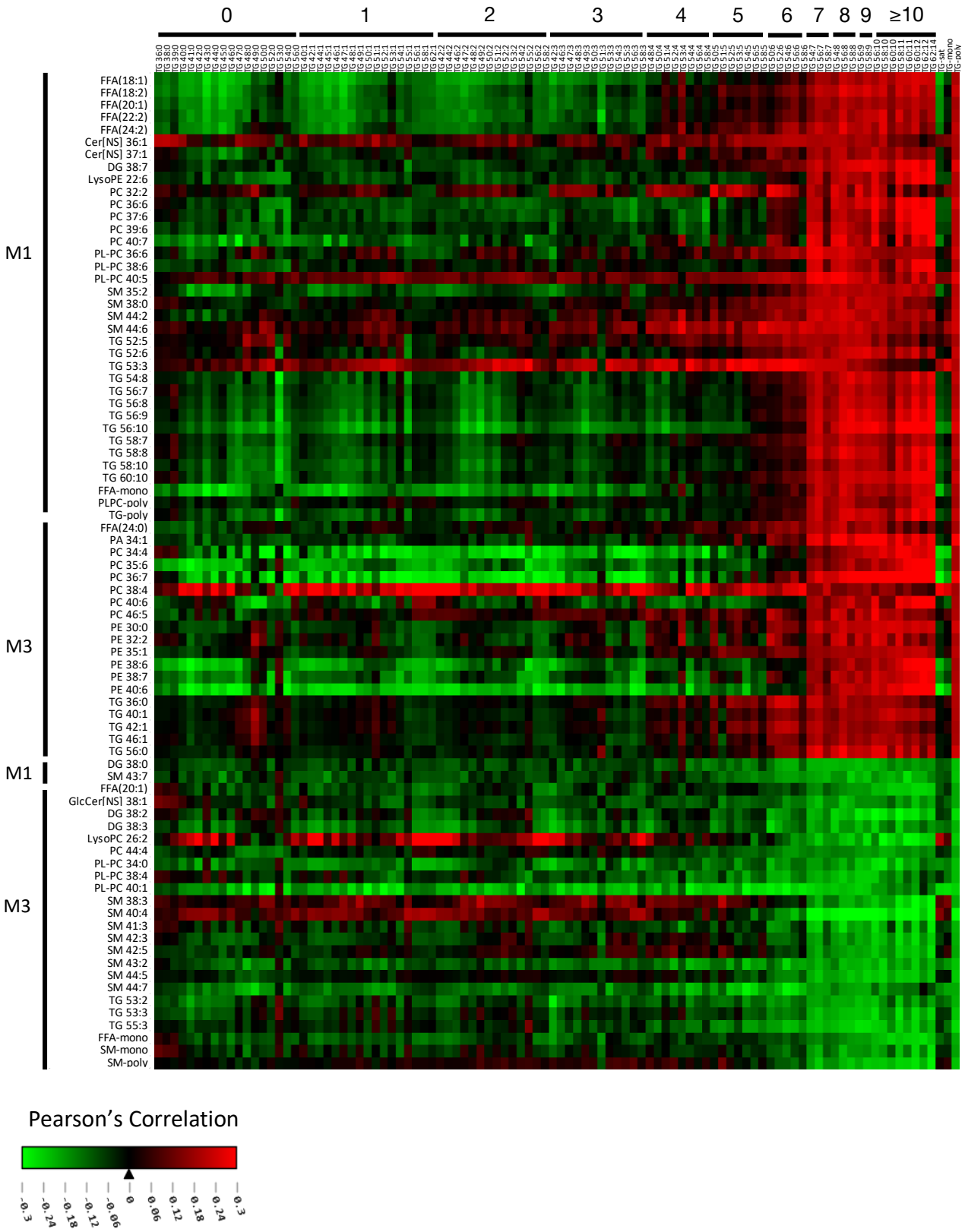

The association between maternal individual lipids and lipid groups with CB TGs was classified using Pearson's correlations. Maternal lipids listed were significantly correlated with the lipid group CB TG-poly (unadjusted p-value α=0.05), suggesting they may modulate CB polyunsaturated TG levels. Maternal lipids (rows) are broken down by positive and inverse associations. Cord blood triglycerides (columns) are ordered by increasing chain length and number of double bonds. CB lipids groups TG-sat, TG-mono, and TG-poly are listed as the last three columns.

References

1. Barker DJP. The origins of the developmental origins theory. J Intern Med. 2007;261:412–7.

2. Brenseke B, Prater MR, Bahamonde J, Gutierrez JC. Current Thoughts on Maternal Nutrition and Fetal Programming of the Metabolic Syndrome. J Pregnancy. 2013;2013:1–13.

3. Susser M, Stein Z. Timing in Prenatal Nutrition: A Reprise of the Dutch Famine Study. Nutr Rev. 1994;52:84–94.

4. Pettitt DJ, Jovanovic L. Birth weight as a predictor of type 2 diabetes mellitus: the U-shaped curve. Curr Diab Rep. 2001;1:78–81.

5. Barker DJP, Eriksson JG, Forsén T, Osmond C. Fetal origins of adult disease: Strength of effects and biological basis. Int J Epidemiol. 2002;31:1235–9.

6. Guasch-Ferré M, Bhupathiraju SN, Hu FB. Use of Metabolomics in Improving Assessment of Dietary Intake. Clin Chem. 2018;64:82–98.

7. Rosato A, Tenori L, Cascante M, De Atauri Carulla PR, Martins dos Santos VAP, Saccenti E. From correlation to causation: analysis of metabolomics data using systems biology approaches. Metabolomics. Springer US; 2018;14:1–20.

8. Pinto J, Barros S, Rosa M, Domingues M, Goodfellow BJ, Galhano E, Pita C, Ceu Almeida M do, Carreira IM, Gil AM. Following Healthy Pregnancy by NMR Metabolomics of Plasma and Correlation to Urine. J Proteome Res. 2015;14:1263–74.

9. Lindsay KL, Hellmuth C, Uhl O, Buss C, Wadhwa PD, Koletzko B, Entringer S. Longitudinal metabolomic profiling of amino acids and lipids across healthy pregnancy. PLoS One. 2015;10:e0145794.

10. Marchlewicz EH, Dolinoy DC, Tang L, Milewski S, Jones TR, Goodrich JM, Soni T, Domino SE, Song PXK, Burant CF, et al. Lipid metabolism is associated with developmental epigenetic programming. Sci Rep. Nature Publishing Group; 2016;6:1–13.

11. Luan H, Meng N, Liu P, Feng Q, Lin S, Fu J, Davidson R, Chen X, Rao W, Chen F, et al. Pregnancy-Induced Metabolic Phenotype Variations in Maternal Plasma. J Proteome Res. 2014;13:1527–36.

12. Hellmuth C, Lindsay KL, Uhl O, Buss C, Wadhwa PD, Koletzko B, Entringer S. Maternal Metabolomic Profile and Fetal Programming of Offspring Adiposity: Identification of Potentially Protective Lipid Metabolites. Mol Nutr Food Res. 2019;63:e1700889.

13. Sandler V, Reisetter AC, Bain JR, Muehlbauer MJ, Nodzenski M, Stevens RD, Ilkayeva O, Lowe LP, Metzger BE, Newgard CB, et al. Associations of maternal BMI and insulin resistance with the maternal metabolome and newborn outcomes. Diabetologia. Diabetologia; 2016;60:518–30.

14. Scholtens DM, Bain JR, Reisetter AC, Muehlbauer MJ, Nodzenski M, Stevens RD, Ilkayeva O, Lowe LP, Metzger BE, Newgard CB, et al. Metabolic networks and

metabolites underlie associations between maternal glucose during pregnancy and newborn size at birth. Diabetes. 2016;65:2039–50.

15. Scholtens DM, Muehlbauer MJ, Daya NR, Stevens RD, Dyer AR, Lowe LP, Metzger BE, Newgard CB, Bain JR, Lowe WL. Metabolomics reveals broad-scale metabolic perturbations in hyperglycemic mothers during pregnancy. Diabetes Care. 2013;37:158–66.

16. Hellmuth C, Lindsay KL, Uhl O, Buss C, Wadhwa PD, Koletzko B, Entringer S. Association of maternal pre-pregnancy BMI with metabolomic profile across gestation. Int J Obes. Nature Publishing Group; 2017;41:159–69.

17. Desert R, Canlet C, Costet N, Cordier S, Bonvallot N. Impact of maternal obesity on the metabolic profiles of pregnant women and their offspring at birth. Metabolomics. Springer US; 2015;11:1896–907.

18. Lowe WL, Bain JR, Nodzenski M, Reisetter AC, Muehlbauer MJ, Stevens RD, Ilkayeva OR, Lowe LP, Metzger BE, Newgard CB, et al. Maternal BMI and glycemia impact the fetal metabolome. Diabetes Care. 2017;40:902–10.

19. Perng W, Rifas-Shiman SL, McCulloch S, Chatzi L, Mantzoros C, Hivert MF, Oken E. Associations of cord blood metabolites with perinatal characteristics, newborn anthropometry, and cord blood hormones in project viva. Metabolism. Elsevier Inc.; 2017;76:11–22.

20. Robinson O, Keski-Rahkonen P, Chatzi L, Kogevinas M, Nawrot T, Pizzi C, Plusquin M, Richiardi L, Robinot N, Sunyer J, et al. Cord Blood Metabolic Signatures of Birth Weight: A Population-Based Study. J Proteome Res. 2018;17:1235–47.

21. Patel N, Hellmuth C, Uhl O, Godfrey K, Briley A, Welsh P, Pasupathy D, Seed P, Koletzko B, Poston L, et al. Cord Metabolic Profiles In Obese Pregnant Women; Insights Into Offspring Growth And Body Composition. J Clin Endocrinol Metab. 2017;103:346–55.

22. Hellmuth C, Uhl O, Standl M, Demmelmair H, Heinrich J, Koletzko B, Thiering E. Cord Blood Metabolome Is Highly Associated with Birth Weight, but Less Predictive for Later Weight Development. Eur J Obes. 2017;10:85–100.

23. Lu Y-P, Reichetzeder C, Prehn C, Yin L-H, Yun C, Zeng S, Chu C, Adamski J, Hocher B. Cord Blood Lysophosphatidylcholine 16:1 is Positively Associated with Birth Weight. Cell Physiol Biochem. 2018;45:614–24.

24. Verburg PE, Tucker G, Scheil W, Erwich JJHM, Dekker A, Roberts CT. Sexual Dimorphism in Adverse Pregnancy Outcomes - A Retrospective Australian Population Study 1981-2011. PLoS One. 2016;11:e0158807.

25. Fenton TR, Kim JH. A systematic review and meta-analysis to revise the Fenton growth chart for preterm infants. BMC Pediatr. 2013;13:1–13.

26. Barbier A, Boivin A, Yoon W, Vallerand D, Platt RW, Audibert F, Barrington KJ, Shah PS, Nuyt AM, Canadian Neonatal Network. New Reference Curves for Head Circumference at Birth, by Gestational Age. Pediatrics. 2013;131:e1158–67.

27. Bligh EG, Dyer WJ. A rapid method of total lipid extraction and purification. Can J Biochem Physiol. 1959;37:911–7.

28. Afshinnia F, Rajendiran TM, Karnovsky A, Soni T, Wang X, Xie D, Yang W, Sha T, Weir MR, He J, et al. Lipidomic Signature of Progression of Chronic Kidney Disease in the Chronic Renal Insufficiency Cohort. Kidney Int Reports. 2016;1:256–68.

29. Gika HG, Macpherson E, Theodoridis GA, Wilson ID. Evaluation of the repeatability of ultra-performance liquid chromatography-TOF-MS for global metabolic profiling of human urine samples. J Chromatogr B. 2008;871:299–305.

30. Kind T, Liu K, Lee DY, Defelice B, Meissen JK, Fiehn O. LipidBlast in silico tandem mass spectrometry database for lipid identification. Nat Methods. 2013;10:755–8.

31. Ejsing CS, Duchoslav E, Sampaio J, Simons K, Bonner R, Thiele C, Ekroos K, Shevchenko A. Automated Identification and Quantification of Glycerophospholipid Molecular Species by Multiple Precursor Ion Scanning. Anal Chem. 2006;78:6202–14.

32. Cetin I, Alvino G, Cardellicchio M. Long chain fatty acids and dietary fats in fetal nutrition. J Physiol. 2009;587:3441–51.

33. Campbell FM, Gordon MJ, Dutta-roy AK. Preferential uptake of long chain polyunsaturated fatty acids by human placental cells. Mol Cell Biochem. 1996;155:77–83.

34. Gázquez A, Uhl O, Ruíz-palacios M, Gill C, Patel N, Koletzko B, Poston L, Larqué E, UPBEAT Consortium. Placental lipid droplet composition: Effect of a lifestyle intervention (UPBEAT) in obese pregnant women. Biochim Biophys Acta Mol Cell Biol Lipids. 2018;1863:998–1005.

35. Basu S, Duren W, Evans CR, Burant CF, Michailidis G, Karnovsky A. Sparse network modeling and Metscape-based visualization methods for the analysis of large-scale metabolomics data. Bioinformatics. 2017;33:1545–53.

36. Sonagra AD. Normal Pregnancy- A State of Insulin Resistance. J Clin Diagnostic Res. 2014;8:1–3.

37. Innis SM. Dietary (n-3) Fatty Acids and Brain Development. J Nutr. 2007;137:855–9.

38. Berghaus TM, Demmelmair H, Koletzko B. Fatty acid composition of lipid classes in maternal and cord plasma at birth. Eur J Pediatr. 1998;157:763–8.

39. Schlörmann W, Kramer R, Lochner A, Rohrer C, Schleussner E, Jahreis G, Kuhnt K. Foetal cord blood contains higher portions of n-3 and n-6 long-chain PUFA but lower portions of trans C18:1 isomers than maternal blood. Food Nutr Res. 2015;59:1–9.

40. Koletzko B, Lien E, Agostoni C, Böhles H, Campoy C, Cetin I, Decsi T, Dudenhausen JW, Dupont C, Forsyth S, et al. The roles of long-chain polyunsaturated fatty acids in pregnancy, lactation and infancy: Review of current knowledge and consensus recommendations. J Perinat Med. 2008;36:5–14.

41. Chambaz J, Ravel D, Manier M-C, Pepin D, Mulliez N, Bereziat G. Essential Fatty Acids Interconversion in the Human Fetal Liver. Biol Neonate. 1985;47:136–40.

42. Szitanyi P, Koletzko B, Mydlilova A, Demmelmair H. Metabolism of 13C-Labeled Linoleic Acid in Newborn Infants During the First Week of Life. Pediatr Res. 1999;45:669–73.

43. Stammers J, Stephenson T, Colley J, Hull D. Effect on placental transfer of exogenous lipid administered to the pregnant rabbit. Pediatr Res. 1995;38:1026–31.

44. Haggarty P, Page K, Abramovich D, Ashton J, Brown D. Long-chain Human Polyunsaturated Fatty Acid Transport Across the Perfused Placenta. Placenta. 1997;18:635–42.

45. Cetin I, Parisi F, Berti C, Mandó C, Desoye G. Placental fatty acid transport in maternal obesity. J Dev Orig Health Dis. 2012;3:409–14.

46. Larqué E, Demmelmair H, Gil-Sánchez A, Prieto-Sánchez M, Blanco J, Pagán A, Faber F, Zamora S, Parrilla J, Koletzko B. Placental transfer of fatty acids and fetal implications. Am J Clin Nutr. 2011;94:1908S-1913S.

47. Martínez-Victoria E, Yago MD. Omega 3 polyunsaturated fatty acids and body weight. Br J Nutr. 2012;107:S107–16.

48. Middleton P, Gomersall J, Gould J, Shepherd E, Olsen S, Makrides M. Omega-3 fatty acid addition during pregnancy (Review). Cochrane Database Syst Rev. 2018;15.

49. O'Tierney-Ginn PF, Davina D, Gillingham M, Barker DJP, Morris C, Thornburg KL. Neonatal fatty acid profiles are correlated with infant growth measures at 6 months. J Dev Orig Health Dis. 2017;8:474–82.

50. Hauner H, Much D, Vollhardt C, Brunner S, Schmid D, Sedlmeier E-M, Heimberg E, Schuster T, Zimmermann A, Schneider K-TM, et al. Effect of reducing the n-6:n-3 long-chain PUFA ratio during pregnancy and lactation on infant adipose tissue growth within the first year of life: An open-label randomized controlled trial. Am J Clin Nutr. 2012;95:383–94.

51. Sedlmeier E, Brunner S, Much D, Pagel P, Ulbrich SE, Ulbrich S, Meyer H, Amann-gassner U, Hauner H, Bader BL. Human placental transcriptome shows sexually dimorphic gene expression and responsiveness to maternal dietary n-3 long-chain polyunsaturated fatty acid intervention during pregnancy. BMC Genomics. 2014;15:1–19.

52. Nguyen LN, Ma D, Shui G, Wong P, Cazenave-Gassiot A, Zhang X, Wenk MR, Goh ELK, Silver DL. Mfsd2a is a transporter for the essential omega-3 fatty acid docosahexaenoic acid. Nature. Nature Publishing Group; 2014;509:503–6.

53. Prieto-Sánchez M, Ruiz-palacios M, Blanco-Carnero J, Pagan A, Hellmuth C, Uhl O, Peissner W, Ruiz-alcaraz AJ, Parrilla JJ, Koletzko B, et al. Placental MFSD2a transporter is related to decreased DHA in cord blood of women with treated gestational diabetes. Clin Nutr. 2017;36:513–21.

54. MacDonald JIS, Sprecher H. Phospholipid fatty acid remodeling in mammalian cells. Biochim Biophys Acta. 1991;1084:105–21.

55. Lagarde M, Bernoud N, Brossard N, Lemaitre-Delaunay D, Thiès F, Croset M, Lecerf J.

Lysophosphatidylcholine as a preferred carrier form of docosahexaenoic acid to the brain. J Mol Neurosci. 2001;16:201–4.

56. Sandoval KE, Wooten JS, Harris MP, Schaller ML, Umbaugh S, Witt KA. Mfsd2a and Glut1 Brain Nutrient Transporters Expression Increase with 32-Week Low and High Lard Compared with Fish-Oil Dietary Treatment in C57Bl/6 Mice. Curr Dev Nutr. 2018;2:1–10.

57. Iqbal J, Walsh MT, Hammad SM, Hussain MM. Sphingolipids and Lipoproteins in Health and Metabolic Disorders. Trends Endocrinol Metab. Elsevier Ltd; 2017;28:506–18.

CHAPTER 3

Lipidome across Pregnancy Influences the Programming of Umbilical Cord Blood Leukocyte DNA Methylation.

Abstract

The maternal metabolic environment may influence DNA methylation levels in the developing fetus, with potential long-term health consequences in the offspring via epigenetic programming. The lipidome provides a comprehensive assessment of maternal lipid levels across gestation. Untargeted shotgun lipidomics was performed on first trimester maternal plasma (M1) and delivery maternal plasma (M3) in 106 mothers from the Michigan Mother-Infant Pair (MMIP) cohort. Infant cord blood (CB) leukocyte DNA methylation was profiled using the Infinium MethylationEPIC (EPIC) bead array. Using empirical Bayes modeling, we classified differential methylation at CpG sites in relation to maternal lipid groups, adjusting for CB blood cell types, sex, and batch effects. M3 saturated lysophosphatidylcholine (LysoPC) was associated with 45 differentially methylated CpG sites and M3 saturated lysophosphatidylethanolamine (LysoPE) was associated with 18 differentially methylated CpG sites. Most of the differentially methylated CpG sites had increased DNA methylation. Many of the differentially methylated CpG sites were localized in CpG islands, including 64% of CpG sites associated with M3 saturated LysoPC and 50% of CpG sites associated with M3 saturated LysoPE. Biological pathways pertaining to differentially methylated CpG sites associated with M3 saturated LysoPCs were involved in cell proliferation and growth. The results of this analysis highlighted the influence of late gestation

maternal lipid levels on the infant epigenome. Future analyses will assess expression of genes with differential methylation.

Introduction

The Developmental Origins of Health and Disease (DOHaD) theory postulates that insults during early life can permanently program the fetus/offspring, influencing long-term health outcomes (1). During gestation, the maternal metabolic environment may alter DNA methylation levels in the fetus, potentially shifting the developmental trajectory of the offspring via epigenetic programming. Profiling the maternal metabolome and lipidome, the low-molecular weight lipid intermediates in metabolism, provides an objective view of maternal nutrient availability during pregnancy. Changes in the maternal metabolome across gestation occur to support the developing needs of the fetus (2) and are influenced by maternal characteristics such as obesity (3–5) and dietary intake (6). Irregular fluctuations in the maternal metabolome may influence the development of the offspring by causing structural changes in fetal organs and tissues to adapt to the intrauterine environment and prepare for the external environment (7).

We have previously assessed the relationship between the maternal lipidome with the umbilical cord blood (CB) lipidome (LaBarre et al, submitted). The umbilical CB lipidome is an approximate snapshot of the infant lipidome in circulation, presenting details on maternal lipid transfer across the placenta. Our results highlight the selective transport of polyunsaturated fatty acids (PUFA) and lysophospholipids (LysoPL) across the placenta into the umbilical CB to support fetal development. Additionally, CB lipid groups containing PUFAs and LysoPLs were associated with birth weight, a common outcome in DOHaD studies due to its association with cardiometabolic disease in adulthood (8,9). We identified maternal PUFAs in early gestation were vital for the establishment of umbilical CB lipids associated with birth weight.

There is growing evidence that epigenetic mechanisms are a major contributor to developmental programming (10). Epigenetics is defined as the mitotically heritable changes in gene expression that occur without altering the DNA sequence. The most extensively studied epigenetic modification is DNA methylation at CpG sites, short-hand for a cytosine and guanine base separated by a phosphate group. Methyl-groups are covalently attached to the 5' carbon of a cytosine preceding a guanine, generating a 5-methylcytosine. Across most tissues, 70% of CpG sites are methylated (11). Regions in the genome with high CpG site frequency are called CpG islands, which are often located at the 5' promotor of genes. The umbilical CB epigenome has previously been associated with maternal dietary intake (12) and maternal BMI (13), as well as infant birth weight (14). Details on the influence and timing of maternal exposures on the offspring DNA methylation patterns continues to be elucidated.

Previous work from our group (15) provided some of the first evidence for a relationship between specific metabolites in the maternal plasma across gestation with DNA methylation in umbilical CB leukocytes. DNA methylation at key genes including *ESR1*, *PPARα*, *IGF2*, and *H19*, which have previously been associated with growth and future cardiovascular disease risk (16–18), was correlated with maternal essential fatty acids (FA) and acylcarnitines. A recent study (19) assessed how the maternal lipidome at ~26 weeks gestation influences DNA methylation in umbilical CB cells using the Infinium HumanMethylation450 (450K) assay. These results found that maternal phospholipids and lysophospholipids were associated with offspring DNA methylation, suggesting the importance of that lipids fraction in establishing methylation patterns.

The objective of our analysis is to provide a deeper understanding of how the maternal lipidome at early gestation and delivery is related to altered DNA methylation patterns in umbilical CB

leukocytes. Our findings provide support that the maternal metabolic environment during gestation influences the infant epigenome, potentially by fetal programming. In particular, we focus our results and discussion on differential methylation in genes associated with lipid metabolism, growth, and metabolic disease. This analysis incorporates high-throughput shotgun lipidomics methodology, profiling 573 lipids, and genome-wide DNA methylation using the EPIC bead array, presenting a comprehensive view of developmental programming.

Subjects and Methods

Study population. Biological samples were analyzed from women and their offspring enrolled in the Michigan Mother Infant Pair (MMIP) cohort (2010-present), an ongoing birth cohort study based out of the University of Michigan (UM) Von Voigtlander Women's Hospital. Recruitment of women took place during their initial prenatal appointment, between 8 and 14 weeks of gestation. Eligibility criteria includes women ages 18 to 42 years, a spontaneously conceived singleton pregnancy, and intention to deliver at the UM Hospital. For this analysis, a subset of mother-infant dyads was selected for lipidomics analyses and genome-wide DNA methylation using the EPIC bead array. Inclusion criteria for the current study include completed demographic, survey, and health information at the initial study visit and availability of all biospecimen for metabolomics and epigenomics analyses (n=100). Study procedures were approved by the UM Medical School Institutional Review Board, and all participants provided written informed consent, which includes consent for measures of lipidomics and DNA methylation. All participants were de-identified.

During the initial study visit between 8 and 14 weeks of gestation, participants provided a blood sample (**M1**) and anthropometry information (weight and height) to calculate an estimated baseline BMI. Maternal venous blood samples (**M3**) was collected upon admittance at UM

Hospital for delivery, and cord blood (**CB**) samples were collected via venipuncture from the umbilical cord. All mother-infant dyads met additional inclusion criteria for this study, including infant birth weight greater than 2500 grams, maternal BMI greater than 18.5 kg/m^2, and no pregnancy complications, such as gestational diabetes.

Lipidomics Profiling. Untargeted shotgun lipidomics was performed as previously detailed (20) using reconstituted lipid extract from M1, M3, and CB plasma samples. Samples were ionized in positive and negative ionization model using a Triple TOF 5600 (AB Sciex, Concord Canada). Chromatographic peaks that represent features are detected using a modified version of existing commercial software (Agilent MassHunter Qualitative Analysis). Pooled human plasma samples and pooled experimental samples were randomized and ran for quality control (21). Detected features were excluded with (1) a relative standard deviation greater than 40% in the pooled samples and/or (2) less than 70% presence in the samples. Missing data were imputed using the K-nearest neighbor method.

Lipids were classified using LIPIDBLAST, a computer generated tandem mass spectral library containing 119,200 compounds from 26 lipid classes (22). After processing, 573 lipids from multiple lipid classes were identified (**Table 2.1**). All lipids will be mentioned with the nomenclature as X:Y, where X is the length of the carbon chain and Y, the number of double bonds.

DNA extraction. At the time of birth, infant umbilical CB was collected into PaxGene Blood DNA tubes (PreAnalytix). Samples were stored at -80°C until extraction. DNA was extracted from CB leukocytes using the PaxGene Blood DNA kit, following standard protocols. At the University of Michigan Advanced Genomics Core, DNA concentration and integrity were quantified using a Qubit Fluorometer and extracts with a concentration greater than 15 ng/μL

were selected for further analysis. Prior to DNA methylation analysis, approximately 500ng of input DNA per sample underwent bisulfite conversion using the EZ-96 DNA Methylation Kit (Zymo).

Genome-wide DNA methylation analysis. DNA methylation analyses were performed by the University of Michigan Epigenomics Core. The Illumina Infinium MethylationEPIC (EPIC) bead array was used to quantify DNA methylation at ~850,000 CpG sites (Illumina Inc, San Diego, CA, USA), following standard protocols. The EPIC bead array detects at single-nucleotide resolution and contains probes the hybridize to loci throughout the genome located within CpG islands, genes, transcription binding sites, open chromatin regions, and more. Umbilical CB samples were run in three experimental batches (sample plates), which are considered in the statistical models (23).

DNA methylation data processing. Raw intensity probe data were processed using the Bioconductor minfi package 1.32.0 (24). The data were generated from reading a red or green signal, signifying if the probe hybridized to a methylated or unmethylated loci. After generation of the signal, a value β between 0 and 1 was provided as β=[*methylated*/(*methylated+unmethylated*)]. Quality of samples and probes was determined by evaluating infant estimated sex (via methylation values on the X and Y chromosomes) versus known sex (as recorded in medical record) and detection and intensity of probe signals. Samples that failed quality check were removed from analysis. The probes located on X and Y chromosomes were excluded from this analysis due to differences in probe intensities for sex chromosomes (25). After quality control, 804108 probes were available for analysis. β-values were converted logarithmically into M-values for statistical analysis. Although β-values are more intuitive for a biological interpretation, M-values are more statistically valid for analysis (26).

Statistical analysis.

Maternal and infant background characteristics.

Table 3.1 summarized maternal and infant population characteristics and estimated proportions of infant CB cell types. To estimate CB proportions of white blood cell types and nucleated red blood cells, we utilized a CB reference dataset (23).

Creating lipid group scores.

The lipidome is highly correlated due to lipids being metabolized by enzymes in a class-specific manner. For this analysis, the lipidome was grouped based on lipid class and the number of double bonds, yielding 41 groups (**Table S2.1**). Lipid groups were scored for each mother-infant dyad using unsupervised Principal Component Analysis. The first principal component was retained, accounting for the largest portion of variance (PROC FACTOR, SAS 9.4 Cary, North Carolina). Within the principal component, each lipid received a factor loading, which is the correlation coefficient between the lipid and the component. Participant scores were created by (1) multiplying the lipid factor loading by the lipid standardized peak intensity and (2) adding together these values for all lipids within a lipid group (PROC SCORE, SAS 9.4 Cary, North Carolina). Lipid scores were considered outliers and removed if exceeding ±3 standard deviations from the mean score. While these values may be biologically relevant, including outliers into the analysis increases risk of false discovery, detecting CpG sites associated with participant variation, rather than the lipid group (27).

Identification of differentially methylated CpG sites and regions.

This analysis sought to identify differential methylation in CB leukocytes associated with the maternal (M1 and M3) lipidome. Differentially methylated sites were classified fitting linear

models using empirical Bayes methodology from the Bioconductor package limma, version 3.42.0 (28). Models were adjusted for sex, EPIC bead array sample plate, and estimated proportions of nucleated red blood cells (nRBC) and B-cells. Results were adjusted for multiple hypothesis testing using the Benjamini-Hochberg method with an FDR threshold for significance of 0.05 (29). Differentially methylated regions (DMR) were identified by the R Bioconductor package DMRcate, version 2.0.0. All DMRs contained at least two CpG sites and were considered significant with an adjusted p-value threshold of 0.05 using the Stouffer's method.

Path analysis.

Biological pathways associated with differentially methylated genes were classified. To avoid bias when performing gene ontology with methylation data (30), we used the gometh function in the R package missMethyl, version 1.20.0 (31), to classify enriched gene ontologies (GO) (32) and KEGG (33) pathways. Pathway analysis was conducted separately for the following lipids groups with multiple significant CpG sites; M3 LysoPC-sat and LysoPE-sat. Differentially methylated CpG sites with an FDR<0.1 were selected to classify enriched biological pathways. Gene ontologies and KEGG biological pathways were considered enriched with an FDR <0.05.

All analyses were performed using R software, version 3.5.3 (The R Foundation for Statistical Computing). Figures were created using GraphPad Prism version 7.4 (La Jolla, California).

Results

Subject Demographics

Maternal and infant population characteristics are reported in **Table 3.1** (n=100). The majority of women were between 30-34 years with an average overweight baseline BMI (25.9 kg/m^2). Most newborns were delivered vaginally (72%). There was a similar distribution of male and female

newborns (53 male, 47 female) with an average birth weight of approximately 3500 grams. Cord blood cell percentages estimated for CD4+T, CD8+T, B cells, granulocytes, monocytes, natural killer cells, and nRBCs are listed in **Table 3.1**.

Relationship between maternal lipid groups with DNA methylation in infant cord blood leukocytes.

Table 3.2 lists the number of CpG sites significantly associated with maternal lipid groups (FDR<0.05), adjusting for infant sex, sample plate, nRBC (%), and B cells (%). Significant sites are shown stratified by "increased" methylation and "decreased" methylation with increasing lipids. The majority of differentially methylated CpG sites were associated with maternal delivery lipid groups. Genes associated with differentially methylated sites are reported in **Table 3.3**.

In M1, only a few lipid groups were associated with single-CpG sites DNA methylation in CB leukocytes. Significant associations were observed between M1 LysoPC-sat and a CpG site in the shore of *MPP5* (logFC= 0.12, probe ID cg07218192) (**Table 3.3**). Early gestation M1 PG-mono is positively associated with a CpG site in the open sea of *PPARGC1B* (logFC=0.17, cg24968215) and a CpG site in the CpG island of *TTC14* (logFC=0.15, cg14930059).

In M3, the LysoPC-sat was associated with 45 differentially methylated CpG sites (**Figure 3.1a**) and LysoPE-sat was associated with 18 differentially methylated CpG sites (**Figure 3.1b**). Many of these CpG sites were located within CpG islands and shores **(Figure 3.1c** and **d**) and had increased DNA methylation. There was overlap in the CpG sites associated with M3 LysoPC-sat and LysoPE-sat including increased methylation at CpG sites related *SLFN5* (cg23010414), *HIST1H1D* (cg15485323), and *DBI* (cg02325290) (**Table 3.3**). Increased methylation was

observed in the CpG island of Diazepam Binding Inhibitor/acyl-CoA binding protein (*DBI*) (**Figure S3.1**); a highly conserved gene that binds medium- and long-chain acyl-Coenzyme A esters and plays a role in lipid metabolism (36).

M3 LysoPC-sat is associated with differential methylation in a variety of other genes related to metabolism and development (**Table 3.3**) including the CpG island of *ATP5G1* (logFC=0.28, cg14103143), which encodes a subunit of mitochondrial ATP synthase; the south shore of *COQ5* (logFC=0.17, cg11075121), a mitochondrial gene that catalyzes the methylation in the *COQ10* synthetic pathways (37); CpG island of *GABBR2* (logFC=0.25, cg11509404), which plays a role in coupling to G-proteins (38) and stimulates phospholipase A2, an enzyme that hydrolyzes phospholipids releasing the sn-2 FA; and the CpG island of *PA2G4* (logFC=0.29, cg21001214), a gene encoding an RNA binding protein involved in growth regulation.

In the DMR analysis, M3 LysoPE-sat was associated with increased methylation across 13 CpGs within the CpG island of FK506 binding protein prolyl isomerase 11 (*FKBP11*) (mean β FC = 0.0064, Stouffer p-value=0.00047) (**Table 3.4**). No additional DMRs were observed.

Pathway analysis of differentially methylated genes

To further investigate the potential biological relevance of the results, pathway analysis was used to classify gene ontologies (GO) and KEGG pathways enriched in genes with differential methylation. Lipid groups selected for pathway analysis had multiple significant CpG hits including M3 LysoPC-sat and LysoPE-sat. Gene ontologies for biological processes (BP), cellular components (CC), and molecular function (MF) and KEGG biological pathways were classified. M3 LysoPC-sat was the only lipid group with significantly enriched gene ontologies (**Table S3.1**) and KEGG biological pathways (**Table S3.2**). The top ten significantly enriched

gene ontologies and biological pathways associated with M3 LysoPC-sat are reported in **Figure 3.2**. From GO analysis, enriched ontologies include cell division (BP), regulation of transcription (BP), the nucleoplasm and nucleus (CC), and DNA, RNA, and protein binding (MF) (**Figure 3.2a-c**). Multiple enriched KEGG pathways are related to cell proliferation including cell cycle, ribosome, human papillomavirus infection, viral carcinogenesis, mTOR signaling pathway, and pathways in cancer (**Figure 3.2d**).

Discussion

In this study using 100 mother-infant dyads from the MMIP cohort, we classified the relationship between the maternal lipidome at early gestation and delivery with DNA methylation profiles in CB leukocytes. An untargeted lipidomics platform quantified almost 600 lipids from a variety of lipid classes at M1 and M3. Measuring the maternal lipidome twice during gestation provided information on how lipid exposure may influence the infant epigenome based on the stage of fetal development. Our results indicate that M3 lysophospholipids with saturated FA tails are associated with differential DNA methylation within umbilical CB CpG sites within CpG islands and shores. These results highlight the importance of the late gestation maternal lipidome in programming the infant epigenome, emphasizing the relevance of specific lipid classes.

Within the 41 lipid groups, M3 LysoPC-sat and LysoPE-sat were the main maternal lipid groups related to differential methylation in CB leukocytes. Most differentially methylated CpG sites associated with this lipid fraction were within CpG islands and shores, increasing the likelihood of potential relevance to programming infant gene expression (39). Both LysoPC-sat and LysoPE-sat were associated with changes in methylation of genes related to lipid metabolism, including increased methylation within the CpG island of *DBI*, the medium- and long-chain acyl-CoA ester binding (36). Long-chain fatty acyl-CoAs play a role in a variety of cellular functions

(40) and are highly expressed in tissues with active lipid metabolism, such as the liver and adipose tissue (41), playing a role in the esterification of long-chain FA into triglycerides and phospholipids (42) as well as FA oxidation (43).

In the DMR analysis, higher M3 LysoPE-sat was associated with increased DNA methylation across 13 CpG sites within the CpG island of *FKBP11*, a gene belonging to a family of FK506 binding proteins. It has been suggested that FK506 binding proteins play a role in the regulation of mechanistic target of rapamycin (mTOR), a master regulator of cell growth (44). The FKBPs-rapamycin complex binds to mTOR and prevents the binding of mTOR substrates (44). A recent study has demonstrated that the *FKBP11* encoded protein, FK506-binding protein 11, mediates the stimulatory effect of XBP1 on the mTOR, leading to cell growth (45).

The relevance of individual CpG site associations was determined using pathway analysis. M3 LysoPC-sat was the only lipid group in maternal plasma with significant pathway enrichment, highlighting enriched cell proliferation and ribosomal metabolism/translation (**Figure 3.2**). Recent analyses by our group (LaBarre et al., submitted) have found that LysoPC and LysoPE are selectively depleted in maternal plasma at M3 and elevated in CB, suggesting selective transfer. We also noted that M1 and M3 LysoPLs, mainly containing saturated FA, are positively correlated with total CB LysoPL levels. A recently published study using the CHAMACOS cohort measured 92 lipids at ~26 weeks gestation and assessed the relationship between the maternal metabolome and DNA methylation in infant CB using the Infinium 450K Bead Chip (19). Their metabolomics platform consisted of diglyceride, phosphatidic acid, lysophospholipid, monoglyceride, phospholipid, sphingolipid, and triglyceride lipid classes mainly composed of FAs tails that are 16:0, 18:0, 18:1, or 20:4. They observed multiple lipids in maternal plasma were associated with infant DNA methylation including four phospholipids and four

lysophospholipids. They found that out of the 28 significant relationships observed, 22 had negative regression coefficients, signifying that increased maternal lipids are associated with decreased infant CB methylation. There was no overlap between the statistically significant CpG sites or related genes identified between our two analyses, potentially due to differences in the maternal metabolome measurement time and the DNA methylation array. In biological pathway analysis, the CHAMACOS cohort found significant differentially methylated genes were involved in biological pathways such as Huntington disease, pyruvate metabolism, and Parkinson disease. Both Huntington disease and Parkinson disease were significantly enriched pathways associated with M3 LysoPC-sat in our analysis (**Table S3.2**). Together with our results, these results emphasize the importance of the maternal lysophospholipid fraction in establishing the infant epigenome during mid-gestation to late gestation.

Mechanisms expanding on the influence of maternal lysophospholipids on the infant epigenome are not clear. Lysophospholipids are formed from the rapid rearrangement and turnover of phospholipids in the cell membrane, known as the Land's cycle (46). In this pathway, phosphatidylcholine in the cell membrane is deacylated by phospholipase A2 (PLA2) forming LysoPC (47). Reacylation of LysoPC mediated by lysophosphatidylcholine acyltransferase (LPCAT) allows for exchange of the sn-2 fatty acyl group, altering the composition of the cellular membrane in response to signals (47). Additionally, phosphatidylcholine is synthesized in the liver and secreted as components of very low density lipoprotein (VLDL), releasing LysoPCs into circulation by LPCAT (48). Once in the plasma, LysoPCs are bioactive molecules with diverse biological functions involved in cell proliferation, as previously demonstrated in cancer cells (49,50) and highlighted in our pathway enrichment analysis. Their role as signaling molecules may be related to metabolic health, as elevations in plasma LysoPCs have been

observed in obesity (51) and in type 2 diabetic subjects (52). Our previous study identified that CB lysophospholipids are positively associated with birth weight. Our results are confirmed by other studies demonstrating CB LysoPCs with varying chain length and saturation are positively associated with newborn BW (53–55), as well as with weight at age 6 months (53).

It has been suggested that maternal lysophospholipids may influence the infant epigenome via the transport of choline to tissues (19). Choline is shuttled into a variety of pathways including acetylcholine synthesis, the production of phosphatidylcholine, and the production of betaine. Betaine is a source of methyl groups for the synthesis of methionine, the precursor to the principal methylating agent, S-adenosylmethioine. During pregnancy, the dynamics of choline metabolism shifts to increase production of phosphatidylcholine via the Kennedy pathway and the phosphatidylethanolamine N-methyltransferase pathway (56). Therefore, alterations in the levels of maternal lysophospholipids may alter the input of choline into the one carbon metabolism pathway, influencing DNA methylation. The discussion of the pregnancy lipidomics analysis from the CHAMACOS cohort explores this possibility (19). While lysophospholipids, in particular LysoPC, may contribute to methyl group donation for one-carbon metabolism, it is unknown why and how differential methylation is occurring in specific genes associated with cell proliferation.

The majority of differentially methylated CpG sites were associated with the M3 lipidome, however a few M1 lipid groups were associated with CpG site methylation. Early gestation M1 PG-mono was positively associated with a CpG site in the open sea of *PPARGC1B*. Peroxisome proliferator-activated receptors (PPAR) and the PPAR gamma co-activator 1 (PGC1) gene families have been previously associated with type 2 diabetes risk (57). In addition, the methylation of the *PPARGC1B* locus in peripheral blood cells was found to be inversely

associated to adherence to a Mediterranean diet (58), which in turn is associated with higher monounsaturated and lower polyunsaturated phospholipid levels (59–61). M1 LysoPC-sat was associated with increased methylation in a CpG site located in the shore of *MPP5*. *MPP5* is a palmitoylated protein coding gene, which is a scaffolding protein in the outer membrane of retinal glial cells (34) and was found to be up-regulated in placenta villus cells of women with intrauterine growth retardation and severe preeclampsia (35).

Previous analyses of the same cohort study (15) used a candidate gene approach to identify metabolite-DNA methylation associations in genes related to lipid metabolism and growth. Maternal very long-chain FA and acylcarnitines were the most consistently associated with DNA methylation. Our current analysis uses different metabolite extraction techniques, which made it unlikely to see similarities in the results. Future work will compare the maternal-infant dyads targeted metabolite profile to DNA methylation data from the EPIC bead array to identify genes related to lipid metabolism and growth with differential methylation.

Conclusion

Our findings provide support that the maternal metabolic environment during gestation, in particular lysophospholipids, influences the umbilical CB epigenome, potentially regulating gene expression. A novelty of this analysis was the incorporation of two ‘omics platforms; an untargeted lipidomics platform with measurements across gestation and the EPIC Bead Array. Multiple maternal measures across gestation determines how maternal lipids influence fetal programming during different periods of gestation. We acknowledge that maternal delivery plasma may not be a true reflect of late gestation lipids due to the stress of parturition. Maternal samples in this analysis were not fasted, presenting challenges in interpreting the results as the epigenome changes in the postprandial state (62). Therefore, infant CB methylation may be a

reflection of maternal fasted or fed state, rather than programming. Lastly, we acknowledge that CB leukocyte methylation may not be the relevant tissue for risk of cardiometabolic disease and additional epigenetic process may also be relevant, such as histone modifications. Future analyses will classify gene expression of relevant genes of interest.

Authorship

Jennifer L. LaBarre, Carolyn McCabe, Muraly Puttabyatappa, Tamara Jones, Peter X.K. Song, Steven E. Domino, Marjorie C. Treadwell, Dana C. Dolinoy, Vasantha Padmanabhan, Jaclyn M. Goodrich, and Charles F. Burant

Acknowledgements

We would like to acknowledge Samantha Milewski and Steven Rogers for help with recruitment, processing of samples, and retrieval of clinical data.

Funding Support

University of Michigan NIEHS/EPA Children's Environmental Health and Disease Prevention Center P01 ES022844/RD 83543601 (VP, DCD, PS, JG), NIH Children's Health Exposure Analysis Resource (CHEAR), 1U2C ES026553 (DD, JG, CFB), Michigan Lifestage Environmental Exposures and Disease (M-LEEaD) NIEHS Core Center P30 ES017885 (VP, DCD, JG, PS, CFB), NIH/NIEHS UG3 OD023285 (VP, DCD), Molecular Phenotyping Core, Michigan Nutrition and Obesity Center P30 DK089503 (CFB, DCD) and Michigan Regional Metabolomics Resource Core R24 DK097153 (CFB), Ruth L. Kirschstein Institutional Training Grant from the NIEHS T32 ES007062 (MP) and The A. Alfred Taubman Research Institute (CFB).

Study Approval

The MMIP study was approved by the University of Michigan Institutional Review Board (HUM00017941). Written informed consent was received from all participants and all plasma samples and metadata were deidentified prior to analysis.

Table 3.1. Characteristics of the MMIP cohort (n=100 mother-infant pairs).

Categorical variables	**N(%)**
maternal age	
25-29	25 (25%)
30-34	54 (54%)
35-45	21 (21%)
newborn sex	
male	53 (53%)
female	47 (47%)
delivery route	
vaginal	72 (72%)
caesarean section	28 (28%)
Continuous variables	**mean±SD (N)**
Maternal	
baseline BMI (kg/m²)	25.9±6.1 (97)
gestational weight gain (kg)	13.2±5.3
Newborn	
gestational age (days)	278±7
birth weight (g)	3504±428
white blood cell count (%)	
CD4+T	15.3.±6.0
CD8+T	12.5±3.8
B cells	8.6±3.2
granulocytes	47.9±8.8
monocytes	8.8±2.5
NK cells	1.4±3.0
nRBC	8.2±4.9

Table 3.2. Number of significant differentially methylated CpG sites in umbilical cord blood leukocytes associated with maternal lipid groups. Differentially methylated sites were classified fitting linear models using empirical Bayes methodology. Models were adjusted for sex, EPIC bead array sample plate, nRBC, and Bcells. Results were adjusted for multiple hypothesis testing using the Benjamini-Hochberg method with an FDR threshold for significance of 0.05. Results reported as the number of CpG sites with significant differential methylation with M1 and M3 lipid groups. Significant site counts are stratified by "Increased" methylation (in red) and "Decreased" methylation (in green).

Lipid Cluster	***Maternal First Trimester (M1)***		***Maternal Term (M3)***	
	Decreased	Increased	Decreased	Increased
AcylCN	0	0	0	0
CE	0	0	0	0
CE-poly	0	0	0	0
CER-sat	0	0	0	0
CER-mono	0	0	0	0
CER-poly	0	0	0	0
DG-sat	0	0	0	0
DG-mono	0	0	0	0
DG-poly	0	0	0	0
FFA-sat	0	0	0	0
FFA-mono	0	0	0	0
FFA-poly	0	0	0	0
GlcCer	0	0	0	0
LysoPC-sat	0	1	2	43
LysoPC-mono	0	0	0	0
LysoPC-poly	0	0	0	1
LysoPE-sat	0	0	0	18
LysoPE-poly	0	0	0	0
PC-sat	0	0	0	0
PC-mono	0	0	0	0
PC-poly	0	0	0	0
PE-sat	0	0	0	0
PE-mono	0	0	0	0
PE-poly	0	0	0	0
PG-sat	0	0	0	0
PG-mono	0	3	0	0
PI-sat	0	0	0	0
PI-mono	0	0	0	0
PI-poly	0	0	0	0
PLPC-sat	0	0	0	0

PLPC-mono	0	0	0	0
PLPC-poly	0	0	0	0
PLPE-sat	0	0	0	0
PLPE-mono	0	0	0	0
PLPE-poly	0	0	0	0
SM-sat	0	0	0	0
SM-mono	0	0	0	0
SM-poly	0	0	0	0
TG-sat	0	0	0	0
TG-mono	0	0	0	0
TG-poly	0	0	0	0

Table 3.3. Classification of significant differentially methylated CpG sites in umbilical cord blood leukocytes associated with maternal lipid groups. Differentially methylated sitres were identified by fitting linear models using empirical Bayes methodology. Models were adjusted for sex, EPIC bead array sample plate, nRBC, and Bcells. Directionality indicated by log fold change. Results were adjusted for multiple hypothesis testing using the Benjamini-Hochberg method with an FDR threshold for significance of 0.05. The CpG site, chromosomal location, related gene, and relation to any CpG Island is reported.

time point	lipid group	CpG site	chromosome	Gene	Relation to CpG Island	logFC	FDR p-value
M1	LysoPC sat M1	cg07218192	chr14	MPP5	N-Shore	0.1196	0.0127
M1	PG mono M1	cg24968215	chr5	PPARGC1B	Open Sea	0.1717	0.0415
M1	PG mono M1	cg14930059	chr3	TTC14	Island	0.1526	0.0415
M1	PG mono M1	ch.19.23069863R	chr19		Open Sea	0.3117	0.0415
M3	LysoPC poly M3	cg01779447	chr6	IFITM4P	N-Shore	0.1682	0.0122
M3	LysoPC sat M3	cg15749322	chr11	ANKRD42	Island	0.3409	0.0471
M3	LysoPC sat M3	cg14103143	chr17	ATP5G1	Island	0.2758	0.0471
M3	LysoPC sat M3	cg21598517	chr19	B9D2	Island	0.1423	0.0471
M3	LysoPC sat M3	cg00598747	chr19	B9D2	Island	0.1547	0.0471
M3	LysoPC sat M3	cg19575351	chr6	C6orf141	Island	0.1247	0.0471
M3	LysoPC sat M3	cg01382153	chr2	CCDC108	Island	0.1795	0.0471
M3	LysoPC sat M3	cg11075121	chr12	COQ5	S-Shore	0.1683	0.0484
M3	LysoPC sat M3	cg04410024	chr8	CRISPLD1	Island	0.1721	0.0471
M3	LysoPC sat M3	cg02325290	chr2	DBI	Island	0.1483	0.0471
M3	LysoPC sat M3	cg01813748	chr18	DLGAP1-AS2	Open Sea	0.1760	0.0471
M3	LysoPC sat M3	cg12709907	chr17	EFTUD2	Island	0.1664	0.0471
M3	LysoPC sat M3	cg18071809	chr19	EID2B	Island	0.1773	0.0471
M3	LysoPC sat M3	cg22045228	chr2	ELMOD3	Island	0.1951	0.0471
M3	LysoPC sat M3	cg01974100	chr14	FAM179B	N-Shore	0.1529	0.0471
M3	LysoPC sat M3	cg11509404	chr9	GABBR2	Island	0.2466	0.0471
M3	LysoPC sat M3	cg07070542	chr7	GARS	Island	0.1816	0.0471
M3	LysoPC sat M3	cg15485323	chr6	HIST1H1D	Open Sea	0.1722	0.0471
M3	LysoPC sat M3	cg19060382	chr12	LOC253724	S-Shore	0.2293	0.0471
M3	LysoPC sat M3	cg17434483	chr19	LOC729991-MEF2B	S-Shore	0.1403	0.0471
M3	LysoPC sat M3	cg25172519	chr6	MOXD1	Island	0.1668	0.0471
M3	LysoPC sat M3	cg17775912	chr14	MTHFD1	Island	0.1542	0.0471
M3	LysoPC sat M3	cg10326891	chr4	NUDT9	Island	0.2125	0.0471
M3	LysoPC sat M3	cg21001214	chr12	PA2G4	Island	0.2869	0.0471
M3	LysoPC sat M3	cg26431298	chr1	PRCC	Island	0.2911	0.0496
M3	LysoPC sat M3	cg17537899	chr3	RPL22L1	S-Shore	0.1982	0.0471
M3	LysoPC sat M3	cg22842064	chr3	RPL22L1	Island	0.1667	0.0471
M3	LysoPC sat M3	cg16696730	chr21	RSPH1	Island	0.2097	0.0471
M3	LysoPC sat M3	cg19049809	chr17	SFRS1	S-Shore	0.1779	0.0471

M3	LysoPC sat M3	cg22398523	chr1	SH3BP5L	Island	0.1501	0.0471
M3	LysoPC sat M3	cg04696559	chr5	SKP2	Island	0.2191	0.0471
M3	LysoPC sat M3	cg23013931	chr22	SLC25A17	N-Shore	0.1928	0.0471
M3	LysoPC sat M3	cg23010414	chr17	SLFN5	Island	0.1801	0.0496
M3	LysoPC sat M3	cg21151651	chr11	SPTY2D1	Island	0.2286	0.0471
M3	LysoPC sat M3	cg25781123	chr3	THUMPD3	N-Shore	0.3710	0.0471
M3	LysoPC sat M3	cg14210275	chr17	TMEM107	Island	0.1611	0.0471
M3	LysoPC sat M3	cg14345069	chr4	UFSP2	Island	0.1598	0.0471
M3	LysoPC sat M3	cg06356912	chr3	VILL	N-Shore	0.2237	0.0471
M3	LysoPC sat M3	cg21665057	chr3	WDR53	Island	0.1210	0.0471
M3	LysoPC sat M3	cg22720041	chr19	ZNF229	Island	0.1516	0.0471
M3	LysoPC sat M3	cg13468174	chr19	ZNF584	Island	0.1577	0.0471
M3	LysoPC sat M3	cg17618194	chr7	ZNHIT1	S-Shore	0.2626	0.0471
M3	LysoPC sat M3	ch.16.79494380F	chr16		Open Sea	0.2426	0.0471
M3	LysoPC sat M3	cg14205309	chr11		Open Sea	-0.1555	0.0471
M3	LysoPC sat M3	ch.4.74730522R	chr4		Open Sea	0.1787	0.0471
M3	LysoPC sat M3	cg26809926	chr7		Open Sea	-0.1877	0.0471
M3	LysoPE sat M3	cg08265188	chr12	ALG10	Island	0.5586	0.0338
M3	LysoPE sat M3	cg22664986	chr11	ANKRD42	Island	0.2278	0.0364
M3	LysoPE sat M3	cg12013332	chr12	BBS10	Island	0.2183	0.0338
M3	LysoPE sat M3	cg12792102	chr5	BNIP1	Open Sea	0.2675	0.0364
M3	LysoPE sat M3	cg19889500	chr14	DAD1	N-Shore	0.2409	0.0364
M3	LysoPE sat M3	cg02325290	chr2	DBI	Island	0.1488	0.0364
M3	LysoPE sat M3	cg15485323	chr6	HIST1H1D	Open Sea	0.1728	0.0364
M3	LysoPE sat M3	cg16666115	chr6	MRPS18A	S-Shore	0.1484	0.0338
M3	LysoPE sat M3	cg16875280	chr19	OPA3	N-Shore	0.2928	0.0338
M3	LysoPE sat M3	cg09367970	chr12	RAD51AP1	Island	0.1812	0.0338
M3	LysoPE sat M3	cg04895581	chr8	RBM12B	Island	0.2021	0.0372
M3	LysoPE sat M3	cg05250654	chr2	RPS7	Island	0.2713	0.0364
M3	LysoPE sat M3	cg16990505	chr14	SDCCAG1	S-Shore	0.1843	0.0364
M3	LysoPE sat M3	cg23010414	chr17	SLFN5	Island	0.1969	0.0338
M3	LysoPE sat M3	cg13045611	chr17	SUPT6H	S-Shore	0.1908	0.0033
M3	LysoPE sat M3	cg23093590	chr15		Island	0.2768	0.0338
M3	LysoPE sat M3	cg07602492	chr1		S-Shore	0.1654	0.0364
M3	LysoPE sat M3	ch.17.51385210R	chr17		Open Sea	0.1546	0.0364

Table 3.4. Classification of differentially methylated regions in umbilical cord blood leukocytes associated with maternal lipid groups. Directionality indicated by β_{max} and β_{min} fold change. Significance denoted by a Stouffer p-value <0.05. Chromosome coordinates, number of differential CpG sites in the region, and related gene are reported.

time point	lipid group	chromosome coordinates	number of CpGs	β_{mean} FC	β_{max} FC	Stouffer p-value	Gene
M3	LysoPE sat M3	chr12:49318740-49319500	13	0.0064	0.0174	0.0005	FKBP11

Figure 3.1. Maternal term saturated lysophospholipids are associated with differential DNA methylation in promoter regions of infant leukocyte genes.

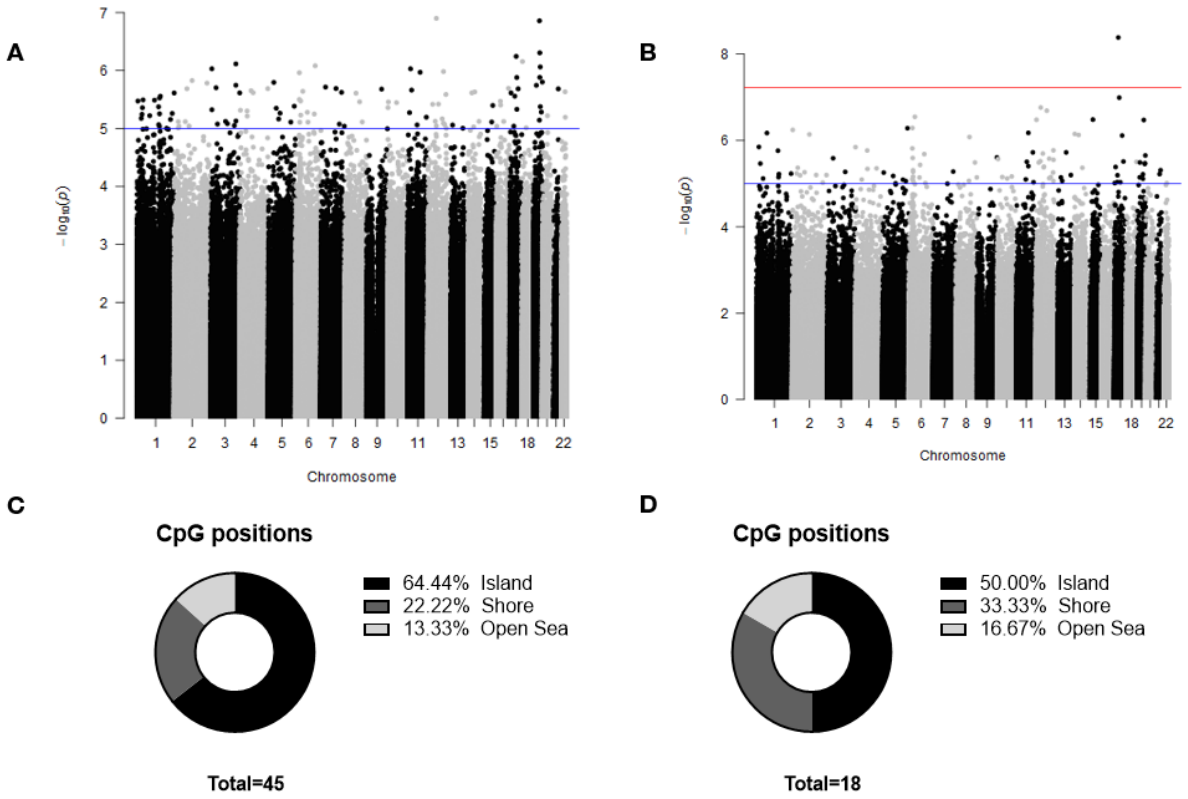

Differentially methylated CpG sites were classified fitting linear models using empirical Bayes methodology. Models were adjusted for sex, EPIC bead array sample plate, nRBC, and Bcells. Represented by Manhattan plots, **(A)** 45 CpG sites were significantly related to M3 LysoPC-sat and **(B)** 18 CpG probes were significantly related to M3 LysoPE-sat (FDR<0.05). Blue line signifies p-value=1e-5. Red line signifies p-value=6e-8. Differentially methylated CpG probes were classified by genomic location. Percentage of statistically significant CpG sites within the CpG Island, shore, shelf, and open sea reported for association with **(C)** M3 LysoPC-sat and **(D)** M3 LysoPE-sat.

Figure S3.1. Maternal term saturated lysophospholipid levels are associated with differential DNA methylation within the CpG Island of Diazepam Binding Inhibitor, Acyl-CoA Binding Protein (DBI).

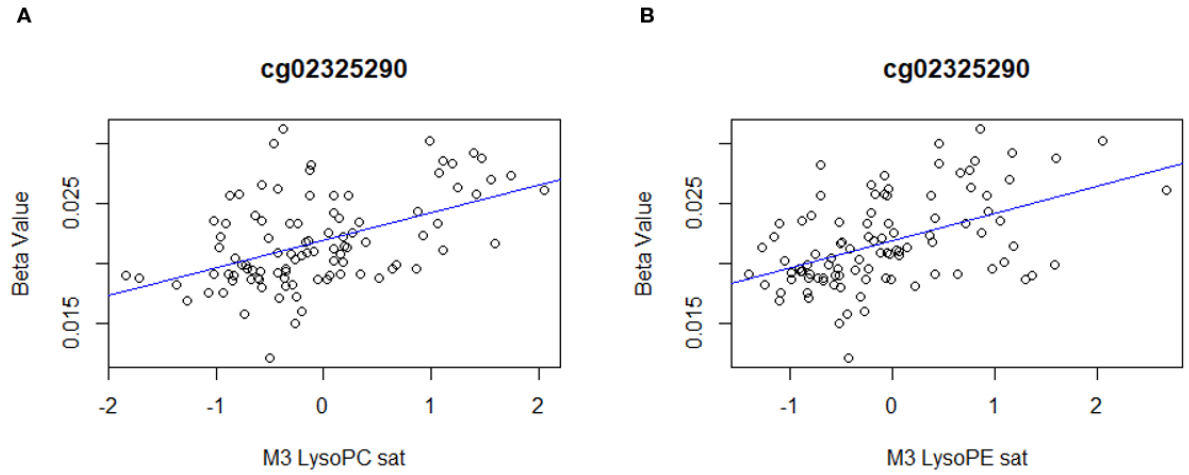

Differentially methylated CpG sites were classified fitting linear models using empirical Bayes methodology. Models were adjusted for sex, EPIC bead array sample plate, nRBC, and Bcells. Both **(A)** M3 LysoPC-sat (logFC=0.15, FDR=0.047) and **(B)** M3 LysoPE-sat (logFC=0.15, FDR=0.036) are positively associated with methylation at a loci (probe ID cg02325290), residing within the CpG island of DBI. Relationship between proportion of DNA methylation at the site (beta values) and lipid group scores are represented.

Table S3.1. Enriched gene ontologies (GO) from differentially methylated sites associated with M3 LysoPC-sat. Differentially methylated sites (FDR<0.1) were selected for pathway analysis. Gene ontologies are classified as "biological processes" (BP), "cellular component" (CC), or "molecular function" (MF). The number of genes within each pathway (N) and the number of genes differentially methylated (DE) are reported. Enriched pathways listed have an FDR<0.05.

Gene Ontology ID	Ontology	Description	N	DE	Fold enrichment	unadjusted p-value	FDR
GO:0005515	MF	protein binding	9664	5966	80.300	2.87E-85	5.01E-81
GO:0005654	CC	nucleoplasm	3123	2179	69.100	9.09E-74	7.94E-70
GO:0005829	CC	cytosol	4871	3139	49.389	7.00E-54	4.08E-50
GO:0005634	CC	nucleus	4561	2861	44.915	2.78E-49	1.21E-45
GO:0003723	MF	RNA binding	1334	961	42.583	7.46E-47	2.61E-43
GO:0005739	CC	mitochondrion	1106	745	20.846	4.90E-25	1.43E-21
GO:0005813	CC	centrosome	447	348	17.969	4.30E-22	1.07E-18
GO:0005737	CC	cytoplasm	3433	2098	17.718	8.77E-22	1.92E-18
GO:0003677	MF	DNA binding	1329	831	11.979	5.41E-16	1.05E-12
GO:0016020	CC	membrane	1853	1185	11.468	1.95E-15	3.40E-12
GO:0000981	MF	DNA-binding transcription factor activity, RNA polymerase II-specific	1537	967	10.698	1.26E-14	2.00E-11
GO:0051301	BP	cell division	344	256	10.138	5.00E-14	7.28E-11
GO:0005743	CC	mitochondrial inner membrane	383	255	8.339	3.41E-12	4.58E-09
GO:0006357	BP	regulation of transcription by RNA polymerase II	917	575	7.818	1.22E-11	1.52E-08
GO:0019901	MF	protein kinase binding	401	292	7.370	3.67E-11	4.26E-08
GO:0000122	BP	negative regulation of transcription by RNA polymerase II	707	481	7.370	3.90E-11	4.26E-08
GO:0016607	CC	nuclear speck	386	275	6.946	1.10E-10	1.13E-07
GO:0045893	BP	positive regulation of transcription, DNA-templated	535	372	6.826	1.59E-10	1.49E-07
GO:0046872	MF	metal ion binding	2267	1352	6.826	1.62E-10	1.49E-07
GO:0016032	BP	viral process	366	259	6.491	3.70E-10	3.23E-07
GO:0006412	BP	translation	165	117	6.278	6.34E-10	5.27E-07
GO:0006614	BP	SRP-dependent cotranslational protein targeting to membrane	89	70	6.143	9.07E-10	7.20E-07
GO:0005524	MF	ATP binding	1451	930	6.039	1.23E-09	9.14E-07
GO:0048471	CC	perinuclear region of cytoplasm	684	455	6.039	1.25E-09	9.14E-07
GO:0008022	MF	protein C-terminus binding	186	145	5.689	2.93E-09	2.05E-06
GO:0016567	BP	protein ubiquitination	419	286	5.632	3.47E-09	2.33E-06
GO:0032991	CC	protein-containing complex	592	389	5.539	4.46E-09	2.89E-06
GO:0000398	BP	mRNA splicing, via spliceosome	224	162	5.461	5.54E-09	3.46E-06
GO:0000184	BP	nuclear-transcribed mRNA catabolic process, nonsense-mediated decay	115	87	5.255	9.23E-09	5.56E-06
GO:0003714	MF	transcription corepressor activity	205	154	5.137	1.25E-08	7.30E-06

GO:0045944	BP	positive regulation of transcription by RNA polymerase II	975	624	5.038	1.64E-08	9.17E-06
GO:0045892	BP	negative regulation of transcription, DNA-templated	485	323	5.038	1.68E-08	9.17E-06
GO:0045296	MF	cadherin binding	280	205	5.025	1.90E-08	9.43E-06
GO:0001650	CC	fibrillar center	131	105	5.025	1.90E-08	9.43E-06
GO:0005925	CC	focal adhesion	397	281	5.025	1.93E-08	9.43E-06
GO:0006413	BP	translational initiation	130	95	5.025	1.94E-08	9.43E-06
GO:0000790	CC	nuclear chromatin	167	128	4.720	4.03E-08	1.91E-05
GO:0043161	BP	proteasome-mediated ubiquitin-dependent protein catabolic process	133	105	4.659	4.81E-08	2.19E-05
GO:0006366	BP	transcription by RNA polymerase II	266	187	4.659	4.89E-08	2.19E-05
GO:0016604	CC	nuclear body	277	198	4.625	5.45E-08	2.37E-05
GO:0008134	MF	transcription factor binding	264	192	4.625	5.56E-08	2.37E-05
GO:0006260	BP	DNA replication	129	102	4.604	5.98E-08	2.49E-05
GO:0019899	MF	enzyme binding	345	238	4.517	7.64E-08	3.04E-05
GO:0003735	MF	structural constituent of ribosome	157	91	4.517	7.66E-08	3.04E-05
GO:0005759	CC	mitochondrial matrix	349	234	4.513	7.91E-08	3.07E-05
GO:0005783	CC	endoplasmic reticulum	850	524	4.455	9.23E-08	3.51E-05
GO:0070125	BP	mitochondrial translational elongation	86	66	4.370	1.15E-07	4.26E-05
GO:0070126	BP	mitochondrial translational termination	88	67	4.212	1.72E-07	6.14E-05
GO:0006974	BP	cellular response to DNA damage stimulus	224	163	4.212	1.72E-07	6.14E-05
GO:0003700	MF	DNA-binding transcription factor activity	480	320	4.094	2.31E-07	8.06E-05
GO:0043231	CC	intracellular membrane-bounded organelle	579	379	4.074	2.46E-07	8.42E-05
GO:0019083	BP	viral transcription	109	79	4.003	2.95E-07	9.93E-05
GO:0000086	BP	G2/M transition of mitotic cell cycle	126	98	3.935	3.52E-07	1.16E-04
GO:0001843	BP	neural tube closure	76	65	3.870	4.16E-07	1.35E-04
GO:0031965	CC	nuclear membrane	234	167	3.752	5.57E-07	1.77E-04
GO:0097711	BP	ciliary basal body-plasma membrane docking	95	76	3.614	7.80E-07	2.43E-04
GO:1901796	BP	regulation of signal transduction by p53 class mediator	131	101	3.600	8.18E-07	2.51E-04
GO:0008380	BP	RNA splicing	143	106	3.265	1.82E-06	5.43E-04
GO:0006977	BP	DNA damage response, signal transduction by p53 class mediator resulting in cell cycle arrest	56	49	3.265	1.83E-06	5.43E-04
GO:1901990	BP	regulation of mitotic cell cycle phase transition	80	65	3.243	1.96E-06	5.71E-04
GO:0019904	MF	protein domain specific binding	255	178	2.929	4.11E-06	1.18E-03
GO:0022625	CC	cytosolic large ribosomal subunit	52	40	2.909	4.37E-06	1.23E-03
GO:0006511	BP	ubiquitin-dependent protein catabolic process	208	143	2.874	4.82E-06	1.34E-03
GO:0000502	CC	proteasome complex	54	46	2.819	5.56E-06	1.52E-03

GO:0031145	BP	anaphase-promoting complex-dependent catabolic process	81	63	2.742	6.73E-06	1.81E-03
GO:0007049	BP	cell cycle	248	170	2.683	7.88E-06	2.07E-03
GO:0006397	BP	mRNA processing	147	105	2.683	7.95E-06	2.07E-03
GO:0004842	MF	ubiquitin-protein transferase activity	224	158	2.671	8.30E-06	2.13E-03
GO:0006364	BP	rRNA processing	124	86	2.638	9.08E-06	2.30E-03
GO:0044877	MF	protein-containing complex binding	256	176	2.581	1.05E-05	2.62E-03
GO:0060071	BP	Wnt signaling pathway, planar cell polarity pathway	88	70	2.563	1.11E-05	2.73E-03
GO:0016579	BP	protein deubiquitination	236	163	2.562	1.13E-05	2.74E-03
GO:0003713	MF	transcription coactivator activity	261	180	2.482	1.38E-05	3.30E-03
GO:0000209	BP	protein polyubiquitination	206	143	2.439	1.54E-05	3.64E-03
GO:0006351	BP	transcription, DNA-templated	101	77	2.421	1.64E-05	3.79E-03
GO:0031625	MF	ubiquitin protein ligase binding	270	187	2.421	1.65E-05	3.79E-03
GO:0016363	CC	nuclear matrix	106	82	2.375	1.86E-05	4.22E-03
GO:0047485	MF	protein N-terminus binding	106	81	2.333	2.07E-05	4.64E-03
GO:0000978	MF	RNA polymerase II proximal promoter sequence-specific DNA binding	379	254	2.317	2.18E-05	4.81E-03
GO:0005839	CC	proteasome core complex	18	18	2.301	2.29E-05	5.00E-03
GO:0005794	CC	Golgi apparatus	820	514	2.299	2.33E-05	5.02E-03
GO:0071013	CC	catalytic step 2 spliceosome	80	62	2.299	2.35E-05	5.02E-03
GO:0043488	BP	regulation of mRNA stability	106	79	2.265	2.58E-05	5.44E-03
GO:0035735	BP	intraciliary transport involved in cilium assembly	40	35	2.231	2.83E-05	5.88E-03
GO:0043066	BP	negative regulation of apoptotic process	488	301	2.185	3.17E-05	6.53E-03
GO:0005814	CC	centriole	124	91	2.175	3.29E-05	6.68E-03
GO:0030496	CC	midbody	154	111	2.162	3.43E-05	6.88E-03
GO:0048013	BP	ephrin receptor signaling pathway	85	69	2.097	4.02E-05	7.99E-03
GO:0006281	BP	DNA repair	194	132	2.094	4.10E-05	8.06E-03
GO:0005819	CC	spindle	114	85	2.083	4.26E-05	8.27E-03
GO:0005929	CC	cilium	187	130	2.081	4.33E-05	8.30E-03
GO:0042645	CC	mitochondrial nucleoid	42	35	2.081	4.37E-05	8.30E-03
GO:0030332	MF	cyclin binding	28	26	2.060	4.64E-05	8.72E-03
GO:0016236	BP	macroautophagy	90	69	2.029	5.03E-05	9.36E-03
GO:0006302	BP	double-strand break repair	54	45	2.008	5.33E-05	9.81E-03
GO:0006890	BP	retrograde vesicle-mediated transport, Golgi to ER	74	58	2.008	5.40E-05	9.83E-03
GO:0051087	MF	chaperone binding	91	68	2.002	5.53E-05	9.96E-03
GO:0000278	BP	mitotic cell cycle	90	69	1.993	5.69E-05	1.02E-02
GO:0042802	MF	identical protein binding	1041	626	1.979	5.95E-05	1.05E-02
GO:0000922	CC	spindle pole	112	84	1.970	6.13E-05	1.07E-02
GO:0031146	BP	SCF-dependent proteasomal ubiquitin-dependent protein catabolic process	68	54	1.944	6.58E-05	1.14E-02
GO:0000139	CC	Golgi membrane	585	372	1.895	7.43E-05	1.27E-02

GO:0006915	BP	apoptotic process	538	333	1.895	7.50E-05	1.27E-02
GO:0006468	BP	protein phosphorylation	434	288	1.872	7.98E-05	1.34E-02
GO:0016055	BP	Wnt signaling pathway	179	129	1.870	8.10E-05	1.35E-02
GO:0072686	CC	mitotic spindle	66	52	1.859	8.39E-05	1.38E-02
GO:0046982	MF	protein heterodimerization activity	497	299	1.838	8.89E-05	1.45E-02
GO:0017148	BP	negative regulation of translation	61	48	1.811	9.55E-05	1.55E-02
GO:0035035	MF	histone acetyltransferase binding	26	24	1.792	1.01E-04	1.62E-02
GO:0042795	BP	snRNA transcription by RNA polymerase II	70	53	1.755	1.11E-04	1.76E-02
GO:0061418	BP	regulation of transcription from RNA polymerase II promoter in response to hypoxia	71	54	1.755	1.12E-04	1.76E-02
GO:0000049	MF	tRNA binding	47	39	1.720	1.22E-04	1.91E-02
GO:0060271	BP	cilium assembly	152	109	1.716	1.24E-04	1.92E-02
GO:0005763	CC	mitochondrial small ribosomal subunit	27	24	1.699	1.30E-04	2.00E-02
GO:0003682	MF	chromatin binding	326	215	1.633	1.53E-04	2.33E-02
GO:0000781	CC	chromosome, telomeric region	50	41	1.608	1.64E-04	2.46E-02
GO:0006521	BP	regulation of cellular amino acid metabolic process	51	40	1.571	1.80E-04	2.69E-02
GO:0006367	BP	transcription initiation from RNA polymerase II promoter	161	113	1.565	1.84E-04	2.72E-02
GO:0071364	BP	cellular response to epidermal growth factor stimulus	43	37	1.559	1.88E-04	2.76E-02
GO:0021766	BP	hippocampus development	63	50	1.555	1.91E-04	2.79E-02
GO:0005694	CC	chromosome	113	81	1.520	2.11E-04	3.02E-02
GO:0043065	BP	positive regulation of apoptotic process	331	214	1.520	2.12E-04	3.02E-02
GO:0006368	BP	transcription elongation from RNA polymerase II promoter	69	52	1.520	2.13E-04	3.02E-02
GO:0005762	CC	mitochondrial large ribosomal subunit	55	39	1.493	2.28E-04	3.21E-02
GO:0014069	CC	postsynaptic density	222	155	1.487	2.33E-04	3.26E-02
GO:0000281	BP	mitotic cytokinesis	48	39	1.473	2.43E-04	3.36E-02
GO:0090090	BP	negative regulation of canonical Wnt signaling pathway	166	115	1.450	2.58E-04	3.54E-02
GO:0005789	CC	endoplasmic reticulum membrane	872	516	1.427	2.74E-04	3.74E-02
GO:0000151	CC	ubiquitin ligase complex	89	67	1.425	2.79E-04	3.76E-02
GO:0005815	CC	microtubule organizing center	142	102	1.425	2.82E-04	3.76E-02
GO:0015630	CC	microtubule cytoskeleton	122	88	1.425	2.83E-04	3.76E-02
GO:1902036	BP	regulation of hematopoietic stem cell differentiation	68	53	1.425	2.84E-04	3.76E-02
GO:0010389	BP	regulation of G2/M transition of mitotic cell cycle	79	59	1.422	2.88E-04	3.78E-02
GO:0004672	MF	protein kinase activity	186	130	1.422	2.90E-04	3.79E-02
GO:0030426	CC	growth cone	124	91	1.407	3.03E-04	3.92E-02
GO:0001701	BP	in utero embryonic development	168	118	1.378	3.26E-04	4.19E-02
GO:0008284	BP	positive regulation of cell proliferation	482	287	1.355	3.46E-04	4.42E-02
GO:0030027	CC	lamellipodium	175	124	1.347	3.56E-04	4.50E-02

GO:0042393	MF	histone binding	99	73	1.346	3.58E-04	4.51E-02
GO:0071889	MF	14-3-3 protein binding	30	27	1.346	3.61E-04	4.51E-02
GO:0006888	BP	ER to Golgi vesicle-mediated transport	144	100	1.320	3.86E-04	4.79E-02
GO:0007094	BP	mitotic spindle assembly checkpoint	18	17	1.308	3.99E-04	4.92E-02

Table S3.2. Enriched KEGG pathways from differentially methylated sites associated with M3 LysoPC-sat. Differentially methylated sites (FDR<0.1) within known genes were selected for pathway analysis. The number of genes within each pathway (N) and the number of genes differentially methylated (DE) are reported. Enriched pathways listed have an FDR<0.05.

KEGG ID	Description	N	DE	Fold enrichment	unadjusted p-value	FDR
path:hsa04110	Cell cycle	124	102	7.004	2.95E-10	9.92E-08
path:hsa03010	Ribosome	153	99	5.463	2.05E-08	3.45E-06
path:hsa05165	Human papillomavirus infection	330	229	4.578	2.36E-07	2.64E-05
path:hsa05203	Viral carcinogenesis	201	139	4.091	9.66E-07	8.12E-05
path:hsa04150	mTOR signaling pathway	153	116	4.068	1.27E-06	8.56E-05
path:hsa05200	Pathways in cancer	531	346	3.960	1.96E-06	1.10E-04
path:hsa04218	Cellular senescence	160	118	3.741	3.78E-06	1.82E-04
path:hsa03040	Spliceosome	135	97	3.704	4.71E-06	1.98E-04
path:hsa04390	Hippo signaling pathway	154	116	3.572	7.18E-06	2.68E-04
path:hsa04714	Thermogenesis	231	149	3.369	1.27E-05	4.28E-04
path:hsa04144	Endocytosis	249	175	3.334	1.68E-05	4.64E-04
path:hsa05220	Chronic myeloid leukemia	76	63	3.334	1.70E-05	4.64E-04
path:hsa05205	Proteoglycans in cancer	204	147	3.334	1.79E-05	4.64E-04
path:hsa05223	Non-small cell lung cancer	66	56	3.273	2.22E-05	5.34E-04
path:hsa01100	Metabolic pathways	1487	861	3.266	2.42E-05	5.42E-04
path:hsa04120	Ubiquitin mediated proteolysis	136	99	2.765	8.63E-05	1.72E-03
path:hsa05222	Small cell lung cancer	92	72	2.765	8.69E-05	1.72E-03
path:hsa05100	Bacterial invasion of epithelial cells	73	59	2.588	1.38E-04	2.58E-03
path:hsa05010	Alzheimer disease	171	112	2.330	2.64E-04	4.68E-03
path:hsa05016	Huntington disease	193	124	2.287	3.13E-04	5.17E-03
path:hsa05163	Human cytomegalovirus infection	225	146	2.287	3.23E-04	5.17E-03
path:hsa05034	Alcoholism	184	110	2.269	3.53E-04	5.38E-03
path:hsa05225	Hepatocellular carcinoma	168	117	2.239	3.95E-04	5.77E-03
path:hsa05226	Gastric cancer	149	106	2.213	4.37E-04	6.12E-03
path:hsa03060	Protein export	23	21	2.169	5.05E-04	6.78E-03
path:hsa04210	Apoptosis	136	94	2.148	5.65E-04	7.11E-03
path:hsa05217	Basal cell carcinoma	63	50	2.148	5.71E-04	7.11E-03
path:hsa04934	Cushing syndrome	155	109	2.105	6.54E-04	7.85E-03
path:hsa05167	Kaposi sarcoma-associated herpesvirus infection	186	121	2.076	7.33E-04	8.40E-03
path:hsa04330	Notch signaling pathway	53	42	2.076	7.50E-04	8.40E-03
path:hsa05212	Pancreatic cancer	76	58	2.043	8.50E-04	9.05E-03
path:hsa05224	Breast cancer	147	104	2.043	8.86E-04	9.05E-03
path:hsa04115	p53 signaling pathway	72	55	2.043	8.89E-04	9.05E-03
path:hsa05166	Human T-cell leukemia virus 1 infection	219	147	2.039	9.25E-04	9.14E-03
path:hsa04140	Autophagy - animal	137	96	1.984	1.08E-03	1.04E-02
path:hsa05215	Prostate cancer	97	71	1.930	1.26E-03	1.17E-02

path:hsa05161	Hepatitis B	162	107	1.834	1.61E-03	1.46E-02
path:hsa04141	Protein processing in endoplasmic reticulum	166	111	1.760	1.96E-03	1.74E-02
path:hsa00510	N-Glycan biosynthesis	50	39	1.740	2.21E-03	1.82E-02
path:hsa05216	Thyroid cancer	37	30	1.740	2.22E-03	1.82E-02
path:hsa05211	Renal cell carcinoma	69	53	1.740	2.23E-03	1.82E-02
path:hsa00514	Other types of O-glycan biosynthesis	23	20	1.740	2.27E-03	1.82E-02
path:hsa05213	Endometrial cancer	58	46	1.734	2.36E-03	1.84E-02
path:hsa05202	Transcriptional misregulation in cancer	186	121	1.705	2.64E-03	1.97E-02
path:hsa01521	EGFR tyrosine kinase inhibitor resistance	79	59	1.705	2.70E-03	1.97E-02
path:hsa00190	Oxidative phosphorylation	133	78	1.705	2.71E-03	1.97E-02
path:hsa04919	Thyroid hormone signaling pathway	119	85	1.705	2.80E-03	1.97E-02
path:hsa03460	Fanconi anemia pathway	54	40	1.705	2.82E-03	1.97E-02
path:hsa03013	RNA transport	165	101	1.704	2.88E-03	1.98E-02
path:hsa05210	Colorectal cancer	86	63	1.638	3.42E-03	2.30E-02
path:hsa04010	MAPK signaling pathway	295	192	1.612	3.76E-03	2.44E-02
path:hsa04211	Longevity regulating pathway	89	64	1.612	3.78E-03	2.44E-02
path:hsa01524	Platinum drug resistance	73	51	1.587	4.08E-03	2.59E-02
path:hsa04520	Adherens junction	71	54	1.582	4.21E-03	2.62E-02
path:hsa04722	Neurotrophin signaling pathway	119	84	1.576	4.36E-03	2.65E-02
path:hsa01212	Fatty acid metabolism	57	43	1.576	4.42E-03	2.65E-02
path:hsa05012	Parkinson disease	142	84	1.576	4.51E-03	2.66E-02
path:hsa04068	FoxO signaling pathway	131	88	1.540	5.02E-03	2.88E-02
path:hsa03440	Homologous recombination	41	32	1.540	5.12E-03	2.88E-02
path:hsa03050	Proteasome	45	34	1.540	5.14E-03	2.88E-02
path:hsa03008	Ribosome biogenesis in eukaryotes	105	55	1.498	5.77E-03	3.18E-02
path:hsa04932	Non-alcoholic fatty liver disease (NAFLD)	149	93	1.489	5.98E-03	3.24E-02
path:hsa04916	Melanogenesis	101	71	1.485	6.13E-03	3.27E-02
path:hsa04070	Phosphatidylinositol signaling system	99	70	1.483	6.27E-03	3.29E-02
path:hsa03018	RNA degradation	79	53	1.413	7.48E-03	3.87E-02
path:hsa00513	Various types of N-glycan biosynthesis	39	31	1.406	7.72E-03	3.93E-02
path:hsa04152	AMPK signaling pathway	120	82	1.393	8.07E-03	4.04E-02
path:hsa05214	Glioma	75	55	1.381	8.45E-03	4.16E-02
path:hsa03030	DNA replication	36	27	1.381	8.55E-03	4.16E-02
path:hsa04728	Dopaminergic synapse	131	88	1.347	9.46E-03	4.50E-02
path:hsa00280	Valine, leucine and isoleucine degradation	48	36	1.347	9.57E-03	4.50E-02
path:hsa04725	Cholinergic synapse	112	77	1.347	9.64E-03	4.50E-02
path:hsa00640	Propanoate metabolism	34	26	1.345	9.81E-03	4.52E-02
path:hsa00310	Lysine degradation	61	45	1.317	1.06E-02	4.82E-02
path:hsa03015	mRNA surveillance pathway	91	59	1.303	1.13E-02	4.98E-02
path:hsa05219	Bladder cancer	41	32	1.303	1.13E-02	4.98E-02
path:hsa04130	SNARE interactions in vesicular transport	34	26	1.303	1.14E-02	4.98E-02

Figure 3.2. Top 10 significantly enriched gene ontologies and biological pathways associated with M3 LysoPC-sat.

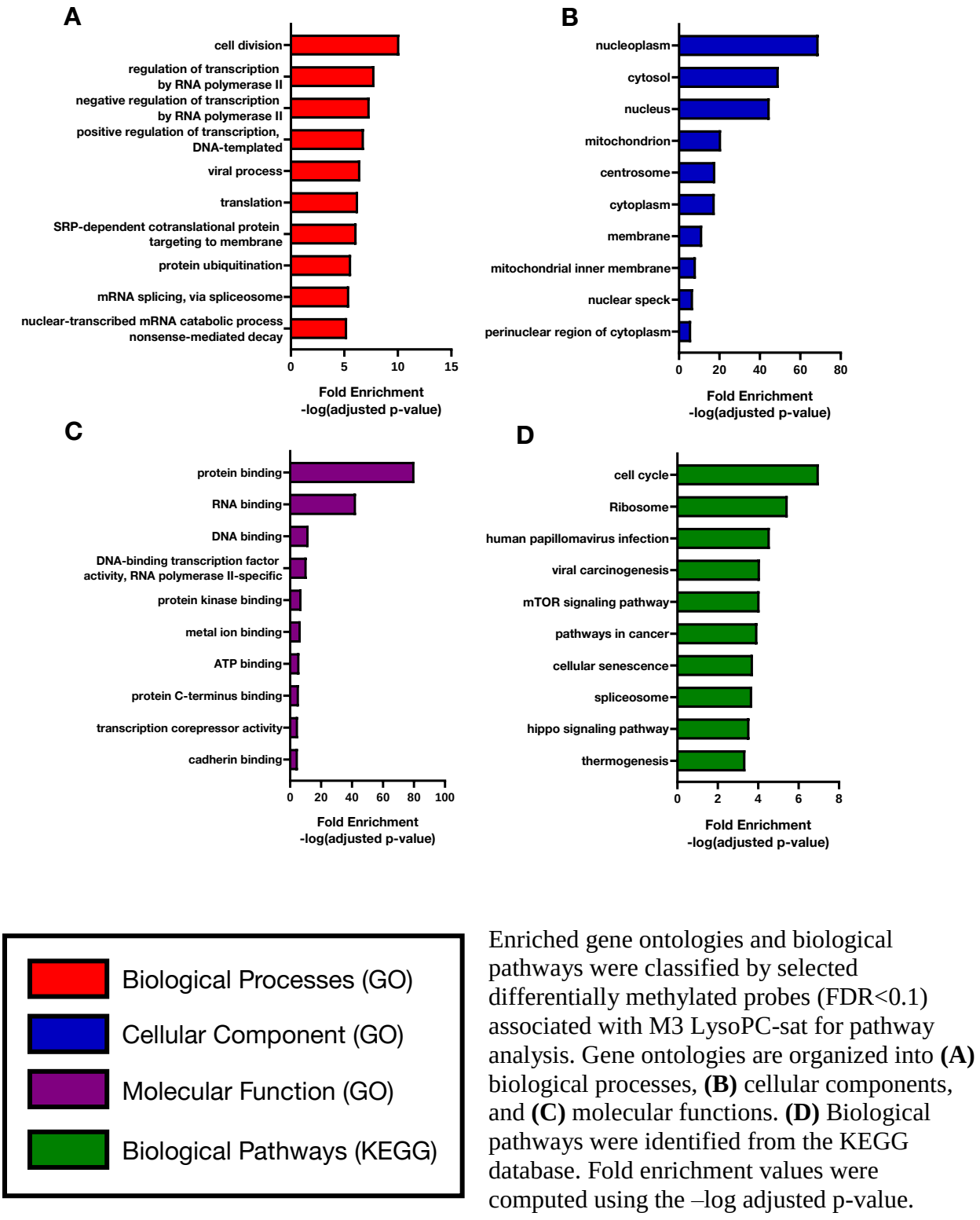

Enriched gene ontologies and biological pathways were classified by selected differentially methylated probes (FDR<0.1) associated with M3 LysoPC-sat for pathway analysis. Gene ontologies are organized into **(A)** biological processes, **(B)** cellular components, and **(C)** molecular functions. **(D)** Biological pathways were identified from the KEGG database. Fold enrichment values were computed using the –log adjusted p-value.

References

1. Barker DJP. The origins of the developmental origins theory. J Intern Med. 2007;261:412–7.

2. Lindsay KL, Hellmuth C, Uhl O, Buss C, Wadhwa PD, Koletzko B, Entringer S. Longitudinal metabolomic profiling of amino acids and lipids across healthy pregnancy. PLoS One. 2015;10:e0145794.

3. Hellmuth C, Lindsay KL, Uhl O, Buss C, Wadhwa PD, Koletzko B, Entringer S. Association of maternal pre-pregnancy BMI with metabolomic profile across gestation. Int J Obes. Nature Publishing Group; 2017;41:159–69.

4. Sandler V, Reisetter AC, Bain JR, Muehlbauer MJ, Nodzenski M, Stevens RD, Ilkayeva O, Lowe LP, Metzger BE, Newgard CB, et al. Associations of maternal BMI and insulin resistance with the maternal metabolome and newborn outcomes. Diabetologia. Diabetologia; 2016;60:518–30.

5. Desert R, Canlet C, Costet N, Cordier S, Bonvallot N. Impact of maternal obesity on the metabolic profiles of pregnant women and their offspring at birth. Metabolomics. Springer US; 2015;11:1896–907.

6. Maitre L, Villanueva CM, Lewis MR, Ibarluzea J, Santa-Marina L, Vrijheid M, Sunyer J, Coen M, Toledano MB. Maternal urinary metabolic signatures of fetal growth and associated clinical and environmental factors in the INMA study. BMC Med. BMC Medicine; 2016;14:1–12.

7. Brenseke B, Prater MR, Bahamonde J, Gutierrez JC. Current Thoughts on Maternal Nutrition and Fetal Programming of the Metabolic Syndrome. J Pregnancy. 2013;2013:1–13.

8. Pettitt DJ, Jovanovic L. Birth weight as a predictor of type 2 diabetes mellitus: the U-shaped curve. Curr Diab Rep. 2001;1:78–81.

9. Barker DJP, Eriksson JG, Forsén T, Osmond C. Fetal origins of adult disease: Strength of effects and biological basis. Int J Epidemiol. 2002;31:1235–9.

10. Gluckman P, Hanson M, Cooper C, Thornburg KL. Effect of In Utero and Early-Life Conditions on Adult Health and Disease. N Engl J Med. 2008;359:61–73.

11. Gu J, Stevens M, Xing X, Li D, Zhang B, Payton JE, Oltz EM, Jarvis JN, Jiang K, Cicero T, et al. Mapping of Variable DNA Methylation Across Multiple Cell Types Defines a Dynamic Regulatory Landscape of the Human Genome. G3. 2016;6:973–86.

12. James P, Sajjadi S, Tomar AS, Saffari A, Fall CHD, Prentice AM, Shrestha S, Issarapu P, Yadav DK, Kaur L, et al. Candidate genes linking maternal nutrient exposure to offspring health via DNA methylation: a review of existing evidence in humans with specific focus on one-carbon metabolism. Int J Epidemiol. 2018;47:1910–37.

13. Sharp GC, Lawlor DA, Richmond RC, Fraser A, Simpkin A, Suderman M, Shihab HA, Lyttleton O, McArdle W, Ring SM, et al. Maternal pre-pregnancy BMI and gestational weight gain, offspring DNA methylation and later offspring adiposity: Findings from the

Avon Longitudinal Study of Parents and Children. Int J Epidemiol. 2015;44:1288–304.

14. Engel SM, Joubert BR, Wu MC, Olshan AF, Haberg SE, Ueland PM, Nystad W, Nilsen RM, Vollset SE, Peddada SD, et al. Neonatal genome-wide methylation patterns in relation to birth weight in the norwegian mother and child cohort. Am J Epidemiol. 2014;179:834–42.

15. Marchlewicz EH, Dolinoy DC, Tang L, Milewski S, Jones TR, Goodrich JM, Soni T, Domino SE, Song PXK, Burant CF, et al. Lipid metabolism is associated with developmental epigenetic programming. Sci Rep. Nature Publishing Group; 2016;6:1–13.

16. Haggarty P, Hoad G, Horgan GW, Campbell DM. DNA Methyltransferase Candidate Polymorphisms, Imprinting Methylation, and Birth Outcome. PLoS One. 2013;8:1–8.

17. Tabano S, Colapietro P, Cetin I, Grati FR, Zanutto S, Mandò C, Antonazzo P, Pileri P, Rossella F, Larizza L, et al. Epigenetic modulation of the IGF2/H19 imprinted domain in human embryonic and extra-embryonic compartments and its possible role in fetal growth restriction. Epigenetics. 2010;5:313–24.

18. Sébert SP, Lecannu G, Kozlowski F, Siliart B, Bard JM, Krempf M, Champ MM-J. Childhood obesity and insulin resistance in a Yucatan mini-piglet model: putative roles of IGF-1 and muscle PPARs in adipose tissue activity and development. Int J Obes. 2005;29:324–33.

19. Tindula G, Lee D, Huen K, Bradman A, Eskenazi B, Holland N. Pregnancy lipidomic profiles and DNA methylation in newborns from the CHAMACOS cohort. Environ Epigenetics. 2019;5:1–11.

20. Afshinnia F, Rajendiran TM, Karnovsky A, Soni T, Wang X, Xie D, Yang W, Sha T, Weir MR, He J, et al. Lipidomic Signature of Progression of Chronic Kidney Disease in the Chronic Renal Insufficiency Cohort. Kidney Int Reports. 2016;1:256–68.

21. Gika HG, Macpherson E, Theodoridis GA, Wilson ID. Evaluation of the repeatability of ultra-performance liquid chromatography-TOF-MS for global metabolic profiling of human urine samples. J Chromatogr B. 2008;871:299–305.

22. Kind T, Liu K, Lee DY, Defelice B, Meissen JK, Fiehn O. LipidBlast in silico tandem mass spectrometry database for lipid identification. Nat Methods. 2013;10:755–8.

23. Bakulski KM, Feinberg JI, Andrews S V, Yang J, Brown S, Mckenney SL, Witter F, Walston J, Feinberg AP, Fallin MD. DNA methylation of cord blood cell types: Applications for mixed cell birth studies. Epigenetics. Taylor & Francis; 2016;11:354–62.

24. Aryee MJ, Jaffe AE, Corrada-Bravo H, Ladd-Acosta C, Feinberg AP, Hansen KD, Irizarry RA. Minfi: A flexible and comprehensive Bioconductor package for the analysis of Infinium DNA methylation microarrays. Bioinformatics. 2014;30:1363–9.

25. Feber A, Guilhamon P, Lechner M, Fenton T, Wilson GA, Thirlwell C, Morris TJ, Flanagan AM, Teschendorff AE, Kelly JD, et al. Using high-density DNA methylation arrays to profile copy number alterations. Genome Biol. 2014;15:1–13.

26. Du P, Zhang X, Huang C, Jafari N, Kibbe WA, Hou L, Lin SM. Comparison of Beta-

value and M-value methods for quantifying methylation levels by microarray analysis. BMC Bioinformatics. 2010;11:1–9.

27. Ghosh J, Mainigi M, Coutifaris C, Sapienza C. Outlier DNA methylation levels as an indicator of environmental exposure and risk of undesirable birth outcome. Hum Mol Genet. 2016;25:123–9.

28. Ritchie ME, Phipson B, Wu D, Hu Y, Law CW, Shi W, Smyth GK. Limma powers differential expression analyses for RNA-sequencing and microarray studies. Nucleic Acids Res. 2015;43:e47.

29. Benjamini Y, Hochberg Y. Controlling the False Discovery Rate: A Practical and Powerful Approach to Multiple Testing. J R Stat Soc Ser B Methodol. 1995;57:289–300.

30. Geeleher P, Hartnett L, Egan LJ, Golden A, Raja Ali RA, Seoighe C. Gene-set analysis is severely biased when applied to genome-wide methylation data. Bioinformatics. 2013;29:1851–7.

31. Phipson B, Maksimovic J, Oshlack A. missMethyl: an R package for analyzing data from Illumina's HumanMethylation450 platform. Bioinformatics. 2016;32:286–8.

32. The Gene Ontology Consortium. Gene ontology: tool for the unification of biology. Nat Genet. 2000;25:25–9.

33. Kanehisa M, Goto S. KEGG: Kyoto Encyclopedia of Genes and Genomes. Nucleic Acids Res. 2000;28:27–30.

34. Neess D, Bek S, Engelsby H, Gallego SF, Færgeman NJ. Long-chain acyl-CoA esters in metabolism and signaling: Role of acyl-CoA binding proteins. Prog Lipid Res. 2015;59:1–25.

35. Malicdan MC V., Vilboux T, Ben-Zeev B, Guo J, Eliyahu A, Pode-Shakked B, Dori A, Kakani S, Chandrasekharappa SC, Ferreira CR, et al. A novel inborn error of the coenzyme Q10 biosynthesis pathway: cerebellar ataxia and static encephalomyopathy due to COQ5 C-methyltransferase deficiency. Hum Mutat. 2018;39:69–79.

36. Nomura R, Suzuki Y, Kakizuka A, Jingami H. Direct detection of the interaction between recombinant soluble extracellular regions in the heterodimeric metabotropic gamma-aminobutyric acid receptor. J Biol Chem. 2008;283:4665–73.

37. Du X, Han L, Guo AY, Zhao Z. Features of methylation and gene expression in the promoter-associated CpG islands using human methylome data. Comp Funct Genomics. 2012;598987.

38. Færgeman NJ, Knudsen J. Role of long-chain fatty acyl-CoA esters in the regulation of metabolism and in cell signalling. Biochem J. 1997;323:1–12.

39. Færgeman NJ, Wadum M, Feddersen S, Burton M, Kragelund BB, Knudsen J. Acyl-CoA binding proteins; structural and functional conservation over 2000 MYA. Mol Cell Biochem. 2007;299:55–65.

40. Huang H, Atshaves BP, Frolov A, Kier AB, Schroeder F. Acyl-Coenzyme A Binding

Protein Expression Alters Liver Fatty Acyl-Coenzyme A Metabolism. Biochemistry. 2005;44:10282–97.

41. Harris FT, Rahman SMJ, Hassanein M, Qian J, Hoeksema MD, Chen H, Eisenberg R, Chaurand P, Caprioli RM, Shiota M, et al. Acyl-coenzyme A-binding protein regulates Beta-oxidation required for growth and survival of non-small cell lung cancer. Cancer Prev Res. 2014;7:748–58.

42. Hausch F, Kozany C, Theodoropoulou M, Fabian A. FKBPs and the Akt/mTOR pathway. Cell Cycle. 2013;12:2366–70.

43. Wang X, Deng Y, Zhang G, Li C, Ding G, May HI, Tran DH, Luo X, Jiang D-S, Li DL, et al. Spliced X-box Binding Protein 1 Stimulates Adaptive Growth Through Activation of mTOR. Circulation. 2019;140:566–79.

44. Lands WE. Metabolism of glycerolipides: A comparison of lecithin and triglyceride synthesis. 1J Biol Chem. 1958;231:883–9.

45. Lands WE. Metabolism of glycerolipids. 2. The enzymatic acylation of lysolecithin. J Biol Chem. 1960;235:2233–7.

46. Law SH, Chan M-L, Marathe GK, Parveen F, Chen CH, Ke LY. An updated review of lysophosphatidylcholine metabolism in human diseases. Int J Mol Sci. 2019;20:1–24.

47. Xu Y, Fang XJ, Casey G, Mills GB. Lysophospholipids activate ovarian and breast cancer cells. Biochem J. 1995;309:933–40.

48. Murph M, Tanaka T, Pang J, Felix E, Liu S, Trost R, Godwin AK, Newman R, Mills G. Liquid Chromatography Mass Spectrometry for Quantifying Plasma Lysophospholipids: Potential Biomarkers for Cancer Diagnosis. Methods Enzymol. 2007;433:1–25.

49. Pietiläinen KH, Sysi-Aho M, Rissanen A, Seppänen-Laakso T, Yki-Järvinen H, Kaprio J, Orešič M. Acquired obesity is associated with changes in the serum lipidomic profile independent of genetic effects--a monozygotic twin study. PLoS One. 2007;2.

50. Rabini RA, Galassi R, Fumelli P, Dousset N, Solera ML, Valdiguie P, Curatola G, Ferretti G, Taus M, Mazzanti L. Reduced Na(+)-K(+)-ATPase activity and plasma lysophosphatidylcholine concentrations in diabetic patients. Diabetes. 1994;43:915–9.

51. Patel N, Hellmuth C, Uhl O, Godfrey K, Briley A, Welsh P, Pasupathy D, Seed P, Koletzko B, Poston L, et al. Cord Metabolic Profiles In Obese Pregnant Women; Insights Into Offspring Growth And Body Composition. J Clin Endocrinol Metab. 2017;103:346–55.

52. Hellmuth C, Uhl O, Standl M, Demmelmair H, Heinrich J, Koletzko B, Thiering E. Cord Blood Metabolome Is Highly Associated with Birth Weight, but Less Predictive for Later Weight Development. Eur J Obes. 2017;10:85–100.

53. Lu Y-P, Reichetzeder C, Prehn C, Yin L-H, Yun C, Zeng S, Chu C, Adamski J, Hocher B. Cord Blood Lysophosphatidylcholine 16:1 is Positively Associated with Birth Weight. Cell Physiol Biochem. 2018;45:614–24.

54. Yan J, Jiang X, West AA, Perry CA, Malysheva O V., Brenna JT, Stabler SP, Allen RH, Gregory JF, Caudill MA. Pregnancy alters choline dynamics: Results of a randomized trial using stable isotope methodology in pregnant and nonpregnant women. Am J Clin Nutr. 2013;98:1459–67.

55. Villegas R, Williams SM, Gao YT, Long J, Shi J, Cai H, Li H, Chen CC, Tai ES, Hu F, et al. Genetic variation in the peroxisome proliferator-activated receptor (PPAR) and peroxisome proliferator-activated receptor gamma co-activator 1 (PGC1) gene families and type 2 diabetes. Ann Hum Genet. 2014;78:23–32.

56. Arpón A, Riezu-Boj J, Milagro F, Marti A, Razquin C, Martinez-Gonzalez M, Corella D, Estruch R, Casas R, Fito M, et al. Adherence to Mediterranean diet is associated with methylation changes in inflammation-related genes in peripheral blood cells. J Physiol Biochem. Journal of Physiology and Biochemistry; 2017;73:445–55.

57. Bondia-Pons I, Martinez JA, de la Iglesia R, Lopez-Legarrea P, Poutanen K, Hanhineva K, de los Angeles Zulet M. Effects of short- and long-term Mediterranean-based dietary treatment on plasma LC-QTOF/MS metabolic profiling of subjects with metabolic syndrome features: The Metabolic Syndrome Reduction in Navarra (RESMENA) randomized controlled trial. Mol Nutr Food Res. 2015;59:711–28.

58. Toledo E, Wang DD, Ruiz-Canela M, Clish CB, Razquin C, Zheng Y, Guasch-Ferre M, Hruby A, Corella D, Gomez-Gracia E, et al. Plasma lipidomic profiles and cardiovascular events in a randomized intervention trial with the Mediterranean diet. Am J Clin Nutr. 2017;106:973–83.

59. Tong TYN, Koulman A, Griffin JL, Wareham NJ, Forouhi NG, Imamura F. A Combination of Metabolites Predicts Adherence to the Mediterranean Diet Pattern and Its Associations with Insulin Sensitivity and Lipid Homeostasis in the General Population: The Fenland Study, United Kingdom. J Nutr. Oxford University Press; 2019;1–11.

60. van Rossum AG, Aartsen WM, Meuleman J, Klooster J, Malysheva A, Versteeg I, Arsanto J-P, Le Bivic A, Wijnholds J. Pals1/Mpp5 is required for correct localization of Crb1 at the subapical region in polarized Muller glia cells. Hum Mol Genet. 2006;15:2659–72.

61. Nevalainen J, Skarp S, Savolainen E-R, Ryynanen M, Jarvenpaa J. Intrauterine growth restriction and placental gene expression in severe preeclampsia, comparing early-onset and late-onset forms. J Perinat Med. 2017;45:869–77.

62. Lai CQ, Wojczynski MK, Parnell LD, Hidalgo BA, Irvin MR, Aslibekyan S, Province MA, Absher DM, Arnett DK, Ordovás JM. Epigenome-wide association study of triglyceride postprandial responses to a high-fat dietary challenge. J Lipid Res. 2016;57:2200–7.

CHAPTER 4

Evidence for Intrinsic Mitochondrial Nutrient Utilization Underlying the Association between Metabolite Levels and Insulin Resistance in Adolescents.

Abstract

A person's intrinsic metabolism, based on underlying physiologic conditions and reflected in the metabolome, may describe the relationship between nutrient intake and metabolic health. Untargeted metabolomics was used to identify metabolites associated with metabolic health and path analysis classified how habitual dietary intake influences BMI z-score (BMIz) and insulin resistance (IR) through changes in the metabolome among 108 girls and 98 boys aged 8-14 years. Data on anthropometry, fasting metabolites, C-peptide, and dietary intake (via a semi-quantitative food frequency questionnaire) were collected from adolescents in the Early Life Exposure in Mexico to ENvironmental Toxicants (ELEMENT) birth cohort. Sex-stratified linear regression identified metabolites associated BMIz and homeostatic model assessment of insulin resistance using C-peptide (HOMA-CP), accounting for puberty, age and muscle and fat area. Path analysis identified clusters of metabolites that underlie the relationship between energy-adjusted macronutrient intake with BMIz and HOMA-CP. Metabolites associated with BMIz include positive associations with diglycerides among girls and positive associations with branched chain and aromatic amino acids in boys. Intermediates in fatty acid metabolism, including medium-chain acylcarnitines (AC), were inversely associated with HOMA-CP. No

direct relationship was observed between macronutrient intake with BMIz and IR. Carbohydrate intake is positively associated with HOMA-CP through decreases in levels of AC, products of β-oxidation. Approaching significance, fat intake is positively associated with HOMA-CP through increases in levels of dicarboxylic fatty acids (DiC-FA), products of omega-oxidation. This cross-sectional analysis suggests that IR in children is associated with reduced fatty acid oxidation capacity. When consuming more grams of fat, there is evidence for increased extra-mitochondrial fatty acid metabolism, while higher carbohydrate intake appears to lead to decreases in intermediates of β-oxidation. Thus, biomarkers of IR and mitochondrial oxidative capacity may depend on macronutrient intake.

Introduction

Obesity rates are increasing in the pediatric population in both developed and developing countries (1), accompanied by an increased prevalence of prediabetes and type 2 diabetes (T2D) (2). With recent advancements in analytical technologies, the profiling of small molecular weight intermediates in metabolism through metabolomics has been used to identify biomarkers and potential pathways associated with obesity and insulin resistance (IR). Branched chain amino acids (BCAA) and their short-chain acylcarnitine (AC) metabolites, propionylcarnitine and butyrylcarnitine, have been consistently increased in obese adolescents (3–5). However, studies are inconsistent regarding the relationship between BCAA and IR in adolescents with findings reporting positive associations (3–5), inverse associations (6), and sex differences (7–9) which may be due to differences in analytical methodologies as well as the variability in the size and characteristic in study populations. Some metabolomics analyses in youth have also identified divergent associations of metabolite levels and metabolic phenotypes compared to those observed in adults. In contrast to adults, fatty acids (FA) were not associated with BMI or IR at

15 years of age (10,11). Additionally, lower levels of fatty acid oxidation (FAO) intermediates, such as dicarboxylic fatty acids (DiC-FA) (4) and medium-chain AC (6), were reported in children with T2D and obesity. These results suggest less imbalance in the delivery and oxidation of substrates in these individuals, perhaps due to the increased substrate utilization to fuel tissue and linear growth in the pubertal period.

The effect of macronutrient intake on metabolic health remains controversial with previous analyses describing a relationship between amount of macronutrient consumed and metabolic outcomes (12), while other analyses suggesting no relationship (13–15). Discrepancies in the results from these studies motivated us to identify molecular mechanisms, via classifying patterns of metabolites, which indicate how habitual diet relates to metabolic health. The ability to fully oxidize substrates within the mitochondria, known as the oxidative capacity, may dictate how nutrient intake influences BMI and IR (16,17).

In this paper, our goal was to expand on the relationship between the metabolome with obesity and IR to identify potential metabolic perturbations in the pubertal period, assessing sex-specific alterations given differences in pubertal hormones and the accumulation of muscle and fat tissue (18). These results build on previous work from our group in identifying metabolites associated with a metabolic risk score (19) and change in metabolic risk (9). Applying an improved untargeted metabolomics pipeline that used new pre-processing methods, we markedly expanded the number of annotated features providing new insights into metabolism in the population. Additionally, we identified how habitual macronutrient intake, in particular energy adjusted carbohydrate and fat intake, is associated with the metabolome. Our final objective was to determine if macronutrient intake could provide additional information on the underlying difference in metabolism that leads to insulin resistance.

Subjects and Methods

Study Population. Participants were enrolled in the Early Life Exposure in Mexico to ENvironmental Toxicants (ELEMENT) project which was started in 1994 and consists of three sequentially-enrolled birth cohorts from Mexico City Maternity Hospitals (20). A subset of these children, age 8-14 years, were contacted through their primary caregiver to provide urine samples, serum samples, anthropometry and complete an interview-based questionnaire (n=250). Subjects for this analysis have baseline and follow data on anthropometry, metabolic biomarkers and adequate serum volume for metabolomics analyses (n=206). This study was evaluated and approved by the Research, Ethics, and Biosafety Committees of the National Institute of Public Health of Mexico, the Institutional Review Board of the University of Michigan, and the Institutional Review Board from the Harvard School of Public Health (21).

Metabolomics Profiling. Fasting serum samples were analyzed using an untargeted metabolomics platform on an Agilent 1200 HPLC/6530 quadrupole Time-of-Flight mass spectrometry (MS) system (Agilent Technologies, Inc., Santa Clara, CA USA) using the Waters Acquity HSS T3 1.8 μm column (Waters Corporation, Milford, MA) (22). The eluent was analyzed in both positive and negative ion mode electrospray ionization. Chromatographic peaks that represent features were detected using a modified version of existing commercial software (Agilent MassHunter Qualitative Analysis). Data normalization followed a recently described method (23), using "pooled" reference samples that were analyzed repeatedly throughout each batch (24). The incorporation of Binner, a new method to visualize closely eluting features, allowed for the removal of redundant features. Missing peak intensities were imputed by K-nearest neighbor-5 in features with at least 70% detection. R package "impute" was used for imputation. Features with less than 70% detection across samples were removed. Annotated

metabolites were identified via comparing their MS/MS spectra to authentic standards, purchased internal or external standards ran on the same instrument. Noteworthy, these analytical technologies are not capable of determining the position of the double bonds and the distribution of carbon atoms between fatty acid side chains. All lipids will be mentioned with the nomenclature as X:Y, where X is the length of the carbon chain and Y is the number of double bonds. The final metabolomics dataset contained 550 annotated metabolites and 2722 unannotated metabolites.

Anthropometric Assessment. Anthropometry was obtained using standardized procedures by trained personnel following Lohman Methodology (25). Weight was measured with scale BAME Mod 420; Catálogo Médico rounded to the nearest 0.1kg; height was recorded with a stadiometer (Perspective Enterprises, Portage, WI, USA) to the nearest 0.5 cm; and waist circumference (WC) was obtained using a non-stretchable measuring tape at the level of the umbilicus (SECA) to the nearest 0.1 cm (21). Weight and height were used to calculate BMI (kg/m2) and participants were classified as obese (BMI z-score≥2) and normal weight (-2≤BMI z-score <1) according to the World Health Organization criteria (26), using WHO Anthro software (version 3.2.2, January 2011, World Health Organization, Geneva, Switzerland). WC and height were used to calculate waist-to-height ratio (WHtR). Skinfold thickness measurements of the triceps (TR), subscapular (SS), and suprailiac (SP) sites were measured using Lange skinfold calipers (Lange, Beta Technology) to the nearest 0.1 mm. These measurements were used to quantify total subcutaneous adiposity (SS+TR) and central subcutaneous adiposity (SS/TR). Weight and height were measured in duplicate and WC and skinfold thickness were measured in triplicate. Arm circumference was measured to the nearest 0.1 cm and used to calculate mid-upper arm muscle area (MUAMA) and mid-upper arm fat area (MUAFA) using standard equations (27).

Metabolic Biomarkers. Metabolic biomarkers were measured using 8-hour fasting serum. Glucose and C-peptide were quantified using an automated chemiluminescence immunoassay (Immulite 1000, Siemens Medical Solutions USA, Inc., Malvern, Pennsylvania). These biomarkers provide a measure of glycemic control, as fasting glucose is an indicator of glucose metabolism and a diabetes screening tool, and C-peptide is a marker of insulin secretion from pancreatic β-cells (28). Insulin levels in plasma were determined by Human Insulin ELISA kit EZHI-14K from Millipore Corporation (Billerica, MA). Insulin measures were below the limit of detection for 86 subjects; therefore, C-peptide was used to assess endogenous insulin levels. There was a significant positive correlation between insulin and C-peptide (r^2 0.7689, $p < 0.001$) (**Figure S4.1**). C-peptide replaced insulin in an adjusted homeostatic model assessment index (HOMA-CP) to evaluate beta-cell function (29).

$$HOMA - CP = \frac{Glucose\ \left(\frac{mg}{dL}\right) * C - peptide\ \left(\frac{ng}{mL}\right) * 1.8395}{135}$$

We measured total cholesterol, triglycerides, and HDL cholesterol in fasting serum samples (mg/dL) using a biochemical analyzer (Cobas Mira Plus, Roche Diagnostics) and calculated LDL cholesterol using Friedewald's equation (30). Leptin was measured using radioimmunoassay (Millipore) and insulin-like growth factor 1 (IGF-1) were measured using an automated chemiluminescence immunoassay (Immulite 1000).

Blood Pressure. Systolic (SBP) and diastolic blood pressure (DBP) were measured in duplicate to the nearest mmHg in the seated position (BPTru monitors; Coquitlam, British Columbia, Canada).

Dietary Intake. Usual dietary intake of children over the past week was determined using a semi-quantitative food frequency questionnaire (FFQ) adapted from the 2006 Mexican Health and Nutrition Survey (31). Separate questionnaires were used for children ages 7-11 years and 12 years or older. Children 7-11 years old were assisted by their mother to improve accuracy and precision of the self-reported intakes. Total calories and grams of macronutrients were extracted from all food items in the FFQ using food composition tables supplied by the United States Department of Agriculture and the Mexican National Institute of Nutrition and Medical Sciences Salvador Zubirán (32). Macronutrients were adjusted for total energy intake using the residual method (33).

Puberty Status. Sexual maturation was measured using Tanner staging where stages 1 indicates no development and stage 5 indicates full development (34,35). Children were examined based on a standardized protocol by a trained pediatrician, who assessed Tanner stages in genital (boys), breasts (girls), and pubic hair (boys and girls) development; see reference (36). Participants were classified as having reached puberty onset if they had a Tanner Stage greater than 1 for pubic hair and genital development (boys) or breast development (girls) (37).

Data Analysis. Prior to the main analysis, we examined sex-specific differences in adiposity measurements, metabolic biomarkers and dietary data. Pearson's chi-square tests were used to identify differences in categorical variables. Paired t-tests were used to identify differences in continuous variables. Pearson's correlations were calculated between select adiposity and glucose regulation measurements to determine associations among variables.

Step 1: Linear regression was used to examine all features (p=3272) separately, and to detect annotated metabolites (p=550) associated with BMIz and HOMA-CP (n=206) (SAS proc

genmod). Important associations were with a false discovery rate (FDR) < 0.10 and nominally significant with an unadjusted p-value < 0.05. All models include sex, age, and puberty onset (dichotomous variable) (Model 1), reducing variability between exposures and outcomes, therefore reducing bias. Sex stratified models were run. Additional models were considered adjusting for specific covariates. The metabolome's association with BMIz was adjusted for HOMA-CP (Model 2), MUAMA (Model 3), MUAFA (Model 4), WHtR (Model 5), or SS+TR (Model 6). The metabolome's association with HOMA-CP was adjusted for BMIz (Model 2), MUAMA (Model 3), MUAFA (Model 4), WHtR (Model 5), or SS+TR (Model 6).

Step 2: Subjects were stratified by sex or obese vs. normal weight to compare raw peak intensity of select metabolites and sums of metabolite classes (t-test).

Step 3: Linear regression was used to classify the relationship between energy-adjusted carbohydrate and fat intake (grams) with HOMA-CP and BMIz, adjusting for sex, age, and puberty onset.

Step 4: Annotated metabolites were correlated using Pearson's correlations and clustered using hierarchical clustering. Clusters were defined using a cut-off on the height of the dendrogram and the tightness of the correlations of the metabolites. Defined clusters were required to have an average tightness r>0.2 (Pearson's correlation) and a minimum of 5 metabolites within, resulting in 34 clusters and 110 singleton metabolites without clusters. A cluster score, 'f1', is created by a weighted linear sum of metabolites with weights of factor loadings of metabolites within the cluster.

Step 5: In the path analysis, we identified beta coefficients describing the relationship between (1) energy-adjusted fat and carbohydrate intake (mean 0, std. deviation 1) with metabolome

clusters (β_1) and (2) metabolome clusters with BMIz and standardized HOMA-CP (β_2), adjusting for sex, age, and puberty onset. Our analysis is composed of two parts: (1) a structural part linking the metabolome to BMIz or HOMA-CP through a linear model such as BMIz = $\beta 0 + f1 * \beta 1$ + puberty onset * $\beta 2$ + age * $\beta 3$ + sex * $\beta 4 + e_1$ and (2) a confirmatory factor analysis model via another linear model such as $f1 = \gamma 0 + Fat * \gamma 1$ + puberty onset * $\gamma 2$ + age * $\gamma 3$ + sex* $\gamma 4 + e_2$. All parameters, including loadings, β values and γ parameters are estimated via a maximum likelihood estimation method using the R package "lavaan".

Step 6: Our hypothesis is that a person's intrinsic metabolism, reflected in the metabolome, influences the consequence of macronutrient intake on BMIz and IR. To assess this relationship, we used path analysis (38), a multiple regression technique used to examine causal relationships between variables. The path effect of an independent variable on a dependent variable is expressed as products of regression parameters from the two models. To obtain confidence intervals for the path effect, Sobel testing was used, which is known as being a conservative but widely used approach for assessing the significance of a path (39).

Unless otherwise state, statistical analyses were performed using SAS 9.4 (Cary, North Carolina). Heatmaps were created using an in-house software, CoolMap. Figures were created using GraphPad Prism version 7.4 (La Jolla, California).

Results

Subject Demographics

Anthropometry, metabolic biomarkers, dietary information and background characteristics were compared between girls (n=108) and boys (n=98), revealing sex-specific differences (**Table 4.1**).

We observed a similar distribution of BMI categories and BMIz in girls and boys, with approximately 50% normal weight in both groups. Girls had greater total subcutaneous adiposity (TR+SS) and mid upper arm fat area (MUAFA), while boys had greater mid upper arm muscle area (MUAMA). Boys showed a slightly higher SBP while girls had higher triglyceride and total cholesterol levels as well as higher leptin and IGF-1 levels. More boys were pubertal than girls measured by 'puberty onset' (boys n=48, girls n=35, p=0.0107). Using Pearson's Correlations, clinical and metabolic phenotypes exhibit strong correlations in both boys and girls, including a significant positive correlation between BMIz and HOMA-CP in boys (r=0.41) and girls (r=0.31) (**Figure S4.2**).

Relationship between the Metabolome and BMIz

Linear regression identified metabolites significantly associated with BMIz (**Figure S4.3**). Initially, we demonstrated the relationship between both annotated and unannotated features (p=3272) with BMIz in the entire cohort (**Figure S4.3a**) and sex stratified in boys (**Figure S4.3b**) and girls (**Figure S4.3c**) (Model 1). The analyses highlighted the associations of 66 features with BMIz in the combined dataset, 35 features with BMIz in boys, and 34 features with BMIz in girls (FDR <0.1).

Using 550 annotated features, we created a series of models that classified association between metabolites with BMIz in the entire cohort (**Figure S4.3d**) and sex stratified in boys (**Figure S4.3e**) and girls (**Figure S4.3f**). We reported metabolites significantly associated with BMIz in Model 1, adjusting for sex, age, and puberty onset, in the entire cohort (**Table S4.1**) and sex stratified in boys (**Table S4.2**) and girls (**Table S4.3**). BMIz was associated with 51 annotated metabolites, which were primarily composed of branched chain and aromatic amino acids and

various lipid species, including phospholipids/ceramides, diglycerides (DG) and FA (Model 1). Most of the compounds showed a positive association with BMIz. Dichotomizing the cohort into girls and boys demonstrated sex-specific associations with BMIz (**Figure 4.1**). Most notable associations with BMIz include the positive association with multiple DG species in girls (**Figure 4.1a**) and the positive association with BCAA and their metabolites, isovalerylcarnitine, AC 3:0, AC 4:0 and AC 5:0 OH, in boys (**Figure 4.1b**). BMIz is positively associated with the aromatic amino acid tyrosine in boys (β=0.4361, p=0.002) and girls (β=0.3526, p=0.0007) (Model 1). Of note, DHEA-S is positively associated with BMIz (β=0.3102, p=0.004) (Model 1). DHEA-S changes rapidly in children during adrenarche and in the pubertal period and has been previously found to be correlated with weight and HOMA-IR in children (40).

To determine if the associations between metabolites and BMIz was due to confounding factors, we added a series of variables that correlate with BMIz into the model, considering differences between boys and girls via sex-stratified models (**Table S4.1-3**). With the addition of HOMA-CP, we observed a reduction in the magnitude of association of metabolites with BMIz; however, the majority associations remained significant including the positive association between DGs and phospholipids with BMIz, driven by the girls (Model 2). In boys, the relationship between BCAA and their metabolites and BMIz was reduced with the addition of HOMA-CP (Model 2) and MUAMA (Model 3), suggesting that BCAAs may be related to IR and muscle mass. With the addition MUAFA (Model 4), WHtR (Model 5), and TR+SS (Model 6) into the model, we observe large shifts in beta coefficients of the metabolite-BMIz relationship overall and in both sexes, with most of metabolite associations becoming non-significant, though nominal p-values were still significant for many DGs in girls. This would suggest that both central and

subcutaneous adipose tissue are driving the majority of the associations observed between BMIz and metabolite levels in plasma.

Of interest, adults with obesity have elevated fasting non-esterified FA levels (41), however in adolescents, the results are contradictory finding no associations between FA with BMIz or IR (10,11). Some studies have observed that overweight adolescents have higher levels of saturated FA and lower levels of polyunsaturated FA in comparison to lean adolescents (42). In our cohort, we observed very few significant associations between individual FA and BMIz in adolescents (Model 1). Using a sum of the peak intensities of the 55 detected fatty acids, there was a trend towards elevated FA in obese children ($p=0.0717$), but no difference between boys and girls ($p=0.8662$) (**Figure S4.4a-b**). Therefore, we explored how BMIz relates to FA chain length and number of double bonds within FA with a chain length of ≥14 carbons. Beta coefficients from the fatty acid-BMIz relationship (Model 1) were plotted vs. FA chain length (**Figure 4.2a**) and number of double bonds (**Figure 4.2b**). Distinct patterns were observed between boys and girls. There was an inverse association between BMIz and FA chain length in boys ($r^2=0.5568$, $p<0.0001$) that was not observed in girls ($r^2=0.00638$, $p=0.5621$) (**Figure 4.2a**). There was no trend between the number of double bond and BMIz in boys ($r^2=0.02262$, $p=0.2731$), however an inverse relationship was observed in girls ($r^2=0.1810$, $p=0.0012$) (**Figure 4.2b**). The majority of FA beta coefficients in girls are positively associated with BMIz, suggesting that in girls the total FA burden is higher.

The untargeted metabolomics platform used has an extraction solvent without chloroform and a hard ionization method, leading to the inability to accurately detect triglycerides. However, DGs are highly correlated with TG levels in plasma. In our analysis, the sum peak intensities of the 19 annotated DGs was positively correlated with clinical triglycerides ($r=0.697128$, $p<0.0001$).

Total DGs were significantly elevated in obese adolescents (p=0.000154) (**Figure S4.4c**) and trended towards being elevated in girls (p=0.0597) (**Figure S4.4d**).

Relationship between the Metabolome and Insulin Resistance

Despite the positive relationship between BMIz and HOMA-CP (**Figure S4.2**), there was minimal impact of adjustment for HOMA-CP on metabolite levels associated with BMIz (Model 2, **Table S4.1-3**). Therefore, we used linear models to assess whether we could identify metabolites associated with HOMA-CP (**Figure S4.5**). We demonstrated the relationship between both annotated and unannotated features (p=3272) with HOMA-CP in the entire cohort (**Figure S4.5a**) and sex stratified in boys (**Figure S4.5b**) and girls (**Figure S4.5c**) (Model 1). This analysis highlighted the associations of 63 features with HOMA-CP in the combined dataset, 64 features with HOMA-CP in boys and 23 features with HOMA-CP in girls (FDR <0.1).

Using 550 annotated features, we created a series of models that classified association between metabolites with HOMA-CP in the entire cohort (**Figure S4.5d**) and sex stratified in boys (**Figure S4.5e**) and girls (**Figure S4.5f**). We reported metabolites significantly associated with HOMA-CP in Model 1, adjusting for sex, age, and puberty onset, in the entire cohort (**Table S4.4**) and sex stratified in boys (**Table S4.5**) and girls (**Table S4.6**). In the entire cohort, HOMA-CP was associated with 40 annotated metabolites, including positive associations with glucose, tyrosine, proline, multiple DGs, and bile acids; along with inverse associations with n-acetylglycine and fatty acid metabolism intermediates, such as short- and medium-chain AC and DIC-FA (Model 1) (**Table S4.4**). There were 11 metabolites that overlapped with those associated with BMIz, consisting of mainly diglycerides (DG 32:0, DG 34:0, DG 30:1, DG 32:1,

DG 34:1, DG 36:1, DG 32:2, and DG 34:3), along with n-acetylglycine, tyrosine, and DHEA-S (Model 1) (**Table S4.1, Table S4.4**). Adding BMIz into the model greatly reduces the associations between DGs and HOMA-CP, especially in the boys (Model 2). The remaining metabolite associations with HOMA-CP, such as n-acetylglycine, proline, bile acids and fatty acid metabolism intermediates, remained significant in the whole group, largely driven by the boys (Model 2). Similar patterns were observed after adjustment for muscle mass (MUAMA) as well as subcutaneous and central fat distribution (MUAFA, WHtR and TR+SS) (Models 3-6).

The inverse relationship between AC and HOMA-CP, adjusting for sex, puberty onset and age, is represented in **Figure 4.3**. Stratifying by sex reduced the number of significant associations, however most beta coefficients remained stable. Adjustments for muscle mass or fat mass did not eliminate the associations, suggesting an intrinsic factor other than weight or body composition drives this association (**Table S4.4-6**). The inverse association became stronger after adjustment for BMIz, primarily in males (Model 2).

Path Analysis Highlighting the Relationship between Macronutrient Intake, the Metabolome, BMIz, and Insulin Resistance

Previous results have been inconsistent when describing a relationship between habitual macronutrient intake and metabolic health in children. In our cohort, energy-adjusted carbohydrate and fat intake were not linearly related to BMIz or HOMA-CP, when adjusting for sex, age, and puberty onset (Path 1, **Table S4.7**). Conducting a path analysis, we assessed how macronutrient intake is reflected in the metabolome, which is associated with obesity and insulin resistance and calculated confidence intervals using Sobel Testing (Path 2, **Figure 4.4**). Due to biological constraints on metabolism, many metabolites are highly correlated. We took

advantage of this to collapse groups of highly correlated metabolites, using weighted sums for each group as a singular value, allowing an increase in power to identify potential causal paths. Individual annotated metabolites were grouped using hierarchical clustering prior to assessing the significance of a path of interest (**Figure 4.5**). We identified 34 clusters and 110 singleton metabolites (described in methods); clusters are classified based on their content metabolites (**Table S4.8**).

Although sex-specific relationships were observed between the metabolome with BMIz and HOMA-CP (**Table S4.2-3, Table S4.5-6**), the majority of beta coefficients were in the same direction in boys and girls, with the relationship between DGs and BMIz emphasized among girls and the relationship between amino acids and BMIz emphasized among boys. Therefore, we will present the following analyses with sex as a covariate, rather than stratifying by boys and girls.

The path analysis identified metabolome clusters associated with the nutrient intake (β_1) and the outcomes (β_2), BMIz (**Table S4.9**) and HOMA-CP (**Table S4.10**), adjusting for sex, age and puberty onset. Seven metabolite clusters were significantly associated with nutrient intake, all revealing positive associations with fat intake and inverse associations with carbohydrate intake (β_1, **Table S4.9-10**), reflecting the inverse relationship we observe between fat and carbohydrate intake. The clusters were composed of BCAAs and their metabolites (Cluster 16), medium-chain hydroxyl-DiC-FA (Clusters 13, 14, and 15), long-chain DiC-FA (Cluster 26), long-chain hydroxyl-DiC-FA (Cluster 14) and medium-chain AC (Cluster 25).

From the seven clusters that are significantly related to macronutrient intake, three of the clusters are associated with HOMA-CP (β_2, **Table S4.10**). Medium-chain ACs (Cluster 25) (-

0.833±0.240, p=0.001), intermediates of β-oxidation, and long-chain DiC-FA (Cluster 26) (-0.383±0.141, p=0.006), intermediates of alpha-oxidation, are inversely related to HOMA-CP. Medium-chain DiC-FA (Cluster 15) (0.361±0.169, p=0.033), intermediates of omega-oxidation, are positively associated with HOMA-CP. These results suggest that intermediates of fatty acid oxidation have differing influences on HOMA-CP dependent on the location of oxidation. None of the seven clusters that are significantly related to macronutrient intake are associated with BMIz (β_2, **Table S4.9**). Additional associations between metabolome clusters with BMIz and HOMA-CP confirmed our reported results using individual metabolites (β_2, **Table S4.9-10**).

Using Sobel tests, we assessed the significance of the causal path of interest. Carbohydrate intake is positively associated with HOMA-CP through decreases in the levels of medium-chain ACs (Cluster 25) (p=0.015) (**Table S4.10**). Fat intake is inversely associated with HOMA-CP through decreases in the levels of medium-chain ACs (p=0.010) (**Table S4.10**), supporting a protection from becoming insulin resistant is the ability to increase FA oxidation flux through the mitochondria. The pathway of macronutrient intake's influence on HOMA-CP through medium-chain DiC-FA (Cluster 15) and long-chain DiC-FA (Cluster 26) were marginally significant (**Table S4.10**). No pathways linking macronutrient intake to BMIz through metabolome clusters reached significance by Sobel tests (**Table S4.9**).

Discussion

In this cross-sectional analysis using untargeted metabolomics, we quantified the relationship between the metabolome with BMIz and IR among 108 girls and 98 boys, focusing on sex-differences in metabolism. Our findings confirm and extend previous results, emphasizing sex-specific differences due to variations in muscle and fat tissue accumulation in puberty. Using

path analyses, we support our hypothesis that person's intrinsic metabolism, reflected in the metabolome, influences the consequence of macronutrient intake on IR.

Our results revealed a positive relationship between diglycerides and BMIz, driven by the girls, that was independent of IR and lean mass (Model 2-3), but dependent on adipose mass (Models 4-6). DGs are building blocks in triglycerides and phospholipid biosynthesis and elevated levels likely reflect increased de novo lipogenesis in adipose tissue and the liver. DGs can serve as intracellular secondary messengers and my activate intracellular pathways leading to IR, defective mitochondrial activity, and endoplasmic reticulum stress (43). However, the relationship between DG levels and HOMA-CP was not evident once we adjusted for BMIz, suggesting that at least at the plasma level in children, they not contributing directly to IR.

Plasma FAs were trending towards being elevated in obese compared to normal weight adolescents however, very few individual FAs were associated with BMIz. In the fasting state, plasma FA levels are a balance between lipolysis of triglycerides within the adipocytes and oxidation of FA. In adults with obesity, plasma FA levels are elevated due to an increase in lipolysis as adipose tissue becomes resistant to insulin action (44). This dynamic is suggested to differ in pubertal adolescents with elevated BMIz (11) due to increased growth hormones (i.e. IGF-1) (45). Increased levels of IGF-1 during puberty, as observed in our cohort (Table S4.11), is associated with IR and an increase in lipolysis, as well as an increase in lipid oxidation (46,47). The ability to increase lipid oxidation during puberty, potentially to sustain energy requirements during growth, may explain why plasma FA levels were not increased with BMIz. We noted a relationship between BMIz with the number of double bonds and the chain length of FAs in boys, supporting the importance of composition of FAs in their association with obesity

(42). Finally, we did not detect any associations of DGs or FAs with dietary macronutrient intake and either IR or obesity in our path analyses.

Previous metabolomics analyses in adolescents have found tyrosine, phenylalanine, and BCAAs are consistently associated with obesity (3–5). In our cohort, we observed positive associations between BCAAs and their degradation products with BMIz, primarily in boys. Our results suggest that BCAAs are in part related to IR and lean mass, as adding HOMA-CP and MUAMA into the model reduced but did not eliminate these associations. Studies in lean adolescents suggest that proteolysis and protein oxidation appear to be reduced during puberty, relative to pre-puberty, which may be also a result of increases in IGF-1 (48). Reduced BCAA catabolism in adipose tissue and skeletal muscle in obesity and IR can result in elevation of plasma BCAA levels (49). Elevations of BCAA may be more apparent in boys due to their increased muscle mass and a relative inability to suppress proteolysis due to IR.

The production of AC is due to an imbalance of entry of acyl-CoAs into the mitochondria and FAO rates, the latter determined by ATP need. Thus, at any ambient supply of FA, lower levels of MC- and LC-AC can be due to either a reduced uptake of acyl-CoAs into the mitochondria, for instance in the presence of elevated malonyl-CoA levels (50), or increased β-oxidation (51). In adults, obesity and IR are characterized by oversupply of FA to the mitochondria and incomplete FAO with increases in AC intermediates (52) and incompletely oxidized FA (50,53). In our study, we observed that MC-ACs (6-14 carbons) are inversely associated with HOMA-CP, independent of muscle mass and BMIz, in both sexes. Previous studies have found similar results (6,8). Mihalik et al. observed decreases in MC-AC species in youth with obesity or T2D compared with normal weight, with no change in LC-AC (6) and proposed that IR in adolescents was associated with enhanced mitochondrial oxidation rather than reduced utilization.

Path analysis demonstrated positive associations between carbohydrate intake and HOMA-CP through decreased MC-AC, with the opposite trend found for dietary fat. These results may suggest that adolescents prone to IR have an increase in selection of carbohydrates for fuel, exacerbated by elevated habitual carbohydrate consumption. Under these conditions, elevated malonyl-CoA would reduce uptake of FA into the mitochondria leading to lipid accumulation in the cytosol, increasing FA metabolites that contribute to IR (54). Habitual fat intake is approaching a positive association with HOMA-CP through increased MC DiC-FA, which are formed from omega-oxidation in the endoplasmic reticulum (55). Our findings may reflect an intrinsic difference in fuel selection by mitochondria related to IR. If insulin resistant individuals do have a relative intrinsic selection for carbohydrate oxidation, a higher dietary fat intake could lead to increases in extra-mitochondrial FAO.

These findings in young, non-diabetic individuals are reminiscent of reduced metabolic flexibility seen in insulin resistant individuals in the setting of obesity where tissues have reduced capacity to alter fuel selection in the face of changes in nutrient supply (56). We do not have respiratory quotient (RQ) measures in the children in this study, which could be used to test the hypothesis of relative differences in fuel utilization. However, Kim et al. (57) has shown that girls with IR associated with polycystic ovarian disease have significantly higher RQ in the fasting state, indicating higher carbohydrate oxidation, which was independent of adiposity and hormone levels. Future studies assessing RQ, metabolite patterns, and response of children to different diets will be needed to test this hypothesis. Additionally, future studies will assess the relationship between cardiorespiratory fitness (oxidative capacity) and fuel selection in children with a varying degree of IR. Previous analyses in humans (58) and animals (59) with higher oxidative capacity show a relative selection of fatty acids and a relative resistance to obesity

(60). In addition, adults with low oxidative capacity have a metabolite profile that is more similar to individuals who have a higher risk of type 2 diabetes (61).

Conclusion

In summary, our study highlights that intrinsic metabolism, in particular the relative ability to oxidize lipid in the mitochondria, may influence the consequence of nutrient intake on metabolic health. Strengths include the availability of a wealth of data in the ELEMENT cohort allowing for the incorporation of anthropometry measurements, metabolic biomarkers, puberty measures, and dietary intake and the use of comprehensive metabolomics methodology assessing both annotated and unannotated features and confirming using hierarchical clustering. The use of path analysis created a strong statistical platform to begin to understand mechanisms describing this relationship.

Despite the strengths of this study, this work is cross sectional therefore causality cannot be confirmed. We are limited by the number of subjects within this study (n=206), acknowledging that stratifying by sex reduces power. Though within this cohort there was a strong correlation between C-peptide and insulin levels, we assess IR using HOMA-CP, due to the large number of subjects (n=86) with plasma insulin levels below the limit of detection. This suggests some caution in interpretation of insulin resistance. In addition, a large number of unannotated metabolites, generated from untargeted metabolomics, were identified to be associated with BMIz and HOMA-CP. These metabolites, once identified may alter or modify the conclusions in the present study.

Authorship

Jennifer L. LaBarre, Karen E. Peterson, Maureen T. Kachman, Wei Perng, Lu Tang, Wei Hao, Ling Zhou, Alla Karnovsky, Alejandra Cantoral, Martha María Téllez-Rojo, Peter XK Song, and Charles F. Burant

Acknowledgements

We would like to thank the research staff at participating hospitals and the American British Cowdray Hospital in Mexico City for providing research facilities.

Funding Support

This work was supported by the following grants: P20 ES018171 (KEP) and P01 ES022844 (KEP) from the National Institute for Environmental Health Sciences; RD83543601 (KEP) from the US Environmental Protection Agency; R24 DK097153 (CFB), P30 DK089503 (CFB), U24 DK097153 (CFB) from the National Institutes of Health and the Taubman Institute of the University of Michigan (CFB).

Figure S4.1. Relationship between insulin and C-peptide at baseline.

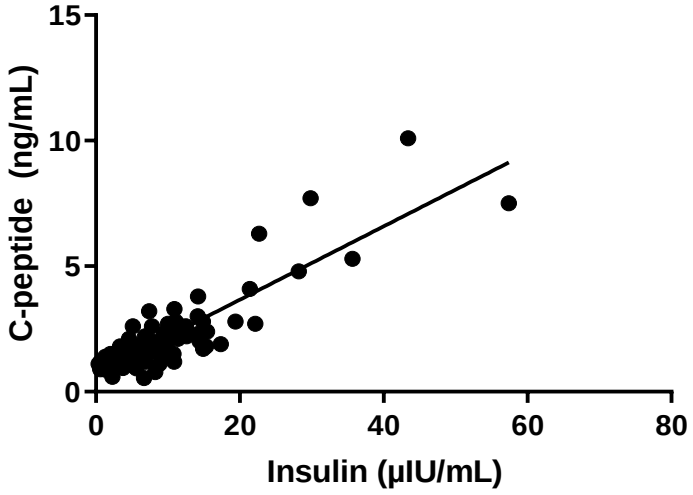

Linear trendline describing relationship (n=120, linear trendline y=0.1461x+0.7379, r^2 = 0.7689, p<0.0001)

Table 4.1. Characteristics of the ELEMENT participants, stratified by sex (n=206). Values are n(%) or mean±SD. [A]Represents Pearson's chi-square test for categorical variables. [B]Represents paired t-test for continuous variables. If sample size differs, mean±SD (n).

Categorical Variables	Boys n(%)	Girls n(%)	p-value[A]
BMI Categories			
Underweight	1 (1.0)	2 (1.9)	0.8859
Lean	47 (48.0)	53 (49.1)	
Overweight	33 (33.7)	32 (29.6)	
Obese	17 (17.3)	21 (19.4)	
Pubic Hair Tanner Stage			
1	80 (83.3)	84 (77.8)	0.7782
2	12 (12.5)	18 (16.7)	
3	3 (3.2)	5 (4.6)	
4	1 (1.0)	1 (0.9)	
5	0 (0.0)	0 (0.0)	
Puberty Onset			
Yes	48 (50.0)	35 (32.4)	0.0107
No	48 (50.0)	73 (67.6)	
Continuous Variables	Boys mean±SD	Girls mean±SD	p-value[B]
Age	10.4±1.6	10.1±1.6	0.3781
Anthropometry			
Weight (kg)	37.8±10.0	37.4±10.0	0.8076
Height (cm)	139.4±10.6	138.3±10.6	0.4368
BMI	19.2±3.2	19.3±3.5	0.7111
BMI z-score	0.91±1.22	0.78±1.28	0.4718
WC (cm)	69.9±9.9	70.7±10.2	0.5752
TR + SS (mm)	25.1±11.1	30.1±11.4	0.0019
SS/TR	0.74±0.22	0.72±0.21	0.6112
MUAMA (mm^2)	26.5±6.9	24.0±6.3	0.0079
MUAFA (mm^2)	15.0±7.1	17.6±7.3	0.0082
WHtR	0.50±0.06	0.51±0.07	0.2639
Metabolic Biomarkers			
SBP (mmHg)	104±10	101±10	0.0177
DBP (mmHg)	65±7	65±7	0.8565
C-peptide (ng/mL)	1.6±1.1	1.8±1.3	0.104
Glucose (mg/dL)	87.8±8.0	87.0±10.2	0.5252
Leptin (ng/mL)	8.4±6.6	13.3±9.3	<0.0001
IGF-1 (ng/mL)	231.9±95.5	271.7±101.3	0.0042
Total Cholesterol (mg/dL)	152.6±27.7	160.7±25.7	0.0314
HDL (mg/dL)	60.0±12.1	57.4±12.2	0.1179
Triglycerides (mg/dL)	78.4±37.0	98.3±47.5	0.0009
LDL (mg/dL)	76.9±23.6	83.6±20.7	0.0301
HOMA-CP	1.9±1.4	2.3±2.3	0.132
Dietary Information (energy adjusted)			

Calories (kcal)	2801±837	2497±842	0.0102
Protein (g)	75.9±11.0	77.0±9.7	0.4442
Carbohydrates (g)	345.3±40.7	341.3±31.4	0.4294
Sugar (g)	54.2±41.3	52.8±41.7	0.8081
Fat (g)	94.2±14.0	95.8±10.8	0.3567
Saturated Fat (g)	28.4±9.2	31.1±10.0	0.041
Monounsaturated Fat (g)	24.4±5.4	25.0±4.9	0.4186
Polyunsaturated Fat (g)	15.6±4.4	15.2±4.3	0.5933
Cholesterol (mg)	291.2±88.0	293.5±102.6	0.8587
Fiber (g)	19.5±6.6	20.4±6.8	0.3207

Figure S4.2. Clinical phenotypes and metabolic biomarkers exhibit strong correlations, sex-stratified.

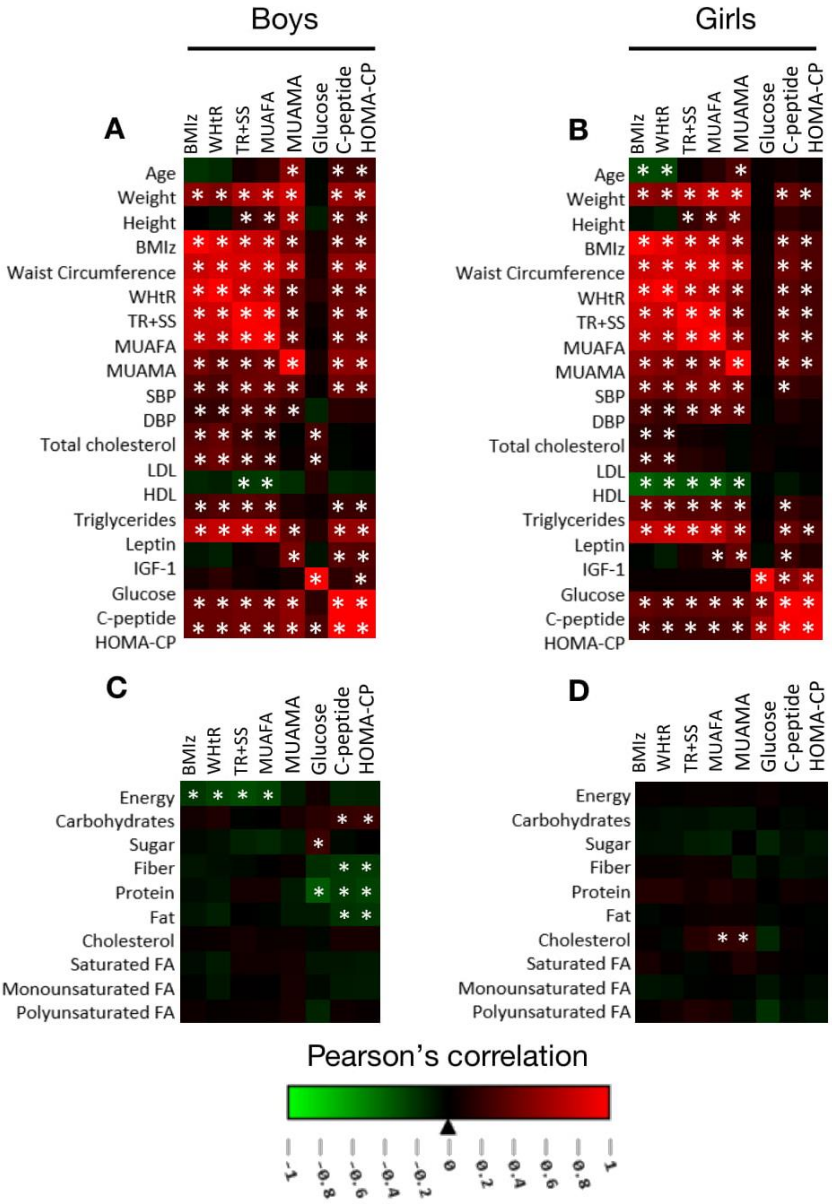

Pearson correlations identified connectivity between adiposity and metabolic biomarkers in **(A)** boys (n=98) and **(B)** girls (n=108) and connectivity between adiposity, metabolic biomarkers, and energy-adjusted dietary macronutrients in **(C)** boys and **(D)** girls. Positive correlation in red and negative correlations in green. Nominal significance denoted with (*) (α=0.05).

Figure S4.3. Association of metabolite features with BMIz, within the entire cohort and sex-stratified.

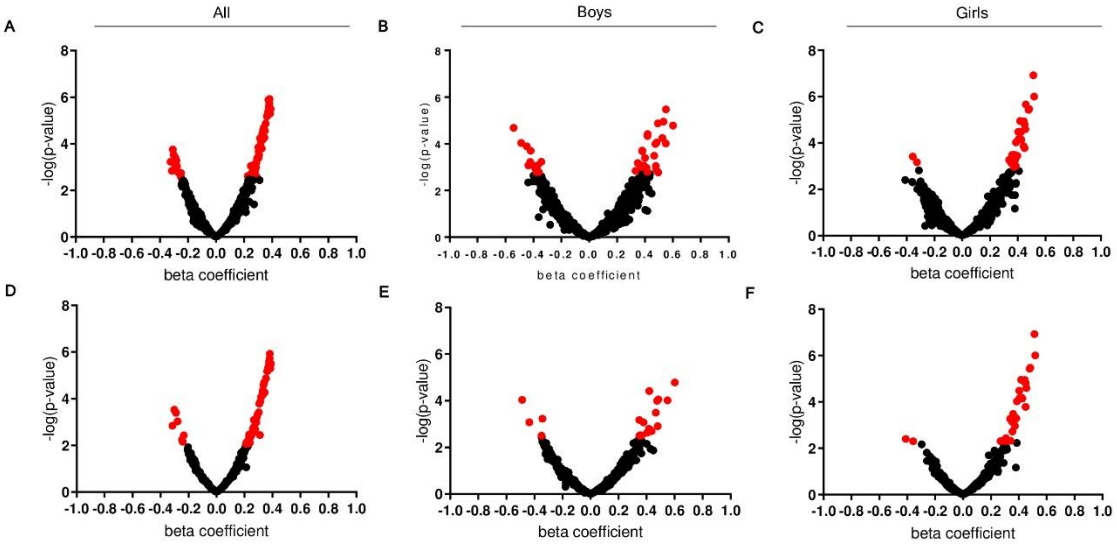

Beta coefficients from linear models are plotted on the x-axis and negative log transformed p-values are plotted on the y-axis. Association between BMIz and both annotated and unannotated features (p=3272) **(A)** within entire cohort (n=206), accounting for age, sex, and puberty onset, and sex stratified in **(B)** boys and **(C)** girls, accounting for age and puberty onset (Model 1). Using solely annotated metabolites (p=550), representing the relationship between metabolites and BMIz **(D)** within the entire cohort and sex stratified in **(E)** boys and **(F)** girls (Model 1). Features in red indicate significant associations after FDR correction (FDR<0.10).

Table S4.1. Association between annotated metabolites and BMIz (n=206). Regression models identifying annotated metabolites (p=550) linearly associated with BMIz. All models were adjusted for sex, age, and puberty onset (Model 1), along with additional phenotypic measures to identify metabolites that drive the association with BMIz including HOMA-CP (Model 2), MUAMA (Model 3), MUAFA (Model 4), WHtR (Model 5) and TR+SS (Model 6). Values reported are β±Std Error. Metabolites with FDR<0.10 highlighted in red and bolded. Metabolites listed have an FDR<0.10 in Model 1 in the combined model and/or the sex-stratified models.

Metabolite	Model 1	Model 2	Model 3	Model 4	Model 5	Model 6
N-acetylglycine	**-0.2456±0.0889**	-0.1135±0.0871	-0.0952±0.0643	0.0061±0.0489	0.041±0.0393	0.0238±0.0487
isovalerylcarnitine	**0.3198±0.0812**	**0.2565±0.0767**	**0.1866±0.0586**	0.0448±0.0459	0.0543±0.0365	0.0288±0.0458
isoleucine	**0.3132±0.082**	**0.2724±0.0765**	**0.1945±0.0588**	0.0328±0.0463	0.004±0.0373	0.0539±0.0456
leucine	0.1858±0.082	0.1479±0.0764	0.0775±0.0587	0.0778±0.0436	0.0773±0.0348	0.0604±0.0435
valine	**0.2612±0.0839**	0.2101±0.0786	0.1438±0.0602	0.0362±0.0462	0.049±0.0368	0.0317±0.0459
phenylalanine	**0.2426±0.0854**	0.1842±0.0801	0.1218±0.0612	0.0486±0.0464	0.0245±0.0374	0.047±0.0461
tyrosine	**0.3852±0.0844**	**0.2863±0.082**	**0.207±0.0621**	0.0906±0.0481	0.032±0.0392	0.0559±0.0485
5-methylthioadenosine	**0.3025±0.0852**	**0.2274±0.0808**	0.1305±0.0623	0.0451±0.0475	0.0146±0.0382	0.0533±0.047
D-ornithine	**0.2128±0.0802**	0.1919±0.0743	0.0939±0.0576	0.0916±0.0427	0.0164±0.035	0.1117±0.0421
L-ornithine	**0.2157±0.0803**	0.1924±0.0745	0.0856±0.0579	0.0932±0.0428	0.0194±0.035	0.1202±0.042
normethanephrine	**0.2427±0.0853**	0.1843±0.0801	0.1218±0.0612	0.0487±0.0464	0.0246±0.0374	0.047±0.0461
D-lyxose	**-0.3152±0.0989**	**-0.3443±0.0907**	**-0.2506±0.0692**	-0.0168±0.0549	0.0176±0.0441	-0.0035±0.0546
5-phospho-alpha-D-ribose-1-diphosphate	**0.2397±0.0899**	0.1979±0.0838	0.0904±0.0649	0.0393±0.0488	0.0577±0.0388	0.0252±0.0486
Cer t36:0(2OH)	**0.3344±0.0837**	**0.3219±0.0772**	**0.2388±0.0593**	0.0001±0.0482	0.0361±0.038	-0.0177±0.0481
PE-Cer d36:1	0.1726±0.0828	0.0971±0.0782	0.129±0.0582	-0.0664±0.045	-0.0207±0.0358	-0.0411±0.0445
PE-Cer d32:3	**0.2347±0.0801**	0.1768±0.0753	**0.1812±0.0562**	-0.0254±0.0445	0.0344±0.035	-0.0085±0.044
PE-Cer d34:3	0.1291±0.0837	0.0884±0.0779	0.1253±0.0586	-0.0589±0.0448	0.0135±0.0357	-0.0314±0.0444
DG 32:0	**0.3822±0.0787**	**0.2757±0.0778**	**0.2117±0.058**	0.05±0.0462	0.0485±0.0368	0.0588±0.0457
DG 34:0	**0.3623±0.0804**	**0.2646±0.0784**	**0.2122±0.0585**	0.0508±0.0465	0.0362±0.0372	0.0599±0.0459
DG 30:1	**0.3299±0.0816**	**0.2388±0.0787**	**0.2023±0.0587**	0.0627±0.046	0.0901±0.0361	0.0671±0.0456
DG 32:1	**0.368±0.0804**	**0.275±0.078**	**0.2349±0.0579**	0.0419±0.0468	0.0747±0.0366	0.049±0.0463

DG 33:1	**0.3317±0.0812**	**0.2585±0.0773**	**0.2361±0.0575**	0.0068±0.0468	0.0754±0.0363	0.0043±0.0465
DG 34:1	**0.3759±0.0799**	**0.2887±0.0772**	**0.211±0.0586**	0.0458±0.0467	0.0784±0.0365	0.0571±0.0461
DG 35:1	**0.3059±0.0812**	**0.2358±0.077**	**0.1743±0.0586**	0.0498±0.0455	0.0557±0.0362	0.0537±0.0451
DG 36:1	**0.3543±0.0814**	**0.2635±0.0787**	0.1546±0.0608	0.0618±0.0465	0.0525±0.0372	0.0729±0.0459
DG 32:2	**0.3805±0.0799**	**0.3004±0.0767**	**0.2359±0.0579**	0.0358±0.047	0.0944±0.0363	0.0494±0.0464
DG 34:2	**0.3365±0.08**	**0.2673±0.076**	**0.2055±0.0577**	0.0087±0.0464	0.0814±0.0358	0.0203±0.0458
DG 35:2	**0.3893±0.0836**	**0.3195±0.0793**	**0.24±0.0605**	0.0469±0.0488	0.0929±0.0379	0.0547±0.0482
DG 34:3	**0.3405±0.0799**	**0.2641±0.0763**	**0.2143±0.0575**	-0.0146±0.0468	0.0787±0.0359	0.0107±0.046
DG 35:3	**0.3738±0.0809**	**0.3275±0.0757**	**0.2543±0.0578**	0.0327±0.0474	0.072±0.037	0.0358±0.0469
DG 36:3	**0.2625±0.0859**	**0.221±0.0801**	0.1599±0.0612	0.0006±0.0476	0.079±0.0371	0.0374±0.0468
DG 36:4	**0.2937±0.084**	**0.2532±0.0783**	**0.1874±0.0599**	0.0549±0.0466	0.0944±0.0365	0.0801±0.0458
DG 38:4	0.2034±0.0851	0.1836±0.0788	0.1183±0.0604	0.0069±0.0462	0.0391±0.0367	0.0321±0.0456
DG 36:5	0.175±0.0834	0.1414±0.0775	0.1088±0.059	-0.0738±0.0453	0.0577±0.0355	-0.0365±0.0448
DG 38:5	**0.2569±0.0865**	0.1853±0.0817	0.1393±0.062	-0.0042±0.0479	0.0558±0.0376	0.0045±0.0474
FA 17:0	**0.2131±0.0814**	0.1952±0.0753	0.1449±0.0575	0.0316±0.0442	0.0379±0.0353	0.0276±0.0439
FA 18:3	**0.2339±0.081**	**0.2231±0.0748**	**0.1636±0.0572**	-0.005±0.0447	0.0336±0.0354	0.0145±0.0442
AC 3:0	**0.2506±0.0859**	0.1874±0.0808	0.1709±0.0608	0.0699±0.0465	0.0168±0.0378	0.088±0.0459
AC 4:0	**0.2597±0.0867**	**0.2489±0.08**	0.0723±0.0635	0.0653±0.0471	0.045±0.0379	0.0653±0.0468
AC 8:1	**0.345±0.0854**	**0.3466±0.0784**	**0.2003±0.0617**	-0.0096±0.0494	0.0207±0.039	-0.0055±0.0489
AC 5:0 (OH)	**0.2855±0.087**	**0.2448±0.081**	0.1742±0.0621	0.1145±0.0468	0.058±0.0382	0.1076±0.0466
FA 8:1 (DiC)	0.1873±0.0861	0.1487±0.0802	0.0233±0.0624	0.05±0.0461	0.0556±0.0368	0.0562±0.0456
FA 9:1 (DiC)	**0.2294±0.0828**	0.1825±0.0774	0.049±0.0606	0.1001±0.0442	0.0858±0.0354	0.0943±0.0439
FA 12:1 (DiC)	**-0.2344±0.0808**	-0.1672±0.0764	-0.1331±0.0577	-0.0044±0.0446	0.0238±0.0358	-0.0003±0.0443
FA 28:2 (DiC)	-0.1725±0.0864	-0.1779±0.0797	-0.0808±0.0614	-0.1118±0.0453	-0.0309±0.037	-0.0727±0.0454
SN-glycero-3-phosphocholine	0.2019±0.084	0.199±0.0775	0.0581±0.0607	0.0605±0.045	0.0404±0.0362	0.0961±0.0442
PC 34:0/PE 37:0	-0.2026±0.0831	-0.1622±0.0775	-0.0952±0.0595	-0.0939±0.0441	-0.0671±0.0355	-0.0694±0.0441
PC 40:4/PE 43:4	**0.2333±0.084**	**0.2222±0.0777**	**0.1808±0.059**	0.0027±0.0462	-0.006±0.037	-0.0211±0.046
PC 31:5/PE 34:5	**0.2675±0.0798**	**0.2083±0.0752**	0.1148±0.0582	0.024±0.0445	0.0752±0.0348	0.0524±0.0437
PC 35:5/PE 38:5	**-0.3013±0.0832**	**-0.2589±0.0777**	-0.1348±0.0609	-0.1009±0.0455	-0.0573±0.0369	-0.0931±0.0453
PE 36:2	**0.2786±0.0845**	**0.2198±0.0795**	0.1431±0.061	0.0205±0.047	0.0691±0.0369	0.0412±0.0464

PS 35:4	**0.2429±0.0832**	0.1717±0.0787	**0.1682±0.0588**	0.0201±0.0457	0.0191±0.0365	0.0043±0.0455
PS 40:4	**-0.2421±0.0897**	-0.1936±0.0837	-0.0814±0.065	-0.0309±0.0488	-0.0634±0.0387	-0.0458±0.0483
PS 42:6	**-0.2779±0.0839**	**-0.2335±0.0784**	-0.1004±0.0616	-0.0753±0.0459	-0.0372±0.0371	-0.093±0.0452
PS 39:7	-0.1555±0.0862	-0.155±0.0796	-0.1432±0.0603	-0.0712±0.0456	-0.0454±0.0367	-0.0247±0.0457
LysoPC 14:0	0.2105±0.0843	0.1276±0.0801	0.116±0.06	0.0085±0.0459	0.0717±0.036	0.0385±0.0452
norhyodeoxycholic acid	0.1515±0.0833	0.1057±0.0778	0.1129±0.0586	0.046±0.0443	0.0483±0.0354	-0.0073±0.0444
SM d36:2	**0.2288±0.0843**	**0.2121±0.078**	**0.1854±0.0591**	-0.0516±0.0467	0.0436±0.0366	-0.0373±0.0462
DHEA sulfate	**0.3102±0.1066**	0.1984±0.1018	0.1064±0.0776	0.0354±0.0584	0.0577±0.0465	0.0512±0.0578
cortisone	**-0.2898±0.0819**	**-0.2819±0.0755**	-0.1509±0.0592	-0.0333±0.0458	0.0143±0.037	-0.0349±0.0454
urate	**0.2769±0.0898**	0.2057±0.0848	0.1038±0.0655	0.0442±0.0493	0.0353±0.0395	0.0326±0.0491
dipeptide (glutamate-phenylalanine)	**0.2669±0.0848**	**0.2382±0.0787**	0.1599±0.0606	0.0729±0.0462	-0.0608±0.038	0.048±0.0462
dipeptide (histidine-tyrosine)	**0.2307±0.0873**	0.1836±0.0815	0.044±0.0638	0.1062±0.0464	0.0315±0.0379	0.1016±0.0461
L-gamma-glutamyl-L-isoleucine	**0.2867±0.0841**	**0.2436±0.0785**	0.1431±0.0609	0.0736±0.0461	0.0592±0.037	0.0877±0.0455

Table S4.2. Association between annotated metabolites and BMIz in boys (n=98). Sex-stratified regression models identifying annotated metabolites (p=550) linearly associated with BMIz. All models were adjusted for age and puberty onset (Model 1), along with additional phenotypic measures to identify metabolites that drive the association with BMIz including HOMA-CP (Model 2), MUAMA (Model 3), MUAFA (Model 4), WHtR (Model 5) and TR+SS (Model 6). Values reported are β±Std Error. Metabolites with FDR<0.10 highlighted in red and bolded. Metabolites listed have an FDR<0.10 in Model 1 in the combined model and/or the sex-stratified models.

Metabolite	Model 1	Model 2	Model 3	Model 4	Model 5	Model 6
N-acetylglycine	-0.1413±0.123	-0.0142±0.1114	-0.0252±0.0873	0.0384±0.0673	0.0781±0.0557	0.0301±0.0667
isovalerylcarnitine	**0.3499±0.1185**	0.2347±0.1087	0.2136±0.0849	0.0295±0.0699	0.0952±0.0559	0.0093±0.0698
isoleucine	**0.4195±0.1019**	**0.3175±0.0942**	0.2334±0.0763	0.0346±0.0655	0.0309±0.0537	0.0525±0.0642
leucine	**0.3478±0.1022**	0.2342±0.0952	0.1961±0.0747	0.0482±0.0615	0.115±0.0484	0.0564±0.0607
valine	**0.3634±0.1229**	0.2164±0.1149	0.2323±0.0876	0.0238±0.0727	0.1154±0.0575	0.0117±0.0724
phenylalanine	0.4285±0.1696	0.3005±0.1528	0.2678±0.1204	-0.0602±0.0994	0.0614±0.0801	-0.0425±0.0983
tyrosine	**0.4361±0.1412**	0.1509±0.1451	0.1965±0.1047	0.086±0.0826	0.03±0.0694	0.0619±0.0826
5-methylthioadenosine	**0.549±0.1407**	0.3859±0.1323	**0.3513±0.1019**	0.0607±0.0883	0.0691±0.0721	0.047±0.088
D-ornithine	0.2173±0.1143	0.1916±0.1004	0.1586±0.0799	0.1114±0.0618	0.0351±0.0525	0.1483±0.0602
L-ornithine	0.2224±0.1155	0.2105±0.1011	0.1601±0.0808	0.112±0.0625	0.033±0.0532	0.1523±0.0608
normethanephrine	0.4286±0.1696	0.3005±0.1529	0.2678±0.1204	-0.0603±0.0994	0.0614±0.0801	-0.0425±0.0983
D-lyxose	-0.2221±0.1386	-0.2741±0.1204	-0.17±0.0967	-0.0285±0.0763	-0.0006±0.0635	-0.0774±0.0748
5-phospho-alpha-D-ribose-1-diphosphate	0.1172±0.135	0.059±0.1193	0.0548±0.0947	-0.1059±0.0733	-0.011±0.0606	-0.0924±0.0727
Cer t36:0(2OH)	0.2584±0.1268	0.2501±0.1108	0.2097±0.0881	-0.0213±0.0719	0.0187±0.0589	-0.0196±0.0713
PE-Cer d36:1	-0.0551±0.1539	0.0119±0.1357	0.0974±0.1082	-0.1614±0.0812	-0.0846±0.068	-0.1917±0.08
PE-Cer d32:3	0.0358±0.1177	0.0257±0.1033	0.1538±0.0815	-0.1252±0.0627	-0.008±0.0524	-0.1092±0.0623
PE-Cer d34:3	-0.1025±0.1289	-0.0611±0.1136	0.0659±0.0916	-0.1443±0.0678	-0.0165±0.0577	-0.1108±0.0678
DG 32:0	0.2981±0.1243	0.1609±0.1147	0.183±0.0882	-0.0201±0.0719	-0.0082±0.0592	-0.0227±0.0713
DG 34:0	0.2236±0.1449	0.083±0.1314	0.1182±0.1023	-0.0041±0.0801	-0.0367±0.0665	-0.0085±0.0795
DG 30:1	0.2259±0.1306	0.1292±0.1172	0.1696±0.0912	-0.0071±0.0728	0.0371±0.0597	-0.0131±0.0722
DG 32:1	0.2309±0.1223	0.1542±0.1092	0.197±0.0847	-0.0552±0.0692	0.0274±0.0563	-0.0506±0.0686

DG 33:1	0.2219±0.1211	0.1859±0.1067	0.1928±0.0838	-0.0794±0.0685	0.0588±0.0551	-0.0673±0.0679
DG 34:1	0.2891±0.1269	0.2156±0.1132	0.1867±0.0896	-0.0555±0.0734	0.0658±0.0588	-0.0405±0.0726
DG 35:1	0.2624±0.1406	0.2045±0.1244	0.2194±0.0976	-0.0327±0.0792	0.0624±0.0642	-0.0156±0.0783
DG 36:1	0.2892±0.1389	0.1886±0.1247	0.1246±0.0998	-0.0144±0.0788	0.0413±0.0643	-0.0062±0.078
DG 32:2	0.1761±0.1302	0.0895±0.1162	0.1405±0.0907	-0.1067±0.072	0.0196±0.059	-0.0981±0.0714
DG 34:2	0.1939±0.1249	0.159±0.11	0.1596±0.0869	-0.1099±0.0698	0.0513±0.0565	-0.088±0.0691
DG 35:2	0.2933±0.129	0.2516±0.1136	0.2617±0.0886	-0.0425±0.0744	0.0774±0.0595	-0.0349±0.0736
DG 34:3	0.1729±0.1208	0.1276±0.1067	0.1634±0.0837	-0.1205±0.0671	0.0263±0.0548	-0.0845±0.0665
DG 35:3	0.1945±0.1216	0.1783±0.1067	0.2407±0.0826	-0.106±0.0681	0.0097±0.0557	-0.1046±0.0675
DG 36:3	0.0779±0.1219	0.1182±0.1068	0.1124±0.0846	-0.0908±0.0658	0.0301±0.0543	-0.0711±0.0653
DG 36:4	0.044±0.1527	0.0717±0.134	0.1446±0.1062	-0.1226±0.0817	-0.0065±0.068	-0.1064±0.0811
DG 38:4	0.0651±0.1186	0.0983±0.104	0.0999±0.0824	-0.0703±0.0639	-0.0156±0.053	-0.0744±0.0634
DG 36:5	-0.0094±0.1177	-0.0193±0.1033	0.0393±0.0823	-0.1612±0.0617	-0.0042±0.0524	-0.1441±0.0615
DG 38:5	0.1965±0.1237	0.2072±0.1079	0.1481±0.0863	-0.0553±0.069	0.0496±0.056	-0.0474±0.0683
FA 17:0	0.2106±0.1216	0.1568±0.1077	0.1926±0.084	0.0059±0.0676	0.029±0.0557	0.0035±0.0671
FA 18:3	0.1565±0.1211	0.1812±0.1057	0.2076±0.0828	-0.0756±0.0668	0.0256±0.0547	-0.0448±0.0661
AC 3:0	**0.6012±0.1396**	**0.4757±0.1277**	**0.3931±0.1013**	0.1886±0.085	0.119±0.0721	0.1561±0.0858
AC 4:0	**0.417±0.1322**	0.3348±0.1182	0.1544±0.0999	0.0842±0.0775	0.104±0.0632	0.0883±0.0767
AC 8:1	**0.4749±0.1221**	**0.4526±0.1058**	**0.3039±0.0884**	0.0303±0.0773	0.1123±0.0607	0.0477±0.076
AC 5:0 (OH)	**0.4027±0.1326**	0.303±0.1196	0.2956±0.0928	0.0981±0.0767	0.0679±0.064	0.0823±0.0765
FA 8:1 (DiC)	**0.4792±0.1483**	0.388±0.1325	0.2619±0.1083	0.0723±0.0881	0.1532±0.0699	0.0316±0.0886
FA 9:1 (DiC)	**0.484±0.1233**	**0.3768±0.1125**	0.2216±0.0947	0.1568±0.0732	0.179±0.0587	0.1244±0.074
FA 12:1 (DiC)	-0.2281±0.1283	-0.1029±0.1166	-0.0888±0.0917	-0.073±0.0703	-0.0328±0.0588	-0.1114±0.0688
FA 28:2 (DiC)	**-0.35±0.1185**	-0.2814±0.1057	-0.088±0.0906	-0.172±0.0652	-0.0596±0.0569	-0.1383±0.0659
SN-glycero-3-phosphocholine	0.024±0.1332	0.0706±0.117	-0.0773±0.0933	0.0616±0.0712	0.0282±0.0592	0.1315±0.0699
PC 34:0/PE 37:0	**-0.343±0.0998**	-0.2548±0.091	-0.1616±0.0747	-0.1065±0.058	-0.1335±0.0464	-0.1146±0.0572
PC 40:4/PE 43:4	0.2676±0.1194	0.2415±0.1048	0.1886±0.0838	0.0445±0.0672	0.0021±0.0563	0.0319±0.0669
PC 31:5/PE 34:5	0.1287±0.1284	0.1402±0.1124	0.0774±0.0899	-0.0464±0.07	0.032±0.0575	-0.0449±0.0694
PC 35:5/PE 38:5	**-0.4873±0.1246**	-0.3443±0.1169	-0.2215±0.0957	-0.128±0.0753	-0.0805±0.0633	-0.094±0.076
PE 36:2	0.1502±0.1283	0.1731±0.1121	0.1246±0.0894	-0.0615±0.0704	0.0521±0.0575	-0.0415±0.0697

PS 35:4	**0.3788±0.1136**	0.2983±0.1021	**0.2917±0.0789**	0.045±0.0683	0.0463±0.0561	0.039±0.0679
PS 40:4	-0.3207±0.1177	-0.1948±0.1086	-0.0436±0.0903	-0.0902±0.0667	-0.127±0.0538	-0.1032±0.0658
PS 42:6	-0.2823±0.1339	-0.1918±0.12	-0.0587±0.0983	-0.0662±0.0746	-0.0125±0.0625	-0.037±0.0745
PS 39:7	**-0.4356±0.1304**	**-0.3915±0.1145**	-0.1769±0.0987	-0.1515±0.0749	-0.1395±0.0617	-0.1769±0.0732
LysoPC 14:0	0.0877±0.1379	0.0751±0.1211	0.1507±0.0955	-0.0735±0.0745	0.0417±0.0614	-0.0687±0.0739
norhyodeoxycholic acid	**0.3564±0.1201**	0.1795±0.1154	0.1516±0.089	0.0579±0.0701	0.0425±0.0581	0.0163±0.0706
SM d36:2	0.23±0.1334	0.2765±0.1157	0.2567±0.0909	-0.028±0.0745	0.0924±0.0599	0.0044±0.0735
DHEA sulfate	0.4019±0.1493	0.2734±0.1356	0.2603±0.1059	0.0604±0.086	0.0733±0.0707	0.0412±0.0858
cortisone	-0.2488±0.1269	-0.306±0.1096	-0.1999±0.0882	0.0818±0.0723	0.0597±0.0594	0.0419±0.0713
urate	0.275±0.1283	0.1759±0.1155	0.1831±0.0903	-0.0703±0.0737	0.0014±0.0601	-0.0713±0.0731
dipeptide (glutamate-phenylalanine)	0.2456±0.1179	0.1739±0.1053	0.1297±0.084	0.074±0.0652	-0.0717±0.0556	0.0356±0.0655
dipeptide (histidine-tyrosine)	0.3489±0.1363	0.2634±0.1219	0.0799±0.1021	0.1414±0.0755	0.0613±0.0642	0.1204±0.0755
L-gamma-glutamyl-L-isoleucine	**0.4662±0.1297**	0.3297±0.1202	**0.3111±0.0926**	0.0766±0.0786	0.1608±0.0615	0.0834±0.0777

Table S4.3. Association between annotated metabolites and BMIz in girls (n=108). Sex-stratified regression models identifying annotated metabolites (p=550) linearly associated with BMIz. All models were adjusted for age and puberty onset (Model 1), along with additional phenotypic measures to identify metabolites that drive the association with BMIz including HOMA-CP (Model 2), MUAMA (Model 3), MUAFA (Model 4), WHtR (Model 5) and TR+SS (Model 6). Values reported are β±Std Error. Metabolites with FDR<0.10 highlighted in red and bolded. Metabolites listed have an FDR<0.10 in Model 1 in the combined model and/or the sex-stratified models.

Metabolite	Model 1	Model 2	Model 3	Model 4	Model 5	Model 6
N-acetylglycine	**-0.3573±0.1271**	-0.2206±0.1297	-0.1855±0.0932	-0.0156±0.0708	-0.0046±0.0554	0.0271±0.0716
isovalerylcarnitine	0.2843±0.1121	0.2325±0.1069	0.1504±0.0816	0.069±0.0603	0.0159±0.0481	0.0529±0.0608
isoleucine	0.1539±0.1319	0.1403±0.1238	0.1286±0.0932	0.0523±0.0683	-0.0381±0.0541	0.0732±0.0681
leucine	-0.0417±0.1276	-0.0335±0.1197	-0.0766±0.0902	0.1221±0.0652	0.0302±0.0516	0.068±0.0657
valine	0.1829±0.1131	0.1634±0.1063	0.0666±0.0816	0.05±0.0592	-0.0026±0.0469	0.0495±0.0593
phenylalanine	0.1831±0.0982	0.1401±0.0934	0.0673±0.0713	0.086±0.0509	0.0126±0.041	0.0773±0.0512
tyrosine	**0.3526±0.1044**	**0.2981±0.1002**	0.2067±0.0767	0.0931±0.0579	0.0334±0.0465	0.0535±0.0592
5-methylthioadenosine	0.1845±0.1054	0.1332±0.1004	0.0143±0.0775	0.0424±0.0554	-0.01±0.044	0.0594±0.0552
D-ornithine	0.1896±0.1124	0.1715±0.1056	0.035±0.082	0.0672±0.0586	-0.0033±0.0467	0.0738±0.0586
L-ornithine	0.1943±0.1115	0.1683±0.105	0.0226±0.0818	0.0674±0.0582	0.0063±0.0464	0.0857±0.058
normethanephrine	0.1832±0.0982	0.1402±0.0934	0.0674±0.0713	0.0861±0.0509	0.0127±0.041	0.0774±0.0512
D-lyxose	**-0.4107±0.1425**	**-0.4257±0.1326**	**-0.3222±0.1004**	-0.0259±0.0795	0.0455±0.0629	0.0712±0.0813
5-phospho-alpha-D-ribose-1-diphosphate	0.3164±0.125	0.2749±0.1183	0.1176±0.0927	0.1763±0.0645	0.1166±0.0515	0.1357±0.0658
Cer t36:0(2OH)	**0.3728±0.1141**	**0.3615±0.1067**	**0.2789±0.0809**	0.0085±0.0655	0.0488±0.0503	-0.0237±0.0662
PE-Cer d36:1	**0.2695±0.0958**	0.1843±0.0953	0.1409±0.0702	-0.019±0.0539	0.0085±0.0417	0.0301±0.053
PE-Cer d32:3	**0.4203±0.1053**	**0.3479±0.1031**	0.2162±0.0802	0.0836±0.0612	0.0815±0.0475	0.0998±0.0607
PE-Cer d34:3	**0.3084±0.1061**	0.2462±0.1023	0.1735±0.0775	0.0105±0.0594	0.0418±0.0459	0.0339±0.059
DG 32:0	**0.4379±0.1005**	**0.347±0.1027**	0.2268±0.0776	0.1102±0.0589	0.0907±0.0461	0.1255±0.0583
DG 34:0	**0.4175±0.0951**	**0.3418±0.095**	**0.2593±0.0708**	0.0834±0.0567	0.0758±0.0441	0.1006±0.0561
DG 30:1	**0.4063±0.1021**	**0.3265±0.1013**	0.2319±0.0764	0.1089±0.0583	0.1322±0.0441	0.1229±0.0578
DG 32:1	**0.4828±0.1039**	**0.3945±0.1054**	**0.2696±0.0799**	0.1325±0.0615	0.1206±0.0477	0.1415±0.0612

DG 33:1	**0.4256±0.1072**	**0.3444±0.106**	**0.2747±0.0785**	0.084±0.0623	0.0939±0.048	0.0707±0.0629
DG 34:1	**0.4441±0.1012**	**0.3603±0.1017**	0.2226±0.0787	0.13±0.0586	0.0913±0.0465	0.1367±0.0584
DG 35:1	**0.3381±0.0977**	0.2727±0.0952	0.1509±0.0742	0.0964±0.0542	0.0562±0.0432	0.094±0.0544
DG 36:1	**0.3867±0.099**	**0.3077±0.0985**	0.1653±0.0771	0.1103±0.0561	0.0605±0.0449	0.1225±0.0557
DG 32:2	**0.5131±0.0969**	**0.4455±0.0958**	**0.3114±0.0745**	0.1435±0.0596	0.1569±0.0447	0.1617±0.0587
DG 34:2	**0.4495±0.104**	**0.3712±0.1031**	0.2381±0.0799	0.1249±0.0603	0.1102±0.047	0.1247±0.0604
DG 35:2	**0.4552±0.1081**	**0.3812±0.1059**	0.2255±0.0836	0.1189±0.0626	0.1072±0.0487	0.1274±0.0624
DG 34:3	**0.4785±0.1034**	**0.3997±0.1029**	**0.2647±0.0796**	0.0868±0.063	0.131±0.0469	0.1035±0.0624
DG 35:3	**0.518±0.1059**	**0.4639±0.1017**	**0.2877±0.0823**	0.1595±0.0627	0.1358±0.0489	0.1662±0.0625
DG 36:3	**0.4491±0.1192**	**0.3723±0.116**	0.2105±0.0911	0.1185±0.0674	0.1368±0.0515	0.1699±0.0655
DG 36:4	**0.4041±0.0973**	**0.356±0.0933**	0.2135±0.0742	0.1515±0.0542	0.1487±0.0415	0.1791±0.053
DG 38:4	**0.3416±0.1209**	0.2944±0.1148	0.1348±0.0903	0.1036±0.0652	0.0999±0.0508	0.1577±0.0637
DG 36:5	**0.3551±0.1143**	0.3112±0.1085	0.1885±0.0843	0.0179±0.0647	0.1266±0.0477	0.0777±0.0633
DG 38:5	0.3117±0.1199	0.2054±0.1189	0.1216±0.0889	0.0527±0.0652	0.0616±0.0508	0.0604±0.0651
FA 17:0	0.2018±0.1093	0.1947±0.1024	0.1015±0.0786	0.0559±0.0575	0.0424±0.0452	0.0495±0.0576
FA 18:3	0.2916±0.1079	0.2664±0.1016	0.1249±0.0799	0.0604±0.0587	0.04±0.0462	0.0696±0.0585
AC 3:0	0.0937±0.1061	0.048±0.1005	0.0664±0.0752	0.0222±0.0549	-0.0257±0.0433	0.0638±0.0545
AC 4:0	0.1474±0.1135	0.1567±0.1062	0.0063±0.0822	0.0619±0.0587	0.0047±0.0466	0.0568±0.0589
AC 8:1	0.2674±0.1175	0.2723±0.1098	0.1044±0.0862	-0.0271±0.0642	-0.0508±0.0503	-0.0366±0.0644
AC 5:0 (OH)	0.1988±0.1143	0.1739±0.1076	0.0794±0.0826	0.1356±0.0582	0.049±0.047	0.1316±0.0584
FA 8:1 (DiC)	0.0546±0.1041	0.0316±0.0979	-0.079±0.0746	0.0382±0.0535	0.0146±0.0421	0.0645±0.0533
FA 9:1 (DiC)	0.0592±0.1087	0.0361±0.1022	-0.0488±0.0777	0.0594±0.0557	0.031±0.0439	0.0737±0.0556
FA 12:1 (DiC)	-0.2365±0.1038	-0.1831±0.0992	-0.1492±0.0744	0.0343±0.0568	0.0648±0.0445	0.0728±0.0573
FA 28:2 (DiC)	0.0256±0.1227	-0.0149±0.1156	-0.0746±0.0872	-0.0595±0.063	0.0003±0.0496	-0.013±0.0632
SN-glycero-3-phosphocholine	**0.3025±0.1077**	0.2859±0.101	0.1502±0.0792	0.0629±0.0588	0.0498±0.0462	0.0782±0.0585
PC 34:0/PE 37:0	0.0256±0.1376	0.0384±0.1291	0.0057±0.0975	-0.0814±0.0706	0.0365±0.0555	-0.0008±0.0709
PC 40:4/PE 43:4	0.2437±0.1205	0.2257±0.1132	0.1532±0.0862	-0.007±0.0648	-0.0161±0.0508	-0.0536±0.0654
PC 31:5/PE 34:5	**0.3597±0.1001**	**0.287±0.0983**	0.1344±0.0777	0.0842±0.0565	0.1078±0.043	0.1283±0.055
PC 35:5/PE 38:5	-0.1497±0.1123	-0.1478±0.1053	-0.0945±0.0799	-0.0738±0.0579	-0.0422±0.0458	-0.0874±0.0578
PE 36:2	**0.3827±0.1101**	0.3023±0.1081	0.1559±0.0844	0.0953±0.0616	0.0866±0.0481	0.1157±0.061

PS 35:4	0.1133±0.1188	0.0406±0.1135	0.0589±0.0845	-0.0121±0.0617	-0.0045±0.0485	-0.034±0.0619
PS 40:4	-0.114±0.1372	-0.1067±0.1287	-0.1346±0.0967	0.0562±0.0712	0.0166±0.0559	0.0337±0.0713
PS 42:6	-0.26±0.1075	-0.2301±0.1015	-0.1235±0.0785	-0.0782±0.0573	-0.0512±0.0452	-0.1269±0.0561
PS 39:7	0.0292±0.1131	0.0087±0.1063	-0.1621±0.0807	-0.0051±0.0582	0.0096±0.0457	0.0857±0.0578
LysoPC 14:0	**0.2963±0.1045**	0.205±0.1037	0.0948±0.0789	0.0662±0.057	0.0946±0.0437	0.1105±0.0558
norhyodeoxycholic acid	-0.0294±0.1126	-0.026±0.1056	0.084±0.0801	0.0418±0.0579	0.0495±0.0454	-0.0248±0.0579
SM d36:2	0.2231±0.1089	0.1863±0.103	0.1293±0.0782	-0.0579±0.0592	0.0091±0.0458	-0.059±0.0593
DHEA sulfate	0.2516±0.1502	0.1358±0.1458	-0.045±0.1116	0.0103±0.0794	0.048±0.0619	0.0605±0.0789
cortisone	-0.2959±0.1093	-0.2729±0.1028	-0.1269±0.0809	-0.1054±0.0583	-0.0157±0.0472	-0.0848±0.0589
urate	0.2483±0.1302	0.1764±0.1246	0.0123±0.0967	0.1601±0.0665	0.0611±0.0538	0.1348±0.0672
dipeptide (glutamate-phenylalanine)	0.3112±0.1215	0.2922±0.1141	0.1754±0.0881	0.0905±0.0651	-0.0517±0.0528	0.0751±0.0656
dipeptide (histidine-tyrosine)	0.1619±0.1128	0.1222±0.1066	0.004±0.0821	0.0973±0.0579	0.0118±0.0464	0.0996±0.0579
L-gamma-glutamyl-L-isoleucine	0.1645±0.1088	0.1509±0.1022	0.0347±0.0789	0.0724±0.0563	-0.0033±0.045	0.0913±0.0561

Figure 4.1. Association of diglycerides and amino acids with BMIz exhibits sex differences.

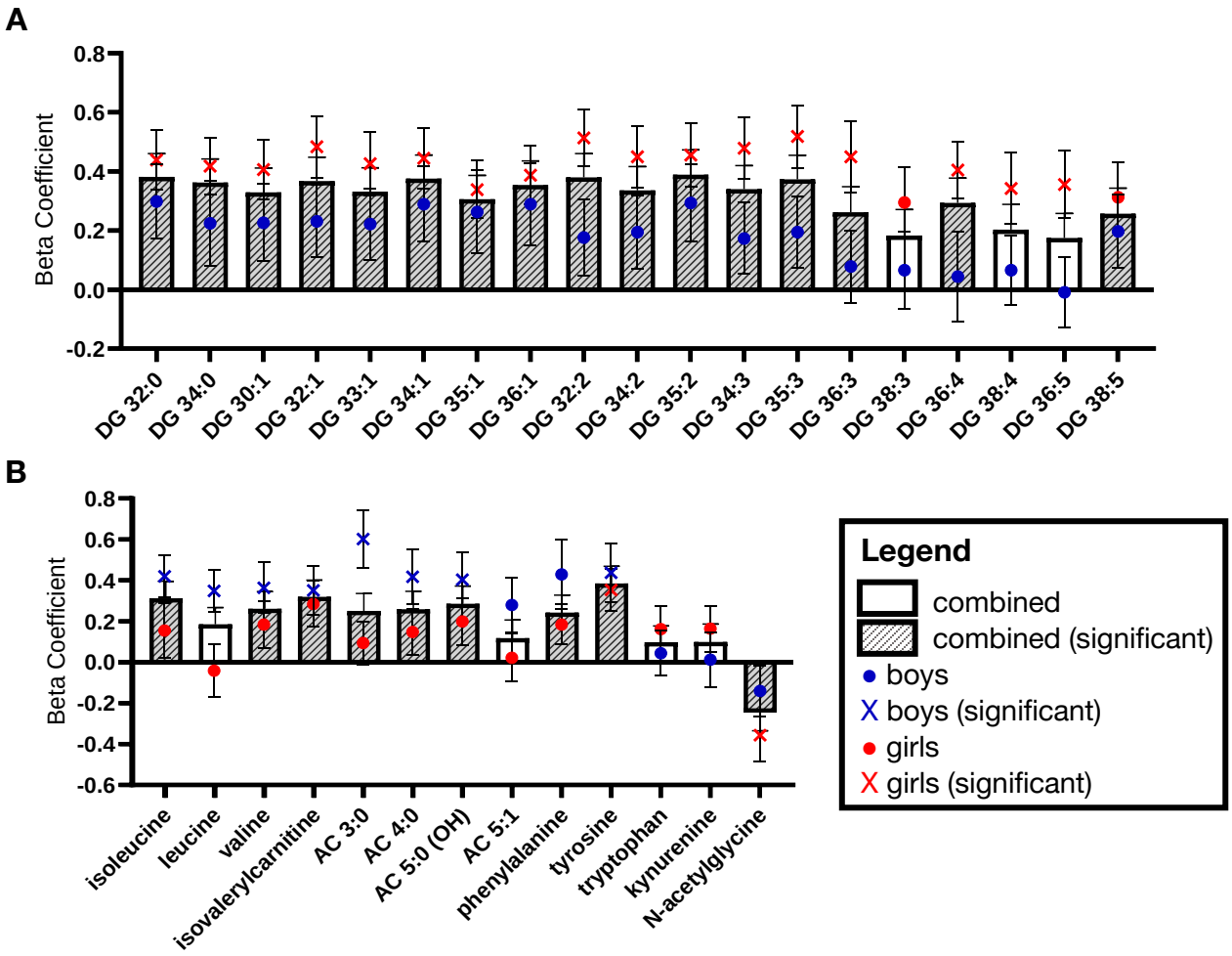

Linear models identified metabolites associated with BMIz in the entire cohort, adjusting for age, sex, and puberty onset, and in sex-stratified models, adjusting for age and puberty onset. Beta coefficients representing the relationship between **(A)** DG metabolites and **(B)** BCAA metabolites with BMIz in the entire cohort (bars) and boys (blue dots) and girls (red dots). Significance in the entire cohort depicted by striped gray bars (FDR<0.10). Signficance in sex-stratified models depicted by "X" (FDR<0.10).

Figure S4.4. Fatty acids and diglycerides stratified by sex and obese (BMIz ≥2) vs. normal weight (-2≤BMIz<1).

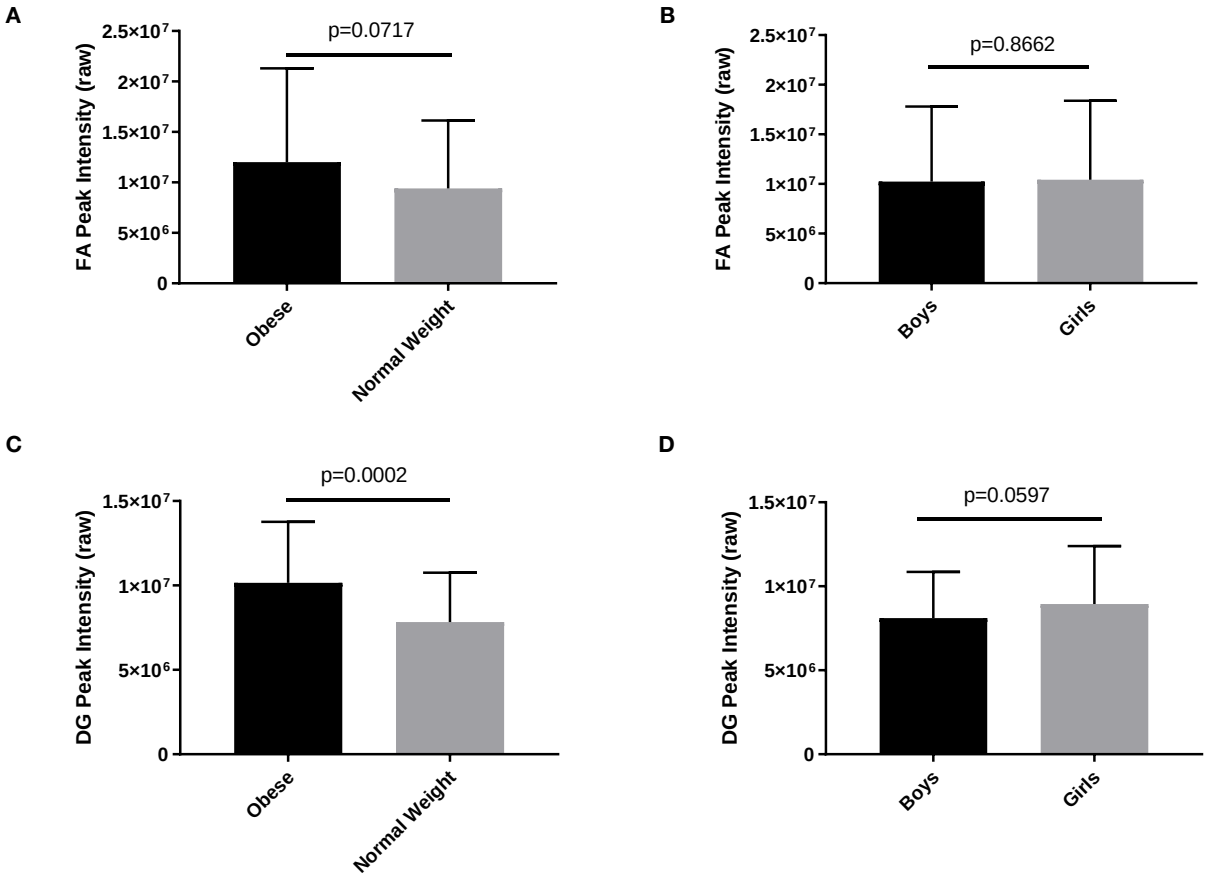

T-tests were used to distinguish differences between metabolite groups. Sum of raw peak intensity values of FA (p=55) stratified by **(A)** obese and normal weight (p=0.0717) and **(B)** by sex (p=0.86662). Sum of raw peak intensity values of DG metabolites (p=19) significantly differs between **(C)** obese and normal weight (p=0.000154) and **(D)** trended to be elevated in girls (p=0.0597).

Figure 4.2. Relationship between fatty acid chain length and number of double bonds with BMIz, sex-stratified.

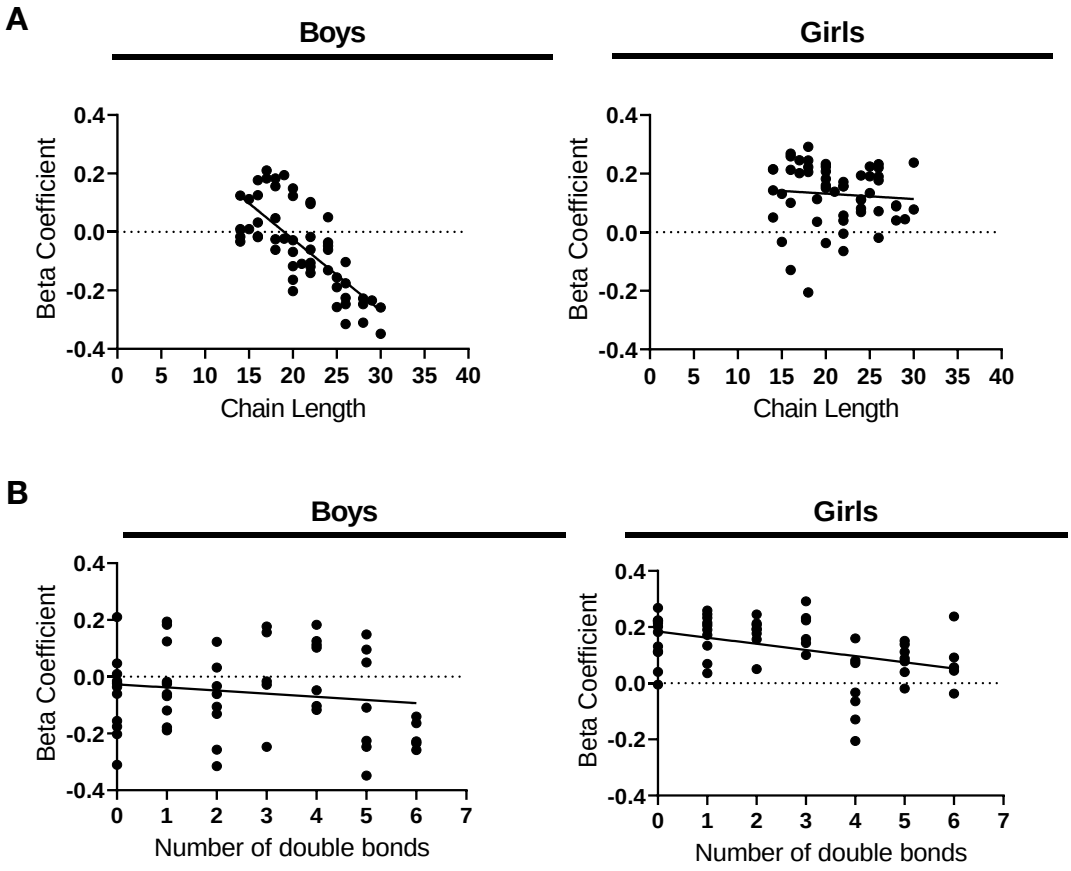

(A) Relationship between beta coefficients describing models between fatty acids and BMIz and fatty acid chain length (14-30 carbons) in boys (r^2=0.5568, p-value<0.0001) and girls (r^2=0.0064, p-value=0.5621). **(B)** Relationship between beta coefficients describing models between fatty acids and BMIz and number of double bonds in boys (r^2=0.0226, p-value=0.2731) and girls (r^2=0.1810, p-value=0.0012).

Figure S4.5. Association of metabolite features with HOMA-CP, within the entire cohort and sex-stratified.

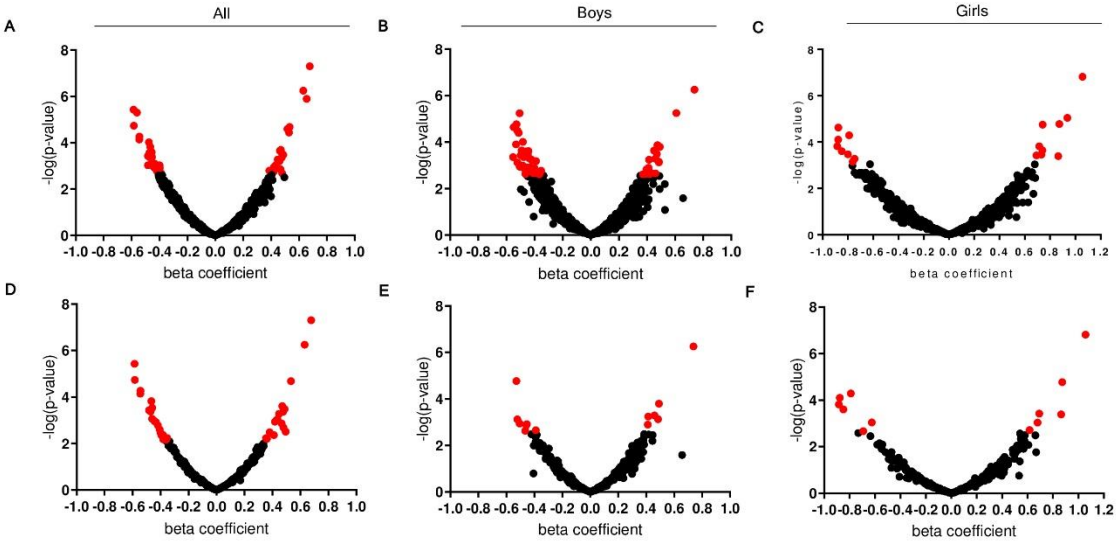

Beta coefficients from linear models are plotted on the x-axis and negative log transformed p-values are plotted on the y-axis. Association between HOMA-CP and both annotated and unannotated features (p=3272) **(A)** within entire cohort (n=206), accounting for age, sex, and puberty onset, and sex stratified in **(B)** boys and **(C)** girls, accounting for age and puberty onset (Model 1). Using solely annotated metabolites (p=550), representing the relationship between metabolites and HOMA-CP **(D)** within the entire cohort and sex stratified in **(E)** boys and **(F)** girls (Model 1). Features in red indicate significant associations after FDR correction (FDR<0.10).

Table S4.4. Association between annotated metabolites and HOMA-CP (n=206). Regression models identifying annotated metabolites (p=550) linearly associated with HOMA-CP. All models were adjusted for sex, age, and puberty onset (Model 1), along with additional phenotypic measures to identify metabolites that drive the association with HOMA-CP including BMIz (Model 2), MUAMA (Model 3), MUAFA (Model 4), WHtR (Model 5) and TR+SS (Model 6). Values reported are β±Std Error. Metabolites with FDR<0.10 highlighted in red and bolded. Metabolites listed have an FDR<0.10 in Model 1 in the combined model and/or the sex-stratified models.

Metabolite	Model 1	Model 2	Model 3	Model 4	Model 5	Model 6
N-acetylglycine	**-0.5841±0.1363**	**-0.4536±0.1302**	**-0.467±0.1292**	**-0.4565±0.1344**	**-0.4378±0.134**	**-0.4529±0.1353**
N-acetyl-L-leucine	0.2169±0.1364	0.1517±0.1269	0.1978±0.126	0.2118±0.1289	0.1535±0.1287	0.2088±0.1292
creatine	**0.4111±0.144**	**0.4385±0.1324**	**0.4188±0.1324**	**0.4306±0.1356**	**0.4352±0.1343**	**0.4297±0.1359**
lysine	**0.4362±0.1317**	0.3173±0.125	0.3219±0.1245	0.3303±0.128	0.3224±0.1269	0.342±0.1277
3,4-hydroxyphenyl-lactate	0.1682±0.1428	0.0913±0.133	0.0728±0.1332	0.1286±0.1354	0.1269±0.1342	0.1315±0.1357
tyrosine	**0.476±0.1352**	0.2707±0.1339	0.3315±0.1294	0.3194±0.1353	0.2882±0.1358	0.3084±0.1371
proline	**0.4877±0.1358**	**0.4092±0.1271**	**0.3938±0.1275**	**0.4115±0.1303**	**0.406±0.1292**	**0.41±0.1307**
glucose	**0.4791±0.1556**	**0.4819±0.1432**	**0.4466±0.1437**	**0.5212±0.1462**	**0.4793±0.1453**	**0.5037±0.1467**
raffinose	0.2699±0.1369	0.1875±0.128	0.1779±0.128	0.2441±0.1296	0.1892±0.1298	0.2506±0.1298
DG 32:0	**0.5326±0.1251**	0.3392±0.1253	**0.3978±0.1202**	**0.3707±0.1284**	**0.3637±0.1264**	**0.3784±0.1281**
DG 34:0	**0.4707±0.1283**	0.2793±0.127	**0.3489±0.122**	0.3097±0.1299	0.2985±0.1285	0.3179±0.1297
DG 30:1	**0.4249±0.1299**	0.2459±0.1269	0.3201±0.1224	0.2809±0.1291	0.2916±0.1264	0.2866±0.1291
DG 32:1	**0.4471±0.1289**	0.2503±0.1276	**0.3378±0.1219**	0.2768±0.1311	0.2877±0.1277	0.2844±0.1309
DG 34:1	**0.4186±0.1289**	0.2149±0.1278	0.2829±0.1231	0.243±0.1312	0.2547±0.1278	0.2528±0.1309
DG 36:1	**0.4301±0.1303**	0.2385±0.1282	0.2686±0.1259	0.2736±0.1306	0.2654±0.1291	0.2827±0.1304
DG 32:2	**0.381±0.1296**	0.1706±0.1284	0.2602±0.1228	0.1935±0.1323	0.2197±0.1278	0.2049±0.1319
DG 34:3	**0.3544±0.1287**	0.1642±0.126	0.2489±0.1213	0.1613±0.1317	0.2056±0.1259	0.1783±0.1307
FA 12:2	**-0.4197±0.1334**	**-0.3597±0.1243**	**-0.3755±0.1236**	**-0.411±0.1259**	**-0.3884±0.1252**	**-0.4105±0.1262**
FA 14:2	**-0.4426±0.1355**	**-0.4579±0.1245**	**-0.4798±0.124**	**-0.5153±0.1271**	**-0.4739±0.1261**	**-0.499±0.1275**
FA 14:3	0.3069±0.1273	0.2644±0.1182	0.2365±0.1187	0.2958±0.1203	0.2822±0.1195	0.2951±0.1206
FA 16:3	**-0.3824±0.1338**	**-0.4752±0.1226**	**-0.4516±0.1224**	**-0.536±0.1264**	**-0.4694±0.1245**	**-0.5229±0.1266**
AC 2:0	**-0.4066±0.1347**	**-0.3824±0.1245**	**-0.3661±0.1247**	**-0.4268±0.1267**	**-0.3972±0.126**	**-0.4193±0.1271**

AC 6:0	**-0.3812±0.1402**	**-0.4653±0.1286**	**-0.4785±0.1284**	**-0.4795±0.132**	**-0.4516±0.1306**	**-0.4747±0.1323**
AC 8:0	**-0.393±0.1382**	**-0.3736±0.1277**	**-0.4253±0.1267**	**-0.3942±0.1303**	**-0.3752±0.1294**	**-0.3941±0.1306**
AC 10:0	**-0.461±0.1384**	**-0.4031±0.1288**	**-0.4725±0.127**	**-0.4232±0.1313**	**-0.4087±0.1305**	**-0.4245±0.1316**
AC 12:0	**-0.3707±0.1334**	**-0.3465±0.1234**	**-0.4089±0.1223**	**-0.3658±0.1259**	-0.3405±0.1252	**-0.3589±0.1263**
AC 10:1	**-0.393±0.1373**	**-0.3712±0.1269**	**-0.4286±0.1259**	**-0.3884±0.1295**	**-0.3739±0.1286**	**-0.3848±0.1299**
AC 12:1	**-0.4827±0.1357**	**-0.5026±0.1244**	**-0.5148±0.1241**	**-0.5256±0.1272**	**-0.5026±0.1262**	**-0.522±0.1276**
AC 14:1	**-0.4714±0.1336**	**-0.4302±0.1239**	**-0.4856±0.1225**	**-0.4638±0.126**	**-0.4375±0.1254**	**-0.4541±0.1265**
AC 10:2	**-0.3995±0.1371**	**-0.3643±0.127**	**-0.3911±0.1263**	**-0.4044±0.1292**	**-0.3735±0.1286**	**-0.4035±0.1295**
AC 12:2	**-0.5864±0.1267**	**-0.5209±0.1183**	**-0.57±0.1164**	**-0.5142±0.1218**	**-0.5289±0.1198**	**-0.5231±0.1217**
AC 14:2	**-0.4589±0.1267**	**-0.4356±0.1171**	**-0.4808±0.116**	**-0.4694±0.1192**	**-0.4436±0.1185**	**-0.4572±0.1197**
AC 11:3	-0.234±0.1247	-0.1659±0.1163	-0.2435±0.1149	-0.1497±0.1198	-0.1917±0.1173	-0.1363±0.1207
AC 6:0 (OH)	**-0.361±0.1336**	**-0.3586±0.1232**	**-0.3701±0.1229**	**-0.4077±0.1257**	**-0.3637±0.1249**	**-0.4036±0.126**
AC 8:0 (OH)	**-0.5435±0.1346**	**-0.4658±0.126**	**-0.5285±0.1237**	**-0.48±0.1286**	**-0.4706±0.1277**	**-0.4829±0.1288**
AC 10:0 (OH)	**-0.5451±0.1373**	**-0.474±0.1282**	**-0.5547±0.1257**	**-0.4843±0.1311**	**-0.4761±0.1301**	**-0.4852±0.1314**
FA 8:0 (DiC)	0.2938±0.135	0.1972±0.1267	0.1123±0.1301	0.2657±0.1279	0.215±0.128	0.2676±0.1281
FA 10:1 (DiC)	-0.0749±0.133	0±0.1238	0.0013±0.1236	-0.0031±0.1267	0.0097±0.1258	-0.0118±0.1268
Keto 14:0	**-0.4328±0.1338**	**-0.3808±0.1244**	**-0.4338±0.123**	**-0.4273±0.1262**	**-0.391±0.1259**	**-0.4219±0.1266**
PA 22:3	**-0.3523±0.1277**	-0.3199±0.1183	-0.2692±0.1195	-0.3274±0.1209	-0.3024±0.1204	-0.3327±0.121
PC 33:3/PE 36:3	**-0.4657±0.1229**	**-0.374±0.1159**	**-0.3463±0.1171**	**-0.4094±0.1174**	**-0.3902±0.117**	**-0.418±0.1173**
PC 38:6/PE 41:6	-0.2292±0.1402	-0.1777±0.1302	-0.1706±0.1301	-0.1988±0.1328	-0.1834±0.1319	-0.1968±0.1331
myo-inositol	**0.4666±0.1458**	**0.4768±0.1341**	**0.5007±0.1336**	**0.4493±0.1378**	**0.4886±0.1358**	**0.4563±0.1379**
LysoPC 14:0	**0.3609±0.132**	0.2423±0.1251	0.283±0.1233	0.2485±0.1284	0.2807±0.1255	0.2663±0.1278
glycochenodeoxycholate	**0.677±0.1241**	**0.6703±0.1136**	**0.6437±0.1143**	**0.6975±0.1158**	**0.6614±0.1156**	**0.6896±0.1163**
glycocholate	**0.6307±0.1261**	**0.6136±0.1159**	**0.5882±0.1165**	**0.6603±0.1177**	**0.6199±0.1174**	**0.644±0.1183**
taurocholate	-0.2432±0.1327	-0.285±0.1223	-0.2724±0.1222	-0.2708±0.1252	-0.2817±0.124	-0.2936±0.1255
norhyodeoxycholic acid	0.1939±0.1313	0.105±0.1228	0.1613±0.1215	0.1315±0.1251	0.1324±0.1239	0.1029±0.1264
DHEA sulfate	**0.4953±0.1674**	0.3226±0.1598	0.3308±0.159	0.3439±0.1635	0.3528±0.161	0.3553±0.1633
cycloheptanecarboxylic acid	0.2935±0.1349	0.2084±0.1263	0.1279±0.1292	0.267±0.1278	0.2244±0.1277	0.2714±0.128
dipeptide (tyrosine proline)	0.193±0.1284	0.1137±0.1199	0.1428±0.1191	0.1297±0.1224	0.1315±0.1212	0.1351±0.1226

Table S4.5. Association between annotated metabolites and HOMA-CP in boys (n=98). Sex-stratified regression models identifying annotated metabolites (p=550) linearly associated with HOMA-CP. All models were adjusted for age and puberty onset (Model 1), along with additional phenotypic measures to identify metabolites that drive the association with HOMA-CP including BMIz (Model 2), MUAMA (Model 3), MUAFA (Model 4), WHtR (Model 5) and TR+SS (Model 6). Values reported are β±Std Error. Metabolites with FDR<0.10 highlighted in red and bolded. Metabolites listed have an FDR<0.10 in Model 1 in the combined model and/or the sex-stratified models.

Metabolite	Model 1	Model 2	Model 3	Model 4	Model 5	Model 6
N-acetylglycine	-0.2982±0.1351	-0.2255±0.1202	-0.2095±0.1185	-0.2089±0.1269	-0.1766±0.123	-0.2061±0.1248
N-acetyl-L-leucine	**0.4153±0.1205**	0.2918±0.1113	**0.341±0.1053**	**0.3437±0.113**	0.2843±0.1123	**0.3199±0.1128**
creatine	0.1014±0.1806	0.068±0.1587	0.073±0.1557	0.0287±0.1663	0.0589±0.1591	0.0039±0.1643
lysine	0.2753±0.1553	0.1409±0.1403	0.1054±0.139	0.1655±0.1459	0.1588±0.1397	0.1861±0.1423
3,4-hydroxyphenyl-lactate	**0.4918±0.1302**	**0.4115±0.1162**	**0.3582±0.1176**	**0.4718±0.1183**	**0.4579±0.1136**	**0.4565±0.117**
tyrosine	**0.7383±0.1475**	**0.5546±0.1415**	**0.5724±0.1349**	**0.5977±0.1461**	**0.5495±0.1428**	**0.5754±0.1455**
proline	0.3841±0.1345	0.3251±0.1189	0.3208±0.1167	0.3149±0.1252	0.3234±0.1193	0.314±0.1231
glucose	0.4463±0.1531	0.3823±0.1352	0.3297±0.1352	**0.4548±0.1385**	0.3798±0.1356	**0.4366±0.1368**
raffinose	**0.4855±0.144**	0.3368±0.1331	0.3251±0.1308	**0.4177±0.1337**	0.3551±0.1319	**0.4088±0.1319**
DG 32:0	0.3424±0.1388	0.1936±0.1278	0.2529±0.1217	0.1899±0.1358	0.1736±0.1296	0.1755±0.134
DG 34:0	0.3365±0.1604	0.222±0.144	0.2546±0.1397	0.2225±0.151	0.1904±0.146	0.2113±0.149
DG 30:1	0.2333±0.1463	0.1157±0.1316	0.1888±0.1265	0.1138±0.1383	0.1237±0.1315	0.1013±0.1364
DG 32:1	0.1854±0.138	0.064±0.1243	0.1585±0.119	0.0372±0.1324	0.0662±0.1245	0.0282±0.1302
DG 34:1	0.1793±0.1446	0.0257±0.1313	0.0974±0.126	-0.0025±0.1404	0.0469±0.1306	-0.0083±0.1377
DG 36:1	0.2458±0.1568	0.0949±0.1421	0.1156±0.1382	0.0897±0.15	0.1015±0.1421	0.0818±0.1475
DG 32:2	0.2063±0.1454	0.114±0.1296	0.1781±0.1253	0.0625±0.1388	0.1152±0.1299	0.0559±0.1364
DG 34:3	0.1076±0.1361	0.0152±0.1211	0.1±0.1172	-0.0483±0.13	0.0205±0.1212	-0.0394±0.1269
FA 12:2	-0.1445±0.1344	-0.0861±0.1189	-0.016±0.1187	-0.1707±0.1226	-0.1227±0.1183	-0.1912±0.1207
FA 14:2	-0.2807±0.1435	-0.2633±0.1257	-0.1697±0.1265	**-0.3651±0.1298**	-0.2992±0.1251	**-0.3697±0.1276**
FA 14:3	0.3856±0.1309	**0.3942±0.113**	**0.346±0.1125**	**0.4413±0.1172**	**0.4229±0.1124**	**0.4412±0.1151**
FA 16:3	-0.1969±0.1392	-0.2978±0.121	-0.14±0.1208	**-0.4129±0.1288**	-0.2932±0.1213	**-0.4333±0.1263**
AC 2:0	-0.2764±0.1427	-0.3398±0.1234	-0.2856±0.1219	**-0.3922±0.1292**	-0.3438±0.1236	**-0.3867±0.1268**

AC 6:0	-0.2553±0.1471	**-0.4295±0.1271**	-0.3622±0.1245	**-0.4447±0.1343**	**-0.3898±0.1274**	**-0.4654±0.1317**
AC 8:0	-0.4041±0.157	**-0.4089±0.1363**	**-0.4234±0.1331**	**-0.4322±0.1419**	-0.4016±0.1368	**-0.4443±0.1393**
AC 10:0	**-0.4648±0.1528**	**-0.4249±0.1338**	**-0.4747±0.129**	**-0.4444±0.1392**	**-0.4192±0.1343**	**-0.4493±0.1367**
AC 12:0	-0.3901±0.1369	**-0.4087±0.118**	**-0.4545±0.1142**	**-0.4258±0.1232**	**-0.3931±0.1188**	**-0.4246±0.1211**
AC 10:1	-0.3668±0.1458	-0.3605±0.1269	**-0.3739±0.1239**	**-0.3892±0.1319**	-0.3585±0.1272	**-0.3997±0.1295**
AC 12:1	-0.421±0.1432	**-0.4637±0.1226**	**-0.4486±0.1204**	**-0.5026±0.1279**	**-0.4507±0.1233**	**-0.4964±0.1256**
AC 14:1	**-0.4575±0.1427**	**-0.4665±0.1229**	**-0.4874±0.1195**	**-0.5102±0.1276**	**-0.4475±0.1239**	**-0.4883±0.1259**
AC 10:2	-0.3609±0.1513	-0.3738±0.1312	-0.354±0.1291	**-0.4386±0.1362**	-0.3598±0.1319	**-0.4333±0.1339**
AC 12:2	-0.2957±0.1418	-0.2516±0.1249	-0.311±0.1208	-0.2609±0.1302	-0.2303±0.126	-0.2697±0.1278
AC 14:2	-0.3378±0.1309	**-0.358±0.1131**	**-0.4036±0.1096**	**-0.3888±0.1178**	**-0.3478±0.1136**	**-0.375±0.116**
AC 11:3	**-0.5279±0.1228**	**-0.4373±0.1106**	**-0.4645±0.106**	**-0.4444±0.1163**	**-0.4583±0.1092**	**-0.4194±0.1164**
AC 6:0 (OH)	-0.1804±0.143	-0.2766±0.1245	-0.2641±0.122	-0.349±0.1317	-0.2524±0.1248	-0.3396±0.1289
AC 8:0 (OH)	**-0.5216±0.1547**	**-0.4715±0.1356**	**-0.5013±0.1314**	**-0.4951±0.141**	**-0.4586±0.1366**	**-0.5015±0.1383**
AC 10:0 (OH)	**-0.5052±0.1553**	**-0.4684±0.1356**	**-0.5151±0.1308**	**-0.4811±0.1415**	**-0.4472±0.1369**	**-0.4867±0.1388**
FA 8:0 (DiC)	0.418±0.1427	0.2429±0.1337	0.2189±0.1323	0.3389±0.1333	0.267±0.1321	0.3203±0.1321
FA 10:1 (DiC)	-0.3826±0.131	-0.3028±0.1171	-0.2771±0.116	**-0.3373±0.1207**	-0.2765±0.119	**-0.3553±0.1179**
Keto 14:0	-0.2845±0.14	-0.2734±0.1223	-0.2349±0.1211	-0.3405±0.1266	-0.2729±0.1226	**-0.354±0.1244**
PA 22:3	-0.2523±0.1482	-0.2229±0.1302	-0.1487±0.1301	-0.2588±0.1351	-0.2295±0.1303	-0.2741±0.1327
PC 33:3/PE 36:3	-0.1924±0.1421	-0.0507±0.1288	-0.0566±0.1258	-0.0918±0.1331	-0.0836±0.1276	-0.0756±0.1316
PC 38:6/PE 41:6	**-0.4542±0.1404**	-0.3415±0.1272	-0.3354±0.1248	-0.3575±0.1327	-0.3411±0.1275	-0.3471±0.131
myo-inositol	0.1016±0.146	0.1201±0.1279	0.104±0.1257	0.0691±0.1339	0.1459±0.1281	0.0945±0.1315
LysoPC 14:0	0.0296±0.1545	-0.0175±0.1359	0.0794±0.1331	-0.057±0.1426	0.0022±0.136	-0.0604±0.1404
glycochenodeoxycholate	0.2999±0.1289	**0.3624±0.1108**	**0.3288±0.1092**	**0.3568±0.1162**	**0.3357±0.1115**	**0.3212±0.1148**
glycocholate	0.365±0.1334	**0.4169±0.1143**	**0.3532±0.1138**	**0.4312±0.1197**	**0.3705±0.1158**	**0.3972±0.1182**
taurocholate	0.1881±0.1245	0.069±0.1128	0.0995±0.1092	0.0947±0.1171	0.0659±0.1132	0.0736±0.1161
norhyodeoxycholic acid	**0.4594±0.1322**	0.2931±0.1251	0.308±0.1205	0.3247±0.13	0.2953±0.1252	0.2953±0.1303
DHEA sulfate	0.3231±0.17	0.1158±0.1572	0.2107±0.149	0.1487±0.1638	0.1331±0.1565	0.1244±0.1621
cycloheptanecarboxylic acid	**0.4161±0.1429**	0.2629±0.1321	0.2428±0.1305	0.3454±0.1329	0.2863±0.1307	0.3285±0.1316
dipeptide (tyrosine proline)	**0.4117±0.1277**	0.3032±0.1161	**0.3355±0.1115**	0.3095±0.122	0.2946±0.117	0.3036±0.12

Table S4.6. Association between annotated metabolites and HOMA-CP in girls (n=108). Sex-stratified regression models identifying annotated metabolites (p=550) linearly associated with HOMA-CP. All models were adjusted for age and puberty onset (Model 1), along with additional phenotypic measures to identify metabolites that drive the association with HOMA-CP including BMIz (Model 2), MUAMA (Model 3), MUAFA (Model 4), WHtR (Model 5) and TR+SS (Model 6). Values reported are β±Std Error. Metabolites with FDR<0.10 highlighted in red and bolded. Metabolites listed have an FDR<0.10 in Model 1 in the combined model and/or the sex-stratified models.

Metabolite	Model 1	Model 2	Model 3	Model 4	Model 5	Model 6
N-acetylglycine	**-0.8848±0.2336**	-0.6984±0.232	**-0.7536±0.2276**	-0.711±0.2374	-0.726±0.2373	-0.725±0.2424
N-acetyl-L-leucine	-0.0425±0.2538	0±0.2384	0.0034±0.2401	0.0705±0.2435	-0.0053±0.2427	0.0848±0.247
creatine	0.5518±0.2134	0.615±0.1982	0.5938±0.2	0.6161±0.2013	0.6115±0.2023	0.6271±0.2035
lysine	0.5171±0.1978	0.4024±0.1903	0.4368±0.1895	0.3988±0.1943	0.4054±0.1951	0.4131±0.1959
3,4-hydroxyphenyl-lactate	-0.1826±0.2508	-0.2311±0.2351	-0.2052±0.2366	-0.2313±0.2383	-0.2224±0.2394	-0.2046±0.2405
tyrosine	0.3363±0.2047	0.1164±0.2041	0.2087±0.1983	0.1665±0.2041	0.1531±0.2075	0.1635±0.2087
proline	0.6061±0.2297	0.5081±0.2186	0.4786±0.2226	0.5261±0.221	0.5061±0.2237	0.5222±0.2239
glucose	0.5391±0.2662	0.6071±0.2481	0.5716±0.2503	0.6044±0.2518	0.5938±0.2531	0.5832±0.2545
raffinose	0.1016±0.216	0.0893±0.2026	0.0813±0.2041	0.1142±0.2052	0.065±0.2066	0.129±0.2073
DG 32:0	**0.6923±0.1947**	0.4767±0.2041	0.534±0.1962	0.5236±0.2027	0.5368±0.2029	0.5524±0.2028
DG 34:0	0.548±0.1876	0.3236±0.196	0.4185±0.1846	0.3629±0.1968	0.3814±0.1959	0.3944±0.1967
DG 30:1	0.5519±0.1995	0.3277±0.2049	0.4095±0.1965	0.3791±0.2036	0.4082±0.2011	0.4065±0.2041
DG 32:1	**0.6784±0.2048**	0.4345±0.2168	0.5123±0.2056	0.4916±0.214	0.5089±0.2134	0.5212±0.2148
DG 34:1	**0.6164±0.1987**	0.3836±0.2079	0.4436±0.2008	0.4414±0.2049	0.4475±0.2068	0.4674±0.2059
DG 36:1	0.5463±0.1927	0.3343±0.1975	0.3724±0.1948	0.386±0.1958	0.3841±0.1987	0.4109±0.1964
DG 32:2	0.5027±0.1995	0.2098±0.2152	0.3295±0.1997	0.2799±0.2118	0.313±0.2084	0.3176±0.2116
DG 34:3	0.5746±0.2064	0.3129±0.2173	0.3996±0.2069	0.3545±0.2192	0.3973±0.2133	0.3912±0.2192
FA 12:2	**-0.6929±0.2256**	-0.6261±0.213	**-0.7506±0.2105**	-0.6277±0.2163	-0.6491±0.2162	-0.619±0.2194
FA 14:2	-0.5821±0.2197	-0.6161±0.2044	**-0.7734±0.2057**	-0.6228±0.2074	-0.6126±0.2085	-0.5945±0.21
FA 14:3	0.2493±0.206	0.1582±0.1955	0.1496±0.1974	0.1775±0.1976	0.1774±0.1987	0.1857±0.1994
FA 16:3	-0.5469±0.2192	-0.6168±0.2036	**-0.7632±0.2059**	-0.6213±0.2068	-0.6157±0.2078	-0.5945±0.2091
AC 2:0	-0.4848±0.2236	-0.3898±0.2126	-0.4416±0.2118	-0.4139±0.2146	-0.4284±0.215	-0.4228±0.2165

AC 6:0	-0.4726±0.2288	-0.4687±0.2141	-0.568±0.2148	-0.4759±0.217	-0.4883±0.2178	-0.4684±0.2193
AC 8:0	-0.3726±0.2112	-0.3329±0.1986	-0.4208±0.1986	-0.3451±0.2011	-0.3446±0.202	-0.3437±0.2031
AC 10:0	-0.4478±0.2144	-0.375±0.2029	-0.4673±0.2016	-0.3898±0.2053	-0.392±0.2062	-0.3937±0.2073
AC 12:0	-0.3368±0.2187	-0.2793±0.2062	-0.3755±0.2059	-0.2939±0.2086	-0.2871±0.2099	-0.2897±0.2109
AC 10:1	-0.3984±0.2208	-0.3557±0.2077	-0.4644±0.2076	-0.3537±0.2107	-0.3672±0.2113	-0.3474±0.2132
AC 12:1	-0.5177±0.2176	-0.5181±0.2034	-0.5639±0.2041	-0.5232±0.2061	-0.532±0.207	-0.5278±0.2081
AC 14:1	-0.465±0.2123	-0.386±0.2012	-0.4844±0.1996	-0.4059±0.2033	-0.4191±0.2037	-0.4135±0.2051
AC 10:2	-0.4191±0.2139	-0.3384±0.2028	-0.4069±0.2018	-0.3566±0.205	-0.3718±0.2053	-0.3693±0.2066
AC 12:2	**-0.7907±0.1953**	**-0.7095±0.1859**	**-0.7565±0.1843**	**-0.6873±0.1918**	**-0.7399±0.1878**	**-0.7049±0.1927**
AC 14:2	-0.5483±0.2083	-0.4857±0.1968	-0.547±0.1959	-0.5154±0.1984	-0.5161±0.1993	-0.5126±0.2006
AC 11:3	0.0029±0.2013	0.0338±0.189	-0.0862±0.1915	0.0769±0.1925	0.0132±0.1923	0.0794±0.1946
AC 6:0 (OH)	-0.4879±0.2149	-0.3969±0.2043	-0.4475±0.2035	-0.422±0.2062	-0.4386±0.2064	-0.4383±0.2075
AC 8:0 (OH)	-0.5417±0.2042	-0.4491±0.1947	-0.5472±0.1919	-0.4491±0.198	-0.4688±0.1977	-0.4586±0.1998
AC 10:0 (OH)	-0.5646±0.2098	-0.4745±0.1997	-0.5872±0.1968	-0.4784±0.2028	-0.4951±0.2028	-0.4834±0.205
FA 8:0 (DiC)	0.2066±0.2135	0.188±0.2004	0.0396±0.2081	0.2311±0.2028	0.186±0.2041	0.2423±0.2048
FA 10:1 (DiC)	0.1834±0.2274	0.2302±0.2131	0.222±0.2146	0.2583±0.2165	0.2307±0.2171	0.2657±0.2189
Keto 14:0	-0.5488±0.218	-0.4671±0.2068	-0.6231±0.2041	-0.4897±0.2088	-0.4914±0.2098	-0.4805±0.2117
PA 22:3	-0.4697±0.1968	-0.4428±0.1847	-0.3897±0.1885	-0.4409±0.1874	-0.4078±0.1899	-0.4392±0.1894
PC 33:3/PE 36:3	**-0.6254±0.1885**	-0.5684±0.1781	-0.5312±0.1822	**-0.5932±0.1795**	-0.5727±0.1816	**-0.6194±0.1803**
PC 38:6/PE 41:6	-0.0244±0.2298	-0.0399±0.2156	-0.0302±0.217	-0.0648±0.2187	-0.0401±0.2195	-0.0599±0.2208
myo-inositol	**0.8641±0.2443**	**0.8667±0.2272**	**0.9425±0.227**	**0.8729±0.2305**	**0.8642±0.2319**	**0.854±0.2336**
LysoPC 14:0	0.5803±0.1967	0.4149±0.1947	0.4263±0.1958	0.4465±0.1957	0.473±0.194	0.4811±0.1947
glycochenodeoxycholate	**1.0568±0.2013**	**0.9764±0.1911**	**0.9682±0.1938**	**1.0281±0.1904**	**0.9957±0.1941**	**1.0545±0.1912**
glycocholate	**0.8732±0.2028**	**0.7845±0.1934**	**0.7939±0.1944**	**0.8528±0.192**	**0.84±0.1937**	**0.8582±0.1939**
taurocholate	**-0.8494±0.2319**	**-0.7462±0.2212**	**-0.7618±0.222**	**-0.7536±0.2246**	**-0.7637±0.2251**	**-0.7897±0.2244**
norhyodeoxycholic acid	-0.0185±0.2127	0.0007±0.1995	0.0814±0.2026	0.0301±0.2027	0.0299±0.2036	-0.0157±0.2041
DHEA sulfate	0.6673±0.2799	0.5156±0.2683	0.4393±0.2779	0.5186±0.2729	0.5529±0.2718	0.5594±0.2731
cycloheptanecarboxylic acid	0.2088±0.2132	0.1889±0.2001	0.0461±0.2075	0.2253±0.2024	0.1864±0.2038	0.241±0.2044
dipeptide (tyrosine proline)	0.0374±0.2126	-0.0016±0.1997	-0.0003±0.2011	0.0412±0.2021	0.032±0.2031	0.0422±0.204

Figure 4.3. Insulin resistance is inversely associated with short- and medium-chain acylcarnitine metabolites.

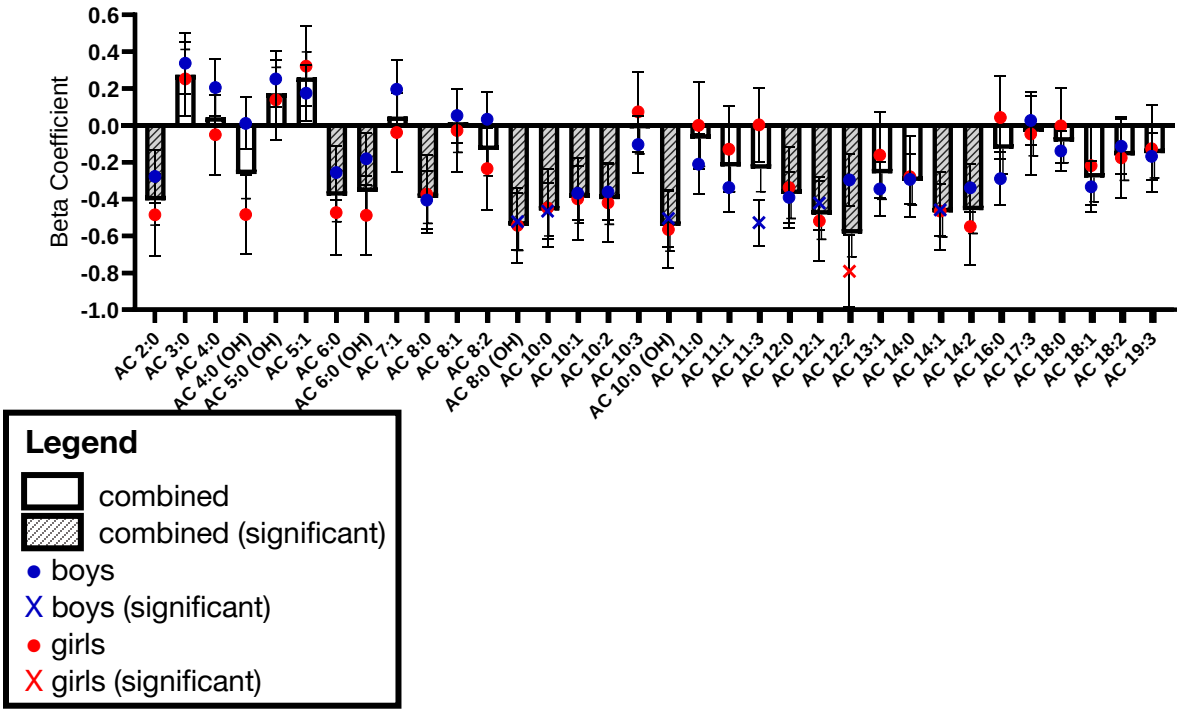

Linear models identified metabolites associated with HOMA-CP in the entire cohort, adjusting for age, sex, and puberty onset, and in sex-stratified models, adjusting for age and puberty onset. Beta coefficients representing the relationship between all AC with HOMA-CP in the entire cohort (bars) and boys (blue dots) and girls (red dots). Significance in the entire cohort depicted by striped gray bars (FDR<0.10). Signficance in sex-stratified models depicted by "X" (FDR<0.10).

Table S4.7. Linear relationship between energy adjusted macronutrient intake with BMIz and HOMA-CP. Carbohydrate and fat intake was adjusted for total energy intake using the residual method and standardized (mean 0, std 1). Linear models assessed the relationship between dietary intake with BMIz or HOMA-CP, adjusting for sex, age, and puberty onset.

	BMIz		HOMA-CP	
	β±SE	**Unadjusted p-value**	**β±SE**	**Unadjusted p-value**
carbohydrate	0.02872±0.085	0.7359	0.15307±0.1332	0.2519
fat	-0.05201±0.0851	0.5418	-0.18161±0.1332	0.1744

Figure 4.4. Structure of path analysis.

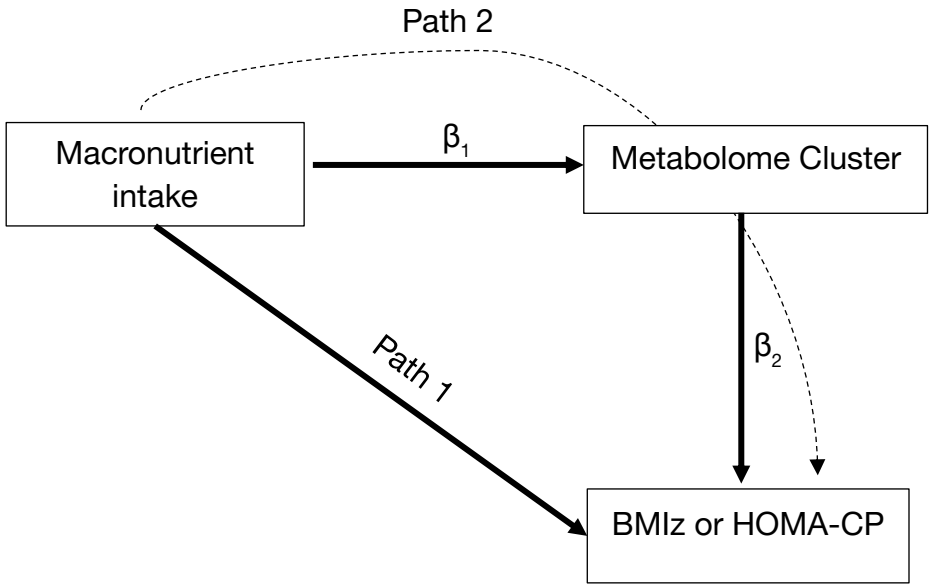

Path analysis classfied the effects of macronutrient intake (independent variable) on BMIz and HOMA-CP (dependent variable) through metabolome clusters. The relationship between the diet and each metabolome cluster is described by β_1. The relationship between each metabolome cluster and the outcome is described by β_2. Path 1 describes the influence of macronutrient intake on BMIz and HOMA-CP. Path 2 describes the influence of macronutrient intake on BMIz and HOMA-CP through metabolome clusters. The independent variables, energy adjusted fat and carbohydrate intake, were standardized (mean 0, standard deviation 1). All models adjusted for sex, puberty onset and age.

Figure 4.5. Clustering of annotated metabolites.

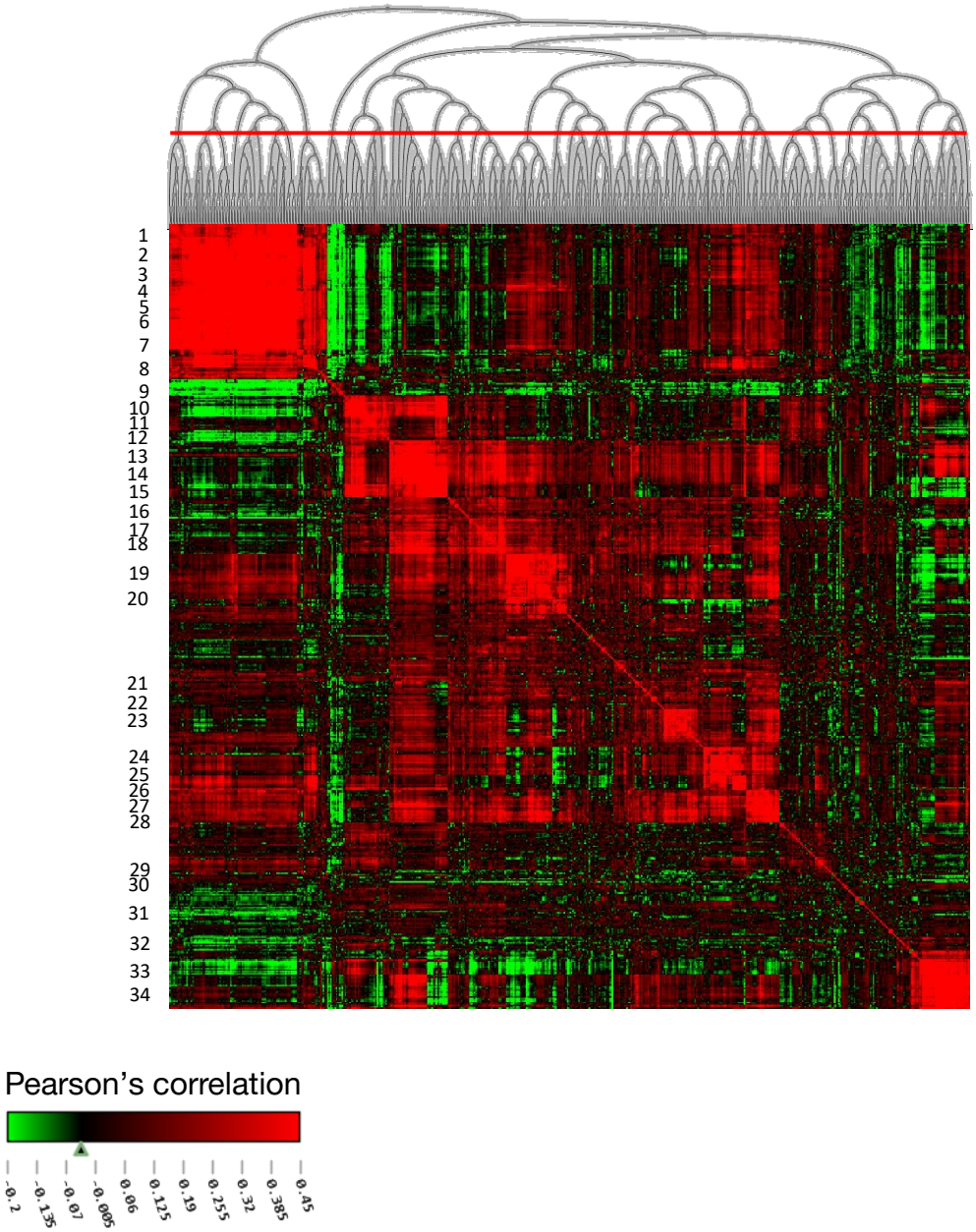

Pearson's correlation and hierarchical clustering identified connectivity between annotated metabolites (p=550). Clusters were formed based on dendrogram height (red line) and tightness of Pearson's correlation coefficient (r>0.2) creating 34 clusters. Cluster number listed next to the heat map.

Table S4.8. Classification of clusters. Annotated metabolites were clustered using hierarchical clustering. Cluster names and metabolites within each cluster are reported.

Cluster Number	Cluster Name	Metabolites
1	LC and VLC-FA (DiC),VLC-FA, PC/PE	FA 18:0 (DiC), FA 18:0 (OH), FA 24:1 (DiC), FA 26:1 (DiC), FA 26:2 (DiC), FA 26:5, estradiol valerate, PE-Cer d36:1, PC 34:0/PE 37:0, PC 36:5/PE 39:5, FA 27:2 (DiC), FA 28:6, FA 28:0, FA 26:3, FA 25:0, PE-Cer d34:2, FA 28:5
2	LC-FA	FA 14:0, FA 16:0, FA 17:2 (DiC), FA 24:1, FA 20:2, FA 18:3, FA 15:0, FA 18:1, FA 18:0, FA 18:2 , FA 16:1, FA 20:1, FA 20:0, FA 22:1, FA 24:2, phytanate
3	LC-FA	FA 22:2, FA 20:3, FA 22:5, FA 22:6, 7-oxo-11-octadecenoic acid, FA 22:3, FA 24:4, FA 17:1, FA 24:5, FA 20:5
4	Cer	Cer 41:0, PC 36:5/PE 39:5, Cer 35:0, Cer d42:1 (2OH), Cer d43:1 (2OH), Cer t40:0(2OH), Cer t41:0(2OH), Cer d40:1 (2OH), Cer 40:0, Cer d44:1 (2OH), Cer t42:0(2OH), PE-Cer d34:1, Cer d38:1 (2OH), Cer t38:0(2OH)
5	TG, Cer	TG 52:8, TG 50:8, TG 49:8, Cer 42:0, Cer 43:0, Cer 44:0
6	VLC-FA, VLC-FA (DiC), VLC-FA (OH)	FA 27:0 (OH), FA 26:2, FA 25:0 (OH), FA 25:2, FA 30:6, FA 24:0 (DiC), FA 26:1 , FA 16:0 (OH), LysoPC 20:4, FA 28:2 (DiC), FA 29:6, FA 26:0 (OH), FA 28:1 (DiC), FA 30:5
7	LysoPE, FA	Cer t34:0(2OH), LysoPC 18:3, FA 26:4, FA 20:4, LysoPE 16:0, LysoPE 18:0, LysoPS 21:0
8	LC-FA, odd-chain LC-FA, Cer	Cer 37:0, Cer 38:0, Cer t36:0(2OH), Cer 36:0, FA 17:0, FA 19:1, FA 14:1, FA 19:0, FA 16:2, FA 12:0, FA 14:2, FA 16:3, Keto 18:0, FA 21:5, dihomoursodeoxycholic acid , FA 24:0 (OH), FA 20:6, FA 27:1 (DiC), 3,7-dihydroxy-5-cholestanoic acid, FA 25:1, FA 22:0
9	bile acids, glucose, PS	1-octadecanoyl-rac-glycerol, glucose, taurocholate, rac-glycerol-1-myristate, norhyodeoxycholic acid , hyodeoxycholic acid, PC 34:2/PE 37:2, PS 39:6, PS 41:6, PS 41:7, PC 36:4/PE 39:4, traumatin
10	malate intermediates, PA, MC-FA (DiC)	2-methylmaleate, citramalate, PA 18:3, FA 9:0, FA 16:4, 9,10,13-Trihydroxy-11-octadecenoic acid, PG 31.4, PA 20:3, cortisol 21-acetate, FA 7:1 (DiC) , FA 8:0 (Dic, OH) , FA 15:4, 5-hydroxytryptophan, FA 13:4
11	Glucose metabolites, BCAA metabolites, xanthine	S-3-methyl-2-oxopentanoate, 4-methyl-2-oxopentanoate, methyl-acetoacetate, allose, glyceraldehyde, malate, xanthine, possible peptide, dipeptide (HIS TYR), diethylstilbestrol
12	Glucose metabolites, acetyl-amino acids	L-histidine, N-acetyl-D-glucosamine, N-acetyl-DL-serine, 3,4-hydroxyphenyl-lactate, 2-deoxy-D-glucose, N-acetylglycine, D-lyxose

13	MC-FA (DiC)	FA 11:1 (DiC,OH), 4-hydroxyphenylethanol, FA 10:0 (DiC), C8 H12 N6 O2, phenylacetic acid
14	MC-FA (DiC OH), LC-FA (DiC, OH)	C8 H14 O2, FA 9:0 (DiC,OH), FA 17:0 (DiC,OH), FA 10:1 (DiC, OH) , FA 11:0 (DiC,OH), FA 9:1 (DiC) , FA 20:3 (DiC, diOH) , porphobilinogen, 5-methoxytryptophol, C9 H16 O2, FA 8:1 (DiC) , FA 11:1 (DiC, OH), chlorpheniramine, FA 18:0 (DiC,OH), FA 10:0 (DiC,OH)
15	odd-chain MC-FA (DiC)	FA 9:0 (DiC) , FA 11:0 (DiC), FA 7:0 (DiC) , 3-hydroxybenzyl alcohol, debrisoquin, FA 5:0 (DiC), FA 6:0 (DiC), FA 9:0 (OH), FA 13:0 (DiC), 17-alpha-hydroxyprogesterone, FA 8:0 (DiC), cycloheptanecarboxylic acid, 3-methyladipic acid, LysoPA 20.5
16	BCAA, BCAA metabolite, reflect mitochondrial metabolism	3-methoxytyrosine, thyroxine, isovalerylcarnitine , AC 4:0, AC 5:1 , leucine, glutarylcarnitine, salsolinol, methyl-jasmonate, N-undecanoylglycine, alpha-tocopherol, FA 22:4, quinolin-2-ol, 2-deoxyinosine, N-cyclohexylformamide
17	homocysteine, phenylalanine metabolite	S-adenosyl-L-homocysteine, sphingosine, dipeptide (glutamate phenylalanine), phenylethanolamine, dipeptide (serine isoleucine/leucine)
18	BCAA, BCAA metabolites, aromatic amino acids, methionine	isoleucine, valine, dipeptide (glutamate isoleucine/leucine), AC 3:0, tyrosine, n-gamma-L-glutamyl-L-methionine , serine, methionine, taurolithocholate, 1-methyladenosine, indolelactic acid, 5-hydroxy-1,4-naphthoquinone, pantothenate, AC 5:0 (OH) , AC 11:0, phenylalanine, normethanephrine, L-gamma-glutamyl-L-isoleucine , 5-methylthioadenosine, S-Allyl-L-cysteine
19	DG, PC/PE, LysoPC	DG 35:1, DG 36:1, DG 35:2, DG 34:1, DG 34:2, DG 34:3, DG 35:3, DG 32:0, DG 32:1, DG 33:1, DG 38:3, DG 38:4, DG 36:3, PE 36:2, 1-oleoyl-rac-glycerol, LysoPC 16:1, LysoPC 20:3, LysoPC 18:0, LysoPC 16:0, LysoPC 14:0, LysoPC 15:0, PC 36:2/PE 39:2, PC 36:3/PE 39:3, PC 36:1/PE 39:1, PS 39:4, PC 34:3/PE 37:3, PS 37:6, PC 34:1/PE 37:1, PC 40:4/PE 43:4, PC 40:5/PE 43:5, DG 38:5, PC 31:5/PE 34:5
20	DG, PC/PE, PS	DG 30:1 , DG 32:2, DG 34:0, PS 35:5 , PS 37:5 , PC 32:1/PE 35:1, PS 35:4, PC 32:2/PE 35:2, PC 32:4/PE 35:4, PS 39:8
21	polar metabolites, urate	2-acetyl-pyrolidine, 3-amino-5-hydroxybenzoic acid, urate, 3-aminoisobutanoate, 4-acetamidobutanoate, pinitol, methyl beta-D-galactoside, AC 7:1, AC 8:2, m-hydroxymandelic acid, SM d36:1, dipeptide (tyrosine proline), 1,3,7-trimethyluric acid, C16 Sphinganine , bilirubin
22	dipeptides, cortisol, vitamin metabolites	deoxyuridine, possible peptide, LysoPE 18:2, PC 41:7/PE 44:7, possible peptide, AC 11:1, AC 13:1, PS 40:7, PC 33:3/PE 36:3, bis(2-ethylhexyl)phthalate, PS 42:6, tricarballylic acid, ascorbate, hypoxanthine, dipeptide (phenylalanine phenylalanine), 15R-PGE2 methyl ester, 15-acetate, 3-dehydroxycarnitine, PC 33:3/PE 36:3, cortisol, 5-methyltetrahydrofolate

23	PC/PE	PC 39:8/PE 42:8, PC 37:4/PE 40:4, PC 35:5/PE 38:5, PS 40:4, PC 43:8/PE 46:8, PC 33:4/PE 36:4, PS 42:3, PS 44:3, PC 35:5/PE 38:5, PS 38:4, PC 34:5/PE 37:5, PC 34:7/PE 37:7, PC 35:3/PE 38:3, PC 37:7/PE 40:7, PC 37:5/PE 40:5, PC 35:4/PE 38:4
24	PC/PE, PS	PC 41:8/PE 44:8, PS 42:3, PC 43:7/PE 46:7, PC 40:8/PE 43:8, PC 38:6/PE 41:6, AC 18:0, possible peptide, tripeptide (cysteine histidine lysine), PS 40:3, PS 38:7, dethiobiotin
25	MC-AC	AC 4:0 (OH), AC 6:0 (OH) , O-adipoylcarnitine, N-acetyl-DL-methionine, pterin, AC 8:0 (OH), AC 10:0 (OH), AC 12:0, AC 8:0, AC 10:0, AC 10:1, AC 14:1 , AC 14:2, AC 12:1 , AC 2:0, AC 6:0, AC 8:1, AC 10:3, AC 10:2, AC 12:2
26	MC/LC-FA (DiC), FA (OH)	FA 10:0 (OH) , 7-oxo-11E-tetradecenoic acid, FA 12:0 (OH), Keto 14:0, 7-oxo-11-hexadecenoic acid, FA 12:2, FA 14:0 (DiC), FA 16:0 (DiC), FA 12:0 (DiC), FA 14:0 (OH)
27	LC AC, SM	SM d40:1, SM d42:1, PC 35:3/PE 38:3, PS 46:6, AC 14:0, AC 18:1, AC 16:0, AC 18:2 , PC 42:7/PE 45:7
28	PI, SM, PC/PE	PI 41:1, PI 42:1, PI 43:1, SM d41:2, SM d42:2, SM d34:1, SM d34:2, SM d36:2, cholesterol, SM d32:1, SM d33:1, PC 34:0, PC 39:5/PE 42:5, PC 32:0/PE 35:0
29	Krebs Cycle intermediates	FA 18:1 (DiC), FA 18:2 (DiC), trans-aconitate, citrate, isocitrate, glucaric acid, glucuronic acid, salicyluric acid, AC 19:3
30	choline, betaine	betaine, 5-aminopentanoate, choline, fluvoxamino acid, pyridoxamine, N-acetyl-L-alanine
31	lactose, MC-FA (keto), amino acids metabolites	16-bromo-9E-hexadecenoic acid , FA 22:2 (DiC), AC 11:3, monoethylhexyl phthalic acid, LL-2,6-diaminoheptanedioate, N-(tert-Butoxycarbonyl)-L-methionine , possible peptide, lactose, N-acetylneuraminate, 5-oxo-7-octenoic acid
32	PA, di-/tri-peptides	Tripeptide (glycine proline valine), tripeptide (tryptophan tyrosine isoleucine/leucine), inosine, guanosine, dipeptide (isoleucine/leucine alanine) , N6,N6,N6-trimethyl-L-lysine, PA 17:3, FA 18:4, PA 19.3, PA 21:3, PA 23:3, PA 22:3, PA 24:3, PA 25:3, FA 15:0 (Dic, OH) , dipeptide (methionine isoleucine/leucine), riboflavin
33	LC-FA (DiC, OH)	FA 12:0 (DiC,OH), FA 16:0 (DiC,OH), FA 18:3 (DiC, diOH) , FA 13:0 (DiC,OH), FA 14:3 (DiC, diOH), FA 14:1 (DiC, OH), testosterone, Methyl 8-2-2-formyl-vinyl-3-hydroxy-5-oxo-cyclopentyl]-octanoate
34	MC-FA (DiC), PI	FA 17:3 (DiC, diOH), PI 36:1, PI 34:1, PC 40:7/PE 43:7, PI 37:1 , PI 38:1 , FA 21:3 (DiC, diOH) , FA 12:1 (DiC), FA 14:1 (DiC), FA 19:3 (DiC, diOH) , FA 10:1 (DiC) , FA 14:0 (DiC,OH)

Table S4.9. Path analysis demonstrating the relationship between macronutrient intake with BMIz through metabolome clusters, adjusting for age, sex and puberty onset. Association between energy-adjusted fat and carbohydrate intake (mean 0, standard deviation 1) and metabolome clusters (β1), adjusting for age, sex and puberty onset. Association between metabolome clusters and BMIz (β2), adjusting for sex, age and puberty onset. Significant relationships in bold and red fill (α=0.05). Sobel testing tested the relationship between the independent variable and dependent variable when including the mediator, the metabolome cluster, in the model. Significant relationships in bold and red fill (α=0.05).

Cluster Number	Cluster Classification	Macronutrient intake and the metabolome		Metabolome and BMIz		Sobel's test	
		β_1±SE	p-value	β_2±SE	p-value	t-statistic	p-value
Carbohydrate							
1	LC and VLC-FA (DiC),VLC-FA, PC/PE	-0.01±0.038	0.799	-0.148±0.164	0.368	0.244	0.807
2	LC-FA	-0.049±0.065	0.449	0.12±0.092	0.189	-0.656	0.512
3	LC-FA	-0.093±0.065	0.151	0.068±0.093	0.462	-0.654	0.513
4	Cer	-0.027±0.065	0.673	0.015±0.092	0.866	-0.156	0.876
5	TG, Cer	-0.041±0.062	0.503	0.003±0.096	0.972	-0.035	0.972
6	VLC-FA, VLC-FA (DiC), VLC-FA (OH)	-0.024±0.062	0.702	-0.108±0.096	0.260	0.363	0.717
7	LysoPE, FA	-0.021±0.062	0.736	0.032±0.096	0.739	-0.237	0.813
8	LC-FA, odd-chain LC-FA, Cer	-0.039±0.032	0.217	0.315±0.202	0.119	-0.968	0.333
9	bile acids, glucose, PS	0.007±0.01	0.452	0.933±1.173	0.427	0.547	0.585
10	malate intermediates, PA, MC-FA (DiC)	-0.088±0.041	**0.030**	0.063±0.151	0.679	-0.407	0.684
11	Glucose metabolites, BCAA metabolites, xanthine	-0.104±0.066	0.118	0.063±0.091	0.487	-0.635	0.525
12	Glucose metabolites, acetyl-amino acids	-0.028±0.038	0.452	0.105±0.179	0.559	-0.461	0.645
13	MC-FA (DiC)	-0.166±0.054	**0.002**	0.071±0.108	0.509	-0.645	0.519
14	MC-FA (DiC OH), LC-FA (DiC, OH)	-0.18±0.055	**0.001**	0.15±0.107	0.159	-1.293	0.196
15	odd-chain MC-FA (DiC)	-0.114±0.055	**0.037**	0.201±0.108	0.062	-1.390	0.164
16	BCAA, BCAA metabolite	-0.067±0.033	**0.046**	0.312±0.23	0.175	-1.123	0.262
17	homocysteine, phenylalanine metabolite	-0.017±0.066	0.798	0.284±0.109	**0.009**	-0.255	0.799
18	BCAA, BCAA metabolites, aromatic amino acids, methionine	-0.062±0.036	0.085	0.467±0.174	**0.007**	-1.450	0.147

19	DG, PC/PE, LysoPC	-0.015±0.06	0.803	0.419±0.098	**0.000**	-0.250	0.803
20	DG, PC/PE, PS	0.043±0.056	0.438	0.26±0.114	**0.022**	0.735	0.462
21	polar metabolites, urate	0.015±0.013	0.226	-0.402±0.585	0.492	-0.597	0.550
22	dipeptides, cortisol, vitamin metabolites	0±0.032	0.994	0.258±0.189	0.171	0.008	0.994
23	PC/PE	-0.055±0.063	0.386	-0.202±0.098	**0.038**	0.800	0.424
24	PC/PE, PS	-0.057±0.05	0.249	-0.122±0.141	0.386	0.693	0.488
25	MC-AC	-0.004±0.001	**0.001**	-0.08±0.149	0.591	0.531	0.596
26	MC/LC-FA (DiC), FA (OH)	-0.132±0.065	**0.043**	-0.078±0.091	0.393	0.787	0.431
27	LC AC, SM	-0.028±0.038	0.455	0.138±0.163	0.398	-0.560	0.575
28	PI, SM, PC/PE	-0.052±0.045	0.244	0.17±0.138	0.220	-0.845	0.398
29	Krebs Cycle intermediates	0.014±0.034	0.690	-0.113±0.2	0.571	-0.326	0.744
30	choline, betaine	-0.052±0.069	0.444	-0.039±0.084	0.644	0.396	0.692
31	lactose, MC-FA (keto), amino acids metabolites	0.069±0.042	0.103	-0.278±0.216	0.197	-1.013	0.311
32	PA, di-/tri-peptides	-0.021±0.026	0.403	-0.236±0.239	0.322	0.639	0.523
33	LC-FA (DiC, OH)	-0.131±0.067	0.050	-0.043±0.088	0.628	0.470	0.638
34	MC-FA (DiC), PI	-0.111±0.058	0.057	-0.098±0.103	0.341	0.851	0.395
	Fat						
1	LC and VLC-FA (DiC),VLC-FA, PC/PE	0.01±0.038	0.789	-0.148±0.164	0.368	-0.257	0.797
2	LC-FA	0.033±0.065	0.606	0.12±0.092	0.189	0.480	0.631
3	LC-FA	0.09±0.065	0.169	0.068±0.093	0.462	0.648	0.517
4	Cer	0.022±0.065	0.735	0.015±0.092	0.866	0.151	0.880
5	TG, Cer	0.036±0.062	0.560	0.003±0.096	0.972	0.035	0.972
6	VLC-FA, VLC-FA (DiC), VLC-FA (OH)	0.025±0.062	0.694	-0.108±0.096	0.260	-0.371	0.711
7	LysoPE, FA	0.01±0.062	0.870	0.032±0.096	0.739	0.147	0.883
8	LC-FA, odd-chain LC-FA, Cer	0.037±0.032	0.240	0.315±0.202	0.119	0.937	0.349
9	bile acids, glucose, PS	-0.005±0.009	0.564	0.933±1.173	0.427	-0.467	0.641
10	malate intermediates, PA, MC-FA (DiC)	0.094±0.041	**0.020**	0.063±0.151	0.679	0.408	0.684
11	Glucose metabolites, BCAA metabolites, xanthine	0.114±0.066	0.086	0.063±0.091	0.487	0.644	0.519
12	Glucose metabolites, acetyl-amino acids	0.03±0.038	0.424	0.105±0.179	0.559	0.472	0.637

13	MC-FA (DiC)	0.159±0.054	**0.003**	0.071±0.108	0.509	0.644	0.520
14	MC-FA (DiC OH), LC-FA (DiC, OH)	0.179±0.055	**0.001**	0.15±0.107	0.159	1.291	0.197
15	odd-chain MC-FA (DiC)	0.131±0.055	**0.017**	0.201±0.108	0.062	1.472	0.141
16	BCAA, BCAA metabolite	0.075±0.034	**0.027**	0.312±0.23	0.175	1.157	0.247
17	homocysteine, phenylalanine metabolite	0.033±0.066	0.622	0.284±0.109	**0.009**	0.484	0.628
18	BCAA, BCAA metabolites, aromatic amino acids, methionine	0.067±0.036	0.060	0.467±0.174	**0.007**	1.539	0.124
19	DG, PC/PE, LysoPC	-0.012±0.06	0.841	0.419±0.098	**0.000**	-0.200	0.842
20	DG, PC/PE, PS	-0.075±0.056	0.181	0.26±0.114	**0.022**	-1.154	0.249
21	polar metabolites, urate	-0.01±0.012	0.380	-0.402±0.585	0.492	0.541	0.589
22	dipeptides, cortisol, vitamin metabolites	0.005±0.032	0.869	0.258±0.189	0.171	0.164	0.870
23	PC/PE	0.091±0.063	0.146	-0.202±0.098	**0.038**	-1.189	0.235
24	PC/PE, PS	0.084±0.05	0.090	-0.122±0.141	0.386	-0.772	0.440
25	MC-AC	0.163±0.042	**0.000**	-0.08±0.149	0.591	-0.532	0.595
26	MC/LC-FA (DiC), FA (OH)	0.16±0.065	**0.014**	-0.078±0.091	0.393	-0.807	0.420
27	LC AC, SM	0.036±0.038	0.350	0.138±0.163	0.398	0.627	0.531
28	PI, SM, PC/PE	0.057±0.045	0.204	0.17±0.138	0.220	0.883	0.377
29	Krebs Cycle intermediates	-0.01±0.034	0.768	-0.113±0.2	0.571	0.262	0.794
30	choline, betaine	0.076±0.068	0.268	-0.039±0.084	0.644	-0.426	0.670
31	lactose, MC-FA (keto), amino acids metabolites	-0.059±0.042	0.160	-0.278±0.216	0.197	0.951	0.342
32	PA, di-/tri-peptides	0.014±0.025	0.591	-0.236±0.239	0.322	-0.473	0.636
33	LC-FA (DiC, OH)	0.102±0.067	0.128	-0.043±0.088	0.628	-0.461	0.645
34	MC-FA (DiC), PI	0.09±0.059	0.124	-0.098±0.103	0.341	-0.809	0.418

Table S4.10. Path analysis demonstrating the relationship between macronutrient intake with HOMA-CP through metabolome clusters, adjusting for age, sex and puberty onset. Association between energy-adjusted fat and carbohydrate intake (mean 0, standard deviation 1) and metabolome clusters (β1), adjusting for age, sex and puberty onset. Association between metabolome clusters and HOMA-CP (β2), adjusting for sex, age and puberty onset. Significant relationships in bold and red fill (α=0.05). Sobel testing tested the relationship between the independent variable and dependent variable when including the mediator, the metabolome cluster, in the model. Significant relationships in bold and red fill (α=0.05).

Cluster Number	Cluster Classification	Macronutrient intake and the metabolome		Metabolome and HOMA-CP		Sobel's test	
		β_1±SE	p-value	β_2±SE	p-value	t-statistic	p-value
Carbohydrate							
1	LC and VLC-FA (DiC),VLC-FA, PC/PE	-0.01±0.038	0.799	0.118±0.257	0.646	-0.222	0.824
2	LC-FA	-0.049±0.065	0.449	-0.052±0.145	0.717	0.327	0.744
3	LC-FA	-0.093±0.065	0.151	-0.017±0.146	0.908	0.116	0.908
4	Cer	-0.027±0.065	0.673	0.024±0.144	0.866	-0.156	0.876
5	TG, Cer	-0.041±0.062	0.503	-0.012±0.151	0.936	0.080	0.936
6	VLC-FA, VLC-FA (DiC), VLC-FA (OH)	-0.024±0.062	0.702	0.055±0.151	0.715	-0.264	0.792
7	LysoPE, FA	-0.021±0.062	0.736	-0.021±0.062	0.739	0.237	0.813
8	LC-FA, odd-chain LC-FA, Cer	-0.039±0.032	0.217	-0.556±0.319	0.081	1.008	0.314
9	bile acids, glucose, PS	0.007±0.01	0.452	-0.941±1.628	0.563	-0.458	0.647
10	malate intermediates, PA, MC-FA (DiC)	-0.088±0.041	**0.030**	0.235±0.238	0.322	-0.901	0.368
11	Glucose metabolites, BCAA metabolites, xanthine	-0.104±0.066	0.118	0.056±0.143	0.695	-0.380	0.704
12	Glucose metabolites, acetyl-amino acids	-0.028±0.038	0.452	-0.026±0.281	0.927	0.091	0.927
13	MC-FA (DiC)	-0.166±0.054	**0.002**	-0.023±0.17	0.894	0.133	0.894
14	MC-FA (DiC OH), LC-FA (DiC, OH)	-0.18±0.055	**0.001**	0.178±0.168	0.288	-1.010	0.312
15	odd-chain MC-FA (DiC)	-0.114±0.055	**0.037**	0.361±0.169	**0.033**	-1.490	0.136
16	BCAA, BCAA metabolite	-0.067±0.033	**0.046**	0.282±0.354	0.427	-0.739	0.460
17	homocysteine, phenylalanine metabolite	-0.017±0.066	0.798	0.155±0.168	0.356	-0.247	0.805
18	BCAA, BCAA metabolites, aromatic amino acids, methionine	-0.062±0.036	0.085	0.487±0.268	0.070	-1.250	0.211

19	DG, PC/PE, LysoPC	-0.015±0.06	0.803	0.423±0.156	**0.007**	-0.249	0.803
20	DG, PC/PE, PS	0.043±0.056	0.438	0.435±0.179	**0.015**	0.739	0.460
21	polar metabolites, urate	0.015±0.013	0.226	-0.848±0.952	0.373	-0.717	0.473
22	dipeptides, cortisol, vitamin metabolites	0±0.032	0.994	-0.271±0.294	0.356	-0.008	0.994
23	PC/PE	-0.055±0.063	0.386	-0.23±0.154	**-0.136**	0.750	0.453
24	PC/PE, PS	-0.057±0.05	0.249	-0.294±0.221	0.184	0.870	0.384
25	MC-AC	-0.004±0.001	**0.001**	-0.833±0.24	**0.001**	2.439	**0.015**
26	MC/LC-FA (DiC), FA (OH)	-0.132±0.065	**0.043**	-0.383±0.141	**0.006**	1.625	0.104
27	LC AC, SM	-0.028±0.038	0.455	-0.418±0.258	0.105	0.679	0.497
28	PI, SM, PC/PE	-0.052±0.045	0.244	0.036±0.216	0.870	-0.162	0.871
29	Krebs Cycle intermediates	0.014±0.034	0.690	0.175±0.316	0.579	0.324	0.746
30	choline, betaine	-0.052±0.069	0.444	-0.114±0.132	0.389	0.572	0.567
31	lactose, MC-FA (keto), amino acids metabolites	0.069±0.042	0.103	-0.241±0.342	0.480	-0.649	0.517
32	PA, di-/tri-peptides	-0.021±0.026	0.403	-0.481±0.379	0.205	0.699	0.485
33	LC-FA (DiC, OH)	-0.131±0.067	0.050	0.004±0.139	0.979	-0.026	0.979
34	MC-FA (DiC), PI	-0.111±0.058	0.057	-0.196±0.162	0.225	1.023	0.307
	Fat						
1	LC and VLC-FA (DiC),VLC-FA, PC/PE	0.01±0.038	0.789	0.118±0.257	0.646	0.231	0.817
2	LC-FA	0.033±0.065	0.606	-0.052±0.145	0.717	-0.296	0.767
3	LC-FA	0.09±0.065	0.169	-0.017±0.146	0.908	-0.116	0.908
4	Cer	0.022±0.065	0.735	0.024±0.144	0.866	0.151	0.880
5	TG, Cer	0.036±0.062	0.560	-0.012±0.151	0.936	-0.080	0.936
6	VLC-FA, VLC-FA (DiC), VLC-FA (OH)	0.025±0.062	0.694	0.055±0.151	0.715	0.267	0.789
7	LysoPE, FA	0.01±0.062	0.870	-0.021±0.062	0.739	-0.147	0.883
8	LC-FA, odd-chain LC-FA, Cer	0.037±0.032	0.240	-0.556±0.319	0.081	-0.974	0.330
9	bile acids, glucose, PS	-0.005±0.009	0.564	-0.941±1.628	0.563	0.408	0.683
10	malate intermediates, PA, MC-FA (DiC)	0.094±0.041	**0.020**	0.235±0.238	0.322	0.911	0.363
11	Glucose metabolites, BCAA metabolites, xanthine	0.114±0.066	0.086	0.056±0.143	0.695	0.382	0.702
12	Glucose metabolites, acetyl-amino acids	0.03±0.038	0.424	-0.026±0.281	0.927	-0.091	0.927

13	MC-FA (DiC)	0.159±0.054	**0.003**	-0.023±0.17	0.894	-0.133	0.894
14	MC-FA (DiC OH), LC-FA (DiC, OH)	0.179±0.055	**0.001**	0.178±0.168	0.288	1.010	0.313
15	odd-chain MC-FA (DiC)	0.131±0.055	**0.017**	0.361±0.169	**0.033**	1.592	0.111
16	BCAA, BCAA metabolite	0.075±0.034	**0.027**	0.282±0.354	0.427	0.748	0.454
17	homocysteine, phenylalanine metabolite	0.033±0.066	0.622	0.155±0.168	0.356	0.435	0.664
18	BCAA, BCAA metabolites, aromatic amino acids, methionine	0.067±0.036	0.060	0.487±0.268	0.070	1.305	0.192
19	DG, PC/PE, LysoPC	-0.012±0.06	0.841	0.423±0.156	**0.007**	-0.199	0.842
20	DG, PC/PE, PS	-0.075±0.056	0.181	0.435±0.179	**0.015**	-1.171	0.242
21	polar metabolites, urate	-0.01±0.012	0.380	-0.848±0.952	0.373	0.625	0.532
22	dipeptides, cortisol, vitamin metabolites	0.005±0.032	0.869	-0.271±0.294	0.356	-0.162	0.871
23	PC/PE	0.091±0.063	0.146	-0.23±0.154	**-0.136**	-1.041	0.298
24	PC/PE, PS	0.084±0.05	0.090	-0.294±0.221	0.184	-1.045	0.296
25	MC-AC	0.163±0.042	**0.000**	-0.833±0.24	**0.001**	-2.587	**0.010**
26	MC/LC-FA (DiC), FA (OH)	0.16±0.065	**0.014**	-0.383±0.141	**0.006**	-1.824	0.068
27	LC AC, SM	0.036±0.038	0.350	-0.418±0.258	0.105	-0.809	0.418
28	PI, SM, PC/PE	0.057±0.045	0.204	0.036±0.216	0.870	0.163	0.871
29	Krebs Cycle intermediates	-0.01±0.034	0.768	0.175±0.316	0.579	-0.260	0.794
30	choline, betaine	0.076±0.068	0.268	-0.114±0.132	0.389	-0.680	0.496
31	lactose, MC-FA (keto), amino acids metabolites	-0.059±0.042	0.160	-0.241±0.342	0.480	0.632	0.528
32	PA, di-/tri-peptides	0.014±0.025	0.591	-0.481±0.379	0.205	-0.495	0.620
33	LC-FA (DiC, OH)	0.102±0.067	0.128	0.004±0.139	0.979	0.026	0.979
34	MC-FA (DiC), PI	0.09±0.059	0.124	-0.196±0.162	0.225	-0.952	0.341

Table S4.11. Differences in IGF-1 levels between pubteral and pre-pubertal children. Puberty levels classified by pubertal onset variable. Values for IGF-1 are in ng/mL. Represents a paired t-test.

Subjects	Pubertal		Pre-Pubertal		t-test	
	Mean	StdDev	Mean	StdDev	t-value	unadjusted p-value
Combined	306	112	217	73	-6.83	<0.0001
Boys	269	109	196	63	-4.00	0.0001
Girls	356	96	231	76	-6.78	<0.0001

References

1. Ng M, Fleming T, Robinson M, Thomson B, Graetz N, Margono C, Mullany EC, Biryukov S, Abbafati C, Abera SF, et al. Global, regional, and national prevalence of overweight and obesity in children and adults during 1980-2013: A systematic analysis for the Global Burden of Disease Study 2013. Lancet. 2014;384:766–81.

2. Roglic G, Varghese C, Riley L, Harvey A, Krung E, Alwan A, Cowan M, Savin S, Armstrong T, Banatvala N, et al. Global report on diabetes. Geneva, Switzerland. 2016.

3. Perng W, Gillman MW, Fleisch AF, Michalek RD, Watkins SM, Isganaitis E, Patti M-E, Oken E. Metabolomic profiles and childhood obesity. Obesity. 2014;22:2570–8.

4. Butte NF, Liu Y, Zakeri IF, Mohney RP, Metha N, Voruganti VS, Goring H, Cole SA, Comuzzie AG. Global metabolomic profiling targeting childhood obesity in the hispanic Population. Am J Clin Nutr. 2015;102:256–67.

5. Mccormack SE, Shaham O, Mccarthy MA, Deik AA, Wang TJ, Gerszten RE, Clish CB, Mootha VK, Grinspoon SK, Fleischman A. Circulating branched-chain amino acid concentrations are associated with obesity and future insulin resistance in children and adolescents. Pediatr Obes. 2013;8:52–61.

6. Mihalik SJ, Michaliszyn SF, De Las Heras J, Bacha F, Lee S, Chace DH, De Jesus VR, Vockley J, Arslanian SA. Metabolomic Profiling of Fatty Acid and Amino Acid Metabolism in Youth With Obesity and Type 2 Diabetes. Diabetes Care. 2012;35:605–11.

7. Mastrangelo A, Martos-Moreno G, García A, Barrios V, Rupérez FJ, Chowen JA, Barbas C, Argente J. Insulin resistance in prepubertal obese children correlates with sex-dependent early onset metabolomic alterations. Int J Obes. 2016;40:1494–502.

8. Newbern D, Gumus Balikcioglu P, Balikcioglu M, Bain J, Muehlbauer M, Stevens R, Ilkayeva O, Dolinsky D, Armstrong S, Irizarry K, et al. Sex Differences in Biomarkers Associated With Insulin Resistance in Obese Adolescents: Metabolomic Profiling and Principal Components Analysis. J Clin Endocrinol Metab. 2014;99:4730–9.

9. Perng W, Tang L, Song PXK, Tellez-rojo MM, Cantoral A, Peterson KE. Metabolomic profiles and development of metabolic risk during the pubertal transition: a prospective study in the ELEMENT Project. Pediatr Res. 2019;85:262–8.

10. Jensen MD, Haymond MW, Rizza RA, Cryer PE, Miles JM. Influence of body fat distribution on free fatty acid metabolism in obesity. J Clin Invest. 1989;83:1168–73.

11. Frohnert BI, Jacobs DR, Steinberger J, Moran A, Steffen LM, Sinaiko AR. Relation between serum free fatty acids and adiposity, insulin resistance, and cardiovascular risk factors from adolescence to adulthood. Diabetes. 2013;62:3163–9.

12. Gow ML, Ho M, Burrows TL, Baur LA, Stewart L, Hutchesson MJ, Cowell CT, Collins CE, Garnett SP. Impact of dietary macronutrient distribution on BMI and cardiometabolic outcomes in overweight and obese children and adolescents: A systematic review. Nutr Rev. 2014;72:453–70.

13. Urrusquieta-Flores HM, Padilla-Raygoza N, Jimenez-García SN, Moreno ER, Guerrero

VB, Arias-rico J. Relationship among macronutrient intake and overweight/obesity in school children from Celaya, Mexico. J child Adolesc Heal. 2017;1:1–4.

14. Sjoberg Brixval C, Andersen LB, Lilienthal Heitmann B. Fat intake and weight development from 9 to 16 years of age: The European youth heart study - A longitudinal study. Obes Facts. 2009;2:166–70.

15. Henderson M, Benedetti A, Gray-Donald K. Dietary composition and its associations with insulin sensitivity and insulin secretion in youth. Br J Nutr. 2014;111:527–34.

16. Simoneau J-A, Veerkamp JH, Turcotte LP, Kelley DE. Markers of capacity to utilize fatty acids in human skeletal muscle: relation to insulin resistance and obesity and effects of weight loss. FASEB J. 1999;13:2051–60.

17. Kelley DE, He J, Menshikova E V, Ritov VB. Dysfunction of Mitochondria in Human Skeletal Muscle in Type 2 Diabetes. 2002;51.

18. Wells JCK. Sexual dimorphism of body composition. Best Pract Res Clin Endocrinol Metab. 2007;21:415–30.

19. Perng W, Hector EC, Song PXK, Tellez Rojo MM, Raskind S, Kachman M, Cantoral A, Burant CF, Peterson KE. Metabolomic Determinants of Metabolic Risk in Mexican Adolescents. Obesity. 2017;25:1594–602.

20. Lewis RC, Meeker JD, Peterson KE, Lee JM, Pace GG, Cantoral A, Téllez-Rojo MM. Predictors of Urinary Bisphenol A and Phthalate Metabolite Concentrations in Mexican Children. Chemosphere. 2013;93:2390–8.

21. Cantoral A, Téllez-rojo MM, Ettinger AS, Hu H, M H-A, Peterson K. Early introduction and cumulative consumption of sugar-sweetened beverages during the pre-school period and risk of obesity at 8-14 years of age. Pediatr Obes. 2016;11:68–74.

22. Evans CR, Karnovsky A, Kovach MA, Standiford TJ, Burant CF, Stringer KA. Untargeted LC-MS Metabolomics of Bronchoalveolar Lavage Fluid Differentiates Acute Respiratory Distress Syndrome from Health. J Proteome Res. 2014;13:640–9.

23. Fernández-Albert F, Llorach R, Garcia-Aloy M, Ziyatdinov A, Andres-Lacueva C, Perera A. Intensity drift removal in LC/MS metabolomics by common variance compensation. Bioinformatics. 2014;30:2899–905.

24. Chen M, Rao RSP, Zhang Y, Zhong CX, Thelen JJ. A modified data normalization method for GC-MS-based metabolomics to minimize batch variation. Springerplus. 2014;3:1–7.

25. Lohman TG, Roche AF., Martorell R. Anthropometric Standardization Reference Manual. Champaign, IL: Human Kinetics Books; 1988.

26. Onis M De, Onyango AW, Borghi E, Siyam A, Nishida C, Siekmann J. Development of a WHO growth reference for school-aged children and adolescents. Bull World Health Organ. 2007;85:660–7.

27. Frisancho A. New norms of upper limb fat and muscles areas for assessment of nutritional

status. Am J Clin Nutr. 1981;34:2540–5.

28. Bonser AM, Garcia-Webb P, Harrison LC. C-peptide measurement: methods and clinical utility. Crit Rev Clin Lab Sci. 1984;19:297–352.

29. Xia L, Zhi-guang Z, Hai-ying Q, Xiao-Yan C, Gan H. Replacement of insulin by fasting C-peptide in modified homeostasis model assessment to evaluate insulin resistance and islet beta cell function. J Cent South Univ Med Sci. 2004;29:419–23.

30. Friedewald WT, Levy RI, Fredrickson DS. Estimation of the concentration of low-density lipoprotein cholesterol in plasma, without use of the preparative ultracentrifuge. Clin Chem. 1972;18:499–502.

31. Denova-gutiérrez E, Ramírez-silva I, Rodríguez-ramírez S, Jiménez-aguilar A, Shamah-levy T, Rivera-dommarco JA. Validity of a food frequency questionnaire to assess food intake in Mexican adolescent and adult population. Salud Pública México. 2016;58:617–28.

32. National Institute of Public Health. The Compiled México-INSP Food Composition Data Bank; National Institute of Public Health. Saitama, Japan; 2002.

33. Willett WC, Howe GR, Kushi LH. Adjustment for total energy intake in epidemiologic studies. Am J Clin Nutr. 1997;65:1220S-1228S.

34. Marshall W a., Tanner JM. Variations in the Pattern of Pubertal Changes in Boys. Arch Dis Child. 1970;45:13–23.

35. Marshall W a., Tanner JM. Variations in the Pattern of Pubertal Changes in Girls. Arch Dis Child. 1969;44:291–303.

36. Chavarro JE, Watkins DJ, Afeiche MC, Zhang Z, Sánchez BN, Cantonwine D, Mercado-García A, Blank-Goldenberg C, Meeker JD, Téllez-Rojo MM, et al. Validity of Self-Assessed Sexual Maturation Against Physician Assessments and Hormone Levels. J Pediatr. 2017;186:172–8.

37. Watkins DJ, Peterson KE, Ferguson KK, Mercado-garcía A, Tamayo M, Cantoral A, Meeker JD, Téllez-rojo MM. Relating Phthalate and BPA Exposure to Metabolism in Peripubescence: The Role of Exposure Timing, Sex, and Puberty. J Clin Endocrinol Metab. 2016;101:79–88.

38. Pedhazur E. Multiple regression in behavioral research. 3rd Editio. Harcourt Brace College Publishers; 1997.

39. Sobel ME. Asymptotic Confidence Intervals for Indirect Effects in Structural Equation Models Stable. Sociol Methodol. 1982;13:290–312.

40. Cano B, Oya M De, Benavente M, Viturro E, Oya I De, Lo L. Dehydroepiandrosterone sulfate (DHEA-S) distribution in Spanish prepuberal children: Relationship with fasting plasma insulin concentrations and insulin resistance. Clin Chim Acta. 2006;366:163–7.

41. Gordon E. Non-esterified fatty acids in blood of obese and lean subjects. Am J Clin Nutr. 1960;8:740–7.

42. Klein-Platat C, Drai J, Oujaa M, Schlienger JL, Simon C. Plasma fatty acid composition is associated with the metabolic syndrome and low-grade inflammation in overweight adolescents. Am J Clin Nutr. 2005;82:1178–84.

43. Souza KD, Nzirorera C, Kienesberger PC. Lipid metabolism and signaling in cardiac lipotoxicity. Biochem Biophys Acta. 2016;1861:1513–24.

44. Sears B, Perry M. The role of fatty acids in insulin resistance. Lipids Health Dis. Lipids in Health and Disease; 2015;14:1–9.

45. Clemmons DR. Metabolic Actions of IGF-I in Normal Physiology and Diabetes. Endocrinol Metab Clin North Am. 2012;41:425–43.

46. Caprio S, Plewe G, Diamond MP, Simonson DC, Boulware SD, Sherwin RS, Tamborlane W V. Increased insulin secretion in puberty: A compensatory response to reductions in insulin sensitivity. J Pediatr. 1989;114:963–7.

47. Arslanian SA, Kalhan SC. Correlations between fatty acid and glucose metabolism. Potential explanation of insulin resistance of puberty. Diabetes. 1994;43:908–14.

48. Kalhan SC, Kalhan C. Protein turnover during puberty in normal children. Am J Physiol Endocrinol Metab. 1996;270:E79–84.

49. Herman MA, She P, Peroni OD, Lynch CJ, Kahn BB. Adipose Tissue Branched Chain Amino Acid (BCAA) Metabolism Modulates Circulating BCAA Levels. J Biol Chem. 2010;285:11348–56.

50. Koves TR, Ussher JR, Noland RC, Slentz D, Mosedale M, Ilkayeva O, Bain J, Stevens R, Dyck JRB, Newgard CB, et al. Mitochondrial Overload and Incomplete Fatty Acid Oxidation Contribute to Skeletal Muscle Insulin Resistance. Cell Metab. 2008;7:45–56.

51. Schooneman MG, Vaz FM, Houten SM, Soeters MR. Acylcarnitines: Reflecting or Inflicting Insulin Resistance? Perspect Diabetes. 2013;62:1–8.

52. Ribel-madsen A, Ribel-madsen R, Brøns C, Newgard CB, Vaag AA, Hellgren LI. Plasma acylcarnitine profiling indicates increased fatty acid oxidation relative to tricarboxylic acid cycle capacity in young , healthy low birth weight men. Physiol Rep. 2016;4:e12977.

53. Mihalik SJ, Goodpaster BH, Kelley DE, Chace DH, Vockley J, Toledo FGS, DeLany JP. Increased Levels of Plasma Acylcarnitines in Obesity and Type 2 Diabetes and Identification of a Marker of Glucolipotoxicity. Obesity. 2010;18:1695–700.

54. Dobbins RL, Szczepaniak LS, Bentley B, Esser V, Myhill J, McGarry JD. Prolonged inhibition of muscle carnitine palmitoyltransferase-1 promotes intramyocellular lipid accumulation and insulin resistance in rats. Diabetes. 2001;50:123–30.

55. Lodhi IJ, Semenkovich CF. Peroxisomes: A nexus for lipid metabolism and cellular signaling. Cell Metab. 2014;19:380–92.

56. Muoio DM. Metabolic Inflexibility: When Mitochondrial Indecision Leads to Metabolic Gridlock. Cell. 2014;159:1253–62.

57. Kim JY, Tfayli H, Michaliszyn SF, Arslanian S. Impaired lipolysis, diminished fat

oxidation, and metabolic inflexibility in obese girls with polycystic ovary Syndrome. J Clin Endocrinol Metab. 2018;103:546–54.

58. Venables MC, Achten J, Jeukendrup AE. Determinants of fat oxidation during exercise in healthy men and women: a cross-sectional study. J Appl Physiol. 2005;98:160–7.

59. Mcclelland GB, Lyons SA, Robertson CE. Fuel Use in Mammals: Conserved Patterns and Evolved Strategies for Aerobic Locomotion and Thermogenesis. Integr Comp Biol. 2017;57:231–9.

60. Zurlo F, Lillioja S, Esposito-Del Puente A, Nyomba BL, Raz I, Saad MF, Swinburn BA, Knowler WC, Bogardus C, Ravussin E. Low ratio of fat to carbohydrate oxidation as predictor of weight gain: study of 24-h RQ. Am J Physiol. 1990;259:E650-7.

61. Morris C, Grada CO, Ryan M, Roche HM, Vito G De, Gibney MJ, Gibney ER, Brennan L. The relationship between aerobic fitness level and metabolic profiles in healthy adults. Mol Nutr Food Res. 2013;57:1246–54.

CHAPTER 5

Conclusion

Significance of Research Findings

The global prevalence of obesity, type 2 diabetes (T2D), and metabolic disease continues to rise; influencing children and adolescents at an earlier age. In the United States, 39.8% of adults have obesity and 18.5% of children and adolescents aged 2-19 years have obesity (1). In part, this is due to increased intake of calorically dense foods, in particular highly processed foods, paired with increases in sedentary activity (2). A top public health priority worldwide is to reduce the prevalence of obesity, with an emphasis on prevention in childhood. Childhood obesity is associated with obesity (3) and T2D (4) in adulthood. There is a high economic burden of obesity and T2D (5,6), presenting an urgent need for public health efforts to save societal resources. In the United States, public health efforts and funding towards combatting obesity are focused on improving lifestyles, such as eating a healthier diet (e.g. MyPlate) and increasing physical activity (e.g. Let's Move!). These programs are valuable for teaching children how to lead healthy lifestyles, however, there are other avenues for intervention and prevention.

This dissertation suggests that the intrauterine environment can have profound implications on the offspring's metabolic health, potentially programming risk to adult cardiometabolic disease. The infant cord blood lipidome and DNA methylome in cord blood leukocytes was correlated with the maternal lipidome across gestation, identifying unique lipid profiles related to growth. Harnessing the findings from our studies, I propose that interventions should be targeted to

women prior to conception to prevent the intergenerational cycle of obesity. Additionally, this dissertation highlights the intrinsic differences in nutrient utilization between individuals, which is related to insulin resistance (IR). In adolescence, we observed differential metabolite profiles associated with obesity and IR. The metabolome is influenced by habitual carbohydrate or fat intake, suggesting that biomarkers of IR may depend on macronutrient intake. Overall, I propose a shift from a "one-size-fits-all" nutrition approach to classifying mitochondrial oxidative capacity to create a precise "dietary prescription" for each individual.

Implications from the pregnancy studies

Fifty years ago, the Developmental Origins of Health and Disease (DOHaD) field originated with the work of David Barker and his colleagues from their epidemiological studies of infant and adult mortality published in *The Lancet* (7–9). Stemming from these results, dietary manipulation studies during pregnancy have demonstrated changes in the risk of adult metabolic disease (10). These studies have demonstrated that nutrient factors including energy intake, fatty acids (10,11), protein (12,13), micronutrients (14), and vitamins, including folic acid (15), have profound influences on fetal programming, varying by timing of exposure. However, in epidemiologic studies, measuring food and nutrient intake is challenging due to random and systematic errors in dietary assessment tools. To assess food intake, researchers rely on memory-based dietary assessment methodologies, such as Food Frequency Questionnaires and 24-hour dietary recalls, which have been debated over their value and validity (16). Therefore, it is necessary to have objective measurements of the maternal intrauterine environment to which the developing fetus is exposed. For this dissertation, the maternal plasma lipidome was measured during first trimester (M1) and at delivery (M3), providing an objective view of maternal nutrient

availability across gestation. Profiling the lipidome presents the opportunity to classify biomarkers and metabolic pathways associated with offspring growth and metabolic health.

Chapter 2 identified maternal lipids related to the development of the infant, measured by birth weight (BW) and the umbilical cord blood (CB) lipidome, a representation of placental transfer and infant metabolism. At each time-point, the maternal and CB lipidome displayed unique correlations between differing lipid classes. The increased number of significant Pearson's correlations in CB compared to M1 and M3 may suggest differences in lipid connectivity, warranting further analyses to recognize biological implications. Most classes of lipids increased in levels from M1 to M3, consistent with previous observations of generalized increases in lipoproteins and associated lipids with advancing pregnancy (17,18). Shifts in the maternal and CB lipidome were consistent with the transport of long-chain (LC) polyunsaturated fatty acids (PUFA) as well as lysophosphatidylcholine (LysoPC) and lysophosphatidylethanolamine (LysoPE) species into CB. These results suggest the selective transfer of PUFAs across the placenta to the fetus (19), seemingly mediated in part by lysophospholipids (LysoPL) (20). Maternal characteristics, such as gestational weight gain (GWG) and baseline BMI, influenced the metabolome, including positive association between BMI and maternal plasma sphingomyelins (SM) as well as GWG and maternal plasma LysoPLs.

Most of the lipids that increased in CB compared to M3 plasma were associated with infant BW with significant positive associations between all classes of CB LysoPC and LysoPE groups (both saturated and unsaturated fatty acid-containing LysoPLs) and Fenton BW z-score. Inverse association were observed between CB diglycerides (DGs) and triglycerides (TGs) containing PUFA and Fenton BW z-score. Maternal first trimester PUFA-containing TGs and phospholipids were inversely correlated with CB LysoPC and LysoPE species, suggesting that early gestational

maternal lipid levels influence the development of the CB lipidome and its relationship with BW. **Figure 5.1** demonstrates the relationship between maternal and CB lipids with BW. While PUFA-containing dietary interventions have been studied in pregnancy, many of these clinical trials started supplements in mid-gestation. Our results suggest the importance of early gestation PUFA levels, therefore, I am proposing that supplementation should begin prior to conception (see Future Studies and Applications section).

Chapter 3 identified epigenetic mechanisms that may contribute to developmental programming of offspring growth and metabolic health (21). We classified how the maternal lipidome at first trimester and delivery is related to altered DNA methylation patterns in umbilical CB leukocytes. Genome-wide DNA methylation was analyzed using the Infinium HumanMethylation850K (EPIC) bead array. Differential methylation at CpG probes and within CpG region was classified using empirical Bayes modeling, adjusting for batch differences, infant sex, and white blood cell types. Our findings provide support that the maternal metabolic environment during gestation influences infant DNA methylation, potentially by fetal programming. M3 saturated LysoPC and LysoPE are associated with differential methylation in CpG islands, with the majority of CpG sites having increased methylation with increased lipid exposure. Biological pathways pertaining to differentially methylated CpGs associated with M3 saturated LysoPCs are involved in cell proliferation. The role of maternal lysophospholipids in the establishment of the infant CB lipidome and epigenome, as well as birth weight, needs further elucidation to understand the biological implications.

Implications in the adolescent periods

Within adults, metabolomics analyses have identified biomarkers of obesity (22) and IR (23), increasing the understanding of the disease pathogenesis. With the increases in obesity (24) and

T2D (25) in the pediatric population, it is important to classify metabolome fluctuations in children and adolescents; a period of physical transition marked by the onset of puberty. We hypothesized the relationship between the metabolome with BMI and IR in the pediatric population will differ from the adult population, due to metabolic changes occurring with puberty. For instance, IR increases across puberty, exhibiting sex-specific changes, potentially in response to changes in muscle and fat mass (26). In parallel, insulin growth factor-1 (IGF-1) increases across puberty (27) and is directly correlated with insulin levels (28). Chapter 4 determines how the metabolome during adolescence is related to obesity and IR, assessing sex-specific alterations given differences in pubertal hormones and the accumulation of muscle and fat tissue (29).

Sex-stratified linear regression identified metabolites associated BMI z-score (BMIz) and homeostatic model assessment of insulin resistance using C-peptide (HOMA-CP), accounting for puberty, age and muscle and fat area. Metabolites associated with BMIz include positive associations with DGs among girls and positive associations with branched chain and aromatic amino acids in boys. Intermediates in fatty acid metabolism, including medium-chain acylcarnitines (AC), were inversely associated with HOMA-CP. These results suggest less imbalance in the delivery and oxidation of substrates in these individuals, perhaps due to the increased substrate utilization to fuel tissue and linear growth in the pubertal period, as observed in previous studies (30).

The effect of macronutrient intake on metabolic health remains controversial with previous analyses describing a relationship between amount of macronutrient consumed and metabolic outcomes (31), while other analyses suggesting no relationship (32–34). In the ELEMENT cohort, no direct relationship was observed between macronutrient intake with BMIz and IR.

Path analysis identified clusters of metabolites that underlie the relationship between energy-adjusted macronutrient intake with BMIz and HOMA-CP. Carbohydrate intake is positively associated with HOMA-CP through decreases in levels of AC, products of β-oxidation. Approaching significance, fat intake is positively associated with HOMA-CP through increases in levels of dicarboxylic fatty acids (DiC-FA), products of omega-oxidation. When consuming more grams of fat, there is evidence for increased extra-mitochondrial fatty acid metabolism, while higher carbohydrate intake appears to lead to decreases in intermediates of β-oxidation. These results may suggest that adolescents prone to IR have an increase in selection of carbohydrates for fuel, exacerbated by elevated habitual carbohydrate consumption. Under these conditions, elevated malonyl-CoA would reduce uptake of FA into the mitochondria leading to lipid accumulation in the cytosol, increasing FA metabolites that contribute to IR (35) (**Figure 5.2A).** Adolescents that are not prone to insulin resistance tend to have a higher mitochondrial oxidative capacity and an increase selection of fatty acids, represented in in humans (36) and animals (37). In these individuals, β-oxidation in the mitochondrial is associated with increases in medium-chain ACs, a reflection of enhanced oxidation (**Figure 5.2B**).

Study Strengths and Limitations

Pregnancy Study

The Michigan Mother-Infant Pairs (MMIP) cohort is an established birth cohort with studies assessing the effect of environmental toxicants on maternal and newborn health (38). This cohort is mainly composed of white women with a high socioeconomic status, limiting the implications of our results to other populations. A strength of this study is the recruitment of women during their first prenatal appointment between 8 and 14 weeks of gestation, as other metabolomics studies assess the influence of the metabolome on offspring health starting at mid-gestation (39).

Fetal organ development is occurring during the first trimester, marking a critical period where the fetus is plastic to exposures. Profiling of the maternal lipidome during the first trimester can suggest the implications of particular lipid classes. Using an established liquid chromatography/mass spectrometry platform, we profiled almost 600 lipids, providing an objective view of the maternal metabolic environment, compared to dietary recall or a targeted lipid platform. Additionally, we have incorporated maternal baseline BMI and GWG to assess how phenotypic differences influence the lipidome.

Infant metabolic health was classified using a variety of measurements including BW, the umbilical CB lipidome, and umbilical CB leukocytes DNA methylation. Infant BW is the most common health outcome studied to determine if the maternal intrauterine environment influences the development of the fetus, allowing for validation of other metabolome analyses. The umbilical CB lipidome is a reflection of infant metabolism as well as maternal metabolite levels, placental transfer, and interaction with other metabolites, such as inhibition by competition or metabolite-induced changes in placental transport activity. The EPIC bead array is a genome-wide measurement of DNA methylation. Applying all three of these methods creates a strong platform to assess how maternal lipid levels across gestation influence infant health. Strong statistical methods were incorporated including clustering techniques of the lipidome by lipid class and number of double bonds. Empirical Bayes models were adjusted for relevant covariates and batch influences when assessing differential methylation, probe-wise and regionally. The novelty of this dissertation is the incorporation of multiple metabolome measurements with the epigenome to gain a broader understanding of a biological system.

Future longitudinal studies with a larger sample size are desired to confirm results in this dissertation. Our sample size of approximately 100 mother-infant dyads was small for an ‘omics

data analysis. Further, maternal blood collection at delivery may not be representative of the metabolic states during the third trimester due to the stress of parturition. Future studies should include a mid-gestation maternal plasma sample. Umbilical CB is not a true representation of infant blood, as it represents placental transport and metabolism. Additional, umbilical CB leukocytes DNA methylation may not be the relevant tissue to examine for risk of metabolic disease and additional epigenetic processes, such as histone modifications, may be more relevant. We did not include a measure of gene expression in this dissertation. Therefore, we cannot be sure if differential methylation is associated with changes in transcription.

Adolescent Study

The Early Life Exposures in Mexico to ENvironmental Toxicants (ELEMENT) project (40) started in 1994 and consists of three sequentially-enrolled birth cohorts from Mexico City Maternity Hospitals (41). This mother-child pregnancy and birth cohort originated to explore if lead exposure and mobilization during pregnancy influences fetal development and whether maternal calcium supplementation can mitigate these adverse effects. A subset of offspring, age 8-14 years, of the original mothers recruited were selected for the metabolomics analyses. Strengths include the availability of a wealth of data in the ELEMENT cohort allowing for the incorporation of anthropometry measurements, metabolic biomarkers, puberty measures, and dietary intake. The liquid chromatography/mass spectrometry based untargeted metabolomics platform is well-established and external standards were run, confirming annotations of metabolites. Linear models were used for both the unannotated and annotated features, incorporating the step-wise addition of covariates such as muscle and fat mass. These models allowed for a deeper understanding of the metabolome's relationship with BMIz and insulin resistance. The use of path analysis created a strong statistical platform to begin to understand

mechanisms describing this relationship. A validated food frequency questionnaire quantified macronutrient intake (42), which was adjusted for total energy intake using the residual method (43). For the path analysis, hierarchical clustering grouped highly correlated metabolites, reducing the number of comparisons.

Despite the strengths of this study, this work is cross sectional therefore causality cannot be confirmed. We are limited by the number of subjects within this study (n=206), acknowledging that stratifying by sex reduces power. The relationship between the metabolome and obesity was measured by BMIz, acknowledging that BMI does not distinguish between muscle and fat tissue. Previous studies have acknowledged the ratio of subcutaneous fat to visceral fat influences risk of IR and T2D (44). Future analyses should consider using dual-energy X-ray absorptiometry (DEXA) to assess the relationship between body composition and the metabolome. A more accurate measurement of insulin resistance would have been using insulin to calculate HOMA-IR, instead of using C-peptide. Lastly, a measure of oxidative capacity would strengthen our findings from path analysis, indicating changes in mitochondrial fatty acid oxidation in adolescents who are prone to IR.

Future Studies and Applications

Molecular Study: Understanding the Transfer of Fatty Acids across the Placenta via MFSD2a

The placenta plays a crucial role in pregnancy connecting the fetus via the umbilical cord to the uterine wall, supporting nutrient transfer, gas exchange, and waste elimination. Therefore, the placenta is a key regulator of fetal growth. This dissertation classified the relationship between maternal plasma lipids and umbilical cord plasma lipids without considering the implications of the placenta. To address, future analyses should quantify expression of lipid transporters on the placenta to understand mechanisms regulating nutrient transport. It is hypothesized that the

placenta might have a crucial role in modulating lipid transport depending on maternal supply and fetal demands (45). A better understanding of placental lipid transfer in relation to the maternal lipidome, as well as phenotypes (e.g. BMI, gestational diabetes), may help provide suggestions for dietary modifications to support fetal development.

Maternal lipids are transported to the fetus across the placenta via a variety of fatty acid transport proteins as well as passive diffusion (46,47). Lipid species are hydrolyzed at the maternal surface of the placenta for transport (48). TGs are hydrolyzed by placental lipoprotein lipase and phospholipids are hydrolyzed by placental endothelial lipase. Previous studies have demonstrated the importance of the phospholipid fraction for the transport of essential LC-PUFA during late gestation (46). Since the sn-2 position of phospholipids tend to be occupied by PUFAs (49), it has been hypothesized that specific placental endothelial lipases cleave sn-1 fatty acids, allowing transport of the PUFA-containing LysoPC to the fetal circulation, perhaps enhancing delivery to the developing fetal brain (20,50). The Major Facilitator Super Family Domain Containing 2a (MFSD2a) protein has been proposed as a NA^{+}-dependent LysoPL transporter in the brain (51) and placenta (52). This transporter provides a mechanism for the active transport of LysoPL from maternal plasma, preferentially transferring LysoPCs with PUFAs (53). Collecting placenta samples, trophoblast cells will be isolated (54) and RNA extracted to quantify MFSD2a gene expression.

Clinical Study: Optimizing the Maternal Intrauterine Environment in a Pre-Conception Weight Loss Study

Through a collaboration between Michigan Weight Management Program and the MMIP cohort, this research has fueled the start of a clinical trial assessing the influence of pre-conception weight loss on the health of the mother-infant dyad. The results from this dissertation have

indicated the importance of the maternal lipidome throughout gestation in establishing the umbilical CB lipidome and infant BW, potentially through fetal programming via epigenetic modifications. Obesity during pregnancy has increased risk of complications including gestational diabetes, hypertensive disorders, and preterm birth (55). Both the metabolome and lipidome are altered with obesity (22). To encourage the best health outcomes for the mother-infant dyad, it is critical to optimize the intrauterine environment. Therefore, in collaboration with Dr. Amy Rothberg, Dr. Vasantha Padmanabhan, Dr. Dana Dolinoy, and Dr. Charles Burant, we hypothesize that pre-conception weight loss will normalize the maternal metabolic environment resulting in more favorable mother-infant health outcomes.

Weight loss is associated with improvements in insulin sensitivity in adipose tissue, the liver, and muscles (56). During a 2-year intensive weight management program at the University of Michigan using a very low energy diet, decreases in BMI and waist circumference were associated with improvements in components of metabolic risk measurements (57). **Table 5.1** represents components influenced by the weight management program, including BMI, fat mass, and HOMA-IR.

Within the Michigan Weight Management program, the lipidome has been analyzed in women that are lean and obese before and after weight loss (**Figure 5.3**). In comparison to lean women, pre-weight loss obese women have higher levels of multiple lipid species including ceramides (Cer), DGs, lysophospholipids (LysoPC, LysoPE), SMs, and TGs (**Figure 5.3a**). After weight loss, many of these lipid species "normalized" closer to the levels seen in lean women. For instance, saturated TGs in women post-weight loss were comparable to the saturated TG levels in lean women (**Figure 5.3b**), even those the women post-weight loss are still obese (**Table 5.1**). Other studies have suggested the metabolome is altered with weight loss (58). Relevant to this

dissertation's findings, others have demonstrated that LysoPLs are decreased in response to weight loss in obese subjects (59). We hypothesize that the LysoPL lipid fraction will be important to modify in obese women prior to pregnancy due to the results of this dissertation and other studies (60–62).

The modification of the metabolome with weight loss must be paired with incorporation of certain nutrients to ensure optimal health for the mother-infant dyad. In a recent review of omega-3 fatty acid supplementation during pregnancy, 70 randomized control trials were compiled to evaluate the influence of PUFA supplementation on maternal-offspring health outcomes (63). In offspring, supplementation reduced preterm birth, perinatal death, and low BW while increased prolonged gestation and large-for-gestational age babies. The influence of omega-3 supplementation on offspring adult body mass was uncertain. In mothers, supplementation was only associated with an increase in gestation length. However, most of the trials started omega-3 supplementations in the second or third trimester. The results of this dissertation suggest the importance of early gestational maternal PUFA levels for modulating the CB lipidome and its relationship with BW. Therefore, PUFA supplementation must begin prior to conception to potentially improve offspring cardiometabolic health. Maternal characteristics may attenuate the effect of PUFA supplementation on mother-infant pregnancy outcomes, including pre-pregnancy BMI (64). This is important to consider when adjusting the dosage of the supplement to fit the study population.

To support placental transport of PUFAs, participants must have adequate choline levels for the formation of LysoPCs. Choline is an essential nutrient during fetal development, which supports cell membrane formation and supplies methyl groups for one carbon metabolism (65). During pregnancy, the dynamics of choline metabolism shifts to increase production of

phosphatidylcholine via the Kennedy pathway and the phosphatidylethanolamine N-methyltransferase (PEMT) pathway (66). The relationship between docosahexaenoic acid (DHA) and choline supplementation during pregnancy needs to be understood. Previous neurodevelopment studies found enhanced hippocampal development with the supplementation of both DHA and choline (67). Monitoring of choline dietary intake and choline blood levels should begin prior to conception. Insufficient evidence is available to suggest addition of a choline supplement.

After conception, participants will meet with a Registered Dietitian to monitor dietary intake. Physicians will monitor GWG in accordance to the recommendations produced by The Institute of Medicine (IOM), which are based on pre-pregnancy BMI (68). The MMIP participants included in this dissertation were stratified based on lean, overweight, and obese baseline BMIs (**Figure 5.4a**). Each BMI baseline group contained women that gained inadequate and excess gestational weight based on the IOM recommendations. In this dissertation, excess GWG was associated with increased in LysoPC and LysoPE in the maternal plasma, suggesting importance in monitoring. Both inadequate and excess GWG is associated with complications for the offspring, including childhood obesity, hypertension, and IR (69). Additionally, we observed a relationship between GWG and infant Fenton BW percentile in lean women (**Figure 5.4b**). A relationship was not observed in overweight nor obese, potentially due to the small sample size within these groups.

Clinical Study: Moving Away from One-Size-Fits-All Nutrition Recommendations to Classifying Intrinsic Differences in Mitochondrial Oxidative Capacity.

Using a cross-sectional study design in the ELEMENT cohort, we identified clusters of metabolites that underlie the relationship between habitual carbohydrate and fat intake with IR,

measured by HOMA-CP. Based on our results, we hypothesize that there are intrinsic differences in fuel selection and the ability to fully oxidize fatty acids, having implications on the development of IR. VO_2 max during exhaustive physical activity corresponds to muscle mitochondrial oxidative capacity (70). Previous analyses in humans (36) and animals (37) with higher oxidative capacity show a relative selection of fatty acids and a relative resistance to obesity (71). Therefore, we propose to analyze fuel selection and oxidative capacity in children undergoing a controlled feeding study following these Specific Aims:

Specific Aim 1. Investigate the correlation between VO_2max, fuel selection, and metabolite profiles during exercise in children. We will recruit metabolically healthy children with a variety of BMI z-scores, including both lean and obese children. Children with T2D will be excluded from this study. All participants will undergo a 3-day standard diet. The day after the standard diet, fasted participants will undergo a treadmill stress test following the Bruce Protocol to obtain maximal oxygen uptake (VO_2 max) (72) with regular blood sampling through an IV catheter. Samples will be analyzed using untargeted metabolomics and lipidomics to determine phenotypes that influence metabolic exercise-responses. We will analyze metabolic processes that are correlated with oxidative capacity and fuel selection, identifying metabolites and metabolic pathways biomarkers of disease risk.

Specific Aim 2. Through a controlled feeding study, classify fasting blood metabolome alterations in response to two different diets (one high in carbohydrates and one high in fat). The metabolome is dynamic and reflective of macronutrient intake derived from diet (73). Post the 3-day standard diet, participants will consume one of two diets, either a high carbohydrate or a high fat diet, for 14-days. Following the first dietary treatment, all participants will consume a 3-day standard diet prior to crossover to other dietary treatment for 14-days.

Blood will be collected before, during, and after this study to assess how the metabolome reflects macronutrient intake. We hypothesize that the metabolome will respond to a feeding study differently in the pediatric population than in adults.

Specific Aim 3. Identify intrinsic and phenotypic differences that influence metabolic response to dietary intervention. Utilizing the information gathered in Specific Aims 1 and 2, models will classify if fuel selection and/or oxidative capacity modulates response to dietary intervention. Saliva samples will be collected to assess genetic influences of fuel selection and oxidative capacity. Results from these models will indicate how intrinsic differences in children may influence metabolic response to dietary interventions allowing for the creation of tailored dietary recommendations.

Public Health Relevance

The results of these Developmental Origins of Health and Disease (DOHaD) studies suggest that the maternal metabolic environment has influences the establishment of the umbilical CB lipidome and infant birth weight, potentially through modulating DNA methylation. Modifying the intrauterine environment paired with dietary recommendations in the postnatal life may prevent adult metabolic disease. Grant funding should be aimed towards understanding mechanisms of the development of disease and assessing clinical relevance of interventions. Public health messages should support pre-conception nutrient recommendations for both the mother.

Figure 5.1. Proposed influence of the maternal and cord blood lipidome on birth weight.

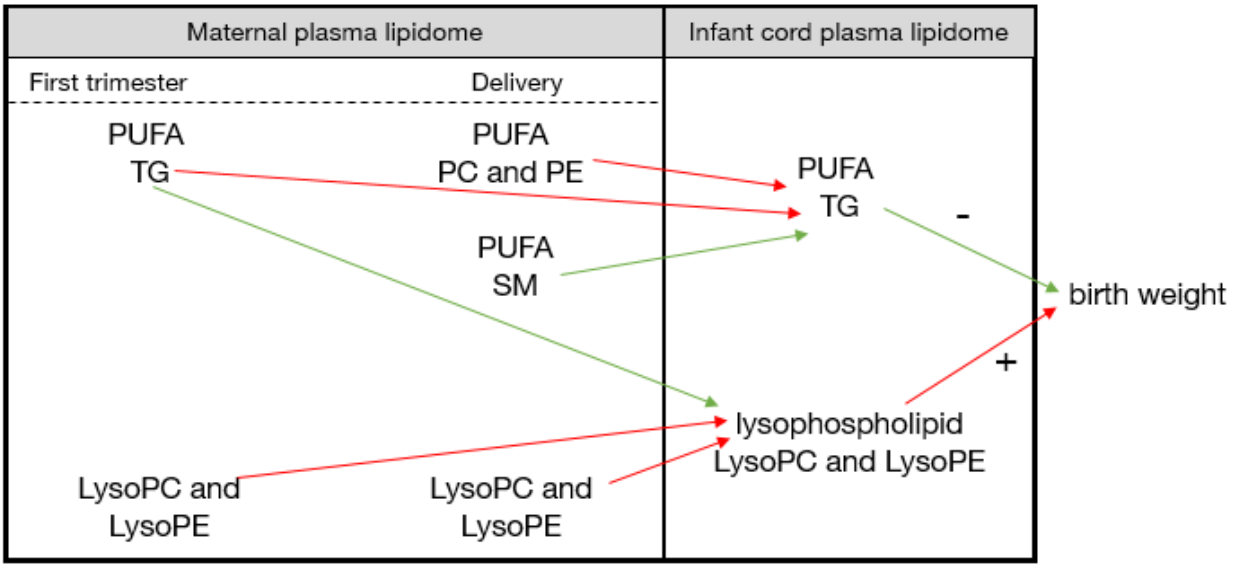

Infant umbilical cord blood lipids associated with birth weight are potentially modulated by the maternal lipidome, beginning in early gestation. CB LysoPC and LysoPE lipid classes are positively associated with infant BW. CB PUFA containing TGs are inversely associated with BW. In the first trimester, maternal PUFA containing TGs are positive associated with CB PUFA containing TGs and inversely associated with CB LysoPLs. At delivery, maternal PUFA containing PCs and PEs are positively association with CB PUFA containing TGs, suggesting the importance in the phospholipid fraction for the transfer of PUFAs late in gestation. Maternal delivery PUFA containing SMs are inversely associated with CB PUFA containing TGs. Across gestation, maternal LysoPL levels are positively associated with CB LysoPL levels. Red arrows indicate positive associations. Green arrows indicate inverse associations.

Figure 5.2. Proposed differences in mitochondrial oxidation in an insulin resistance and insulin sensitive cell.

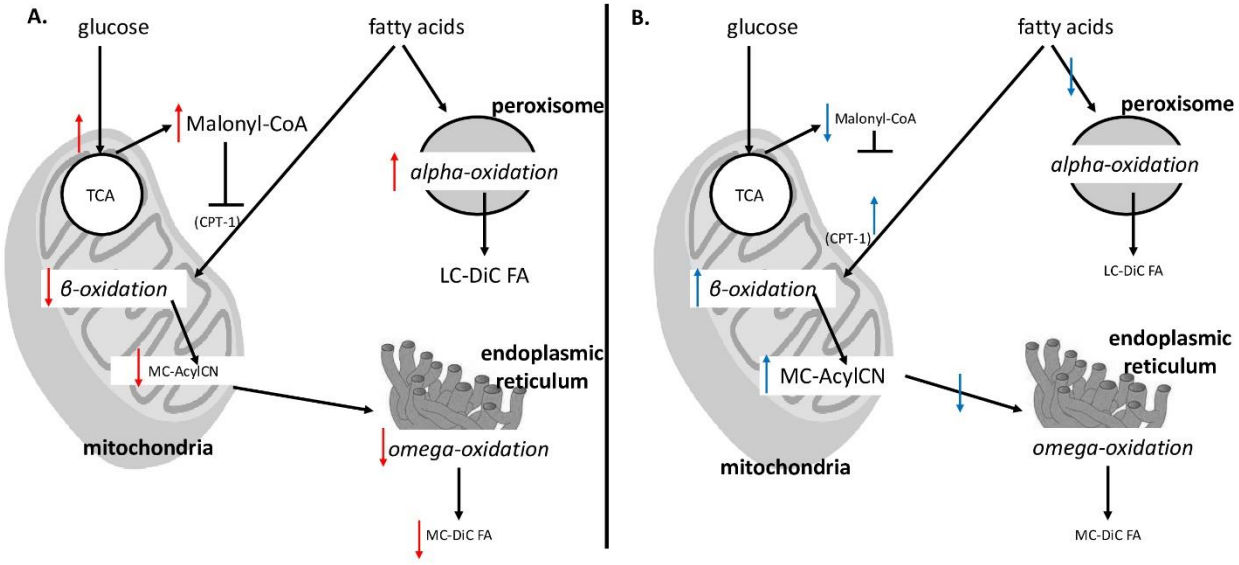

(A) In an insulin resistant cell, carbohydrates are the preferred fuel source. An increased glucose flux into the TCA cycle produces excess malonyl-CoA, inhibiting fatty acid entry into the mitochondria via CPT-1 and reducing β-oxidation. Fatty acids will accumulate in the cytosol. Very long-chain fatty acids can be shuttled to the peroxisomes for alpha-oxidation, producing long-chain dicarboxylic fatty acids. **(B)** In an insulin sensitive cell, fatty acids are the preferred fuel source. Fatty acids are shuttled from the cytosol into the mitochondria via CPT-1 to undergo β-oxidation. Increases in β-oxidation produce medium-chain acylcarnitines. Rescue pathways of fatty acids oxidation, alpha oxidation and omega oxidation, are able to oxidize fatty acid oxidation intermediates. Habitual dietary intake may exacerbate intrinsic mitochondrial differences in individuals.

Table 5.1. Effect of weight loss on clinical measures. Clinical characteristics of 11 lean and 31 obese women, pre-weight loss and post-weight loss.

	Average ± SD			ANOVA p-value		
	Lean (n=11)	**Obese, pre-WL (n=31)**	**Obese, post-WL (n=31)**	**Lean v. obese, pre-WL**	**Lean v. obese, post-WL**	**obese pre-WL v. post-WL**
Age	40.3±1.2	41.4±0.5	41.4±0.5	1.00E-18	2.10E-11	3.00E-09
BMI (kg/m2)	22.0±0.3	40.8±0.3	33.8±0.4	4.00E-07	0.0001	0.013
Total fat mass (kg)	16.6±0.9	55.2±0.9	41.9±0.8	2.80E-07	5.50E-06	0.02
Total FFM (kg)	42.7±0.8	55.7±0.6	51.8±0.5	7.10E-17	1.03E-10	3.00E-05
% fat	27.7±1.2	49.6±0.3	44.3±0.5	7.10E-17	1.03E-10	3.00E-05
REE/FFM (kcal/kg)	31.7±1.2	33.4±0.3	33.2±0.3	NS	NS	NS
VO2max/FFM (mL/kg/min)	52.2±1.5	41.2±0.6	44.7±0.8	4.00E-05	1.50E-02	0.074
Fasting glucose (mg/dL)	88.8±1.4	104.1±1.4	92.3±1.9	3.30E-01	NS	0.0006
Fasting insulin (mIU/l)	9.5±0.6	22.0±0.6	13.3±0.3	2.10E-06	5.00E-03	1.50E-07
HOMA-IR	2.1±0.1	5.8±0.2	3.0±0.1	1.10E-05	0.007	1.50E-07

Figure 5.3. Effect of weight loss on the plasma lipidome.

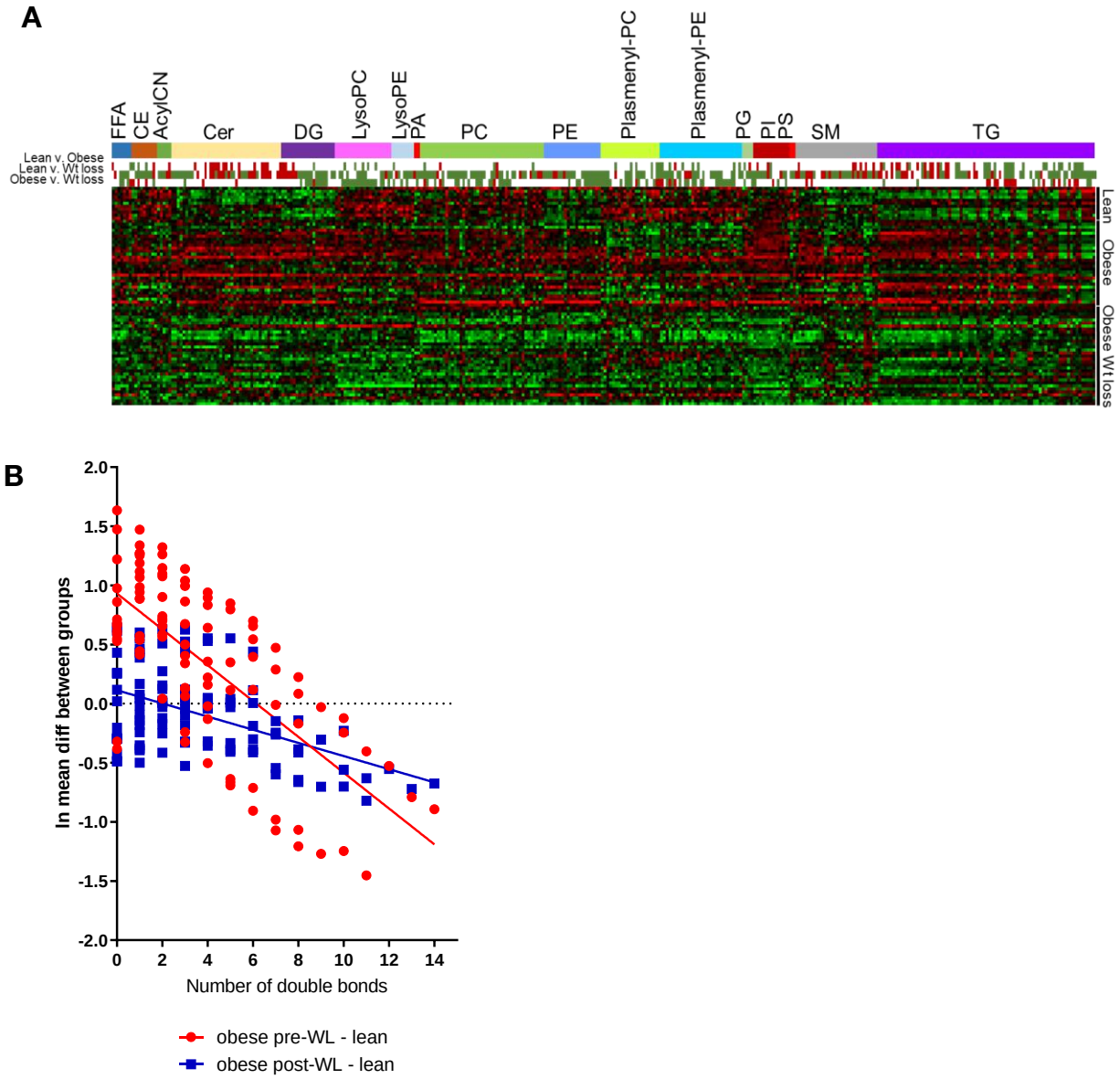

(A) Heat Map of standardized peak intensity for individual lipids (mean 0, standard deviation 1). Lipids are grouped by lipid class with increasing total chain length and double bond from left to right in each lipid class. Beneath metabolite labels, colored bar indicate significantly changed metabolites (t-test, α=0.05) and direction of change (red denotes a significant increase, green denotes a significant decrease). **(B)** Individual triglycerides sorted by the number of double bonds. Plot of mean differences between obese, pre-WL minus lean (red) and obese, post-WL minus lean (blue).

Figure 5.4. Relationship between the Institute of Medicine gestational weight gain recommendations, pre-pregnancy BMI category, and Fenton BW percentile.

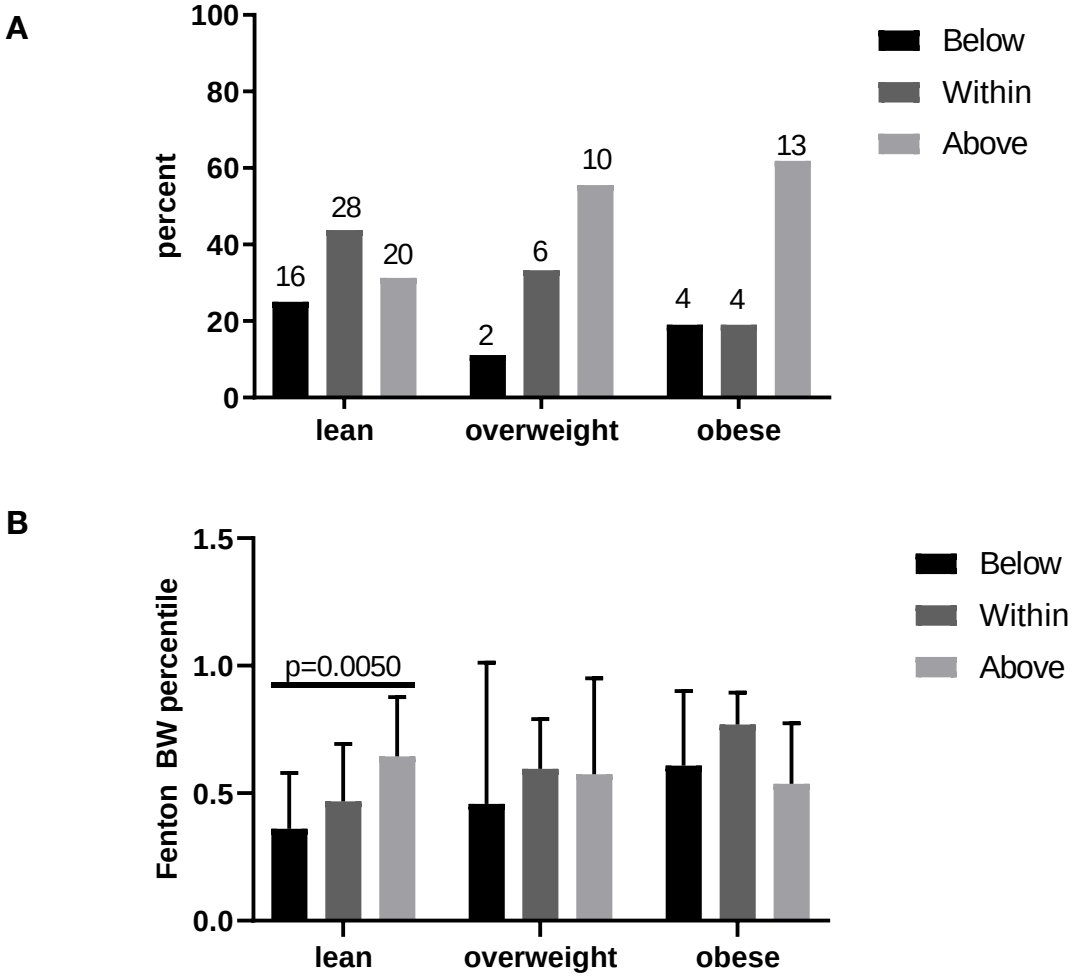

(A) Percentage of women that are below, within, or above IOM recommendations stratified by pre-pregnancy BMI. Number of women within each category listed above columns. **(B)** Comparison of Fenton BW percentile within BMI categories between women who were below, within, or above IOM GWG recommendations. There was a significant effect of IOM GWG recommendation on Fenton BW percentile in leans (F= 5.79, p=0.0050).

References

1. NCHS, National Health and Nutrition Examination Survey, 2015–2016.
2. Mcallister EJ, Dhurandhar N V, Keith SW, Aronne LJ, Barger J, Baskin M, Benca RM, Biggio J, Boggiano MM, Eisenmann JC, et al. Ten putative contributors to the obesity epidemic. Crit Rev Food Sci Nutr. 2009;49:868–913.
3. Simmonds M, Llewellyn A, Owen CG, Woolacott N. Predicting adult obesity from childhood obesity: a systematic review and meta-analysis. Obes Rev. 2016;17:95–107.
4. Abbasi A, Juszczyk D, van Jaarsveld CHM, Gulliford MC. Body Mass Index and Incident Type 1 and Type 2 Diabetes in Children and Young Adults: A Retrospective Cohort Study. J Endocr Soc. 2017;1:524–37.
5. Tremmel M, Gerdtham U, Nilsson PM, Saha S. Economic Burden of Obesity: A Systematic Literature Review. Int J Environ Res Public Health. 2017;14:1–18.
6. Bommer C, Sagalova V, Heesemann E, Manne-goehler J, Atun R, Barnighausen T, Davies J, Vollmer S. Global Economic Burden of Diabetes in Adults: Projections From 2015 to 2030. Diabetes Care. 2018;41:963–70.
7. Barker DJP, Osmond C. Infant mortality, childhood nutrition, and ischaemic heart disease in England and Wales. Lancet. 1986;1:1077–87.
8. Barker DJP, Winter PD, Osmond C, Margetts B, Simmonds SJ. Weight in infancy and death from ischaemic heart disease. Lancet. 1989;2:577–80.
9. Barker DJP, Gluckman PD, Godfrey KM, Harding J, Owens J, Robinson J. Fetal nutrition and cardiovascular disease in adult life. Lancet. 1993;341:938–41.
10. Kereliuk SM, Brawerman GM, Dolinsky VW. Maternal Macronutrient Consumption and the Developmental Origins of Metabolic Disease in the Offspring. Int J Mol Sci. 2017;18:1–27.
11. Mennitti L V., Oliveira JL, Morais CA, Estadella D, Oyama LM, Oller do Nascimento CM, Pisani LP. Type of fatty acids in maternal diets during pregnancy and/or lactation and metabolic consequences of the offspring. J Nutr Biochem [Internet]. Elsevier Inc.; 2015;26:99–111. Available from: http://dx.doi.org/10.1016/j.jnutbio.2014.10.001
12. de Brito Alves J, de Oliveira J, Ferreira D, Barros M, Noqueira V, Alves D, Vidal H, Leandro C, Laqranha C, Pirola L, et al. Maternal protein restriction induced-hypertension is associated to oxidative disruption at transcriptional and functional levels in the medulla oblongata. Clin Exp Pharmacol Physiol. 2016;43:1177–84.
13. Chen J, Martin-gronert MS, Tarry-adkins J, Ozanne SE. Maternal Protein Restriction Affects Postnatal Growth and the Expression of Key Proteins Involved in Lifespan Regulation in Mice. PLoS One. 2009;4:1–7.
14. Haider B, Bhutta Z. Multiple-micronutrient supplementation for women during pregnancy. Cochrane Database Syst Rev. 2017;

15. Pannia E, Cho CE, Kubant R, Diana S, Huot PSP, Anderson GH. Role of maternal vitamins in programming health and chronic disease. Nutr Rev. 2016;74:166–80.

16. Archer E, Marlow ML, Lavie CJ. Controversy and debate: Memory-Based Methods Paper 1: the fatal flaws of food frequency questionnaires and other memory-based dietary assessment methods. J Clin Epidemiol. Elsevier Inc; 2018;104:113–24.

17. Pinto J, Barros S, Rosa M, Domingues M, Goodfellow BJ, Galhano E, Pita C, Ceu Almeida M do, Carreira IM, Gil AM. Following Healthy Pregnancy by NMR Metabolomics of Plasma and Correlation to Urine. J Proteome Res. 2015;14:1263–74.

18. Cetin I, Alvino G, Cardellicchio M. Long chain fatty acids and dietary fats in fetal nutrition. J Physiol. 2009;587:3441–51.

19. Campbell FM, Gordon MJ, Dutta-roy AK. Preferential uptake of long chain polyunsaturated fatty acids by human placental cells. Mol Cell Biochem. 1996;155:77–83.

20. Gázquez A, Uhl O, Ruíz-palacios M, Gill C, Patel N, Koletzko B, Poston L, Larqué E, UPBEAT Consortium. Placental lipid droplet composition: Effect of a lifestyle intervention (UPBEAT) in obese pregnant women. Biochim Biophys Acta Mol Cell Biol Lipids. 2018;1863:998–1005.

21. Gluckman P, Hanson M, Cooper C, Thornburg KL. Effect of In Utero and Early-Life Conditions on Adult Health and Disease. N Engl J Med. 2008;359:61–73.

22. Rangel-Huerta O-D, Pastor-Villaescusa B, Gil A. Are we close to defining a metabolomic signature of human obesity? A systematic review of metabolomics studies. Metabolomics. Springer US; 2019;15:1–31.

23. Pallares-méndez R, Aguilar-salinas CA, Cruz-bautista I, Bosque-plata L del. Metabolomics in diabetes, a review. Ann Med. 2016;48:89–102.

24. Ng M, Fleming T, Robinson M, Thomson B, Graetz N, Margono C, Mullany EC, Biryukov S, Abbafati C, Abera SF, et al. Global, regional, and national prevalence of overweight and obesity in children and adults during 1980-2013: A systematic analysis for the Global Burden of Disease Study 2013. Lancet. 2014;384:766–81.

25. Roglic G, Varghese C, Riley L, Harvey A, Krung E, Alwan A, Cowan M, Savin S, Armstrong T, Banatvala N, et al. Global report on diabetes. Geneva, Switzerland. 2016.

26. Moran A, Jacobs DR, Steinberger J, Hong CP, Prineas R, Luepker R, Sinaiko AR. Insulin resistance during puberty: Results from clamp studies in 357 children. Diabetes. 1999;48:2039–44.

27. Kanbur NÖ, Derman O, Kinik E. The relationships between pubertal development, IGF-1 axis, and bone formation in healthy adolescents. J Bone Miner Metab. 2005;23:76–83.

28. Caprio S, Plewe G, Diamond MP, Simonson DC, Boulware SD, Sherwin RS, Tamborlane W V. Increased insulin secretion in puberty: A compensatory response to reductions in insulin sensitivity. J Pediatr. 1989;114:963–7.

29. Wells JCK. Sexual dimorphism of body composition. Best Pract Res Clin Endocrinol

Metab. 2007;21:415–30.

30. Mihalik SJ, Michaliszyn SF, De Las Heras J, Bacha F, Lee S, Chace DH, De Jesus VR, Vockley J, Arslanian SA. Metabolomic Profiling of Fatty Acid and Amino Acid Metabolism in Youth With Obesity and Type 2 Diabetes. Diabetes Care. 2012;35:605–11.

31. Gow ML, Ho M, Burrows TL, Baur LA, Stewart L, Hutchesson MJ, Cowell CT, Collins CE, Garnett SP. Impact of dietary macronutrient distribution on BMI and cardiometabolic outcomes in overweight and obese children and adolescents: A systematic review. Nutr Rev. 2014;72:453–70.

32. Urrusquieta-Flores HM, Padilla-Raygoza N, Jimenez-García SN, Moreno ER, Guerrero VB, Arias-rico J. Relationship among macronutrient intake and overweight/obesity in school children from Celaya, Mexico. J child Adolesc Heal. 2017;1:1–4.

33. Sjoberg Brixval C, Andersen LB, Lilienthal Heitmann B. Fat intake and weight development from 9 to 16 years of age: The European youth heart study - A longitudinal study. Obes Facts. 2009;2:166–70.

34. Henderson M, Benedetti A, Gray-Donald K. Dietary composition and its associations with insulin sensitivity and insulin secretion in youth. Br J Nutr. 2014;111:527–34.

35. Dobbins RL, Szczepaniak LS, Bentley B, Esser V, Myhill J, McGarry JD. Prolonged inhibition of muscle carnitine palmitoyltransferase-1 promotes intramyocellular lipid accumulation and insulin resistance in rats. Diabetes. 2001;50:123–30.

36. Venables MC, Achten J, Jeukendrup AE. Determinants of fat oxidation during exercise in healthy men and women: a cross-sectional study. J Appl Physiol. 2005;98:160–7.

37. Mcclelland GB, Lyons SA, Robertson CE. Fuel Use in Mammals: Conserved Patterns and Evolved Strategies for Aerobic Locomotion and Thermogenesis. Integr Comp Biol. 2017;57:231–9.

38. Goodrich JM, Ingle ME, Domino SE, Treadwell MC, Dolinoy DC, Burant C, Meeker JD, Padmanabhan V. First trimester maternal exposures to endocrine disrupting chemicals and metals and fetal size in the Michigan Mother-Infant Pairs study. J Dev Orig Health Dis. 2019;10:447–58.

39. Sandler V, Reisetter AC, Bain JR, Muehlbauer MJ, Nodzenski M, Stevens RD, Ilkayeva O, Lowe LP, Metzger BE, Newgard CB, et al. Associations of maternal BMI and insulin resistance with the maternal metabolome and newborn outcomes. Diabetologia. Diabetologia; 2016;60:518–30.

40. Perng W, Tamayo-ortiz M, Tang L, Sánchez BN, Cantoral A, Meeker JD, Dolinoy DC, Roberts EF, Martinez-mier EA, Lamadrid-figueroa H, et al. Early Life Exposure in Mexico to ENvironmental Toxicants (ELEMENT) Project. BMJ Open. 2019;9:e030427.

41. Lewis RC, Meeker JD, Peterson KE, Lee JM, Pace GG, Cantoral A, Téllez-Rojo MM. Predictors of Urinary Bisphenol A and Phthalate Metabolite Concentrations in Mexican Children. Chemosphere. 2013;93:2390–8.

42. Denova-gutiérrez E, Ramírez-silva I, Rodríguez-ramírez S, Jiménez-aguilar A, Shamah-

levy T, Rivera-dommarco JA. Validity of a food frequency questionnaire to assess food intake in Mexican adolescent and adult population. Salud Pública México. 2016;58:617–28.

43. Willett WC, Howe GR, Kushi LH. Adjustment for total energy intake in epidemiologic studies. Am J Clin Nutr. 1997;65:1220S-1228S.

44. McLaughlin T, Lamendola C, Liu A, Abbasi F. Preferential fat deposition in subcutaneous versus visceral depots is associated with insulin sensitivity. J Clin Endocrinol Metab. 2011;96:1756–60.

45. Jansson T, Powell TL. Role of placental nutrient sensing in developmental programming. Clin Obstet Gynecol. 2013;56:591–601.

46. Larqué E, Demmelmair H, Gil-Sánchez A, Prieto-Sánchez M, Blanco J, Pagán A, Faber F, Zamora S, Parrilla J, Koletzko B. Placental transfer of fatty acids and fetal implications. Am J Clin Nutr. 2011;94:1908S-1913S.

47. Gil-Sánchez A, Demmelmair H, Parrilla JJ, Koletzko B, Larqué E. Mechanisms involved in the selective transfer of long chain polyunsaturated fatty acids to the fetus. Front Genet. 2011;2:1–8.

48. Hanebutt FL, Demmelmair H, Schiessl B, Larque E, Koletzko B. Long-chain polyunsaturated fatty acid (LC-PUFA) transfer across the placenta. Clin Nutr. 2008;27:685–93.

49. MacDonald JIS, Sprecher H. Phospholipid fatty acid remodeling in mammalian cells. Biochim Biophys Acta. 1991;1084:105–21.

50. Lagarde M, Bernoud N, Brossard N, Lemaitre-Delaunay D, Thiès F, Croset M, Lecerf J. Lysophosphatidylcholine as a preferred carrier form of docosahexaenoic acid to the brain. J Mol Neurosci. 2001;16:201–4.

51. Nguyen LN, Ma D, Shui G, Wong P, Cazenave-Gassiot A, Zhang X, Wenk MR, Goh ELK, Silver DL. Mfsd2a is a transporter for the essential omega-3 fatty acid docosahexaenoic acid. Nature. Nature Publishing Group; 2014;509:503–6.

52. Prieto-Sánchez M, Ruiz-palacios M, Blanco-Carnero J, Pagan A, Hellmuth C, Uhl O, Peissner W, Ruiz-alcaraz AJ, Parrilla JJ, Koletzko B, et al. Placental MFSD2a transporter is related to decreased DHA in cord blood of women with treated gestational diabetes. Clin Nutr. 2017;36:513–21.

53. Sandoval KE, Wooten JS, Harris MP, Schaller ML, Umbaugh S, Witt KA. Mfsd2a and Glut1 Brain Nutrient Transporters Expression Increase with 32-Week Low and High Lard Compared with Fish-Oil Dietary Treatment in C57Bl/6 Mice. Curr Dev Nutr. 2018;2:1–10.

54. Kolokol'tsova TD, Saburina NN, Poltavtseva PA, Sukhikh GT. Isolation and Culturing of Trophoblasts from Human Terminal Placenta. Cell Technol Biol Med. 2015;158:532–6.

55. Howell KR, Powell TL. Effects of maternal obesity on placental function and fetal development. Reproduction. 2017;153:R97–108.

56. Magkos F, Fraterrigo G, Yoshino J, Luecking C, Kirbach K, Kelly SC, de las Fuentes L, He S, Okunade AL, Patterson BW, et al. Effects of Moderate and Subsequent Progressive Weight Loss on Metabolic Function and Adipose Tissue Biology in Humans with Obesity. Cell Metab. 2016;23:591–601.

57. Rothberg AE, Mcewen LN, Kraftson AT, Ajluni N, Fowler CE, Nay CK, Miller NM, Burant CF, Herman WH. Impact of weight loss on waist circumference and the components of the metabolic syndrome. BMJ Open Diabetes Res Care. 2017;5.

58. Palau-Rodriguez M, Garcia-Aloy M, Minarro A, Bernal-Lopez MR, Brunius C, Gomez-Huelgas R, Landberg R, Tinahones FJ, Andres-Lacueva C. Effects of a long-term lifestyle intervention on metabolically healthy women with obesity: Metabolite profiles according to weight loss response. Clin Nutr. 2019;S0261-5614.

59. Cantero I, Abete I, Maria del Bas J, Caimari A, Arola L, Zulet MA, Martinez JA. Changes in lysophospholipids and liver status after weight loss: the RESMENA study. Nutr Metab (Lond). Nutrition & Metabolism; 2018;15:1–11.

60. Patel N, Hellmuth C, Uhl O, Godfrey K, Briley A, Welsh P, Pasupathy D, Seed P, Koletzko B, Poston L, et al. Cord Metabolic Profiles In Obese Pregnant Women; Insights Into Offspring Growth And Body Composition. J Clin Endocrinol Metab. 2017;103:346–55.

61. Hellmuth C, Uhl O, Standl M, Demmelmair H, Heinrich J, Koletzko B, Thiering E. Cord Blood Metabolome Is Highly Associated with Birth Weight, but Less Predictive for Later Weight Development. Eur J Obes. 2017;10:85–100.

62. Lu Y-P, Reichetzeder C, Prehn C, Yin L-H, Yun C, Zeng S, Chu C, Adamski J, Hocher B. Cord Blood Lysophosphatidylcholine 16:1 is Positively Associated with Birth Weight. Cell Physiol Biochem. 2018;45:614–24.

63. Middleton P, Gomersall J, Gould J, Shepherd E, Olsen S, Makrides M. Omega-3 fatty acid addition during pregnancy (Review). Cochrane Database Syst Rev. 2018;15.

64. Monthe-Dreze C, Penfield-Cyr A, Smid MC, Sen S. Maternal Pre-Pregnancy Obesity Attenuates Response to Omega-3 Fatty Acids Supplementation During Pregnancy. Nutrients. 2018;10.

65. Zeisel SH. Choline: critical role during fetal development and dietary requirements in adults. Annu Rev Nutr. 2006;26:229–50.

66. Yan J, Jiang X, West AA, Perry CA, Malysheva O V., Brenna JT, Stabler SP, Allen RH, Gregory JF, Caudill MA. Pregnancy alters choline dynamics: Results of a randomized trial using stable isotope methodology in pregnant and nonpregnant women. Am J Clin Nutr. 2013;98:1459–67.

67. Rajarethnem HT, Megur K, Bhat R, Jc M, Gopalkrishnan SK, Babu R, Gopalram M, Rai KS. Combined Supplementation of Choline and Docosahexaenoic Acid during Pregnancy Enhances Neurodevelopment of Fetal Hippocampus. Neurol Res Int. 2017;

68. Johnson J, Clifton RG, Roberts JM, Myatt L, Hauth JC, Spong CY, Varner MW, Wapner RJ, Thorp JM, Mercer BM, et al. Pregnancy outcomes with weight gain above or below

the 2009 institute of medicine guidelines. Obstet Gynecol. 2013;121:969–75.

69. Tam CHT, Ma RCW, Yuen LY, Ozaki R, Li AM, Hou Y, Chan MHM, Ho CS, Yang X, Chan JCN, et al. The impact of maternal gestational weight gain on cardiometabolic risk factors in children. Diabetologia. Diabetologia; 2018;61:2539–48.

70. Szendroedi J, Phielix E, Roden M. The role of mitochondria in insulin resistance and type 2 diabetes mellitus. Nat Publ Gr. Nature Publishing Group; 2012;8.

71. Zurlo F, Lillioja S, Esposito-Del Puente A, Nyomba BL, Raz I, Saad MF, Swinburn BA, Knowler WC, Bogardus C, Ravussin E. Low ratio of fat to carbohydrate oxidation as predictor of weight gain: study of 24-h RQ. Am J Physiol. 1990;259:E650-7.

72. Barbosa e Silva O, Riberio Saraiva LC, Sobral Filho DC. Treadmill stress test in children and adolescents: higher tolerance on exertion with ramp protocol. Arg Bras CArdiol. 2007;89:391–7.

73. Esko T, Hirschhorn JN, Feldman HA, Hsu Y-HH, Deik AA, Clish CB, Ebbeling CB, Ludwig DS. Metabolomic profiles as reliable biomarkers of dietary composition. Am J Clin Nutr. 2017;105:547–54.